Terms and Conditions of Use of Digitised Theses from Trinity College Library Dublin

Copyright statement

All material supplied by Trinity College Library is protected by copyright (under the Copyright and Related Rights Act, 2000 as amended) and other relevant Intellectual Property Rights. By accessing and using a Digitised Thesis from Trinity College Library you acknowledge that all Intellectual Property Rights in any Works supplied are the sole and exclusive property of the copyright and/or other IPR holder. Specific copyright holders may not be explicitly identified. Use of materials from other sources within a thesis should not be construed as a claim over them.

A non-exclusive, non-transferable licence is hereby granted to those using or reproducing, in whole or in part, the material for valid purposes, providing the copyright owners are acknowledged using the normal conventions. Where specific permission to use material is required, this is identified and such permission must be sought from the copyright holder or agency cited.

Liability statement

By using a Digitised Thesis, I accept that Trinity College Dublin bears no legal responsibility for the accuracy, legality or comprehensiveness of materials contained within the thesis, and that Trinity College Dublin accepts no liability for indirect, consequential, or incidental, damages or losses arising from use of the thesis for whatever reason. Information located in a thesis may be subject to specific use constraints, details of which may not be explicitly described. It is the responsibility of potential and actual users to be aware of such constraints and to abide by them. By making use of material from a digitised thesis, you accept these copyright and disclaimer provisions. Where it is brought to the attention of Trinity College Library that there may be a breach of copyright or other restraint, it is the policy to withdraw or take down access to a thesis while the issue is being resolved.

Access Agreement

By using a Digitised Thesis from Trinity College Library you are bound by the following Terms & Conditions. Please read them carefully.

I have read and I understand the following statement: All material supplied via a Digitised Thesis from Trinity College Library is protected by copyright and other intellectual property rights, and duplication or sale of all or part of any of a thesis is not permitted, except that material may be duplicated by you for your research use or for educational purposes in electronic or print form providing the copyright owners are acknowledged using the normal conventions. You must obtain permission for any other use. Electronic or print copies may not be offered, whether for sale or otherwise to anyone. This copy has been supplied on the understanding that it is copyright material and that no quotation from the thesis may be published without proper acknowledgement.

The analysis of the modulatory effect of rosiglitazone on glial cells *in vitro* and *in vivo*

Brian Deighan

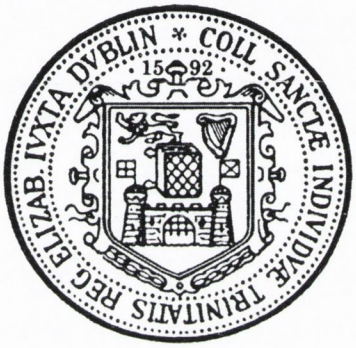

A thesis submitted to

Trinity College Dublin

for the degree of

Doctor of Philosophy

Supervisor: Professor Marina A. Lynch

Department of Physiology

Trinity College Dublin

2010

Declaration of Authorship

This thesis is submitted by the undersigned for the degree of Doctor of Philosophy at the University of Dublin. I declare that this thesis is entirely my own work with the following exceptions; certain results were produced in collaboration with Dr. David Loane, Dr Rebecca Griffin, Dr Áine Murphy, Lauren Averill and Dónal Carney. This work has not been submitted in whole or in part to this or any other university for any other degree. The author gives permission to the library to lend or copy this work upon request.

Brian Deighan

Abstract

Microglial activation is believed to play an important role in the pathogenesis of neurodegenerative and neuroinflammatory diseases. This study focussed on assessing the role of rosiglitazone as an anti-inflammatory agent and analysis was carried out to evaluate its effect *in vitro* and *in vivo*. The specific mechanism by which rosiglitazone might exert its effect was investigated and its effect on different glial cell types was also assessed.

Pretreatment of mixed glia with rosiglitazone attenuated both the LPS-induced increase in the mRNA expression of IL-1β and the release of IL-1β. Rosiglitazone also attenuated the LPS-induced increases in IL-6 and TNFα mRNA and inhibited the LPS-induced increase in expression of two markers of microglial activation CD40 and CD11b. In purified astrocytes, but not purified microglia, pretreatment with rosiglitazone attenuated the LPS-induced increase in the supernatant concentration of IL-1β. This identifies a cell-associated differential effect of rosiglitazone and it can be concluded that the ability of rosiglitazone to inhibit IL-1β release from mixed glia can be attributed to its action on astrocytes. Rosiglitazone also induced an increase in the supernatant concentration of IL-4 in mixed glia and astrocytes, however it did not increase IL-4 in microglia. The potential importance of IL-4 in mediating the modulatory effect of rosiglitazone was demonstrated as rosiglitazone attenuated the LPS-induced increase in IL-1β in mixed glia obtained from wildtype mice, but no attenuation was observed in mixed glia from IL-4$^{-/-}$ mice. A novel PPARγ agonist MDG79, like rosiglitazone, attenuated the LPS-induced increase in IL-1β, TNFα and IL-6, and the expression of the markers of microglial activation CD40 and CD11b. Analysis of the modulatory effect of the PPARγ antagonist, GW9662, on MDG79-associated changes, revealed that the modulatory role of MDG79 on pro-inflammatory cytokines is PPARγ-independent and the ability of MDG79 to attenuate the LPS-induced increase in CD40 and CD11b mRNA expression is likely to be PPARγ-dependent.

Microglial activation and pro-inflammatory cytokine production were examined in the CNS prior to, and following, onset of clinical symptoms of EAE. The data showed an increase in IL-1β and TNFα mRNA expression in the spinal cord prior to the onset of clinical symptoms, accompanied by an increase in CD40 mRNA expression in the hippocampus and spinal cord at the onset of symptoms; the evidence, which demonstrated an inverse relationship between expression of CD40 and CD200, provides further evidence that CD200 ligand-receptor interaction modulates microglial activation. Pro-inflammatory cytokines, IL-1β, IL-6 and TNFα were increased at the peak of disease in hippocampus and spinal cord. This was associated with a decrease in IL-4 mRNA expression in the hippocampus suggesting that an imbalance between pro- and anti-inflammatory cytokines may be a significant factor in the pathogenesis of the disease. The potential role of IL-4 in EAE was investigated by inducing EAE in IL-4$^{-/-}$ mice compared with wildtype mice but no significant differences in clinical symptoms were reported over the disease progression. IL-1β was increased in the spinal cord of IL-4$^{-/-}$ mice with EAE compared with wildtype mice with EAE and significantly CD40 mRNA, which was again shown to be inversely related to CD200 mRNA was also increased to a greater extent in IL-4$^{-/-}$, compared with wildtype, mice with EAE. While the results again highlight the role of IL-4 in modulating microglial activation, the impact of IL-4 on EAE as a whole appears to be quite minor. The ability of rosiglitazone to modulate microglial activation was also investigated in the EAE disease model. There was no significant difference in clinical score between rosiglitazone-treated group and control, and analysis of the spinal cord revealed that rosiglitazone administration decreased IL-1β expression in the spinal cord of mice with EAE.

The most important findings of this study are that the PPARγ agonists rosiglitazone and MDG79 can modulate microglial activation *in vitro*. The data suggest that the ability of

rosiglitazone to increase IL-4 may be an important contributory factor in the mechanism of action of rosiglitazone, although other mechanisms cannot be ruled out.

Acknowledgements

Firstly I would like to thank my supervisor, Prof Marina Lynch. From the moment I first met her in the third year of my undergraduate study she has been encouraging, supportive and a guiding figure in my scientific career to date. The advice and motivation she shared along the way is unquantifiable. She picked me up when times were tough, and she kicked me along when I needed to move (those abstracts!!). Along with the highs and lows of Munster rugby every day has been memorable, and most importantly enjoyable.

I would like to extend a huge thank you to all members of the MAL lab. Some have come and gone, but the help and support offered by all was greatly appreciated. So in no particular order; Anto, Anne Marie, Thelma, Petra, Noreen, Joan, Mel, Áine, Laura, Keith, Kevin, Julie Ann, Belinda, Fionnuala, Lauren, Dónal, Tara, Stephanie, Niamh, Alessia, Becky, Florry, Ronan, Christoph, Derek, Dave, Aileen, Darren, Michelle, Eric and Joe. The atmosphere created by everyone in the lab maintained a steady work rate, but also a relaxed environment, everyone was willing to help out if a problem arose, so thanks gang.

I would like to thank all the staff in the Department of Physiology; in particular Ann, Lesley, Doreen, Aidan, Quentin, Alice and Kieran. I would like to acknowledge Dr. David Lloyd and the Molecular Design Group in the School of Biochemistry and Immunology for providing me with the compound MDG79. I would also like to thank the Health Research Board (HRB) and Trinity College Dublin for funding this research.

I must mention in detail a few who have gone beyond the call of duty in helping me along the road to my PhD. David Loane was my mentor as I entered the lab as a quiet summer student. He instilled in me the drive, perseverance and belief required in the lab, and also the banter that is needed to push through to the end.

I cannot leave out the Murphys, I'm sure a Murphy will rule the world someday! Áine, now Dr Áine, but always Murph to me, was a hard task master and EAE guru, but a true friend both in the lab and outside too. I have to mention Kevin Murphy, my partner in crime. The chats, the "talent spotting", the pranks, the laughs

(at my bad jokes) and the fun nights out, all helped to bring some normality to the PhD. There is only room for one "nice guy" in any lab, and it's Kevin.

To my other write up buddies, the three J's, Joe, Julie Ann and Janis. We pushed through the tough days, followed the protocols and got there in the end. Good job guys.

I'd like to thank John Breen, my former first year room-mate and now one of my lifelong friends. The cups of tea and lunches in the sun were what were needed on those tough summer lab days, he is the best chemist I know and will go very far.

I cannot forget my housemates Áine, Martin, Patrick and Tomás. "33" has become a home from home; the nice dinners, pots of tea and chats were always a great end to any day. We may not agree on everything, such as composers, football teams or what to watch on the television, but the times we shared during the course of my PhD were great.

It takes patience to put up with the strange demands of animal work, lab work and the busy times of writing up, so I have to thank the "lovely" Laura for being patient, positive and her usual brilliant self.

A special thank you to my sister Orla who went ahead and set the high standards in everything she did, it's great to have someone to aspire to.

And finally to my parents, who have never stopped encouraging me. Thanks for the positive attitude and the continuous support in every way imaginable. They are always there to offer a helping hand, before I even ask. I guess they have accepted that seeing me once every so often is normal, but there's no place like home.

To the brave and the faithful nothing is impossible

Abbreviations The following abbreviations have been used:

AD	Alzheimer's Disease
ADAM	A disintegrin and mellatoprotease
AMP	Adenosine Monophosphate
BBB	Blood Brain Barrier
BDNF	Brain derived neurotrophic factor
Ca^{2+}	Calcium
CD	Cluster differentiation
CFA	Complete Freund's Adjuvant
ChAT	Choline Acetyl transferase
CNS	Central nervous system
COX	Cyclooxygenase
CREB	cAMP response element binding protein
CSF	Cerbrospinal fluid
DD	Death domain
DMEM	Dulbecco's Modified Eagles Medium
DMSO	Dimethyl sulfoxide
DNA	Deoxy ribose nucleic acid
dNTP	Deoxy nucleoside triphosphate
EAE	Experimental Autoimmune Encephalomyelitis
ELISA	Enzyme linked immunosorbent assay
FGF	Fibroblast growth factor
FADD	Fas associated death domain
g	acceleration due to gravity
GDNF	Glial derived neurotrophic factor

GFAP	Glial fibrillary acidic protein
GMCSF	Granulocyte macrophage colony stimulating growth factor
h	Hour
HDAC	Histone deacetylase
HIF1α	Hypoxia inducible factor 1α
ICAM	Intracellular adhesion molecule
IFNγ	Interferon γ
IgSF	Immunoglobulin superfamily
IKK	IκB kinase
IL	Interleukin
IL-1R	Interleukin-1 receptor
IL-1RAcP	IL-1R accessory protein
iNOS	inducible nitric oxide synthase
IP-10	Chemokine ligand 10
IRAK	IL-1R associated kinase
JAK	Janus activated kinase
LBD	Ligand binding domain
LPL	Lipoprotein lipase
LPS	Lipopolysaccharide
min	Minute
ml	millilitre
μg	microgram
μl	microlitre
μm	micrometre
MAPK	Mitogen activated protein kinase
MBP	Myelin basic protein

MCP-1	Monocyte chemoattractant protein
mCSF	Macrophage colony stimulating factor
MDG	Molecular Design Group
MOG	Myelinoligodendrocyte glycoprotein
MRI	Magnetic resonance imaging
mRNA	messenger Ribonucleic acid
MS	Multiple Sclerosis
NCAM	Neural cell adhesion molecule
NGF	Nerve growth factor
NFκB	Nuclear factor κ B
NK cells	Natural killer cells
PAGE	Polyacrylamide gel electrophoresis
PAMP	Pathogen associated molecular pattern
PCR	Polymerase Chain Reaction
PD	Parkinson's Disease
PGJ_2	Prostaglandin J_2
PI3K	Phosphoinositide 3-kinase
PLP	Phosopholipase
PPAR	Peroxisome proliferator activated receptor
PPRE	Peroxisome proliferator response element
Ppm	Parts per million
PPMS	Primary progressive MS
PRMS	Progressive relapsing MS
PT	Pertussis Toxin
P2X7	Purinergic receptor P2X, ligand gated ion channel 7
RANTES	Chemokine ligand 5

Rpm	revolutions per minute
RRMS	Relapsing remitting MS
RXR	Retinoid X receptor
SDS	Sodium Dodecyl sulphate
SOCS	Suppressor of cytokine signalling
SPMS	Secondary progressive MS
STAT	Signal transducers and activators of transcription
TACE	TNFα converting enzyme
TEER	Transendothelial electrical resistance
TGFβ	Transforming growth factor β
Th	T helper
TIR	Toll/Interleukin-1 receptor
TLR	Toll-like receptor
TNF	Tumour necrosis factor
TRAF	TNF receptor associated factor
T reg	T regulatory
VCAM	Vascular cellular adhesion molecule

Table of Contents

Chapter 2 Methods

List of Figures

Chapter 3

Chapter 6

Chapter 1

Introduction

1.1. Central Nervous System

The nervous system is one of the most complex and plastic examples of the process of evolution. It is responsible for the detection of internal and external changes, the processing of this information, and the execution of the appropriate response in the muscles, glands and organs.

The cell types of the central nervous system (CNS) are the neurons and the glial cells. Neurons primary functional role is the transmission of stimuli along the length of their axon by electrochemical signalling and subsequent interaction with adjacent cells. Their role as the functional unit in the nervous system was proposed in the 20th century by a Spanish anatomist Santiago Ramón y Cajal. His work describing the neurons as discrete functional units that communicate at synaptic junctions has become known as the *neuron doctrine* and is the foundation of much of modern day neuroscience. The glial cells of which there are four types; microglia, astrocytes, ependymal cells and oligodendrocytes, function to support the neurons and to maintain homeostasis.

1.1.1. The Brain

The cerebral cortex is the largest portion of the human brain, composing 80% of total brain weight in humans. It plays a key role in the most sophisticated of neuronal functions and is the most complex integrating area of the brain. The cerebral cortex is composed of an outer layer of gray matter with densely packed neurons covering an inner layer of white matter composed of myelinated axons. The cortex has been divided in four functional anatomical lobes; the occipital lobe, the temporal, parietal, and frontal lobe.

The hippocampus is a region of the brain that forms part of the limbic system with very important roles in memory and spatial navigation. The hippocampus is located inside the medial temporal lobe, beneath the cortical surface and its shape is responsible for its distinctive name. The sixteenth century Greek anatomist Julius Caesar Aranzi described it as similar to a sea horse; hippos meaning horse and kampos meaning monster. The hippocampus is a region of the brain very susceptible

to damage and age- and disease-related deficits in memory and cognition are associated with changes in hippocampal function.

1.1.2. The Spinal Cord

The spinal cord is approximately 45cm long and 2 cm in diameter. The vertebral column serves to protect this delicate tube of nerve cells. The cord itself is composed of white and gray matter as in the brain, but in contrast the gray matter forms an inner butterfly shaped region on the inside that is surrounded by an outer white matter layer. Similar to the brain the gray matter is composed of both neurons and glial cells.

1.1.3. Importance of the maintenance of homeostasis in CNS

Neurons are fragile and very sensitive to changes in their microenvironment, and the CNS has evolved both anatomically and physiologically to protect its delicate and vital functions from damaging immune responses.

Three barrier layers limit and regulate the molecular exchange at the interfaces between the blood and the neural tissue or the cerebrospinal fluid (CSF) in the fluid spaces (Abbott et al., 2006). The first is the blood brain barrier (BBB) formed by the cerebrovascular endothelial cells between the blood and the brain interstitial fluid, the second is the choroid plexus epithelium between the blood and ventricular CSF and the third is the arachnoid epithelium between the blood and the subarachnoid CSF. The close proximity of neurons to the blood capillary (8-20μm) highlights the BBB as the most important of the three barriers (Abbott et al., 2006). The structure of the barriers prevent the movement of immune cells, and other hydrophilic molecules from the blood into the brain, thus maintaining a stable environment for neurons. The presence of the BBB led scientists to propose that the brain was an immune privileged organ due to its compartmentalisation from the immune system.

1.1.4. Blood Brain Barrier

The BBB is a selective barrier formed by the endothelial cells that line cerebral microvessels (Abbott et al., 2006). It acts as a 'physical barrier' because complex tight junctions between adjacent endothelial cells force most molecular traffic to take a transcellular route across the BBB, rather than moving paracellularly through the junctions, as in most endothelia (Hawkins and Davis, 2005). It is generally accepted that the BBB limits the entry of plasma components, red blood cells, and leukocytes into the brain. As a result, the brain exhibits its own innate immune response that resembles, in many aspects the classical immune system. In the mammalian CNS, the BBB has been shown to consist of at least two major components, the barrier itself, which is endothelial and a second astrocytic component which has been implicated in the induction and maintenance of the barrier phenotype by both grafting studies and co-culture experiments.

A great deal is now known about the specific features of the brain endothelium. Studies using freeze fracture images show that tight junctions are more complex in the brain endothelium thus distinguishing them from the endothelium of peripheral tissues (Wolburg and Lippoldt, 2002). Studies of the molecular structure of tight junctions have identified two transmembrane proteins that contribute considerably to tight junction formation; they are occludin and claudin (Hawkins and Davis, 2005; Wolburg and Lippoldt, 2002; Yu et al., 2005). Occludin is a 60-65kDa protein with its main function being regulation of the tight junctions and claudin is a 20-27kDa protein with its main function contributing to maintenance of the high transendothelial electrical resistance (TEER) (Wolburg and Lippoldt, 2002), which restricts the movement of small ions cross the BBB (Hawkins and Davis, 2005; Yu et al., 2005). The presence of the tight junctions restricts transport of molecules. Although small gaseous molecules such as O_2 and CO_2 can diffuse freely through the lipid membranes, as well as lipophilic molecules, large hydrophilic molecules must cross the BBB either via receptor-mediated transcytosis or adsorptive transcytosis (Abbott et al., 2006).

The astrocytes are the second component of the BBB and are thought to act as important regulators of the balance between endothelial stability and permeability

(Argaw et al., 2006). The earliest histological studies showed that brain capillaries are closely associated with the perivascular endfeet of astrocytes and in close proximity to microglia (Prat et al., 2001) and that it is the close structural relationship between astrocytes and endothelia that mediates this regulation of BBB phenotype (Davson and Oldendorf, 1967). *In vitro* experiments indicated that astrocytes are able to secrete a range of chemical agents, including transforming growth factor-β (TGF-β), glial cell derived neurotrophic factor (GDNF) and basic fibroblast growth factor (bFGF) that can induce BBB phenotype in endothelial cells *in vitro* (Igarashi et al., 1999; Lee et al., 2003).

The term barrier suggests that it is a fixed permanent structure, but it is known that many features of BBB phenotype are subject to change (Abbott et al., 2006). Opening of the BBB tight junctions can occur in inflammation, and changes in transporter activity can be altered in starvation and hypoxia (Boado and Pardridge, 2002). The importance of the BBB is evidenced in several neurodegenerative disease pathologies where BBB breakdown is evident in the early phase of disease pathology (Abbott et al., 2006), involving disturbances in the endothelial-astroglial cell interaction. Bradykinin, which is produced during inflammation in stroke or brain trauma, acts on endothelial and astrocyte receptors which can lead to an increase in intracellular Ca^{2+}. This has been shown to result in the production of interleukin-6 (IL-6) via nuclear factor-κB (NFκB) from astrocytes which can impact on BBB permeability (Schwaninger et al., 1999). Other pro-inflammatory cytokines involved in inflammation such as tumour necrosis factor-α (TNFα), and interleukin-1β (IL-1β), produced by both microglia and astrocytes have previously been shown to impact on BBB stability and permeability (Didier et al., 2003; Schwaninger et al., 1999). Multiple Sclerosis (MS), which is associated with BBB breakdown has been linked to IL-1β, which causes a shift to plasticity and permeability, through the hypoxia inducible factor 1α- vascular endothelial growth factor-a (HIF1α-VEGF A) pathway. VEGF A is a potent angiogenic factor that has also been linked to BBB permeability (Argaw et al., 2006).

While the focus of much research in neurodegenerative diseases is on maintaining the BBB and sealing it up, the issue of transient opening of the tight

junctions to facilitate drug delivery is the subject of significant research (Rapoport, 2001). Attempts have been made to produce controlled opening using bradykinins but further studies are required to define the process. Understanding the endothelial-astrocytic interaction is of importance and could help design future therapies for regulation of BBB in disease.

1.2. The Immune System

The immune system along with the nervous system are the two most complex and vital systems in the human body. Immunity is the body's ability to resist or eliminate harmful foreign materials or abnormal cells. The immune system can be divided into two different components; the innate immune system and the adaptive/acquired immune system. Both the innate and acquired systems are interdependent components that differ in their timing and selectivity of their defence mechanisms.

The innate immune system is the first line of defence of the body. The principal cells of the innate immune response develop from the common myeloid progenitor cell. These are the macrophages, granulocytes, dendritic cells and mast cells. Granulocytes is a broad term for cells including neutrophils, eosinophils, basophils and the macrophage precursor the monocyte. Neutrophils and macrophages, both phagocytic cells, play a key role in the innate immune response.

Macrophages are resident in almost all tissues of the body where they perform several functions including phagocytosis of harmful foreign cells, cellular debris and also the release of cytokines and chemokines. Macrophages and dendritic cells provide an important link between the innate and acquired immune system as they have the ability to present antigen to cells of the acquired immune system. Following phagocytosis of a pathogen, dendritic cells express antigens on their surface that allows them to interact with lymphocytes of the acquired immune response (Murphy et al., 2008).

The acquired immune response primarily involves cells derived from the common lymphoid progenitor; B lymphocytes (B cells), T lymphocytes (T cells) and

natural killer (NK) cells. In the absence of infection the B and T cells are in an inactive state. It is the interaction of the cell surface receptors, B cell antigen receptors and T cell antigen receptors, with antigen that results in their activation. Activated B cells differentiate into plasma cells from which they secrete antibodies for the specific antigen and activated T cells differentiate and proliferate into one of several different functional types of effector T cells. The different subsets of effector T cells include; cytotoxic T cells, helper T (Th) cells, and regulatory T (Treg) cells. Cytotoxic T cells are capable of inducing cell death in the cells infected with antigen such as viruses and pathogens or otherwise damaged or dysfunctional cells. Helper T ($CD4^+$) cells promote antigen specific B cell differentiation and also play an important role in macrophage recruitment. The final subset, the regulatory T cells, suppress activity of lymphocytes and control immune responses therefore maintain immune homeostasis.

The spleen combines the innate and adaptive immune system in a uniquely organised way making it an important organ for immune homeostasis. Located in the abdomen, directly beneath the diaphragm, connected to the stomach, it is the body's largest filter of blood. As well as having haematologic and vascular reservoir functions, the spleen is also an important lymphoid organ. The structure of the spleen enables it remove older erythrocytes from the circulation by phagocytosis playing an important role in removal of blood-borne microorganisms and cellular debris.

In an immune response to disease or infection the dendritic cells in the circulation, having captured bacteria in the blood are transported to the spleen where they mediate the initial differentiation of and survival of B cells to become antibody-producing plasmablasts (Mebius and Kraal, 2005). On entry of antigen presenting cells to the white pulp region of the spleen, T cells become activated and they can assist the B cells. The spleen is an important immune-related organ and the relative expression of different cytokines here will be important in the differentiation and activation of specific T cell subsets during the development of disease (Mebius and Kraal, 2005).

1.3. CNS and the Immune System and their interaction

There is now extensive evidence of the immune-mediated events in the CNS parenchyma (Aloisi, 2001). Macrophages and dendritic cells have been identified in the meninges and choroid plexuses (McMenamin, 1999). Perivascular macrophages at the BBB surround the small and medium sized cerebral vessels where they display phagocytic and immune-mediated functions (Williams et al., 2001).

Beyond the protective shield of the BBB, the brain does harbour its own innate immune cells (Aloisi, 2001), the microglia. They are derived from the myeloid precursor cell, the same precursor of peripheral innate immune cells, and they function as the macrophages of the brain. They function to survey the CNS environment and phagocytose unwanted or foreign material. Microglia exist usually in a resting state, similar to macrophages, but in response to invasion they are activated and express cell surface markers and produce both cytokines and chemokines. This inflammatory response is beneficial in removing the foreign invading pathogens.

Inflammation is generally a beneficial response of an organism to infection but, when prolonged or inappropriate, it can be detrimental (Simi et al., 2007a). It has been proposed that, in the CNS, neuroinflammation associated with age and disease involves cells of the periphery, and innate immune cells contribute to the resultant disruption of CNS homeostasis and the consequent neurodegeneration.

1.3.1. LPS as a model of neuroinflammation in vitro

Lipopolysaccharide (LPS) is the most frequently used immune modulatory molecule (Lund et al., 2006). It is an amphipathic molecule which is a component of the cell wall of gram-negative bacteria that acts as a non-specific activator of the immune system (Lacosta et al., 1999). LPS consists of three distinct chemical moieties: the hydrophobic lipid A moiety, which anchors it to the outer membrane; a well-conserved surface-exposed hydrophilic oligosaccharide, designated the core, and a hypervariable polysaccharide, the O antigen (Steeghs et al., 2001).

A key hallmark of the innate immune system is the recognition of specific elements of invading pathogens, such as gram negative bacteria. These elements are called pathogen associated molecular patterns (PAMPs) which are recognised by specific cells of the immune system, i.e. microglia, as innate mechanisms to mount a rapid response to bacterial infection (Takeuchi and Akira, 2001). This bacterial recognition system was first identified in Drosophila, where it mediated defence against fungal infection, and was named Toll like receptor (TLR), as it resembled the Toll receptor involved in determining the dorsal-ventral axis of the fruit fly *drosophila melanogaster* (Hashimoto et al., 1988).

LPS activates the cell by binding to CD14, a 55kDa glycoprotein which leads to the formation of receptor complex with the MD2 and Toll-like receptor 4 (TLR4) proteins (Shimazu et al., 1999). Activation of TLR4 results in the recruitment of adaptor proteins, MyD88 and Mal. From this point on, LPS shares a signalling pathway similar to that of IL-1β. Downstream signalling via IL-1R-associated kinase-4 (IRAK-4) leads to activation of the mitogen activated protein kinase (MAPK) and NFκB. Activation of these transcription factors, particularly NFκB, leads to pro-inflammatory gene transcription and protein translation resulting in the production of inflammatory molecules, including inducible NO synthase (iNOS) and cyclooxygenase-2 (COX-2) (Tetsuka et al., 1996), which forms the basis of the innate inflammatory response.

1.4. Cells which play a role in neuroinflammation: Microglia

Microglia were first described by del Rio Hortega (1932) as a unique cell type differing in morphology from other glia and neurons, comprising of about 12% of the brain (Block and Hong, 2005). Most of the evidence currently suggests that microglia are derived from a bone marrow precursor of the mononuclear phagocytic lineage that populate the brain early in development, relating it to other organ specific macrophage populations such as the Kupffer cells of the liver and bone osteoclasts (Vilhardt, 2005).

The unique point about microglia is that they are both supportive glia and immunocompetent defence cells (Streit et al., 2004). Microglia interact dynamically with other glial cells and neurons to fulfil important neurotrophic roles (Vilhardt, 2005). They play an active role in late embryonic brain development and early postnatal brain maturation. During this remodelling and maturation, microglia are believed to assist in the clearance of cells destined for elimination through programmed cell death (Barron, 1995).

Described as the resident immune cells of the brain, microglia perform functions similar to those of tissue macrophages in the periphery such as phagocytosis, antigen presentation and the production of cytokines and chemokines (Benveniste, 1998). This constitutes the first line of defence against invading pathogens.

In the mature adult brain, most phagocyte effector function is downregulated, resting microglia exhibit a characteristic ramified morphology and function as supportive glia and are responsible for immune surveillance (Block and Hong, 2005). Neuron-microglia communication plays a key role in shaping the quiescent and reactive states of microglia (Aloisi, 2001). Neurotrophins such as nerve growth factor (NGF) and brain-derived neurotrophic factor (BDNF) along with astrocyte-produced TGFβ have been shown *in vitro* and *in vivo* as important regulators of microglia activity (Aloisi et al., 1997; Neumann et al., 1998; Vincent et al., 1997). The identification of CD200 membrane-bound glycoprotein, which is expressed on neurons, has highlighted the importance of neuron-glia cell contact in microglial regulation (Hoek et al., 2000). The interaction of CD200 with its receptor, CD200R which is expressed on microglia, has a role in regulation of microglial activity, an area discussed in more detail later (see section 1.9.).

Microglia are particularly sensitive to changes in their microenvironment and readily become activated in response to immunological stimuli, infection or injury (Liu and Hong, 2003). The transformation from a resting to an activated state has been clearly recognised for almost a century (Merzbacher, L. 1909 in (Kreutzberg, 1996). The activation results in a visible change in microglial morphology, from resting highly branched (ramified) cells with a small amount of perinuclear

cytoplasm, to cells that become hypertrophied with short processes which exhibit a bushy appearance (Benveniste, 1998). Of critical importance to the prompt response to a variety of infectious or inflammatory stimuli is their ability to detect their presence via a larger array of cell surface receptors (Aloisi, 2001). These receptors include pattern recognition receptors that can recognise pathogen-associated molecules such as LPS, complement receptors which enhance and mediate phagocytosis (Aloisi, 2001), and cytokine receptors, such as IL-1R, interferon-γ (IFNγ)R and TNFR through which specific cytokines can induce or amplify microglial activation (Benveniste, 1998). These receptors are an important determinant in inducing and regulating microglial immune functions (Aloisi, 2001).

Reports show that activated microglia increase expression of class I and II major histocompatability complex (MHC) antigens (Dickson et al., 1993; McGeer et al., 1993), adhesion molecules such as intracellular adhesion molecule-1 (ICAM 1) and co-stimulatory molecules like CD40 (Aloisi et al., 1999; Tan et al., 1999) and CD11b (Benveniste, 1998). This is accompanied by increased production of the pro-inflammatory cytokines including IL-1β, IL-6 and TNFα. Each of these will be discussed in more detail below (see section 1.6.).

1.5. Cells which play a role in neuroinflammation: Astrocytes

Astrocytes form the largest portion of glial cells in the CNS and have a number of important physiological properties related to CNS homeostasis (Dong and Benveniste, 2001). One of the obvious roles of the astrocytes is in forming the BBB with the endothelial cells, where they contribute to both its structural and functional integrity (see above, section 1.1.4.).

Astrocytes provide metabolic and neurotrophic support to neurons and modulate synaptic activity (Takuma et al., 2004). There is considerable evidence for the role of astrocytes in the defence against oxidative stress-mediated neuronal cell death (Tanaka et al., 1999) and in their ability to regulate brain energy metabolism. For example, glycogen the energy reserve of the brain is located in astrocytes and astrocytes release growth factors; BDNF, FGF and NGF that result in sustained

modulatory action in neighbouring neurons (Albrecht et al., 2002; Bruno et al., 2001; Mizuta et al., 2001; Takuma et al., 2004).

Astrocytes also play a role in synaptic transmission. Recent evidence indicates that there is a dynamic two-way communication between astrocytes and neurons at the synapse (Newman, 2003). Release of neurotransmitters from the presynaptic terminal evokes an increase in the Ca^{2+} concentration of adjacent glia (Pasti et al., 1997; Porter and McCarthy, 1996), which results in the release of glutamate and ATP from astrocytes (Bezzi et al., 1998; Kang et al., 1998; Pasti et al., 1997; Pasti et al., 2001). Transmitters released from glial cells, such as glutamate, are termed gliotransmitters to distinguish them from (neuronally-derived) neurotransmitters. It has been shown that gliotransmitters can feedback on the presynaptic terminal either to enhance or depress further release of neurotransmitters (Araque et al., 1998a; Araque et al., 1998b; Kang et al., 1998), or they can also stimulate postsynaptic neurons, producing either excitatory or inhibitory responses.

Like microglia the involvement of astrocytes in the immune response is considered to be a double-edged sword. While they possess the ability to detect infectious agents and endogenous danger signals, they produce factors that target neighbouring cells promoting leukocyte infiltration and inflammation.

Astrocytes have been shown to express the TLRs, mannose receptors, complement receptors and scavenger receptors (Farina et al., 2007). Much debate has arisen over the last decade as to the ability of astrocytes to function as competent antigen presenting cells (APCs) and their ability to interact with T cells. Evidence supports the expression of MHCII on astrocytes *in vitro* in response to IFNγ and TNFα (Panek et al., 1994; Wong et al., 1984), but the ability to detect changes in MHCII expression in astrocytes in the diseased brain is controversial. In conjunction with this, astrocyte expression of the co-stimulatory molecules B7 and CD40 is the cause of much controversy (Dong and Benveniste, 2001).

Activation of astrocytes in response to stimuli results in astrogliosis. This is the increased synthesis of glial fibrillary acidic protein (GFAP) (Holley et al., 2003; Wu and Schwartz, 1998) and astrocyte hypertrophy. GFAP is the major intermediate

filament protein of mature astrocytes and its prominent increase is the main identifying marker of reactive astrocytes (Holley et al., 2003). Recent evidence has shown that the pro-inflammatory cytokine IL-1 as a key mediator in astrocyte induced inflammation in the brain (Moynagh, 2005).

Data from both *in vitro* and *in vivo* studies show that the pro-inflammatory cytokines IL-1β, TNFα, and IFNγ are also associated with the induction of cytokine release (IL-1, IL-6, IL-10, IFNγ) (Corbin et al., 1996; Giulian et al., 1988; Yong et al., 1991) and chemokine release (RANTES, monocyte chemoattractant protein 1 (MCP1), IP-10) from astrocytes (Dong and Benveniste, 2001; Hua and Lee, 2000) as well as cell surface expression of adhesion molecules (ICAM and vascular cellular adhesion molecule (VCAM)) (Dong and Benveniste, 2001). Increased expression of both ICAM and VCAM by astrocytes has been reported in diseases such as MS and Alzheimer's disease (AD) (Brosnan et al., 1995; Rosenman et al., 1995; Shrikant et al., 1994). This list of potent immunologically-relevant cytokines and chemokines shows that astrocytes play a pivotal role in the type and extent of CNS immune and inflammatory responses (Dong and Benveniste, 2001).

1.6. Pro-inflammatory cytokines

1.6.1. IL-1β

IL-1, often referred to as the prototypic inflammatory cytokine, is a family of closely-related proteins that are products of separate genes located in a cluster on chromosome 2 (Rothwell and Luheshi, 2000). Members of the IL-1 family are expressed at low or undetectable levels by endogenous cells in the healthy brain, but in response to various brain insults including ischemia, trauma, hypoxia or inflammatory stimuli, their expression is rapidly upregulated (Simi et al., 2007a). The members of the IL-1 family, which has recently been expanded to a total of ten includes IL-1α and IL-1β.

Both IL-1α and IL-1β are synthesised as precursor proteins that lack a leader sequence. As a precursor, pro-IL-1α is active but pro-IL-1β requires cleavage to

become active. Pro-IL-1β is cleaved by an enzyme cysteine-aspartate protease caspase 1, to form active IL-1β (Thornberry et al., 1992). The biological actions of IL-1 are exerted by binding to the receptor IL-1RI, which then associates with IL-1R accessory protein (IL-1RAcP) (Wesche et al., 1997) to activate intracellular signalling pathways (Cao et al., 1996; Greenfeder et al., 1995; Muzio et al., 1997). The IL-1RI signals through a conserved intracellular region termed TIR (Toll/interleukin-1 receptor) domain, which recruits adaptors such as MyD88 and TRAF-6. This results in the activation of downstream signalling pathways including the MAPK and the NFκB (Rothwell and Luheshi, 2000). There is a second IL-1 receptor, type II receptor (IL-1RII), that binds IL-1 but it lacks an intracellular domain and does not initiate signal transduction (Sims et al., 1993). The importance and dependence of the signalling of IL-1 through IL-1RI is shown in studies where deletion of the IL-1RI gene abolishes all pro-inflammatory effects of IL-1, from activation of NFκB to production of other pro-inflammatory cytokines (Allan et al., 2005; Lucas et al., 2006; Relton and Rothwell, 1992; Yamasaki et al., 1995).

The IL-1 family also includes the IL-1R antagonist (IL-1Ra). It is a highly selective, competitive receptor antagonist that binds IL-1RI, but does not trigger IL-1R and AcP association and does not result in intracellular signalling (Mrak and Griffin, 2001). Exogenous administration of IL-1Ra is neuroprotective in animal models of ischemia (Relton and Rothwell, 1992), excitotoxicity (Lawrence et al., 1998) and trauma (Tehranian et al., 2002).

Expression of IL-1 has been shown in microglia, astrocytes, oligodendroglia, neurons, cerebrovascular cells and circulating immune cells (Simi et al., 2007a) although the regulation of expression, cleavage and release of IL-1β from the cell is still poorly understood. The proposed mechanism comes from data on IL-1 release from monocytes of the periphery. It is proposed that the release of IL-1β from microglia and astrocytes requires purinergic P2X7 receptor activation by extracellular ATP which can regulate the cleavage and release of IL-1β (Ralevic and Burnstock, 1998; Sanz and Di Virgilio, 2000; Simi et al., 2007b).

It remains uncertain whether endogenous IL-1 plays a physiological role in the body. On the one hand, the levels in the healthy brain are very low, and mice

lacking genes for IL-1 develop normally and do not suffer from any obvious physiological changes. However endogenous IL-1 has been shown to be involved in sleep pattern (Krueger et al., 1998) and it plays a significant role in fever (Kluger et al., 1998). The majority of actions of IL-1 in the brain are associated with responses to local or systemic insults. IL-1 is not toxic to neurons in culture, but it does induce an indirect negative effect (Viviani et al., 2003). IL-1 can induce the production of ceramide, which results in the activation of NMDAR which causes an influx of Ca^{2+}, leaving the neuron vulnerable to other insults (Strijbos and Rothwell, 1995). Most effects of IL-1β have been described in astrocytes where it promotes astrocyte proliferation and astrogliosis. It has been shown that IL-1 is the key stimulus in the induction of expression of adhesion molecules (ICAM 1 and VCAM) and chemokines (MMPs and IL-8) in astrocytes (Moynagh et al., 1994; Rosenman et al., 1995; Shrikant et al., 1994). IL-1 has also has been shown to increase the release of the pro-inflammatory cytokines, IL-6 and TNFα from astrocytes (Lee et al., 1993b). IL-1 activation of IL-1R in astrocytes has been shown to induce caspase-dependent neuronal death, which is dependent on the release of free radicals (Thornton et al., 2006).

Increases in IL-1β are associated with inflammation and pathogenesis of diseases such as MS, Parkinson's Disease (PD) and AD (Lucas et al., 2006). For example IL-1 is thought to exacerbate acute brain damage associated with cerebral ischemia (Touzani et al., 1999). AD is an example of a condition in which there is sustained chronic overexpression of IL-1 and in which IL-1 overexpression has been implicated in both the initiation and progression of the characteristic neuropathological changes (Griffin, 2006).

In addition, patients suffering from MS have elevated levels of IL-1 in the CSF when the disease is active (Hauser et al., 1990), while IL-1 is also thought to play a role in autoimmune destruction of myelin (Merrill, 1992). It has been concluded that IL-1 is an important element in the inflammatory mechanism in neurodegeneration and increased understanding would undoubtedly contribute to the design of future therapies.

1.6.2. IL-6

IL-6 is a 26kDa pleotropic inflammatory cytokine (Haegeman et al., 1986) that belongs to the family of cytokines that have a four helical structure (Scheller and Rose-John, 2006). IL-6 is secreted by a wide range of cells including fibroblasts, monocytes, B cells, endothelial cells, T cells, microglia and astrocytes (Benveniste, 1998). Astrocytes appear to be the main producers of IL-6 and can be activated to express IL-6 in response to a wide array of stimuli such as LPS, TNFα, IL-1β and TGFβ (Benveniste et al., 1990; Lee et al., 1993b; Sawada et al., 1992).

IL-6 exerts it activity by binding to specific cell surface receptors which belong to the cytokines type 1 receptor family (Darnell et al., 1994). On binding with its receptor, IL-6R, the IL-6-IL-6R complex associates with two molecules of the signal transducing protein gp130 (Taga and Kishimoto, 1997). The formation of this complex activates the intracellular tyrosine kinases of the Janus kinase family (JAK). Activated JAKs phosphorylate transcription factors of the signal transducers and activators of transcription (STAT) family, in particular STAT 3 which, through translocation to the nucleus, regulates IL-6 specific genes. The binding of IL-6 to its receptor can also activate an alternative pathway which involves the G-protein Ras, and can result in the activation of MAPK (Gadient and Otten, 1993).

IL-6 and IL-6R expression has been reported in neurons, microglia and astrocytes (Schobitz et al., 1993; Yan et al., 1992). The mechanisms controlling IL-6 synthesis and release are identical in all three cell types. The fact that IL-6 synthesis in brain cells can be induced by pro-inflammatory cytokines, infections, pathogens, as well as neurotransmitters, supports the concept of tight communication between neurons and glia involving IL-6 (Gadient and Otten, 1993).

IL-6 is elevated rapidly within the CNS after brain damage (Woodroofe et al., 1991) and it has been suggested that one of the inflammatory mediators causally involved in AD pathology is IL-6 (Gadient and Otten, 1993). It has also been shown that IL-6 immunoreactivity is markedly elevated in the nigrostriatal dopaminergic region of a patient suffering from PD (Mogi et al., 1994) although whether IL-6 is

causative to the neurodegeneration events or if it is a consequence of on-going inflammation induced by neuronal damage is still debated (Gadient and Otten, 1993).

1.6.3. TNFα

TNFα was identified three decades ago as a product of lymphocytes and macrophages that caused the lysis of certain cell types, especially tumour cells (Carswell et al., 1975; Grange et al., 1969). TNFα is a type 2 transmembrane protein that can exist in a membrane-associated form as well as a cleaved, soluble mature form (Locksley et al., 2001). Its structure is described as a self-assembly non-covalent trimer, whose individual structures fold as compact "jelly roll" β sandwiches and interact at hydrophobic interfaces. TNFα-converting enzyme (TACE or ADAM-17) cleaves the membrane-bound form to release the soluble cytokine (Black et al., 1997). Both forms are biologically active and can be synthesised in the CNS by microglia, astrocytes and neurons and in the adipocytes in the periphery (Lorenzo et al., 2008; McCoy and Tansey, 2008).

The members of the TNF ligand family exert their biological functions by interacting with their cognate membrane receptors, the TNF receptor family. Two types of receptors are known; TNF-R1 and TNF-R2. TNF-R1 is expressed in most tissues but TNF-R2 is found mainly in the cells of the immune system.

The ligand-receptor interaction generates downstream signalling that occurs via two classes of cytoplasmic adaptor proteins: TNF receptor-associated factors (TRAFs) and "death domain" (DD) molecules (Fesik, 2000). Recruitment of adaptor protein DD, such as Fas-associated death domain (FADD) or TNFR associated death domain (TRADD) results in activation of a downstream signalling cascade and ultimately the activation of caspases, and cell death. Recruitment of TRAF leads to activation of the transcription factor NFκB and activation of c-jun-N-terminal kinase (JNK) (Locksley et al., 2001).

There is strong evidence implicating TNFα in the pathology underlying neuroinflammatory diseases such as MS. Serum and CSF TNFα concentrations were reported to be increased in patients with MS compared with control (Beck et al.,

1988; Sharief and Hentges, 1991) and treatment with anti-TNFα antibodies are protective against disease severity (Probert et al., 1995).

1.7. Anti-inflammatory cytokines

1.7.1 IL-4

IL-4 is a typical anti-inflammatory cytokine that plays a critical role in the regulation of immune responses. It is a glycoprotein with a molecular weight of 20kDa and is composed of 129 amino acids (Sholl-Franco et al., 2009). IL-4 was discovered in the 1980s and is typically released from Th2 cells where it is responsible for the maturation and differentiation of T and B cells. The production of IL-4 has also been shown by basophils, mast cells and natural killer cells (Seder and Paul, 1994).

IL-4 exerts its biological action through the interaction with and binding to cell surface receptors that form the assembly of a receptor complex consisting of the IL-4Rα chain and the common gamma chain (γc). After dimerisation of the IL-4R complex, cytoplasmic tails of receptors become phosphorylated and act as docking sites for different signalling molecules. This results in a series of phosphorylation events mediated by receptor-associated kinases (Nelms et al., 1999). Three members of the JAK family, JAK-1, JAK-2 and JAK-3, have been demonstrated to be activated in response to IL-4R engagement (Nelms et al., 1999). It has been shown that engagement of the receptor results in phosphorylation of STAT-6, which translocates to the nucleus and regulates transcription of IL-4 responsive genes (Haque et al., 1998). *In vitro* experiments show that IL-4 inhibits IFNγ induced production of hydrogen peroxide in human cultured monocytes (Lehn et al., 1989), and IL-4 induced a decrease in IL-1β and TNFα in human cultured monocytes from cancer patients and also in peripheral macrophages (Lehn et al., 1989).

Most of the data published was obtained from peripheral cells but there is growing evidence of its action in the CNS. IL-4 and IL-4 mRNA expression have been detected on microglia and astrocytes, although there is debate about the issue of

astrocyte expression of IL-4 (Abbas et al., 2002; Hulshof et al., 2002; Suzumura et al., 1994). Accumulating evidence has indicated that IL-4 reduces the production of inflammatory mediators, including iNOS, TNFα, COX2 and MCP-1 from activated microglia both *in vivo* and *in vitro* (Chao et al., 1993; Ledeboer et al., 2000; Park et al., 2005). Evidence from this lab has shown that IL-4 downregulates IL-1β in tissue prepared from aged rats (Nolan et al., 2005).

1.8. Markers of glial activation

1.8.1. CD40

CD40 is a 48kDa phosphorylated glycoprotein protein that is expressed on the surface of various cells including B lymphocytes, dendritic cells, endothelial cells, and activated macrophages and microglia (Alderson et al., 1993; Armitage et al., 1992). CD40 a member of the TNFR family, that includes TNFR1, TNFR2 and Fas (D'Aversa et al., 2002).

It interacts with its natural ligand CD40L or CD154, 39kDa type II transmembrane protein of the TNF superfamily, which is expressed on $CD4^+$ T cells (Egeler et al., 2000). CD40-CD40L interactions have a crucial role in the development of many immune responses and inflammatory processes (Aloisi et al., 1999). CD40-CD40L interaction has been shown to upregulate; co-stimulatory molecule expression (ICAM1, VCAM1, MHC II), pro-inflammatory cytokines (IL-1, IL-6, TNF, IL-8 and IL-12) and chemokines (macrophage inflammatory protein (MIP)-1α and MCP-1) (Chen et al., 2006).

Microglial expression of CD40 is usually very low (Tan et al., 1999), but in response to stress, or challenge (LPS or pro-inflammatory cytokines) CD40 expression dramatically increases (Aloisi et al., 1999; Tan et al., 1999). The pro-inflammatory cytokines TNFα and IL-1β are known inducers of CD40 expression in microglia (Aloisi et al., 2000) but IFNγ is the most potent, increasing CD40 expression 20-fold (Chen et al., 2006).

CD40-CD40L interaction initiates a complex signalling cascade that involves the activation of various protein tyrosine kinases and transcription factors (Chen et al., 2006). Due to the lack of enzymatic activity in the cytoplasmic c-terminus of CD40, the signalling is mediated via TNF receptor-associated factors (TRAFs). The TRAF family consists of 6 members TRAF 1-6. These adaptors link CD40 to the multiple downstream pathways that include phosphoinositide 3-kinase (PI3K) (Chen et al., 2006; Tan et al., 1999), phospholipase C, MAPK (Calingasan et al., 2002), and NFκB (Chen et al., 2006).

CD40-CD40L interactions are implicated in participating in a variety of CNS diseases. Increased expression of CD40 and CD40L has been detected in AD (Togo et al., 2000) and MS (Gerritse et al., 1996). The fact that depletion of CD40 and CD40L gene in mouse models of MS or AD renders the animal resistant to disease progression defines a detrimental role for these molecules in promoting inflammation in the CNS (Chen et al., 2006)

1.8.2. CD11b

CD11b is a cell surface antigen expressed on cells of the myeloid lineage including neutrophils, monocytes, macrophages and microglia. It is expressed at low or undetectable levels in the resting state, and its expression increases steadily during myeloid differentiation (Dziennis et al., 1995). CD11b acts as a binding protein for ICAM-1 and Cb3i, both of which are expressed on a variety of cell types including leukocytes and endothelial cells. It has been reported in several models of neuroinflammatory diseases that CD11b expression corresponds with the severity of microglia activation. It has been shown that this upregulation in CD11b in response to microglial activation is driven by NO (Roy et al., 2008).

1.9. CD200

CD200 is a type-1 membrane glycoprotein of the immunoglobulin superfamily (IgSF) of cell surface proteins. CD200, or OX-2 membrane glycoprotein

as it was previously known, contains two IgSF domains and is expressed on a variety of lymphoid and non-lymphoid cells, including the kidney glomeruli, vascular endothelium and subsets of neurons (Adams et al., 1998; Barclay, 1981; Bukovsky et al., 1983).

While CD200 has been studied for many years an important discovery was made by Preston et al., (1997) with the identification of CD200R on the surface of resident macrophage obtained from the peritoneal cavity of rats and mice. The structure of CD200R was identified as being similar to CD200, membrane bound and having two immunoglobulin-like domains. It is highly expressed on cells of the myeloid lineage (macrophages, microglia, neutrophils and monocytes) and also on T cells, but differs structurally from its ligand as it has a longer cytoplasmic tail containing no signalling motifs (Preston et al., 1997; Wright et al., 2000).

The importance of the control of myeloid cells, including microglia, has been emphasised already. The CD200-CD200R interaction provides a cell-cell contact regulatory interaction for myeloid cells (Jenmalm et al., 2006). It is the inhibitory signal to myeloid cells resulting from CD200-CD200R receptor interaction that is important to the inflammatory control. As I mentioned CD200R differs from the ligand by virtue of a longer cytoplasmic domain. The tail contains three conserved tyrosine residues, one of which is contained within an NPXY motif (Wright et al., 2000). It has been shown that signalling occurs via phosphorylation of the NPXY motif that recruits to Dok 1 and Dok 2 phosphorylation and subsequently inhibits Ras/MAPK pathways (Zhang et al., 2004).

There is a growing body of evidence for the significant role that CD200-CD200R interactions play in the modulating tissue inflammation in various inflammatory forms, such as arthritis, allograft rejection and neurodegeneration (Walker et al., 2009). Studies using mice with a CD200 deletion have shed light on the dynamics of the CD200-CD200R interactions. Deletion of CD200 resulted in myeloid cell dysregulation and enhanced susceptibility to autoimmune inflammation in experimental autoimmune encephalomyelitis (EAE) and collagen-induced arthritis, therefore suggesting that immune suppression is generated through interaction with CD200R (Hoek et al., 2000). Further to this, a study showed that a soluble form of

CD200 administered to mice reduced autoimmune inflammation in an arthritis model (Gorczynski et al., 2001).

Recent evidence has shown the importance of CD200 in rodent models of neurodegeneration. It is reported that microglial activation in the hippocampus of aged (Frank et al., 2006; Lyons et al., 2007a) and Aβ treated rats (Lyons et al., 2007a) were accompanied by decreased expression of neuronal CD200. This was accompanied by *in vitro* data that show treatment of hippocampal neurons with the anti-inflammatory cytokine IL-4 increased CD200 expression (Lyons et al., 2007a).

1.10. PPAR

Peroxisome proliferator-activated receptors (PPAR) are members of a superfamily of proteins termed nuclear receptors (Kapadia et al., 2008). As a nuclear receptor, PPAR acts as an agonist-activated transcription factor that regulates specific target gene transcription. There are three subtypes of PPAR; PPARα, PPARβ and PPARγ.

1.10.1. PPARγ

The role of PPARγ in controlling lipid and glucose metabolism is well established (Drew et al., 2006). However, the fact that these receptors are also capable of modulating the immune response has only recently become appreciated. PPARγ is similar to other nuclear receptors in that it possesses a modular structure composed of two domains. The first of these is a DNA binding domain (DBD). It consists of two zinc fingers that specifically bind the PPAR response element (PPRE) in the regulatory region of the PPAR responsive genes. The second is the ligand binding domain (LBD), the portion to which PPARγ agonists and coactivators bind. Crystalographic analysis has shown the LBD to contain 13-α helices and a small 4-stranded β-sheet, and the ligand-binding pocket of PPARγ is quite large, thus allowing it to interact with a broad range of natural and synthetic ligands (Nolte et al., 1998).

Prior to binding with the ligand, PPARγ is in an inactive state complexed with nuclear co-repressors and histone deacetylases (HDACs). The co-repressors function to keep the receptor in a repressed inactive state while the HDAC maintains the surrounding chromatin in a condensed state through histone deacetylation, thus inhibiting gene expression (Jepsen and Rosenfeld, 2002; Sundararajan et al., 2006). On binding of the ligand to the LBD on PPARγ, the repressors displace, and PPARγ forms a heterodimer with a retinoid X receptor (RXR). This allows PPARγ to bind to the PPRE and recruitment of transcriptional activators occurs. The co-activators include nuclear co-activators (N-CoAs) and cyclic-AMP response elements protein (CREB)-binding protein (CBP)/protein 300 (p300). The result is an increase in gene transcription (Berger and Moller, 2002; Bernardo and Minghetti, 2006).

1.10.2. PPARγ, role in lipid and glucose metabolism

PPARγ is predominantly expressed in adipose tissue, the adrenal gland and in the spleen. It acts in the body as a lipid sensor where it functions to regulate a unique subset of genes responsible for lipid and energy metabolism (Kersten et al., 2000). They play a particularly important role in both lipid and carbohydrate metabolism and participate in the regulation of serum glucose levels as well as regulating insulin sensitivity (Landreth et al., 2008). From its role in lipid metabolism it is not surprising that the natural agonists are long chain fatty acids, eicosanoids and prostaglandins. Synthetic agonists of PPARγ belong to a class of drugs called thiazolidinediones, or glitazones (Combs et al., 2000). Currently on the market for the treatment of type II diabetes are the glitazones, ciglitazone, rosiglitazone and pioglitazone. The binding of the thiazolidinedione to PPARγ has been shown to improve lipid metabolism and insulin sensitivity (Berger and Moller, 2002).

In adipocytes, PPARγ regulates numerous genes involved in lipid metabolism including aP2, acetyl co-A synthase (Berger and Moller, 2002) as well as CD36 and lipoprotein lipase (LPL) which are important for lipid uptake into adipocytes (Hodgkinson and Ye, 2003). PPARγ has also been shown to downregulate leptin, which is an adipocyte-selective protein that inhibits feeding (De Vos et al., 1996;

Kallen and Lazar, 1996). PPARγ also modulates the transcription of several genes that affect insulin action. Interestingly, the pro-inflammatory cytokine, TNFα, which is expressed by adipocytes, has been associated with insulin resistance and diminished insulin signal transduction (Hofmann et al., 1994) and PPARγ agonists inhibit the expression of TNFα and prevent TNFα-induced insulin resistance (Hofmann et al., 1994; Miles et al., 1997).

1.10.3. PPARγ and a role in neuroinflammation

It was the inhibitory effects of PPARγ agonists on TNFα that led to several research groups examining the possibility that these agents possess anti-inflammatory properties. This was strengthened by evidence showing the expression of PPARγ on T cells, B cells, macrophages and monocytes (Clark, 2002; Jiang et al., 1998; Ricote et al., 1998; Yang et al., 2002). Pivotal early experiments showed that PPARγ expression was upregulated in activated macrophages and monocytes (Jiang et al., 1998; Ricote et al., 1998) and that expression of iNOS and release of pro-inflammatory cytokines such as TNFα and IL-6 are attenuated by treatment with natural and synthetic PPARγ agonists (Jiang et al., 1998; Ricote et al., 1998). Further studies have shown the anti-inflammatory properties of PPARγ agonists in animal models of aging, PD, MS and many more neurodegenerative conditions.

Despite the ever-growing evidence that both natural and synthetic PPARγ agonists are important in the regulation of the inflammatory response, the exact mechanism by which this response occurs is still debated. While PPARγ agonists can clearly lead to transcription factor activation, it is now clear that some actions are independent of the nuclear receptor. This recent evidence has shown that the anti-inflammatory effects of PPARγ agonists may control gene expression independently of binding to PPRE, by a mechanism called receptor-dependent transrepression (Drew et al., 2006). This is believed to result from physical interaction of the receptor with other transcription factors.

It has been demonstrated that 15d-PGJ_2, a natural PPARγ agonist and the major metabolite from prostaglandin D2 that is derived from sequential metabolism

of arachidonic acid, suppressed TNFα, NO and MHCII expression by primary rat microglia. It was also demonstrated that ciglitazone, suppressed the production of the cytokines in a similar manner, suggesting a PPARγ-dependent mechanism (Bernardo et al., 2000). In addition, the expression of PPARγ was found to be upregulated in the spinal cord of mice with EAE, an animal model of multiple sclerosis, supporting a role of this receptor in modulating disease (Diab et al., 2002). Recent studies have also demonstrated that thiazolidinediones block the production of inflammatory cytokines from microglia and astrocytes and protect neurons, but more importantly a PPARy antagonist, GW9662, blocked thizolidinedione protection of cortical neurons, suggesting a receptor-mediated suppression and protection (Luna-Medina et al., 2005).

On the other hand there is evidence suggesting that PPARγ agonists are capable of inhibiting inflammatory responses in glia through receptor-independent mechanisms (Drew et al., 2006). In primary astrocytes the anti-inflammatory effects, inhibition of TNFα, IL-1β and IL-6 gene expression, were observed to be independent of PPARγ activation (Giri et al., 2004). It was shown that 15d-PGJ_2 inhibited the inflammatory response by inhibiting IκB kinase (IKK) activity, which inhibits the translocation of the NFκB subunit p65 to the nucleus and thus the activity of NFκB (Giri et al., 2004; Ward et al., 2002). Recent evidence from this lab has shown that the anti-inflammatory action of rosiglitazone in the brain of aged rats is independent of PPARγ; the data here indicated that the PPARγ antagonist GW9662 failed to abrogate the inhibitory effect of rosiglitazone (Loane et al., 2009).

Recent evidence also shows that PPARγ agonists can also act to inhibit the JAK STAT signalling cascade in a PPARγ independent manner. The JAK STAT signalling pathway is an essential pathway mediating immune responses and one which is tightly regulated. A recent study identified protein suppressors of cytokine signalling (SOCS), that are usually expressed at low levels but are upregulated by inflammatory stimuli (Park et al., 2003), which negatively regulate the response of immune cells by inhibiting JAK STAT activity. Evidence shows that the PPARγ agonists, rosiglitazone and 15d-PGJ_2, induced the transcription of SOCS1 and SOCS3 in microglia and astrocytes. This increase in SOCS activity was accompanied by the

inhibition of JAK activation, thus reducing inflammatory signalling (Park et al., 2003) and is another example of PPARγ independent anti-inflammatory action. It is therefore evident that further studies are required to more definitively determine the mechanisms by which PPARγ agonists modulate inflammatory responses in the CNS.

1.10.4. PPARγ, a novel agonist, MDG79

The role of PPARγ agonists in modulating neuroinflammation is becoming more established. The withdrawal of the drug troglitazone from the market 1997, due to its association with drug induced-hepatotoxicity, has encouraged the research and development of novel PPARγ agonists that are more specific for the nuclear receptor and free of contraindications. At this present moment there are 30 known agonists undergoing clinical trials

The Molecular Design Group in Trinity College has recently identified a novel agonist for PPARγ referred to as MDG79. MDG79 is a small molecule, less than 500Da that is structurally different from glitazones and thiazolidinediones. Analysis has shown, using the established silico AMDE (Absorption, Distribution, Metabolism and Elimination) prediction model, that MDG79 is expected to cross the BBB. Preliminary experiments were carried out to investigate the protective role of MDG79 in PD and the results indicate that MDG79 offers neuroprotection against the neurotoxin N-methyl-4-phenylpyridium (MPP+) in the PC12 dopaminergic cell line, at a low concentration of 1μM (Davey et al., unpublished).

1.11. Multiple Sclerosis

MS is a chronic inflammatory demyelinating disease of the CNS. It is the most common cause of neurological disability arising between early to middle adulthood, affecting approximately 2 million people worldwide (Oksenberg and Barcellos, 2005). Interestingly it has been shown that females are twice as likely to develop the disease than males (Ebers and Dyment, 1998).

1.11.1. History of MS

A French man Jean Martin Charcot has been credited with the first distinct description of the disease in 1868 when he reported the pathology as "sclerose en plaques" (Poser and Brinar, 2004). Charcot's determination to explain the relationship between symptom presentation in his patients at the Hôpital de la Salpetriere, and the presence of lesions observed by autopsy in the CNS, led to the characterisation of the disease. During a series of three lectures in 1868 entitled "Leçons du mardi" Charcot described symptoms such as nystagmus, intention tremor and scanning speech in his patients combined with his detailed macroscopic and microscopic artistic representations of lesions in the brain of the patients. This complete picture cemented the concept of "sclerose en plaques" or MS as a distinct disease (Murray, 2009).

From the first steps and descriptions by Charcot in the late 19th century, our understanding of the disease has evolved to reflect the advances in technology in the late 20th and early 21st centuries. A modern textbook definition of MS defines it as a chronic neurological disease caused by a destructive immune response resulting in the formation of hard sclerotic lesions or plaques in the white matter of the CNS (Murphy et al., 2008). The plaques themselves are composed of areas of dissolution of myelin, the insulating layer surrounding the axons, along with other inflammatory infiltrates and immune cells (Murphy et al., 2008).

This representation of the disease is effective at communicating the essential concept of the disease, but the specific mechanisms of disease initiation and progression require further investigation. Many rewarding areas of research are contributing to our further understanding of the disease. In the last few decades detailed studies of the pathology of MS have intensified, advances in MRI have provided more specific information on the disease and experimental drug therapies provide valuable insights into the immunological and biological elements in the disease pathology (McFarland and Martin, 2007).

1.11.2. Subtypes of MS

Despite the advances, a common problem is the variability of disease progression from individual to individual. Clinical symptoms may be episodic or progressive, mild or severe, disseminated or even specific to the spinal cord (Ramagopalan and Ebers, 2008). This variability has prompted the classification of MS into four subtypes. They are; Relapsing Remitting MS (RRMS), Secondary Progressive MS (SPMS), Primary Progressive MS (PPMS) and Progressive Relapsing MS (PRMS). RRMS is defined by a relapse or flare up of symptoms followed by a remission or recovery period, this can be full or almost full recovery. SPMS is a form that develops from initial RRMS, defined by prolonged relapses during which disability increases without remission. PPMS is the most common form of MS, particularly prevalent in the older population. It is defined by symptoms that become progressively worse with increasing disability without any periods of remission. The final subtype is PRMS, it is defined as the progressive worsening of symptoms, but with clear acute relapses, with or without recovery (Ramagopalan and Ebers, 2008).

1.11.3. MS and the immune system: overview

It has been established that the cells of the immune system play an important role in the pathogenesis of the disease. MS is characterised by chronic inflammation, myelin loss, gliosis, varying degrees of axonal and oligodendrocyte pathology and progressive neuronal dysfunction, resulting in the development of lesions. The use of magnetic resonance imaging (MRI) has highlighted the importance of the BBB in the initial stages of MS pathogenesis (Stone et al., 1995). A general consensus is that MS begins with the formation of acute inflammatory lesions characterised by the breakdown of the BBB (McFarland and Martin, 2007) allowing the migration the $CD4^+$ T cells from the blood into the brain. In brief, the interaction of the T cells, which have a Th1 and Th17 phenotype with their antigen, presented on microglia, results in an increased inflammatory response. The antigen is usually the proteins of the myelin sheath, myelin basic protein (MBP), proteolipid protein (PLP) and myelin

oligodendrocyte glycoprotein (MOG) (Swanborg, 1995). The inflammatory response involves the recruitment of T cells, B cells, dendritic cells, glial cells, production of chemokines and cytokines all exacerbating the inflammatory response which results in the demyelination of the axon and the production of the MS lesion.

Most of what is known about the BBB, T cell infiltration and microglial driven inflammation is the result of both studies on MS patients and animal models of MS such as experimental autoimmune encephalomyelitis (EAE).

1.12. EAE

1.12.1. History of EAE

The origins of EAE date back to the 1920's when early experiments by Koritschoner and colleagues induced spinal cord inflammation and encephalitis in rabbits by inoculation with human spinal cord (Baxter, 2007; Koritschoner and Schweinburg, 1925). In the 1930's researchers in the Rockerfeller Institute at John Hopkins University attempted to reproduce the encephalitic complications associated with rabies vaccine by repetitive immunisation of rhesus monkeys with CNS tissue (Gold et al., 2006; Rivers et al., 1933). They found that histological examination of the brains of monkeys revealed the presence of perivascular infiltrates and distinct areas of demyelination (Baxter, 2007; Rivers et al., 1933). Further experiments by Rivers and colleagues resulted in the development of a model of encephalomyelitis, experimental allergic encenphalomyelitis, in monkeys. The monkeys displayed clinical symptoms such as clumsy gait and muscle weakness following injection of rabbit brain emulsion and this was accompanied by perivascular infiltrates and myelin degeneration in the spinal cord (Baxter, 2007; Rivers and Schwentker, 1935).

1.12.2. EAE models

This model has successfully been refined and frequently modified over the past 75 years. Even the name has changed from experimental allergic

encephalomyelitis to experimental autoimmune encephalomyeilits (EAE) (Steinman and Zamvil, 2006).

The first important modification was the development of a new oil-based adjuvant by Jules Freund, complete Freund's adjuvant (CFA), that when combined with brain extract allowed the fast tracking of disease progression (Kabat et al., 1951). In Rivers' initial work, numerous injections over a 1-year period were required but using Freund's adjuvant (CFA) only a single injection was required at the initiation of the disease. The second important development was addition of heat-inactivated mycobacterium tuberculosis to the adjuvant (CFA) (Kabat et al., 1951). This was proven to further enhance the progression of the symptoms.

Initial EAE models were confined to the monkey, rat and guinea pig, due to a lower disease incidence in mice. Pioneering work by Yasuda (1975) and Bernard and Carnegie (1975) using Pertussis toxin in combination with CFA and mycobacteria tuberculosis developed a successful murine version of the EAE model. In addition the success of their mouse model was that they selectively chose more susceptible mouse strains for the induction of the disease (Bernard and Carnegie, 1975; Yasuda et al., 1975). There are now a number of standard EAE mouse models in use including PLP139-151 peptide-induced relapsing EAE in SJL mice, MBP-induced disease in PL/J mice, chronic progressive models of MOG protein or MOG_{35-55} peptide-induced disease in C57BL/6 mice, or MOG that induces a relapsing-remitting disease in Biozzi ABH mice (Gold et al., 2006). Each model reflects certain aspects of the pathology seen in MS such as demyelination associated with axonal degeneration (Zamvil et al., 1985), but the pathology and clinical course of EAE in the mouse is determined by both genetic and immunogen/adjuvant factors used to induce disease. It is important to note that in the literature no one model of EAE is used as standard, thus making comparisons across studies difficult.

Despite the successful development of a reproducible EAE model it has been argued that EAE does not have the ability to point towards a meaningful therapy or therapeutic approach to MS (Steinman and Zamvil, 2006). It has also received criticism for the large number of potential therapies that have showed promise in the model but failed to demonstrate clinical efficacy in MS (Sriram and Steiner, 2005).

However EAE is the best characterised animal model of human autoimmune disease and it has played a valuable role in identifying and characterising aspects of immune surveillance, inflammation and immune-mediated tissue injury (Baxter, 2007).

1.12.3. EAE and the immune system

The immunological basis of acute disease activity in MS has only recently been well documented by studies in EAE and MS (Niino et al., 2001b). In the following section I attempt to review the different cell types that are involved in disease progression.

1.12.3.1. T cells

It is well established that $CD4^+$ T helper (Th) type cells play an important role in the initiation of lesion formation. Th1 cells are characterised by the production of TNFα and IFNγ (McFarland and Martin, 2007). Elevated levels of both cytokines have been found in the CNS of EAE models and it was thought that Th1 cells production of these cytokines was primarily responsible for disease (Beck et al., 1988; Martin and Near, 1995). Recent evidence now points towards a T cell that produces IL-17 as important in driving inflammation and disease progression in EAE (McKenzie et al., 2006). IL-17 is an inflammatory cytokine associated with inflammation in rheumatoid arthritis (Koenders et al., 2006), lupus (Pernis, 2009) and allograft rejection (Atalar et al., 2009). Th17 cells ($CD4^+$ Th17 cells) as they are called, represent a lineage distinct from Th1 and Th2 phenotypes (McFarland and Martin, 2007; McKenzie et al., 2006); polarization of Th17 cells requires the cytokine IL-23 (Brok et al., 2002), IL-6 and TGF-β (Veldhoen et al., 2006).

1.12.3.2. Dendritic cells

Although much of the focus of research is on T cell responses in EAE, the role of dendritic cells in influencing the outcome of the response is becoming better

understood (McFarland and Martin, 2007). EAE is induced by priming of the activation, and population expansion, of the $CD4^+$ T cells in response to CNS myelin antigens normally sequestered in the brain. Re-presentation of myelin epitopes (MBP, MOG or PLP) by APCs is required for the initiation of the disease. Studies have shown that dendritic cells alone, acting as APCs, are sufficient to initiate EAE (Bailey et al., 2007).

1.12.4. EAE and Glial cells

The initial immunopathological event of EAE and MS starts when auto-reactive T cells in the systemic immune compartment are activated and cross the blood brain barrier (Magnus and Rao, 2005). This leads to their reactivation and rapid expansion which in turn stimulates microglia and astrocytes to increase their activities which results in increased demyelination and axonal degeneration. The presence of activated microglia and astrocytes has been demonstated in the brain and spinal cord in MS and EAE (Aharoni et al., 2005; Brown and Sawchenko, 2007; Liedtke et al., 1998).

Microglia are active participants in myelin breakdown, their phagocytosis of myelin proteins in the lesions is a reliable indicator of ongoing demyelinating activity. Activated microglia in MS have been shown to express molecules critical for antigen presentation such as MHC II (Bauer et al., 1994) and another immunologically relevant antigen expressed by microglia in the MS brain is CD40 (Alderson et al., 1993). CD40 interaction with CD40L on T cells is proposed to play a role in further activation of monocytic cells and important in the initiation of the disease (Alderson et al., 1993). Evidence exists that astrocytes, like microglia, express MHC class II molecules in active MS lesions (Lee et al., 1990; Zeinstra et al., 2003) and they have the required co-stimulatory molecules, B7-1 and B7-2 that enables them to act as antigen-presenting cells to T cells (Zeinstra et al., 2003). Astrocyte gliosis is also a common feature of MS, which is characterised by increased astrocyte proliferation, hypertrophy and increased synthesis of GFAP (Holley et al., 2003).

Both activated microglia and astrocytes produce pro-inflammatory cytokines and chemokines that contribute to the disease progression, inflammation and the resultant motor and cognitive impairment in MS /EAE (Benveniste, 1997). Cytokine production by both cell types has the potential to enhance inflammation in the brain and spinal cord with high levels of IL-1β, TNFα and IL-6 found in association with active MS lesions (Cannella and Raine, 1995; Samoilova et al., 1998). Elevated levels of IL-1β have been recorded in the CSF of patients with MS (Hauser et al., 1990). The presence of increased IL-1β has been shown to be important in the breakdown of the BBB (Bush et al., 1999) associated with the reactive astrogliosis that occurs simultaneously (Brosnan et al., 1995; Herx and Yong, 2001). Both IL-1β and TNFα have been shown to be of vital importance in the onset and development of the early stages of EAE (Bauer et al., 1994; Murphy et al., 2002). TNFα production by microglia along with NO, has been documented to contribute to the demyelination process in the CNS (Selmaj et al., 1991). It has been documented in the literature that IL-6 is elevated in the CSF of MS patients and increased levels in the brain in EAE where it promotes chemokine expression and upregulation of adhesion molecule expression (Navikas et al., 1996).

Activated microglia and astrocytes produce and release chemokines and chemotactic cytokines that selectively recruit specific subsets of leukocytes into the CNS. INFγ and MCP-1 which are released by astrocytes attract leukocytes and myelin degrading macrophages into the brain (Ghirnikar et al., 1998). Upregulation of the expression of MIP-1 and MIP2 was shown *in vitro* and *in vivo* on astrocytes in a model of EAE which the authors suggest was responsible for increased movement of monocytic cell into the CNS (Kennedy and Karpus, 1999; Simpson et al., 1998; Sorensen et al., 1999).

1.12.5. Hippocampus and MS/EAE

The hippocampus has been identified as a key brain area for memory formation and cognition (see section 1.1.1.). Loss of cognitive function is described as one of the earliest manifestations of MS (Peyser et al., 1990; Rao et al., 1991a).

Studies indicate that 50-70% of individuals suffering from MS experience cognitive dysfunction and, in particular, difficulties in learning and remembering new information (Thornton et al., 2002). Differences in cognitive deficits do differ in the disease subtypes; for example verbal memory deficits are observed in PPMS and visuospatial memory deficits are observed in RRMS (Sicotte et al., 2008).

Despite the knowledge of cognitive deficits occurring in MS, little research has been undertaken to address hippocampal changes which accompany EAE. However the presence of demyelinating lesions in pathological specimens obtained from the hippocampus of MS patients has been reported (Geurts et al., 2007; Vercellino et al., 2005) and signal abnormalities have been detected in areas of the hippocampus using MRI (Roosendaal et al., 2008). There is also evidence of progressive and selective hippocampal atrophy in CA1 region which is associated with deficits in memory encoding and retrieval (Sicotte et al., 2008). In a model of EAE, very recent evidence shows a decrease in the activity of the enzyme choline acetyl transferase (ChAT) in the hippocampus after induction of EAE (Sajad et al., 2009). The decrease in ChAT is associated with cholinergic neuronal degeneration, and the results show a strong role for NO involvement in this process. The authors note that further research needs to be carried out to assess the degenerating mechanism involved in hippocampal cognitive decline in MS/EAE (Sajad et al., 2009).

1.13. Modulation of EAE

The first drug treatment successfully identified in EAE was glatiramer acetate. Glatiramer acetate under the trade name Copaxone, was approved in 1996 for the treatment of relapsing remitting MS. Studies have shown that this random copolymer, named Copolymer 1, composed of glutamate, tyrosine, alanine and lysine, was able to suppress the induction of EAE (Teitlebaum et al., 1971). A number of mechanisms of action of glatiramer acetate relating to its ability to suppress EAE have been proposed. Studies have shown that glatiramer acetate antigen specifically modulates the immune response to MBP (Sela, 1999) and this leads to a shift in the balance of

cytokines from Th1 cytokines to those associated with the Th2 response (Duda et al., 2000). Others have shown that glatiramer acetate has the ability to bind to MHC II molecules (Fridkis-Hareli et al., 1997), allowing it interfere with antigen presentation to T cells (Ruiz et al., 2001).

Researchers have attempted to target the infiltration of T cells into the EAE brain in an attempt to control disease progression. In the 1990's experiments were carried out to find the molecule involved for T cell adhesion in the inflamed brains of EAE mice (Yednock et al., 1992). More than 20 monoclonal antibodies to the adhesion molecules available at the time were used but only antibodies binding α4 or β1 integrin molecules inhibited adhesion of lymphocytes to blood vessels in the brain (Yednock et al., 1992). Further progress was made when it was observed that the antibody α4β1 integrin inhibited the development of paralysis in EAE (Yednock et al., 1992). This antibody for α4β1 integrin was modified and improved, and it is now used in the treatment of MS under the trademark Natalizumab.

With the realisation of the importance of pro-inflammatory cytokines and chemokines in disease progression, the focus has also shifted to ways of attenuating pro-inflammatory cytokines in the CNS in disease. Microglial and astrocyte production of cytokines and chemokines contributes to the recruitment of leukocytes from the periphery as well as the migration of microglia to the site of inflammation (Babcock et al., 2003). Consequently treatments that control the activation of microglia and astrocytes may be effective at diminishing disease severity. There has been a recent increase in investigations into the use of PPARγ agonists in EAE.

The effects of PPARγ agonists in modulating EAE were first investigated by Niino and colleagues (2001) who demonstrated that administration of troglitazone inhibited the development of EAE in C57BL/6 mice. Interestingly treatment with troglitazone was more effective in the effector phase of the EAE model than in the induction phase. Their results also suggest that the amelioration in EAE was not due to any alterations in T cell proliferation, but that it attributed to the attenuation of pro-inflammatory cytokine gene expression (Niino et al., 2001b).

Investigations have also been carried out to assess the potential therapeutic effects of pioglitazone, rosiglitazone and ciglitazone in EAE. It has been demonstrated that oral administration of pioglitazone reduces the incidence, clinical severity and associated inflammation and demyelination that occurs with EAE (Feinstein et al., 2002). Further data support the idea that pioglitazone suppresses the priming activation and proliferation of T cells suggesting a possible mechanism for pioglitazone action in EAE (Feinstein et al., 2002). In a parallel experiment it was shown that rosiglitazone reduced the maximal clinical score when orally administered in EAE but did not alter maximal disease incidence (Feinstein et al., 2002). Treatment with ciglitazone or $15dPGJ_2$ decreased the duration and clinical severity of disease progression and this decrease in disease severity was accompanied by a decrease in IL-12 production (Natarajan and Bright, 2002), and further *in vitro* investigation led the authors to conclude that these PPARγ agonists regulate EAE by inhibiting IL-12 production, IL-12 signalling via JAK STAT pathway and Th1 differentiation (Natarajan and Bright, 2002).

It is evident from the data that PPARγ agonists do have a role to play in ameliorating disease pathogenesis although different PPARγ agonists may vary in the distinct mechanisms of action. These findings suggest that the anti-inflammatory and anti-proliferative properties of oral PPARγ agonists could provide therapeutic benefits in the treatment of MS.

1.14. CD200 and EAE/MS

CD200 is a type 1 membrane glycoprotein as described in detail in a previous section. In the context of neurodegenerative disease it is the interaction of CD200 which is expressed on neurons and its receptor CD200R expressed on cells of the myeloid lineage that is of interest. It has been shown that CD200-CD200R interaction in inflammatory disease models exerts an inhibitory signal to the myeloid cells thus protecting the CNS from inflammatory damage by T cell induced myeloid cell activation (Banerjee and Dick, 2004; Copland et al., 2007).

In the context of EAE and MS, the importance of CD200 receptor-ligand interaction is evidenced in studies that assessed EAE disease progression and microglial activation in $CD200^{-/-}$ mice compared with controls. MOG-induced EAE onset was 3 days earlier in mice deficient in CD200 and microglial activation throughout the CNS was increased in $CD200^{-/-}$ mice, indicating that CD200 can modulate the disease processes to which microglia contribute (Hoek et al., 2000). *Wld*s mice are spontaneously-occurring mutants with a phenotype of protection against several forms of axonal injury, including CNS nerve transection (Perry et al., 1991), vincristine-induced neuropathy (Wang et al., 2001) and axonal transection (Steward and Trimmer, 1997). *Wld*s mice develop a delayed onset and exhibit an attenuated disease progression in EAE (Kaneko et al., 2006). Additional studies show that this was mediated by selective elevation of CD200 on CNS neurons which, in turn, resulted in diminished accumulation of macrophages and microglia in the CNS, and reduced expression of pro-inflammatory cytokines (Chitnis et al., 2007). Further evidence indicates that antibody-mediated blockade of CD200R leads to aggravated clinical course and outcome of EAE in rats and *in vitro* blockade of CD200R results in enhanced IFNγ induced release of IL-6 and neuronal cell death in macrophage neuronal co-cultures (Meuth et al., 2008a). Therefore upregulation of CD200 expression in the CNS may be a relevant neuroprotective strategy in neuroinflammatory diseases such as MS.

1.15. Aims and Objectives

Microglial activation is associated with an increase in pro-inflammatory cytokines such as IL-1β, TNFα and IL-6 that contribute to the inflammatory process. Both microglial activation and the release of pro-inflammatory cytokines have been shown in the literature to play an important role in the neurodegeneration associated with aging, and also in diseases such as MS and AD. The overall aim of this thesis is to understand the mechanism by which microglial activation can be modulated as this is believed to play an important role in the pathogenesis of neurodegenerative diseases.

Recent evidence suggests that a class of drugs termed PPARγ agonists, currently on the market for type two diabetes have anti-inflammatory properties and have the ability to downregulate pro-inflammatory cytokines. This thesis focuses on the role of rosiglitazone, a PPARγ agonist, as an anti-inflammatory agent, and analysis is carried out to investigate its effects on glial cells *in vitro*. The use of LPS as a model of neuroinflammation *in vitro* has contributed significantly to the understanding of the inflammatory process in the brain. In this thesis the ability of rosiglitazone to modulate LPS-induced increases in inflammatory mediators is assessed on different glial cells types. Evidence has also shown that rosiglitazone treatment reverses the age-related decrease in the anti-inflammatory cytokine IL-4, highlighting a link between it and IL-4. The potential of IL-4 as a mediator of the anti-inflammatory mechanism of rosiglitazone is also investigated.

It has been reported in the literature that some PPARγ agonists have negative side effects. Reports have indicated that despite the ability of rosiglitazone to modulate inflammation and its success in type two diabetes, it has been suggested that the administration of rosiglitazone is associated with an increased risk of myocardial infarction. Researchers are now developing novel PPARγ agonists that could provide similar beneficial effects without the negative side effects. As part of this thesis a novel PPARγ agonist MDG79 is assessed for its ability to modulate LPS-induced changes in pro-inflammatory cytokines and markers of microglial activation in mixed glial cultures. It is also investigated whether or not the modulatory role of MDG79 on LPS-induced changes in mixed glia is PPARγ-dependent.

LPS administration serves as potent stimulator of the immune response and microglial activation, but also both MS and its animal model EAE are inflammatory diseases associated with activated glial cells. An aim of this thesis is to monitor pro-inflammatory cytokine production in EAE both prior to and after the onset of clinical symptoms in the spleen, spinal cord and hippocampus. Evidence in the literature suggests the importance of cell-cell interactions, in particular neuron-glia interactions, in the control of microglial activation, in particular CD200. The role of CD200 in EAE is assessed and a further aim of this study is to establish whether changes in CD200 are correlated with changes in microglial activation in this

condition. Previous research has shown a relationship between IL-4 and CD200, and the role of IL-4 in EAE disease progression is also investigated here through the use of IL-4$^{-/-}$ mice.

Interventions targeting the activated glia may prove to be beneficial in the modulation of disease progression such as in EAE and MS. Current drugs on the market for the treatment of MS focus on modulating the immune response. The final aim of this study is to examine the ability of rosiglitazone to modulate EAE disease progression and the subsequent microglial activation and inflammation, in the CNS associated with the disease.

Chapter 2

Methods

2.1. *In vitro* experiments

2.1.1. Preparation of primary rat and mouse cortical mixed glia

Primary cortical glial cells were prepared from 1-day old Wistar rats, C57 mice and IL-$4^{-/-}$ mice (BioResources Unit, Trinity College, Dublin, Ireland). The following procedures were carried out in a laminar flow hood (Advanced Biosafety Cabinet Class II; AGB Scientific Ltd., Ireland). The rats were decapitated, the cerebral cortices were dissected and the meninges were removed. Tissue was bi-directionally chopped using a sterile scalpel (Schwann-Mann, UK). Tissue was placed in 15ml falcon tubes (Sarstedt, Ireland) containing warm filter-sterilized DMEM (2ml; GIBCO, UK) supplemented with 10% heat inactivated foetal calf serum (FCS) (Sigma, UK), streptomycin (100U/ml; GIBCO, UK) and penicillin (100U/ml; GIBCO, UK). The tissue was incubated for 20min (37°C; 5% CO_2:95% air; Nuaire Flow CO_2 incubator; Jencons, UK). Tissue was then triturated using a sterile plastic Pasteur pipette (Sarstedt, Ireland), the suspension was filtered through a sterile mesh filter (40µm; Becton Dickinson Labware, France), centrifuged at 2000 x g for 3min at 20°C (Sorvall Legend RT, US) and the pellet resuspended in warmed DMEM.

Cell counts were calculated by diluting cells (1:10) in trypan blue (Sigma, UK). A 10µl volume of the cell suspension was loaded onto a disposable haemocytometer (Hycor Biomedical, UK). Viable cells (i.e. those which did not stain and appear light under a light microscope) were counted.

Resuspended cells (250µl/well) were pipetted onto poly-L-lysine-coated (60µg/ml) coverslips in 24 well plates at a density of 1.0 x 10^6 cells and incubated for 2h before addition of warmed DMEM (400µl). Cells were grown at 37°C in a humidified 5% CO_2:95% air environment and media was changed every 3 days for 12-14 days until cells reached greater than 70% confluence. Mixed glia were treated as outlined in culture treatment protocols.

2.1.2. Preparation of rat cortical microglia and astrocytes

Microglia and astrocyte cultures were prepared from 1-day old Wistar rats (BioResources Unit, Trinity College, Dublin, Ireland) in a laminar flow hood (Advanced Biosafety Cabinet Class II; AGB Scientific Ltd., Ireland). The rats were decapitated, the cerebral cortices were dissected and the meninges were removed. Tissue was bi-directionally chopped using a sterile scalpel (Schwann-Mann, UK). Tissue was placed in 15ml falcon tubes, one brain per falcon tube, (Sarstedt, Ireland) containing warm filter-sterilized DMEM (2ml; GIBCO, UK) supplemented with 10% heat inactivated FCS (Sigma, UK), streptomycin (100U/ml; GIBCO, UK) and penicillin (100U/ml; GIBCO, UK). The tissue was incubated for 20min (37°C; 5% CO_2:95% air; Nuaire Flow CO_2 incubator; Jencons, UK). Tissue was triturated; the suspension was filtered through a sterile mesh filter (40μm; Becton Dickinson Labware, France), centrifuged at 2000 x g for 3min at 20°C (Sorvall, Legend RT) and the pellet resuspended in warmed DMEM (2ml).

The contents of each falcon tube were added to separate, labeled T25 flasks (Sarstedt, Ireland) using a plastic Pasteur pipette and incubated for 2h before addition of complete DMEM to each flask (8ml). Cells were grown at 37°C in a humidified 5% CO_2:95% air environment (Nuaire Flow CO_2 incubator; Jencons, UK) and media was changed at day 1 and day 7. The media at both these time points was supplemented with M-CSF (20ng/ml; stock of 50μg/ml diluted 1/2500 in DMEM). At day 12 the flasks were removed from the incubator and photographs were taken using the light microscope (Olympus 1X51, Olympus Ltd, UK). Parafilm (Alcan, USA) was wrapped around the neck and cap of each flask and they were placed on an orbital shaker (Bibby, Stuart Scientific, UK) at room temperature at 110rpm for 2h. The flasks were returned to the sterile flow hood and each one tapped on the side 30 times. The contents of the flasks were poured into one falcon tube, giving a total volume of approximately 50ml. This falcon tube was spun at 2,000 rpm for 5min at 20°C. The resulting pellet is a microglial cell pellet. The supernatant was removed and the pellet resuspended in 1ml DMEM. A cell count was performed by diluting cells (1:10) in trypan blue (Sigma, UK). A 10μl volume of the cell suspension was then loaded onto a disposable haemocytometer (Hycor Biomedical, UK). Viable

cells, which did not stain and appear light under a light microscope, were counted. Resuspended microglial cells were pipetted onto poly-L-lysine-coated (60μg/ml) coverslips in 24 well plates at a density of 5.0 x 10^4 cells/ml and incubated for 2h before addition of warmed DMEM. Microglial cells were treated 24h later as outlined in the treatment protocols.

The astrocytes, i.e. the adherent cells, were harvested by incubating in the presence of 1ml Trypsin-EDTA (Sigma, UK) for 15min at 37°C and centrifuging at 2,000 rpm for 5min at 20°C to provide the astrocyte pellet. The supernatant was removed and the pellet resuspended in 1ml DMEM. A cell count was performed by diluting cells (1:10) in trypan blue (Sigma,UK). A 10μl volume of the cell suspension was loaded onto a disposable haemocytometer (Hycor Biomedical, UK). Viable cells were counted. Resuspended astrocytes were pipetted onto poly-L-lysine-coated (60μg/ml) coverslips in 24 well plates at a density of 5.0 x 10^4 cells per ml and incubated for 1h before addition of warmed DMEM. Astrocytes were treated 24h later as outlined in the treatment protocols.

2.1.3. Culture Treatment Protocols

All compounds used for treating cells were diluted to the required concentration in the appropriate pre-warmed supplemented media and all solutions were filtered through a syringe with a cellulose acetate membrane filter (0.2μM Supor membrane; Acridisc syringe filters; Pall Corporation, UK).

LPS from Escherichia coli (Alexis, Switzerland) was diluted to a final concentration of 1μg/ml in media (DMEM, GIBCO, UK). Cells were treated with LPS for 24h. Rosiglitazone (Alexis, Switzerland) was prepared as a stock solution (50μM in dimethyl sulfoxide; DMSO) and diluted to its final concentration (20μM) in DMEM (GIBCO, UK). Cells were pretreated with rosiglitazone for 24h prior to LPS treatment. Recombinant IL-4 (R&D Systems, UK) was prepared as a stock solution in sterile PBS (Sigma, UK) and diluted to a final concentration (20ng/ml) in DMEM (GIBCO, UK). Cells were pretreated for 24h with IL-4 prior to LPS treatment. MDG79 (supplied by the Molecular Design Group, Trinity College

Dublin) was prepared as a stock solution in DMSO and diluted to a final concentration (10-100μM) in DMEM (GIBCO, UK). GW9662 was prepared as a stock solution in DMSO and diluted to its final concentration (20μM) in DMEM (GIBCO, UK).

2.1.4. Cell harvest

Following treatments, supernatants were removed using a sterile Pasteur pipette and aliquoted into fresh tubes and stored at -80°C until required for analysis. Cells were harvested for PCR by washing once in ice-cold PBS and adding 60μl cell lysis mastermix to each coverslip (Nucleospin RNA II, Macherey-Nagel, Ireland). Samples were stored at -80°C prior to RNA extraction.

2.2. *In vivo* experiments

2.2.1. Animals

Specific pathogen-free C57BL/6 mice were purchased from Harland UK Ltd., Bicester, Olac, UK, and IL-$4^{-/-}$ mice were provided from the breeding colony held in the Bioresources Unit, Trinity College Dublin. All animals were maintained according to the local regulations and guidelines, and under licence from Department of Health and Children, Ireland with the approval of the local Ethics Committee. All mice used were female, young animals were between 8-10 weeks old at the start of the experiments.

2.2.2. Induction of EAE in C57BL/6 mice using MOG_{35-55}

To induce EAE, 8-10 week C57BL/6 mice were injected subcutaneously (s.c.) with 150μg MOG_{35-55} peptide (Cambridge Biosciences, UK) in Complete Freund's Adjuvant (CFA; DIFCO, UK) supplemented with 5mg/ml H37RA (*Mycobacteria tuberculosis*, DIFCO, UK). The animals were also injected intraperitoneally (i.p.) with 500ng Pertussis Toxin (PT) (Kakasukin, Japan) on day 0 and day 2 post

immunisation. EAE was scored according to a 0-5 scale as follows: limp tail, 1; wobbly gait, 2; hind limb weakness, 3; hind limb paralysis, 4; tetra paralysis, 5. Body weight was monitored throughout the duration of the study. Mice were killed by cervical dislocation 21 days* post immunisation; spinal cord, spleen and hippocampus were removed and snap frozen in liquid nitrogen for mRNA analysis or stored in Krebs solution containing calcium at -80°C for protein analysis. *In the EAE timecourse study mice were killed 0.5, 3, 5, 7 and 10 days after immunisation also.

2.2.3. Induction of EAE in IL-4$^{-/-}$ mice using MOG$_{35-55}$

The induction of EAE was as in 2.2.2, mice were female and 8-10 week old at the beginning of the experiment.

2.2.4. Oral administration of rosiglitazone

Prior to inducing EAE, mice were divided randomly into two groups, one group was fed on a diet of normal laboratory mouse chow and the second group mouse chow supplemented with rosiglitazone at a dose of 6mg/kg/day for three weeks prior to inducing EAE. Oral administration of rosiglitazone was continued throughout the disease progression.

2.2.5. Preparation of tissue for analysis

Tissue was washed three times in Krebs solution containing calcium. It was subsequently homogenised in 1ml Krebs solution containing calcium. Tissue homogenate was spun at 2000 x g for 3min and the pellet removed. Supernatant was used for protein determination and analysis.

2.2.6. Protein assay

Protein concentration of tissue isolated from mice was determined using a BCA assay kit (Pierce, US). Reagent 1 (25ml) was mixed with 500µl reagent 2 to form a working solution. A standard curve was prepared using a range of concentrations of BSA in the same buffer as the samples to be tested. Triplicate samples, standards and blanks (25µl) and working solution (200µl) were added to designated wells of a 96 well plate. The plate was incubated at 37°C for 30min to develop the colour, after which the absorbance was read at 562nm.

2.2.7. Cell Viability assay

The viability of the mixed glial cells in response to each of the treatments was determined using a MTS assay (Promega, US). MTS solution was added to the supernatant in the wells for each treatment group of a 24-well plate at a 1:5 dilution (50µl MTS per 250µl of DMEM). The cell culture plate was then placed in the incubator at 37°C for 2-4h. The plate was removed from the incubator and 100µl of the MTS/DMEM was removed from each well and plated onto a 96 well plate and the absorbance was read at 490nm. To correct for the background, absorbance reading of DMEM and MTS alone without any cells was subtracted from the absorbance reading for each treatment group.

2.3. Preparation of RNA

2.3.1. RNA isolation

Cells from *in vitro* studies which were stored in cell lysis mastermix (Nucleospin RNA II, Macherey-Nagel, Ireland) and tissue from *in vivo* studies was homogenised in 350µl of cell lysis mastermix (Nucleospin RNA II, Macherey-Nagel, Ireland) for extraction of RNA. Lysate was filtered using NucleoSpin Filter, collected in an Eppendorf tube and centrifuged (11,000 x g, 1min). Ethanol (70%, 350µl) was added to the filtrate, mixed and loaded onto NucleoSpin RNA II columns. Tubes

were centrifuged (8,000 x g, 30s) and the RNA binds to the column. The silica membrane was desalted by adding membrane desalting buffer (350µl) and centrifuged (11,000 x g, 1min) to dry the membrane. To digest the DNA, DNase reaction mixture (95µl) was added to the column and incubated at room temperature for 15min. The silica membrane was washed and dried. RNA was eluted by adding RNase free H_20 and centrifuged (11,000 x g, 1min) and RNA concentration was quantified.

2.4. Reverse Transcription for cDNA synthesis

2.4.1. cDNA synthesis

Total mRNA (1µg) was reverse transcribed into cDNA using high-capacity cDNA archive kit (Applied Biosystems, Darmstadt, Germany) according to the protocol provided by the manufacturer. Briefly, RNA (3µg) was added to fresh tubes containing the appropriate volume of nuclease-free H_20 to make a 25µl volume. A 2x mastermix was prepared containing the appropriate volumes of 10x RT buffer, 25x dNTPs, 10x random primer multiscribe reverse transcriptase (50U/µl). The mastermix (25µl) was added to the RNA and nuclease free H_20. Tubes were incubated for 10min at 25°C followed by 2h at 37°C on a thermocycler (PTC-200, Peltier Thermal Cycler, MJ Research, Biosciences Ireland)

2.4.2. Real-time PCR

Real-time PCR primers and probes were delivered as "TaqMan® Gene Expression Assays" for the rat genes IL-1β, TNFα, IL-6, CD40 and CD11b, and for the mouse genes IL-1β, TNFα, IL-6, IL-4, CD40, CD11b and CD200 (Table 2; Applied Biosystems, Darmstadt, Germany). Real-time PCR was performed on Applied Biosystems ABI Prism 7300 Sequence Detection System v1.3.1 in 96-well format and 25µl reaction volume per well. cDNA samples (200pg/well) were mixed with Taqman Universal PCR Mastermix (Applied Biosystems, Darmstadt, Germany) and the respective target gene assay. Mouse and rat β-actin RNA (# 4352341E, Applied Biosystems, Darmstadt, Germany) were used as reference. Each sample was

measured in duplicate in a single RT-PCR run. Forty cycles were run with the following conditions: 2min at 50°C, 10min at 95°C and for each cycle 15s at 95 °C for denaturation and 1min at 60°C for transcription.

2.4.3. Real-time PCR analysis

The ΔΔCT method (Applied Biosystems RQ software, Applied Biosystems, UK) was used to assess gene expression for all real-time PCR analysis. This method is used to assess gene expression by comparing gene expression of treated/experimental samples to a normal or untreated sample (control), rather than quantifying the exact copy number of the target gene. In this manner the fold-difference (increase or decrease) can be assessed between treated and control samples. The fold-difference is assessed using the cycle number (CT) difference between samples. Briefly, a threshold for fluorescence is set, against which CT is measured. To accurately assess differences between gene expression the threshold is set when the PCR reaction is in the exponential phase, when the PCR reaction is assumed to be 100% efficient. Thus samples, with low CT readings demonstrate high fluorescence, indicating greater amplification and hence, greater gene expression. When a PCR is 100% efficient a one-cycle difference between samples means a 2-fold difference in copy number (2^2), similarly a 5-fold difference is a 32-fold difference (2^5).

To measure this fold difference relative to control, the CT of the endogenous control (β-actin) is subtracted from the CT of the target gene for each sample ($CT_{\text{target gene}} - CT_{\beta\text{-actin}}$), thus accounting for any difference in cDNA quantity that may exist. This normalised CT value is called the ΔCT ($CT_{\text{target gene}} - CT_{\beta\text{-actin}} = \Delta CT$).

The ΔCT is then normalised to a reference, by subtracting the ΔCT of the reference from the ΔCT of every experimental sample, this is the ΔΔCT value ($\Delta CT_{\text{sample}} - \Delta CT_{\text{reference}}$). In all experiments the ΔCT of a control sample (a biological sample from the control group in the experiment) was used as the reference. Thus subtracted from itself to give a ΔΔCT=0 ($\Delta CT_{\text{control}} - \Delta CT_{\text{control}} = 0$), and from every other sample to give each sample a ΔΔCT.

The ΔΔCT is then converted into a fold-difference. As one-cycle difference corresponds to a two-fold increase or decrease relative to control, 2 to the power of ΔΔCT gives the fold-difference in gene expression between the control and treated samples. The control sample always has a ΔΔCT value of 0, thus 2^0 gives 1, against which all other samples are referenced.

2.5. Analysis of cytokine expression by ELISA

The concentrations of IL-1β, IL-6, TNFα, and IL-4 were assessed by ELISA in either tissue homogenates or supernatants prepared from mice and rats.

2.5.1. Analysis of IL-1β, IL-6, IL-4 and TNFα concentration in mixed glia, isolated microglia and astrocyte supernatants, and tissue homogenate

The concentrations of IL-1β, IL-6, IL-4 and TNFα were assessed by ELISA (R&D Systems, UK) in supernatants from cultured mixed glial cells, isolated microglia, astrocytes and tissue homogenates. Elisa plates (NUNC, Thermo Fisher Scientific, Denmark) were coated with capture antibody (see Table 1). Elisa plates were covered with Parafilm (Alcan, USA) and incubated overnight at room temperature. The plates were washed three times with wash buffer (0.05% Tween-20 in PBS, pH 7.4), blocking buffer (0.5% BSA in PBS) was added and incubation continued for 1h at room temperature. Plates were washed three times with wash buffer and triplicate standards (see Table 1) or samples (100μl) were added to wells and incubated for 2h. The wells were washed three times and detection antibody (see Table 1) was added and incubation continued for 2h at room temperature. The wells were washed and incubated in horseradish peroxidase-conjugated streptavidin (1:200 dilution in PBS containing 1% BSA) for 20min at room temperature in the dark, washed again and substrate solution (R&D Systems, UK; 1:1 ratio) was added and incubated in the dark at room temperature for 30min. The reaction was stopped using 1M H_2SO_4 and absorbance was read at 450nm. IL-1β, IL-4, TNFα and IL-6

concentrations were measured in pg/ml for supernatant and pg/mg of protein for tissue homogenate.

2.6. SDS- Polyacrylamide gel electrophoresis

2.6.1. Preparation of samples

Hippocampal tissue from control and EAE mice was thawed rapidly, washed three times with Krebs solution containing calcium and homogenised in Krebs solution containing calcium. Protein concentration was assessed (as in 2.2.6.) and samples were equalised for protein concentration, diluted to equal protein concentration, and aliquots were added to a volume of sample buffer (NuPAGE LPS Sample Buffer, NuPage Reducing Agent and deoionized water) and heated to 70°C for 10min.

2.6.2. Gel Electrophoresis

Gel electrophoresis was carried out on precast 10-12% NuPage Novex Bis Tris Mini Gels (Invitrogen, UK) using the XCell SureLock Mini Cell (Invitrogen, UK). The outer chamber was filled with 1x SDS Running Buffer and the inner chamber filled with 1x SDS Running Buffer containing NuPAGE Antioxidant. Samples (10µl) were loaded into the wells and a pre-stained molecular weight standard was also loaded (5µl; Bio-Rad,USA). Proteins were separated by application of 200V constant for 50min (expected current of 100/125mA/ gel at start and 60-80mA/gel).

2.6.3. Western Transfer

The gel was removed from the gel apparatus and a piece of nitrocellulose transfer membrane moistened in transfer buffer (1x NuPAGE Transfer Buffer; 5% 20x NuPAGE Transfer Buffer, 10% methanol, 85% deionised water) was placed on top, air bubbles removed from the contact face and the membrane was cut to fit the

gel. Filter paper (Standard Grade No.3 Whatman, UK) was placed on top and beneath the nitrocellulose/gel forming a sandwich. Two blotting pads soaked in transfer buffer were placed in the cathode core of the XCell Blot II Blot Module and the sandwich on top, with the gel portion of the nitrocellulose/gel portion of the sandwich closest to the cathode. Three more fibre pads were placed on the sandwich so that the blotting pads rose 0.5cm over the rim of the cathode core. The anode core was gently pressed down on top of the pads and slid gently into the guide rails of the lower buffer chamber of the gel dock system. The gel tension wedge was inserted into the lower buffer chamber to lock the XCell Blot II module in position. The lower chamber was filled with 1x NuPAGE Transfer Buffer and the outer chamber filled with deionised water. Proteins were separated by application of a constant voltage of 30Vfor 1h.

2.6.4. Western Immunoblot analysis of CD200L

Non-specific binding was blocked by incubating nitrocellulose membranes for 1h in 5% bovine serum albumin (BSA) in TBS-T (20mM Tris-HCl, 150mM NaCl; pH 7.4 containing 0.05% Tween-20). Membranes were incubated in primary antibody (CD200; 1:500 in TBS-T containing 2% BSA; R&D Systems) at 4°C overnight. The membrane was washed (4 x 15min washes in TBS-T), incubated in secondary antibody anti-goat horseradish peroxidase (HRP; 1:1000 in TBS-T containing 5% BSA; Sigma, UK) for 1h at room temperature. Membranes were washed (4 x 10min) and protein complexes were visualised using ECL Plus Western Blotting Detection System (GE Health Care, UK).

2.6.5. Stripping and reprobing

Following development of blots, the nitrocellulose membranes were washed in TBS-T, placed in stripping solution ReBlot Plus Strong Solution (1:10 in ddH_20; Chemicon Int., UK) for 4min at room temperature, washed in TBS-T (5 x 1min washes) and blocked overnight in blocking buffer (5% Marvel in TBS-T).

Membranes were reprobed with primary β-actin antibody (1:10,000 in TBS-T containing 1% Marvel) for 2h. The membrane was washed (4 x 15min washes in TBS-T), incubated in secondary antibody anti-mouse HRP (1:1000 in TBS-T containing 5% BSA; Sigma, UK) for 1h at room temperature. Membranes were washed (4 x 10min) and protein complexes were visualised using ECL Plus Western Blotting Detection System (GE Health Care, UK).

2.7. Statistical Analysis

Statistical analysis was performed using the computer based statistical package GraphPad Prism. Data are expressed as mean ± standard error of the mean (SEM).

The data from Chapter 3 were analysed using a two-way ANOVA and if any significant changes were detected post hoc comparisons were performed using Newman Keuls test. In Chapter 4, where mixed glia were pretreated with MDG79, and MDG79 in combination with GW9662 (Figures 4.6-4.8), in the presence or absence of LPS the data were analysed by one way ANOVA and if any significant changes were detected post hoc comparisons were performed using Newman Keuls test. In Chapter 5 data were analysed using a 1-way ANOVA and if any significant changes were detected post hoc comparisons were performed using Newman Keuls test. In Chapter 6, data were analysed using a repeated measures 2-way ANOVA. Post hoc comparisons were performed using Newman Keuls test in the event of main effects of EAE and or rosiglitazone or strain.

Data were accepted as significant at the 95% confidence level ($p<0.05$)

Chapter 3

Assessment of the anti-inflammatory properties of rosiglitazone on glial cells

3.1. Introduction

Microglia and astrocytes are the principal glial cells of the brain and spinal cord, and are responsible for the production of the pro-inflammatory cytokines IL-1β, TNFα and IL-6. Microglia exist in the brain in a resting or ramified state and play an important role in immune surveillance and can be activated in response to immunological stimuli, infection or injury. Activated microglia undergo a conformational change, express a variety of cell surface markers such as, CD40 and CD11b, and produce a variety of pro- and anti-inflammatory cytokines that are characteristic of their activated state. Astrocytes form an important component of the blood brain barrier and they also, along with microglia, are involved in the innate immune response of the brain in the production of the pro-inflammatory cytokines. *In vitro*, LPS, a component of the cell wall of gram negative bacteria is used as a model of neuroinflammation. Previous evidence shows that LPS induces an increase in pro-inflammatory cytokines in cultures of mixed glia, microglia and astrocytes (Luna-Medina et al., 2005).

Inflammation is generally described as a beneficial response of an organism to infection, but when it is prolonged or inappropriate it can be detrimental (Simi et al., 2007b). This glial driven inflammation has been shown to contribute to the pathogenesis of aging, AD, MS and PD. As a result there is an increased focus on the ability to modulate or ameliorate this inflammation.

It was the ability of a class of drugs, the PPARγ agonists, to inhibit the expression of TNFα and TNFα-induced insulin resistance that suggested to researchers that these drugs might have anti-inflammatory properties. PPARγ is a nuclear receptor or an agonist activated nuclear transcription factor that regulates target gene transcription. The role of these drugs in the control of lipid metabolism is well established and they are used in the treatment of type II diabetes. Synthetic agonists of PPARγ are the class of drugs the thiazolidinediones or glitazones, of which there are three on the market; pioglitazone, ciglitazone and rosiglitazone. Previous studies have shown the ability of PPARγ agonists to attenuate LPS-induced increases in pro-inflammatory cytokines, and age and disease associated increases also (Giri et al., 2004; Loane et al., 2009; Storer et al., 2005). However there is still

debate over the mechanism by which this attenuation in microglial activation and cytokine release occurs.

Recent evidence from this lab has shown pretreatment of aged rats with rosiglitazone attenuated the age related increase in the pro-inflammatory cytokines IL-1β and IL-6. Rosiglitazone treatment also reversed the age related decrease in IL-4 (Loane et al., 2009). This highlights the importance of the maintenance of the inflammatory profile in the brain and the balance of pro- and anti-inflammatory cytokines.

The aim of this chapter was to assess the anti-inflammatory properties of the PPARγ agonist rosiglitazone to modulate the LPS-induced inflammation in mixed glial cells. A mixed glial cell culture preparation is composed of approximately 70% astrocytes and 30% microglia and as a result the ability of rosiglitazone to modulate inflammation in isolated microglia and astrocytes was further assessed. Previous evidence has shown that rosiglitazone treatment reverses the age related decrease in IL-4, highlighting a link between it and IL-4. Mixed glia were pretreated with IL-4 in an attempt to mimic the anti-inflammatory action of rosiglitazone. Also the ability of rosiglitazone to modulate inflammation was assessed in mixed glia cells from wild type and IL-4$^{-/-}$mice.

3.2. Methods

Mixed glial cells, isolated microglia and astrocytes were prepared from one day old Wistar rats, cultured for 10-14 days and treated with rosiglitazone (20μM) in the presence and absence of LPS (1μg/ml) (see section 2.1. for specific details). Mixed glial cells were also prepared from one day old Wistar rats, cultured as before for 10-14 days and treated with IL-4 (20ng/ml) in the presence and absence of LPS (1μg/ml). Finally mixed glia were also prepared from wildtype (C57BL/6) and IL-4$^{-/-}$ mice, cultured for 10-14 days and treated with rosiglitazone (20μM) in the presence and absence of LPS (1μg/ml). Analysis of supernatant cytokine concentrations were assessed by ELISA, cytokine and microglial marker mRNA expression by Q-PCR (see sections 2.3., 2.4. and 2.5. for specific details). Data are expressed as means ±

standard error of the mean. A 2-way ANOVA was performed to determine whether significant differences existed and if significance was detected post hoc comparisons were performed using Newman Keuls test. In Figure 3.13 a Students *t* test was performed to determine whether IL-4 was significantly increased following rosiglitazone treatment in astrocyte and microglia cultures (see section 2.7. for specific details).

3.3. Results

Anti-inflammatory effects of rosiglitazone in vitro.

It is known that glial cells are the primary source of pro-inflammatory cytokines IL-1β, TNFα and IL-6 in the CNS. The importance of anti-inflammatory cytokines such as IL-4 and IL-10 in modulating the production of these pro-inflammatory cytokines by glia has been recognised. Recent evidence has indicated that PPARγ agonists possess anti-inflammatory properties. The objective of the following experiments was to establish whether rosiglitazone might modulate the LPS-induced inflammatory changes in mixed glia, astrocytes and microglia.

Mixed glial cultures were pretreated with three different doses of rosiglitazone (5μM, 20μM or 100μM) in the presence or absence of LPS and the supernatants were assessed for IL-1β concentration. Figure 3.1 shows that there was a significant increase in mean IL-1β concentration in supernatant prepared from LPS-treated (1110 pg/ml ± 174.3; n=6) compared with control-treated, mixed glia (136.6 pg/ml ± 46.45; n=6; ***$p<0.001$; ANOVA). Pretreatment of mixed glia with rosiglitazone (5μM) did not attenuate the LPS-induced increase in supernatant concentration of IL-1β (921.22 pg/ml ± 209.9; n=6; ANOVA). However pretreatment of mixed glia with rosiglitazone (20μM and 100μM) significantly attenuated the LPS-induced increase in the supernatant concentration of IL-1β (436.4 pg/ml ± 110.4; 100.5 pg/ml ± 30.4; n=6; $^{\#\#}p<0.01$; ANOVA). In subsequent experiments 20μM concentration of rosiglitazone was used to evaluate its effect on LPS-induced changes. The effect of both treatments LPS (1μg/ml) and rosiglitazone (20μM) alone and in combination did

not significantly change the viability of mixed glia compared to controls (b; ANOVA; versus control).

Figure 3.2 shows that LPS induced a significant increase in mean IL-1β mRNA expression (a; 67.04 RQ ±14.4; n=6) and the supernatant concentration of IL-1β (b; 106.2 pg/ml ± 28.91; n=6) compared with control-treated mixed glia mRNA (a; 1.49 RQ ± 0.39; n=6; ***$p<0.001$) and protein (b; 7.40pg/ml ± 1.97; n=6; ***$p<0.001$). Pretreatment of mixed glia with rosiglitazone significantly attenuated the LPS-induced increase in IL-1β mRNA expression (a; 23.85 RQ ± 3.22; n=6; $^{\#\#}p<0.01$; ANOVA) and the supernatant concentration of IL-1β (b; 11.84 pg/ml ± 4.83; n=6; $^{\#}p<0.05$; ANOVA). IL-1β mRNA expression and supernatant concentration were similar in control-treated samples which were incubated in the presence and absence of rosiglitazone.

Figure 3.3 shows that LPS induced a significant increase in mean IL-6 mRNA expression (a; 15.78 RQ ± 2.98; n=6) and the supernatant concentration of IL-6 (b; 2934 pg/ml ± 784.1; n=6) compared with control-treated mixed glia mRNA (a; 1.41 RQ ± 0.14; n=6; ***$p<0.001$; ANOVA) and protein (b; 24.08pg/ml ± 16.19; n=6; **$p<0.01$; ANOVA). Pretreatment of mixed glia with rosiglitazone significantly attenuated the LPS-induced increase in IL-6 mRNA expression (a; 4.64 RQ ± 1.45; n=6; $^{\#\#}p<0.01$; ANOVA) but not supernatant concentration of IL-6 (b; 3304pg/ml ± 913.5; n=6; ANOVA). IL-6 mRNA expression and supernatant concentration of IL-6 were similar in control-treated samples which were incubated in the presence and absence of rosiglitazone.

Figure 3.4 shows that LPS induced a significant increase in mean TNFα mRNA expression (a; 12.27 RQ ± 2.30; n=6) and the supernatant concentration of TNFα (b; 441.6 pg/ml ± 111.7; n=6) compared with controls (a; 2.08 RQ ± 0.548; n=6; ***$p<0.001$; ANOVA) and (b; 111.7 pg/ml ± 14.18; n=6; **$p<0.01$; ANOVA). Pretreatment of mixed glia with rosiglitazone significantly attenuated the LPS-induced increase in TNFα mRNA expression (a; 5.51 RQ ± 1.83; n=6; $^{\#}p<0.05$; ANOVA) and but not supernatant concentration of TNFα (b; 402pg/ml ± 75.96; n=6; ANOVA). TNFα mRNA expression and protein concentration were similar in

control-treated samples which were incubated in the presence and absence of rosiglitazone.

Figure 3.5 shows that LPS induced a significant increase in mean CD40 mRNA expression (a; 6.95 RQ ± 1.18; n=6) and CD11b mRNA expression (b; 2.32 RQ ± 0.190; n=6) compared with controls (a; 1.18 RQ ± 0.284; n=6; ***$p<0.001$; ANOVA) and (b; 0.935 RQ ± 0.045; n=6; *$p<0.05$; ANOVA). Pretreatment of mixed glia with rosiglitazone significantly attenuated the LPS-induced increase in CD40 (a; 2.41 RQ ± 0.899; n=6; $^{\#\#}p<0.01$; ANOVA) and CD11b (b; 1.27 RQ ± 0.087; n=6; $^{\#\#\#}p<0.001$; ANOVA). CD40 mRNA mRNA expression was similar in control-treated samples which were incubated in the presence and absence of rosiglitazone, however CD11b mRNA expression does appear to be increased in the presence of rosiglitazone, although this did not reach statistical significance.

Mixed glial cultures contain about 70% astrocytes and 30% microglia and data obtained from mixed glia do not identify the cell responsible for the observed changes. Therefore cultured purified microglia and astrocytes were prepared and examined from LPS-induced changes and for the modulatory effect of rosiglitazone.

Figure 3.6 shows that LPS induced a significant increase in mean IL-1β mRNA expression (a; 279.8 RQ ± 26.55; n=6) and supernatant concentration of IL-1β (b; 62.78 pg/ml ± 12.46; n=6) compared with controls (a; 5.34 RQ ± 2.11; n=6; ***$p<0.001$; ANOVA) and (b; 2.93 pg/ml ± 0.42; n=6; **$p<0.01$; ANOVA). Pretreatment of microglia with rosiglitazone significantly attenuated the LPS-induced increase in IL-1β mRNA expression (a; 76.32 RQ ± 6.11; n=6; $^{\#\#\#}p<0.001$; ANOVA) but not supernatant concentration of IL-1β (b; 101.1 pg/ml ± 34.15; n=6; ANOVA). IL-1β mRNA and the supernatant concentration of IL-1β were similar in control-treated samples which were incubated in the presence and absence of rosiglitazone.

Figure 3.7 shows that LPS induced a significant increase in supernatant concentration of IL-6 (b; 595.7 pg/ml ± 27.13; n=6) but failed to induce an increase in IL-6 mRNA expression (a; 3.575 RQ ± 1.45; n=6) compared with controls (b; 290.2pg/ml ± 25.65; n=6; ***$p<0.001$; ANOVA) and mRNA (a; 2.575 RQ ± 1.02; n=6; ANOVA). Pretreatment of microglia with rosiglitazone significantly attenuated

the LPS-induced increase in the supernatant concentration of IL-6 (b; 464.9 pg/ml ± 33.58; n=6; $^{\#}p<0.05$; ANOVA) but not mRNA expression (a; 4.28 RQ ± 1.806; n=6; ANOVA). IL-6 mRNA expression and protein concentration were similar in control-treated samples which were incubated in the presence and absence of rosiglitazone.

Figure 3.8 shows that LPS induced a significant increase in mean TNFα mRNA expression (a; 31.25 RQ ± 3.05; n=6) and the supernatant concentration of TNFα (b; 598.9 pg/ml ± 20.19; n=6) compared with controls (a; 2.46 RQ ± 0.597; n=6; ***p<0.001; ANOVA) and (b; 112.8 pg/ml ± 16.59; n=6; ***p<0.001; ANOVA). Pretreatment of microglia with rosiglitazone significantly attenuated the LPS-induced increase in TNFα mRNA expression (a; 9.15 RQ ± 1.54; n=6; $^{\#\#\#}p<0.001$; ANOVA) and supernatant concentration of TNFα (b; 304.9 pg/ml ± 34.56; n=6; $^{\#\#\#}p<0.001$; ANOVA). TNFα mRNA expression and supernatant concentration of TNFα were similar in control-treated samples which were incubated in the presence and absence of rosiglitazone.

Figure 3.9 shows that LPS induced a significant increase in mean CD40 mRNA expression (a; 9.28 RQ ± 1.07; n=6) and CD11b mRNA expression (b; 3.70 RQ ± 0.47; n=6) compared with controls (a; 0.95 RQ ± 0.11; n=6; ***p<0.001; ANOVA) and (b; 0.68 RQ ± 0.01; n=6; ***p<0.001; ANOVA). Pretreatment of microglia with rosiglitazone significantly attenuated the LPS-induced increase in CD40 (a; 4.86 RQ ± 1.05; n=6; $^{\#}p<0.05$; ANOVA) and CD11b (b; 1.196 RQ ± 0.194; n=6; $^{\#\#}p<0.01$; ANOVA). CD40 and CD11b mRNA expression were similar in control-treated samples which were incubated in the presence and absence of rosiglitazone.

Similar experiments were conducted in astrocytes. Figure 3.10 shows that LPS induced a significant increase in mean IL-1β mRNA expression (a; 45.57 RQ ± 16.98; n=6) and supernatant concentration of IL-1β (b; 125.55 pg/ml ± 11.07; n=6) compared with controls (a; 0.74 RQ ± 0.09; n=6; *p<0.05; ANOVA) and (b; 1.24 pg/ml ± 0.59; n=6; ***p<0.001; ANOVA). Pretreatment of astrocytes with rosiglitazone did not significantly attenuate the LPS-induced increase in IL-1β mRNA expression (a; 30.91 RQ ± 17.22 n=6; ANOVA) but did significantly attenuate the LPS-induced increase in supernatant concentration of IL-1β (b; 44.44

pg/ml ± 2.32; n=6; $^{###}$p<0.001; ANOVA). IL-1β mRNA and supernatant concentration were similar in control-treated samples which were incubated in the presence and absence of rosiglitazone.

Figure 3.11 shows that LPS induced a significant increase in supernatant concentration of IL-6 (b; 4435 pg/ml ± 609.8; n=6) but failed to induce an increase in IL-6 mRNA expression (a; 13.65 RQ ± 8.57; n=6) compared with controls (b; 0.068 pg/ml ± 0.023; n=6;***p<0.001; ANOVA) and (a; 12.68 RQ ± 7.38; n=6; ANOVA). Pretreatment of astrocytes with rosiglitazone significantly attenuated the LPS-induced increase in supernatant concentration of IL-6 (b; 2141 pg/ml ± 177.8; n=6; $^{#}$p<0.05; ANOVA) but not mRNA expression (a; 13.14 RQ ± 7.361; n=6; ANOVA). IL-6 mRNA expression and supernatant concentration of IL-6 were similar in control-treated samples which were incubated in the presence and absence of rosiglitazone.

Figure 3.12 shows that LPS induced a significant increase in mean TNFα mRNA expression (a; 12.19 RQ ± 2.19; n=6) and supernatant concentration of TNFα (b; 587.3 pg/ml ± 50.82; n=6) compared with controls (a; 1.05 RQ ± 0.44; n=6; ***p<0.001; ANOVA) and (b; 1.03 pg/ml ± 0.07; n=6; ***p<0.001; ANOVA). Pretreatment of astrocytes with rosiglitazone did not significantly attenuate the LPS-induced increase in TNFα mRNA expression (a; 14.62 RQ ± 4.2; n=6; ns; ANOVA) but did significantly attenuate the LPS-induced increase in supernatant concentration of TNFα (b; 217.2 pg/ml ± 12.73; n=6; $^{###}$p<0.001; ANOVA). TNFα mRNA expression and protein concentration were similar in control-treated samples which were incubated in the presence and absence of rosiglitazone

Rosiglitazone induced a significant increase in IL-4 in mixed glial cells and astrocytes

Figure 3.13 shows that pretreatment of cortical mixed glial cells with rosiglitazone induced a significant increase in mean IL-4 protein concentration (a; 17.64 pg/ml ± 1.975; n=6) compared with control-treated mixed glia (a; 9.45 pg/ml ± 3.58; n=6; *p<0.05; Student's *t* test). Pretreatment of astrocytes with rosiglitazone induced a significant increase in IL-4 protein concentration (b; 10.02 pg/ml ± 1.63;

n=6) compared with control-treated astrocytes (b; 6.68 pg/ml ± 0.78; n=6; *p<0.05; Student's *t* test). In contrast similar treatment of microglia with rosiglitazone failed to increase the supernatant concentration of IL-4 (c; 9.46 pg/ml ± 2.07; n=6) compared with control-treated microglia (c; 7.53 pg/ml ± 1.30; n=6; Student's *t* test). LPS (1μg/ml) did not significantly affect IL-4 protein concentration (a; 10.39 pg/ml ± 0.89; n=6) compared with control-treated mixed glia (a; 9.45 pg/ml ± 3.58; n=6; ns; Student's *t* test).

To further investigate the role of IL-4 in mediating rosiglitazone-induced changes, its effect on LPS-induced IL-1β production was investigated in mixed glia prepared from IL-$4^{-/-}$ and wild type, mice. Figure 3.14 shows that there was a significant increase in IL-1β concentration in supernatant prepared from LPS-treated mixed glia obtained from wildtype mice (23.75 pg/ml ± 1.99; n=6) compared with control-treated mixed glia (2.97 pg/ml ± 0.72; n=6; ***p<0.001; ANOVA) Pretreatment of mixed glia, obtained from wildtype mice, with rosiglitazone significantly attenuated the LPS-induced increase in supernatant concentration of IL-1β (16.09 pg/ml ± 1.5; n=6; $^{\#\#}$p<0.01, ANOVA). There was no significant change in IL-1β concentration in supernatant of mixed glia pretreated with rosiglitazone. Although LPS also induced a significant increase in IL-1β in cells prepared from IL-$4^{-/-}$ mice (27.38 pg/ml ± 2.9 versus 3.3 pg/ml ± 1.99; n=6;***p<0.001; ANOVA), rosiglitazone did not attenuate the LPS-induced change (26.00 pg/ml ± 3.91; n=6; ANOVA).

Anti-inflammatory effects of IL-4 in vitro

If the effect of rosiglitazone is dependent on IL-4 as suggested by the data presented, it must be predicted that treatment of mixed glia with IL-4 will mimic the effect of rosiglitazone and therefore its effect on LPS-induced changes was assessed. Pretreatment of mixed with IL-4 instead of rosiglitazone did mimic rosiglitazone. The results are described below in more detail but in summary pretreatment with IL-4 mimicked rosiglitazone treatment by attenuating the LPS-induced increase in IL-1β

protein and failing to attenuate the LPS-induced increase in IL-6 and TNFα in mixed glia.

Figure 3.15 shows as that LPS induced a significant increase in mean IL-1β (a; 31.76 RQ ± 3.40; n=6) mRNA expression compared to control (a; 0.74 RQ ± 0.09; n=6; *p<0.05). LPS induced a significant increase IL-1β protein concentration (b; 855.8 pg/ml ± 85.30; n=6) compared with control-treated mixed glia (b; 0.056 pg/ml ± 0.021; n=6; ***p<0.001; ANOVA). Pretreatment of mixed glia with IL-4 (20 ng/ml) significantly attenuated the LPS-induced increase in IL-1β protein concentration (b; 636.9 pg/ml ± 66.52; n=6; $^{\#}$p<0.05; ANOVA) but failed to attenuate IL-1β mRNA expression (a; 39.77 RQ ± 2.34; n=6; ANOVA).

Figure 3.16 shows that LPS induced a significant increase in mean IL-6 mRNA expression (a; 6.88 RQ ± 2.16; n=6) and IL-6 protein concentration (b; 6404 pg/ml ± 299.2; n=6) compared with control-treated mixed glia mRNA (a; 3.99 RQ ± 1.6; n=6; *p<0.05; ANOVA) and protein (b; 7.57 pg/ml ± 7.6; n=6; ***p<0.001; ANOVA). Pretreatment of mixed glia with IL-4 did not attenuate the LPS-induced increase in IL-6 mRNA expression (a; 9.76 RQ ± 2.67; n=6; ANOVA) and IL-6 protein concentration (b; 7476 pg/ml ± 524; n=6; ANOVA). IL-6 mRNA expression and protein concentration was similar in control-treated samples which were incubated in the presence and absence of IL-4.

Figure 3.17 shows that LPS induced a significant increase in mean TNFα mRNA expression (a; 14.28 RQ ± 4.45; n=6) and TNFα protein concentration (b; 2979 pg/ml ± 316.4; n=6) compared with control-treated mixed glia mRNA (a; 1.12 RQ ± 0.31; n=6; *p<0.05; ANOVA) and protein (b; 0.87 pg/ml ± 0.26; n=6; ***p<0.001; ANOVA). Pretreatment of mixed glia with IL-4 did not attenuate the LPS-induced increase in TNFα mRNA expression (a; 17.28 RQ ± 8.58; n=6; ANOVA) and TNFα protein concentration (b; 2833 pg/ml ± 244.8; n=6; ANOVA). TNFα mRNA expression and protein concentration was similar in control-treated samples which were incubated in the presence and absence of IL-4.

Figure 3.18 shows that LPS induced a significant increase in mean CD40 mRNA expression (a; 7.17 RQ ± 1.26; n=6) and CD11b mRNA expression (b; 1.13 RQ ± 0.15; n=6) compared with control-treated mixed glia (a; 2.56 RQ ± 0.70; n=6; **p<0.01; ANOVA) and (b; 0.75 RQ ± 0.09; n=6; **p<0.01; ANOVA). Pretreatment of mixed glia with IL-4 (20ng/ml) did not attenuate the LPS-induced increase in CD40 mRNA expression (a; 16.17 RQ ± 5.05; n=6; ANOVA) and CD11b mRNA expression (b; 1.30 RQ ± 0.15; n=6; ANOVA). CD40 and CD11b mRNA expression was similar in control-treated samples which were incubated in the presence and absence of IL-4.

3.4. Discussion

The objectives of this study were to examine the modulatory effect of rosiglitazone on LPS-induced changes in mixed glia, microglia and astrocytes and to determine whether its action is IL-4 dependent. The data indicate that rosiglitazone attenuates the LPS-induced increase in IL-1β in mixed glia and astrocytes but not in microglia. This effect of rosiglitazone was mimicked by IL-4, which was released from astrocytes in response to rosiglitazone.

In this study, dose response analysis revealed that pretreatment of cells with rosiglitazone for 24h at a concentration of 20 and 100μM significantly attenuated the LPS-induced increase in IL-1β from mixed glia. Therefore the concentration chosen for future experiments was 20μM. Different *in vitro* concentrations of PPARγ agonists, including rosiglitazone, varying from 10-100μM have been used in previous studies in the literature. Woster and Combs (2007) found that pretreatment of microglia with 10μM and 50μM of rosiglitazone attenuated LPS-induced increases in TNFα, whereas Storer and colleagues (2005), found that pretreatment of primary mouse microglia and astrocytes with rosiglitzone at 50μM, 200μM and 300μM attenuated LPS-induced increases in IL-1β, TNFα and IL-6 respectively (Storer et al., 2005; Woster and Combs, 2007).

The action of rosiglitazone was first assessed *in vitro* in mixed glia obtained from the cortex of neonatal rats. LPS which is a widely-accepted model of inflammation induced a significant increase in IL-1β, without affecting cell viability, as has been extensively shown *in vitro* in both mixed glia (Loane et al., 2009) and in microglial and astrocyte cell cultures (Kim et al., 2004; Storer et al., 2005). Pretreatment with rosiglitazone attenuated this increase in supernatant concentration of IL-1β and this was accompanied by a significant decrease in IL-1β mRNA. This is consistent with published data; where oral administration of rosiglitazone for a three week period attenuated the aged-related increase in IL-1β mRNA in the rat hippocampus, pretreatment of mixed glia with rosiglitazone attenuated the LPS-induced increase in IL-1β mRNA (Loane et al., 2009).

In addition to IL-1β, activated glial cells also release other pro-inflammatory cytokines including TNFα and IL-6. The present data show that pretreatment of mixed glia with rosiglitazone attenuated the LPS-induced increases in TNFα and IL-6 mRNA. In contrast it did not attenuate the increase in the supernatant concentration of either TNFα or IL-6. The results would suggest that rosiglitazone may be acting to attenuate cytokine mRNA expression and not cytokine release, an similar differences in the abilityto attenuate TNFα and IL-1β mRNA and protein are obsereved in the literature. Evidence in the literature shows that pretreatment of cultured astrocytes with $15dPGJ_2$ attenuated the LPS/IFN-γ-induced increase in TNFα, IL-1β and IL-6 mRNA (Giri et al., 2004). However, Storer and colleagues (2005) investigating the anti-inflammatory action of rosiglitazone in microglia and astrocytes found at a dose of 50μM, no attenuation in IL-6 or TNFα concentration was recorded, but there is evidence reporting that other PPARγ agonists such as $15dPGJ_2$, can attenuate TNFα and IL-6 production in astrocytes (Giri et al., 2004) and microglia (Bernardo et al., 2000).

In addition to the release of pro-inflammatory cytokines, activated microglia express a number of cell surface molecules, these include MHC I and II, CD40, CD11b, complement receptors and intracellular adhesion molecules (Minagar et al., 2002). In this study a significant increase in both CD11b and CD40 mRNA was recorded following LPS stimulation in the same mixed glia that showed changes in cytokines. Increased expression of CD40 and CD11b mRNA have been recorded in microglia in response to LPS treatment (Qin et al., 2005; Roy et al., 2006). It is important to note that CD11b, is also expressed constitutively at moderate levels in resting microglial cells (Dziennis et al., 1995) but activation triggers an increase in expression. Pretreatment with rosiglitazone significantly attenuated the expression of both of these markers. Interestingly pretreatment with rosiglitazone appears to increase CD11b mRNA expression when compared to control-treated glial cells, however this did not reach statistical significance. Investigations into the role of rosiglitazone as an anti-inflammatory agent have shown that rosiglitazone downregulated the microglial expression of CD40 in the hippocampus of an animal model of epilepsy (Sun et al., 2008). Similarly in a mouse model of PD rosiglitazone

treatment decreased the expression of CD11b in the hippocampus (Schintu et al., 2009).

In this study, FACS analysis of mixed glial cells revealed that they consist of approximately 70% astrocytes and 30% microglia. The precise cell population responsible for pro-inflammatory cytokine production is only partly understood and is likely to be stimulus-dependent (Ledeboer et al., 2000). For example, it has been proposed that in LPS-activated mixed glial cultures it is mainly the astocytic cells that produce NO and IL-1β (Vincent et al., 1996). It has also been suggested that TNFα and IL-6 are produced primarily by microglial cells under these conditions (Lee et al., 1993a). However the ability of primary astrocytes to express IL-6 in response to a combination of IL-1β and TNFα or LPS has been demonstrated (Benveniste et al., 1990). To further assess this question, isolated microglial and astrocytic cell cultures were prepared and the production of pro-inflammatory cytokines induced by LPS was investigated, and the modulatory effect of rosiglitazone on LPS-induced changes was investigated in both cell types.

The data show that treatment with LPS induced a significant increase in IL-1β, IL-6 and TNFα in the supernatant obtained from isolated microglia. This is consistent with extensive evidence from the literature both in isolated microglial cell cultures and microglial cell lines (Ledeboer *et al.*, 2000; Luna-Medina *et al.*, 2005; Petrova *et al.*, 1999). Interestingly pretreatment with rosiglitazone attenuated the LPS-induced increase in IL-6 and TNFα, but not IL-1β in these cells. Evidence in the literature supports these data, where pretreatment of isolated microglia with different PPARγ agonists attenuates the release of pro-inflammatory cytokines and chemokines. Pretreatment of BV2, the microglial cell line, with the PPARγ agonists NP00111 and NP01138, both of which are heterocyclic thiazolidinediones, attenuated the LPS-induced increase in TNFα and IL-6 (Luna-Medina et al., 2005). In a similar manner pretreatment of primary mouse microglial cells with $15dPGJ_2$, rosiglitazone and pioglitazone attenuated the LPS-induced increase in TNFα and IL-6, but also IL-β which differs from this study (Storer et al., 2005). The ability of rosiglitazone to attenuate the increase in IL-1β may be due to the differences in the experimental set up. Storer and colleagues (2005) used LPS (2μg/ml) compared with LPS (1μg/ml),

and they used rosiglitazone at a higher concentration (50μM). The resultant IL-1β production was higher in that study (160pg/ml) compared with this study (100pg/ml).

In astrocytes, LPS induced a significant increase in IL-1β, IL-6 and TNFα in supernatant; which was significantly attenuated by pretreatment with rosiglitazone, which is consistent with the evidence from the literature. Rosiglitazone has previously been shown to attenuate LPS-induced release of IL-1, IL-6, TNFα from astrocytes (Storer et al., 2005) and other PPARγ agonists; NP00111 and NP01138 (Luna-Medina et al., 2005) and $15dPGJ_2$ (Giri et al., 2004) exerted similar effects. This attenuation of the production of the pro-inflammatory cytokines was mirrored by a decrease in their mRNA expression of the same cytokines (TNFα, IL-1β and IL-6) (Giri et al., 2004). Interestingly in this study, LPS induced an increase in the supernatant concentration of IL-6 in both astrocytes and microglia but failed to induce an increase in IL-6 mRNA expression in both cell types. While the experiment was repeated twice, the inability to detect any change in IL-6 mRNA in both cell types in response to LPS suggests a problem with the primer used in the PCR reaction, and would benefit the data greatly if it was repeated.

PPARγ agonists have been shown to result in a downregulation of pro-inflammatory cytokine secretion, in particular at the mRNA level which is suggested to be mediated through its ability to modulate transcription factors for genes involved in the inflammatory response including AP1, STAT-1 and NFκB (Jiang et al., 1998; Ricote et al., 1998). Pascual and colleagues (2005) suggest that PPARγ agonists block NFκB dependent gene expression in macrophages through co-repressor interference. Inflammatory genes are normally repressed through the association of the co-repressors present in the promoters of these genes. Pretreatment of macrophages with rosiglitazone followed by LPS stimulation, inhibited iNOS gene expression and they propose this occurs due to the binding of rosiglitazone with its PPRE. This activates the ligand binding domain of PPARγ which undergoes a SUMOylation with the nuclear receptor co-repressor (NCoR)-histone deacetylase-3 (HDAC3), on the inflammatory gene promoter. This prevents the removal of the co-repressor and therefore inhibits gene activation (Pascual et al., 2005).

Giri and colleagues (2004) present evidence that the ability of $15dPGJ_2$ to attenuate LPS/IFNγ induced increases in iNOS and NFκB activity were not altered by the PPARγ antagonist GW9662 or by overexpression of PPARγ, which suggest a PPARγ independent mechanism of this modulatory effect. Treatment of astrocytes with $15dPGJ_2$ modulated the LPS/IFNγ-induced increase in pro-inflammatory cytokine expression (IL-1β, TNFα, IL-6, iNOS) by inhibiting IκB kinase (IKK) activity which results in the inhibition of IκB degradation and therefore in turn prevents the translocation of p65 to the nucleus, thereby regulating the NFκB pathway (Giri et al., 2004). They also state that in astrocytes $15dPGJ_2$ inhibited the recruitment of coactivator compounds such as p300/CREB-binding protein, which is required for maximal NFκB activity (Giri et al., 2004). Another novel PPARγ independent mechanism of the anti-inflammatory action of PPARγ agonists was suggested following work in microglia and astrocytes investigating JAK-STAT signalling in the inflammatory response. Treatment of microglia and astrocytes with rosiglitazone (20μM) and $15dPGJ_2$ (10μM) inhibited the LPS and IFNγ induced phosphorylation of JAK 1 and JAK2 as well as STAT1 and STAT3. They subsequently examined the effect of this on MCP-1 and IP-10, two chemokines whose expression requires the activation of JAK STAT signalling. IFNγ and LPS rapidly increased the transcription of both genes, but this induction was inhibited by $15dPGJ_2$ and rosiglitazone (Park et al., 2003).

While the mechanism of IL-1 maturation and release is incompletely understood, it is known that the activation of the IL-1β inflammasome complex is required for the cleavage of inactive pro-IL-1β by caspase 1 to active IL-1β which is released from the cell (Ferrari et al., 2006). As rosiglitazone attenuates the LPS-induced increase in IL-1β in the supernatant of glial cells it suggests a possible ability of PPARγ agonists to modulate protease or caspase activity, in particular caspase 1 and this is an avenue that might merit further investigation.

The present data highlight one difference between microglia and astrocytes. Rosiglitazone attenuated the LPS-induced increases in all three cytokines in astrocytes but the LPS-induced increase in IL-1β release from microglia was not blocked by rosiglitazone pretreatment. This difference in the response of different cell

types leads to the question of how rosiglitazone is exerting its modulatory effect on the inflammatory profile of glial cells in the brain.

The importance of maintaining the balance of pro- and anti-inflammatory cytokines in the brain has been highlighted previously. It has been shown that the increase in pro-inflammatory cytokines IL-1 and IL-6 which have been reported with age and in neurodegenerative diseases is accompanied by a decrease in the anti-inflammatory cytokines IL-4 and IL-10. This apparent imbalance in pro- and anti-inflammatory cytokines is thought to contribute to the deficit in LTP (Lynch *et al.*, 2007; Maher *et al.*, 2005; Nolan *et al.*, 2005). Consistently, evidence has indicated the importance of IL-4 as a regulator of inflammation in the brain and it has been reported that IL-4 downregulates IL-1β protein in tissue prepared from aged rats (Maher et al., 2005).

Previous data suggested that rosiglitazone may act in an IL-4 mediated manner (Loane et al., 2009) and therefore its effect on IL-4 production was investigated in mixed glia, isolated astrocytes and isolated microglia. The data show that rosiglitazone induced a significant increase in IL-4 in mixed glia and astrocytes, but not in microglia suggesting that the source of IL-4 is probably astrocytes. The ability of rosiglitazone to induce an increase in IL-4 mirrors data observed *in vivo* which demonstrated that the age-related decrease in IL-4 concentration in the hippocampus was restored to concentrations observed in the hippocampus of young animals pretreated orally with rosiglitazone (Loane et al., 2009). This finding suggests that the possible anti-inflammatory action of rosiglitazone may be mediated through the production of the anti-inflammatory cytokine IL-4. If rosiglitazone exerts its modulatory effects by inducing IL-4 then it follows that it will fail to exert any action in IL-$4^{-/-}$ mice. This was investigated by analysing the effect of rosiglitazone on LPS-induced changes in mixed glia prepared from C57 wildtype and IL-$4^{-/-}$ mice. The data show that LPS significantly increased IL-1β in cells prepared from both C57 and IL-$4^{-/-}$ mice. Pretreatment with rosiglitazone significantly attenuated the LPS-induced increase in IL-1β in cells prepared from C57 mice but not in IL-$4^{-/-}$ mice, confirming that the anti-inflammatory action of rosiglitazone is IL-4 dependent. This was further confirmed by previous data (Loane et al., 2009), and in this study it was

demonstrated that rosiglitazone attenuated the LPS-induced increase in MHCII mRNA in wildtype, but not IL-4$^{-/-}$ mice (Loane et al., 2009). It is noted that rosiglitazone treatment induced an increase in the supernatant concentration of IL-1β in IL-4$^{-/-}$ mice in the absence of LPS, but this increase did not reach statistical significance.

It must be predicted that if IL-4 mediates the effect of rosiglitazone that then IL-4 will mimic its effects. To investigate this, mixed glial cells were pretreated with recombinant IL-4 (20ng/ml) and as previously observed, LPS induced a significant increase in the supernatant concentrations of IL-1β, TNFα and IL-6. Pretreatment with IL-4 attenuated the LPS-induced increase in supernatant concentration of IL-1β but not TNFα or IL-6. However, it has been shown that pretreatment of co-cultures of rat astroglial and microglial cells with IL-4 (5-50 U/ml) induced a dose dependent suppression of LPS-induced IL-6 and TNFα concentration (Chao et al., 1993; Ledeboer et al., 2000). The authors report that IL-4 (5 or 50 U/ml) significantly attenuated the LPS-induced increase in TNFα (5 U/ml) and IL-6 (50 U/ml) but failed to attenuate IL-1β at either concentration (Ledeboer et al., 2000). It was also reported that pretreatment of microglia with IL-4 (3ng/ml) attenuated LPS-induced increase in TNFα (Chao et al., 1993). Both soluble and membrane bound IL-4 receptor have been found in astrocytes (Brodie et al., 1998) however microglia in culture have been shown to express IL-4 receptor but do not express IL-4 when evaluated by RT-PCR (Suzumura et al., 1994). However IL-4 pretreatment failed to attenuate the LPS-induced increase in both markers of microglial activation CD40 and CD11b. The ability of IL-4 to attenuate markers of microglial activation has been demonstrated before both *in vitro* and *in vivo,* administration of IL-4 (200ng/ml) attenuated Aβ induced increase in MHC II in cultured cortical glia (Lyons et al., 2007b). IL-4 administration attenuated the IFNγ-induced increase in MHC II mRNA in the hippocampus (Clarke et al., 2008).

It has long been established that the role of PPARγ agonists in controlling lipid and glucose metabolism occurs in a PPARγ dependent mechanism but the data presented here suggests that IL-4 plays an important role in the anti-inflammatory actions. It is known that the binding of a PPARγ agonist to the nuclear receptor

results in a conformational change in PPARγ such that it binds to the DNA and recruitment of transcriptional activators occurs. This results in an increase in gene expression. PPARγ regulates the expression of numerous genes in adipocytes and it is this role that is important as a treatment for type II diabetes. In adipocytes, PPARγ regulates the expression of numerous genes involved in lipid metabolism such as aP2, acyl-CoA synthase, LPL and CD36. These genes are important in the control of lipid uptake into adipocytes but whether alterations in transcription of one or more of these genes plays a role in the anti-inflammatory action of PPARγ agonists is not clear.

Early evidence showed that the anti-inflammatory action of PPARγ agonists was in fact mediated through activation of PPARγ (Jiang *et al.*, 1998; Ricote *et al.*, 1998). Treatment of peritoneal macrophages and monocytes with the endogenous PPARγ agonist $15dPGJ_2$ (0.1μM) attenuated IFNγ induced macrophage activation (Ricote et al., 1998) and the production of pro-inflammatory cytokines by monocytes (Jiang et al., 1998). In one study the authors tested the hypothesis that PPARγ activation was mediating this action (Luna-Medina et al., 2005). HT22 cells were transfected with a reporter construct containing three consensus PPARγ response elements (PPRE-tk-luc) and in these cells an increase in luciferase activity would represent activation of PPARγ. They reported a significant increase in luciferase activity following treatment with two PPARγ agonists NP00111 and NP01138. They subsequently investigated whether the anti-inflammatory action of these agonists was also mediated through PPARγ activation. Astrocytes and microglia were treated with the PPARγ antagonist GW9662 and with NP00111 (50μM) or NP00138 (50μM), followed by LPS treatment (10μg/ml). The PPARγ agonists attenuated the LPS-induced increase in IL-6, TNFα and nitrite production, and this attenuation was significantly reversed by GW9662, indicating a PPARγ dependent action (Luna-Medina et al., 2005).

In contrast, numerous reports have previously suggested that the anti-inflammatory effects of PPARγ agonists are independent of PPARγ activity. Castrillo and colleagues (2000) demonstrated that $15dPGJ_2$ inhibited TNFα and IL-6 secretion in a murine microglial cell line that is known to express negligible PPARγ. It was also demonstrated that rosiglitazone had an anti-inflammatory action in BV2 murine

microglia cell line, despite undetectable levels of PPARγ transcripts (Park et al., 2003). Further evidence of the PPARγ-independent mechanism in modulating pro-inflammatory cytokine secretion is the demonstration that $15dPGJ_2$, troglitazone and ciglitazone attenuated LPS-induced and IFN-γ-induced increases in cytokines in macrophages prepared from wildtype and PPARγ-deficient mice. Recent evidence from this lab suggests also that rosiglitazone acts in a manner which is independent of PPARγ, as the presence of the PPARγ antagonist GW9662 failed to reverse the ability of rosiglitazone to attenuate the LPS-induced increase in IL-1β in mixed glial cells (Loane et al., 2007). The suggestions for an alternative PPARγ independent mechanism are that it may work through the modulation NFκB activation (Petrova et al., 1999). Others have suggested that $15dPGJ_2$ and rosiglitazone-induced transcription of suppressor of cytokine signalling (SOCS) 1 and 3 are responsible for the anti-inflammatory effects (Benveniste, 1998; Storer et al., 2005).

The results presented here suggest that rosiglitazone has the ability to modulate the release of pro-inflammatory cytokines from mixed glia, isolated microglia and astrocytes. The evidence suggests that it does so in an IL-4 dependent manner since IL-4 mimics many of the effects of rosiglitazone and its actions are absent in cells prepared from IL-$4^{-/-}$ mice. Importantly, the data indicate that astrocytes are responsible for the increase in IL-4 but the mechanism by which rosiglitazone increases IL-4 remains to be established.

Chapter 3
Figures

Figure 3.1. Rosiglitazone dose-dependently attenuated the LPS-induced increase in IL-1β in cortical mixed glial cultures .

LPS (1μg/ml) induced a significant increase in mean IL-1β protein concentration in supernatant of mixed glia (***p<0.001, versus control-treated glia). Pretreatment with rosiglitazone (20μM and 100μM) significantly attenuated the LPS-induced increase ($^{\#\#}$p<0.01, versus LPS-treated glia). Values are presented as means (±SEM; n=6) and expressed as pgIL-1β/ml.
LPS (1μg/ml) or rosiglitazone (20μM) treatments did not alter the viability of mixed glial cells (ANOVA; versus control-treated glia).

(a) 2-way ANOVA; LPS_{effect} F(1,21)=47.85; p<0.001, rosiglitazone $10\mu M_{effect}$ F(1,21)=1.37; p=0.2556, rosiglitazone $20\mu M_{effect}$ F(1,21)=12.39; p<0.01, rosiglitazone $100\mu M_{effect}$ F(1,21)=27.52; p<0.01, $Interaction_{effect}$ F(1,21)=16.80; p<0.001.
(b) 2-way ANOVA; LPS_{effect} F(1,4)=0.49; p=0.5225, $rosiglitazone_{effect}$ F(1,4)=0.02; p=0.9066, $Interaction_{effect}$ F(1,4)=2.16; p=0.215.

a

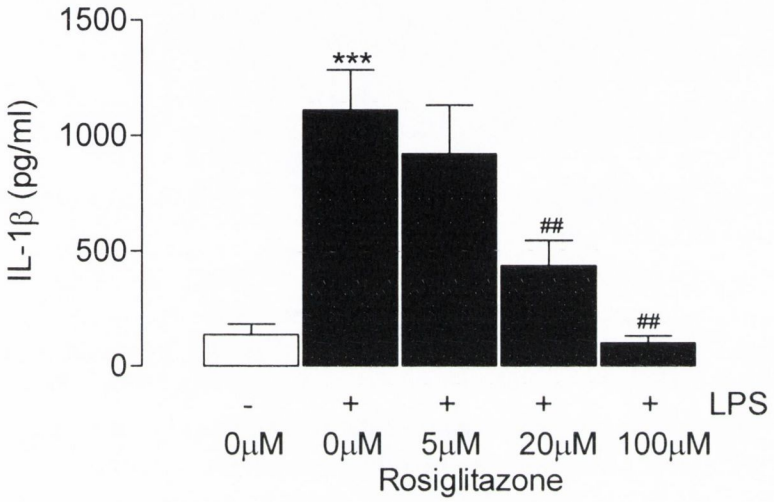
1500
1000
500
0
IL-1β (pg/ml)
***
##
##
-
+
+
+
+
LPS
0μM
0μM
5μM
20μM
100μM
Rosiglitazone

b

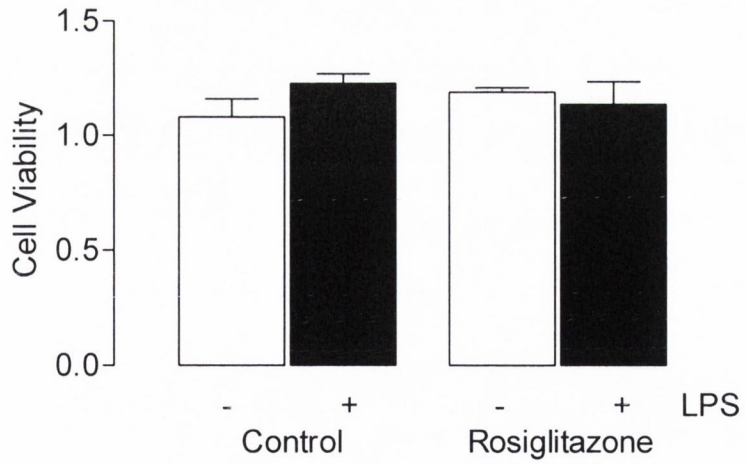
1.5
1.0
0.5
0.0
Cell Viability
-
+
-
+
LPS
Control
Rosiglitazone

Figure 3.2. Rosiglitazone attenuated the LPS-induced increase in IL-1β in cultured mixed glia.

LPS (1μg/ml) induced a significant increase in mean IL-1β mRNA expression and supernatant concentration of IL-1β in mixed glia, compared with controls (a; ***p<0.001; b; ***p<0.001; ANOVA). Pretreatment of mixed glia with rosiglitazone (20μM) significantly attenuated the LPS-induced increase in IL-1β mRNA and supernatant concentration of IL-1β (a; $^{\#\#}$p<0.01; b; $^{\#}$p<0.05; ANOVA; versus LPS-treated glia). Rosiglitazone (20μM) pretreatment did not significantly affect IL-1β mRNA expression or protein concentration. Values are presented as means (±SEM; n=6) and expressed as IL-1β:β-actin (RQ) or pg IL-1β/ml.

(a). 2-way ANOVA; LPS_{effect} F(1,16)=46.82; p<0.001, $rosiglitazone_{effect}$ F(1,16)=11.43; p<0.01, $Interaction_{effect}$ F(1,16)=10.93; p<0.01.
(b). 2-way ANOVA; LPS_{effect} F(1,20)=19.21; p<0.001, $rosiglitazone_{effect}$ F(1,20)=5.88; p<0.05, $Interaction_{effect}$ F(1,20)=5.47; p<0.05.

a

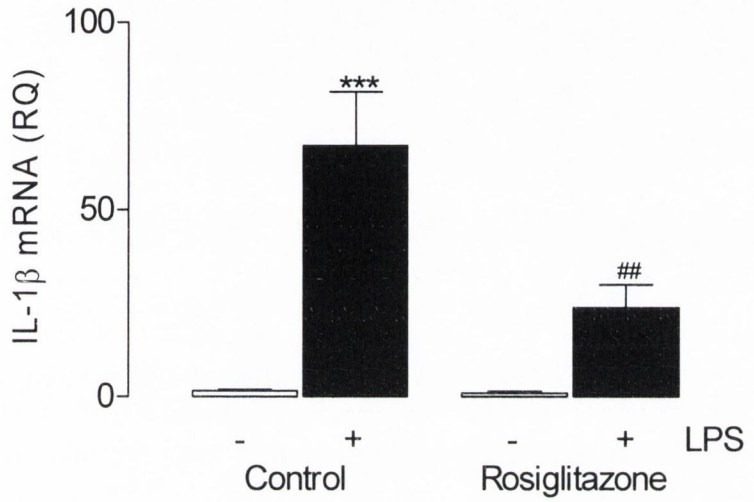
100
50
0
IL-1β mRNA (RQ)
***
##
-
+
-
+
LPS
Control
Rosiglitazone

b

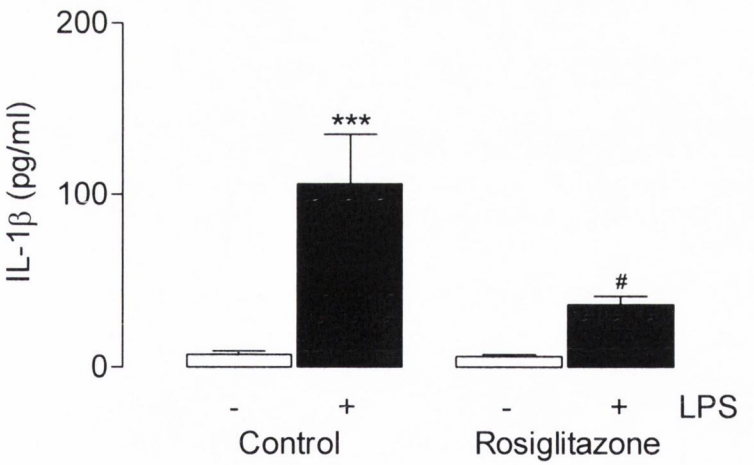
200
100
0
IL-1β (pg/ml)
***
#
-
+
-
+
LPS
Control
Rosiglitazone

Figure 3.3. Rosiglitazone attenuated the LPS-induced increase in IL-6 mRNA in cultured mixed glia.

LPS (1μg/ml) induced a significant increase in mean IL-6 mRNA expression and supernatant concentration of IL-6 in mixed glia, compared with controls (a; ***p<0.001; b;**p<0.01; ANOVA). Pretreatment of mixed glia with rosiglitazone (20μM) significantly attenuated the LPS-induced increase in IL-6 mRNA (a; $^{\#\#}$p<0.01; ANOVA; versus LPS-treated glia) but not supernatant concentration of IL-6 (b; ANOVA; versus LPS-treated glia). Rosiglitazone (20μM) pretreatment did not significantly affect IL-6 mRNA expression or supernatant concentration of IL-6. Values are presented as means (±SEM; n=6) and expressed as IL-6:β-actin (RQ) or pg IL-6/ml.

(a). 2-way ANOVA; LPS_{effect} F(1,16)=29.66; p<0.001, $rosiglitazone_{effect}$ F(1,16)=12.24; p<0.01, $Interaction_{effect}$ F(1,16)=10.24; p<0.01.
(b). 2-way ANOVA; LPS_{effect} F(1,35)=15.52; p<0.01, $rosiglitazone_{effect}$ F(1,35)=0.01; p=0.912, $Interaction_{effect}$ F(1,35)=0.03; p=0.8721.

a

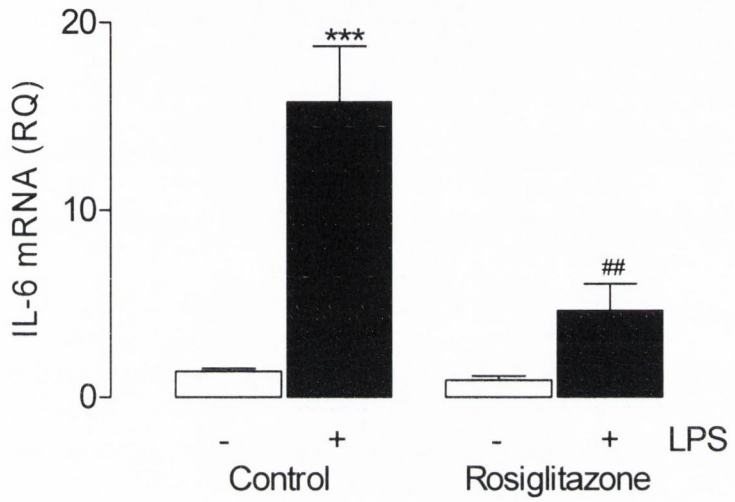
20
10
0
IL-6 mRNA (RQ)
***
##
-
+
-
+
LPS
Control
Rosiglitazone

b

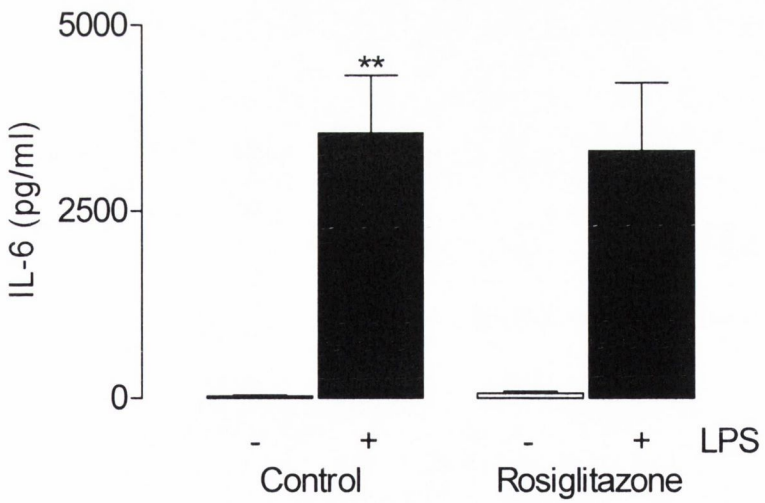
5000
2500
0
IL-6 (pg/ml)
**
-
+
-
+
LPS
Control
Rosiglitazone

Figure 3.4. Rosiglitazone attenuated the LPS-induced increase in TNFα mRNA in cultured mixed glia.

LPS (1μg/ml) induced a significant increase in mean TNFα mRNA expression and supernatant concentration of TNFα in mixed glia, compared with controls (a; ***p<0.001; b;**p<0.01; ANOVA). Pretreatment of mixed glia with rosiglitazone (20μM) significantly attenuated the LPS-induced increase in TNFα mRNA (a; $^{\#}$p<0.01; ANOVA; versus LPS-treated glia) but not the supernatant concentration of TNFα (b; ANOVA; versus LPS-treated glia). Rosiglitazone (20μM) pretreatment did not significantly affect TNFα mRNA expression or supernatant concentration. Values are presented as means (±SEM; n=6) and expressed as TNFα:β-actin (RQ) or pg TNFα/ml.

(a). 2-way ANOVA; LPS_{effect} F(1,15)=21.34; p<0.001, $rosiglitazone_{effect}$ F(1,15)=6.06; p<0.05, $Interaction_{effect}$ F(1,15)=3.18; p=0.0947.
(b). 2-way ANOVA; LPS_{effect} F(1,20)=8.80; p<0.01, $rosiglitazone_{effect}$ F(1,20)=0.42; p=0.5219, $Interaction_{effect}$ F(1,20)=0.88; p=0.3586.

a

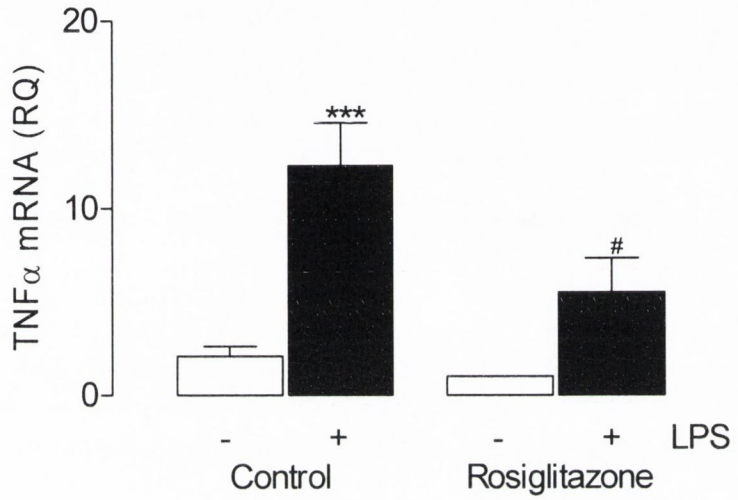
20
10
0
TNFα mRNA (RQ)
***
#
-
+
-
+
LPS
Control
Rosiglitazone

b

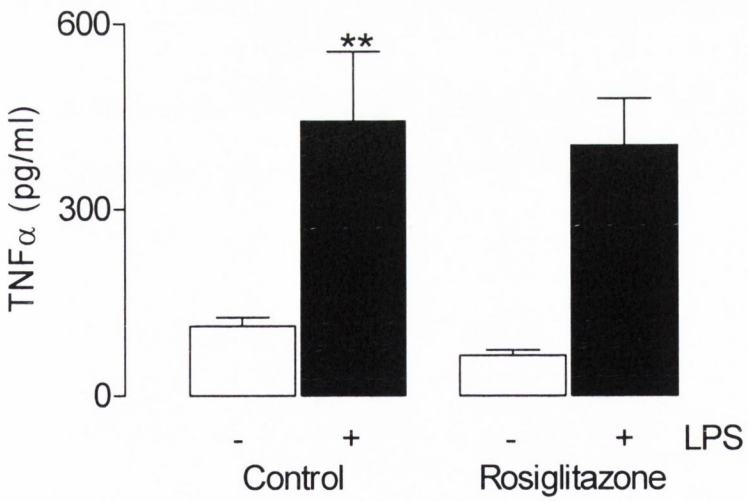
600
300
0
TNFα (pg/ml)
**
-
+
-
+
LPS
Control
Rosiglitazone

Figure 3.5. Rosiglitazone attenuated the LPS-induced increase in CD40 and CD11b in cultured mixed glia.

LPS (1μg/ml) induced a significant increase in mean CD40 mRNA and CD11b mRNA expression in mixed glia, compared with controls (a; ***p<0.001; b; *p<0.05; ANOVA). Pretreatment of mixed glia with rosiglitazone (20μM) significantly attenuated the LPS-induced increase in CD40 and CD11b mRNA (a; $^{\#\#}$p<0.01; b; $^{\#\#\#}$p<0.001; ANOVA; versus LPS-treated glia). Rosiglitazone (20μM) pretreatment did not significantly affect CD40 or CD11b mRNA expression. Values are presented as means (±SEM; n=6) and expressed as CD40:β-actin (RQ) or CD11b:β-actin (RQ).

(a). 2-way ANOVA; LPS_{effect} F(1,15)=22.64; p<0.001, $rosiglitazone_{effect}$ F(1,15)=9.82; p<0.01, $Interaction_{effect}$ F(1,15)=8.36; p=0.0112.
(b). 2-way ANOVA; LPS_{effect} F(1,23)=5.52; p<0.05, $rosiglitazone_{effect}$ F(1,23)=18.13; p<0.001, $Interaction_{effect}$ F(1,23)=0.33; p=0.4729.

a

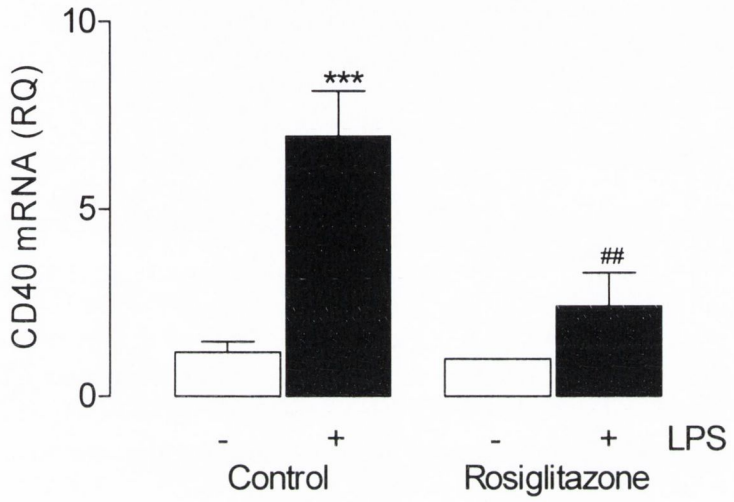
10
5
0
CD40 mRNA (RQ)
***
##
-
+
-
+
LPS
Control
Rosiglitazone

b

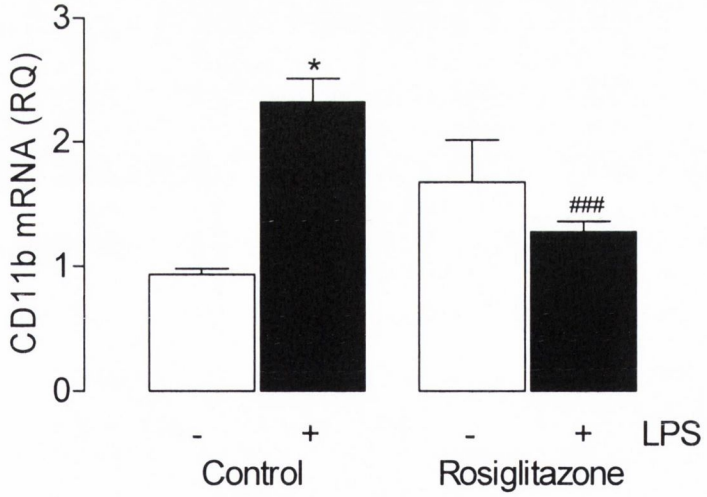
3
2
1
0
CD11b mRNA (RQ)
*
###
-
+
-
+
LPS
Control
Rosiglitazone

Figure 3.6. Rosiglitazone attenuated the LPS-induced increase in IL-1β mRNA in cultured microglia.

LPS (1μg/ml) induced a significant increase in mean IL-1β mRNA expression and supernatant concentration of IL-1β in microglia, compared with controls (a; ***p<0.001; b; **p<0.01; ANOVA). Pretreatment of microglia with rosiglitazone (20μM) significantly attenuated the LPS-induced increase in IL-1β mRNA (a; $^{###}$p<0.001; ANOVA versus LPS-treated microglia) but not supernatant concentration of IL-1β (b; ANOVA versus LPS-treated microglia). Rosiglitazone (20μM) pretreatment did not significantly affect IL-1β mRNA expression or protein concentration. Values are presented as means (±SEM; n=6) and expressed as IL-1β:β-actin (RQ) or pg IL-1β/ml.

(a). 2-way ANOVA; LPS_{effect} F(1,20)=138.21; p<0.001, $rosiglitazone_{effect}$ F(1,20)=45.52; p<0.001, $Interaction_{effect}$ F(1,20)=57.95; p<0.001.
(b). 2-way ANOVA; LPS_{effect} F(1,20)=13.65; p<0.01, $rosiglitazone_{effect}$ F(1,20)=0.72; p=0.4093, $Interaction_{effect}$ F(1,20)=0.79; p=0.3858.

a

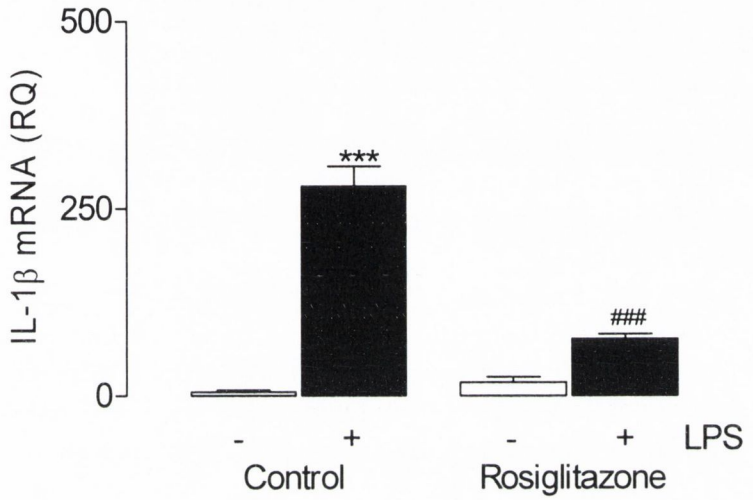
500
250
0
IL-1β mRNA (RQ)
***
###
- + - + LPS
Control
Rosiglitazone

b

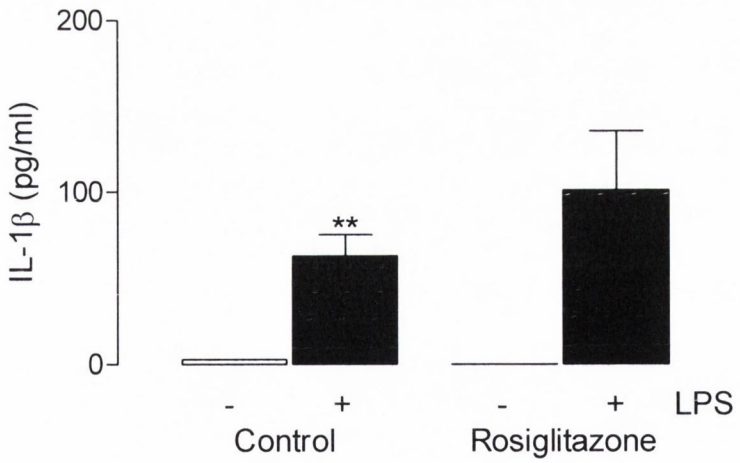
200
100
0
IL-1β (pg/ml)
**
- + - + LPS
Control
Rosiglitazone

Figure 3.7. Rosiglitazone attenuated the LPS-induced increase in IL-6 in cultured microglia.

LPS (1μg/ml) induced a significant increase in supernatant concentration of IL-6 in microglia, compared with controls (b; ***p<0.001; ANOVA). LPS failed to increase IL-6 mRNA in isolated microglia, compared with controls (a; ANOVA). Pretreatment of microglia with rosiglitazone (20μM) significantly attenuated the LPS-induced increase in supernatant concentration of IL-6 (b; $^{\#}$p<0.05; ANOVA versus LPS-treated microglia). Rosiglitazone (20μM) pretreatment did not significantly affect IL-6 mRNA expression or protein concentration. Values are presented as means (±SEM; n=6) and expressed as IL-6:β-actin (RQ) or pg IL-6/ml.

(a). 2-way ANOVA; LPS_{effect} F(1,19)=0..01; p=0.9240, $rosiglitazone_{effect}$ F(1,19)=1.03; p=0.3226, $Interaction_{effect}$ F(1,19)=0.05; p=0.8219.
(b). 2-way ANOVA; LPS_{effect} F(1,20)=70.39; p<0.001, $rosiglitazone_{effect}$ F(1,20)=7.01; p=0.0155, $Interaction_{effect}$ F(1,20)=2.74 p=0.1133.

a

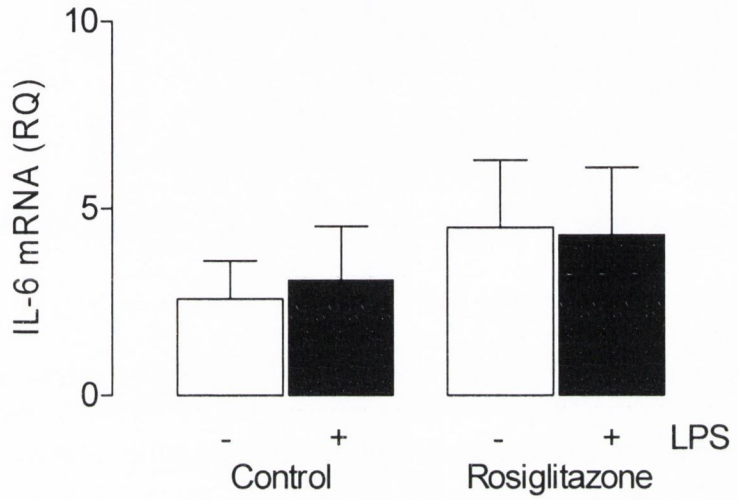
10
5
0
IL-6 mRNA (RQ)
-
+
-
+
LPS
Control
Rosiglitazone

b

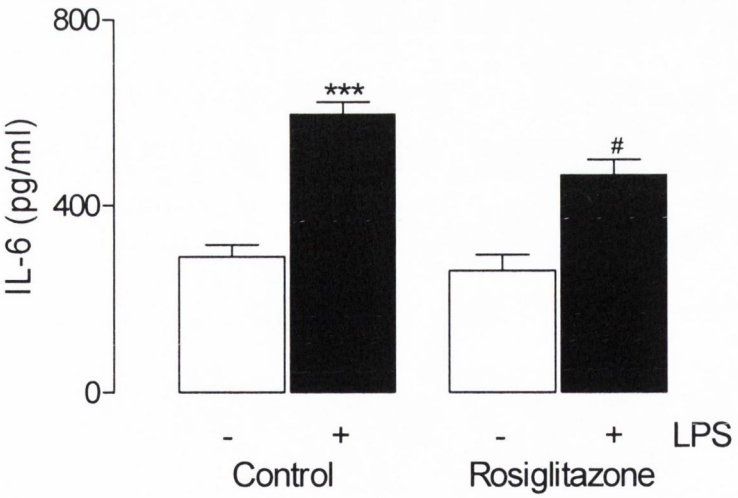
800
400
0
IL-6 (pg/ml)
***
#
-
+
-
+
LPS
Control
Rosiglitazone

Figure 3.8. Rosiglitazone attenuated the LPS-induced increase in TNFα in cultured microglia.

LPS (1μg/ml) induced a significant increase in mean TNFα mRNA expression and supernatant concentration of TNFα in microglia, compared with controls (a; ***p<0.001; b; ***p<0.001; ANOVA). Pretreatment of microglia with rosiglitazone (20μM) significantly attenuated the LPS-induced increase in TNFα mRNA and supernatant concentration of TNFα (a; $^{###}$p<0.001; b; $^{###}$p<0.001; ANOVA versus LPS-treated microglia). Rosiglitazone (20μM) pretreatment did not significantly affect TNFα mRNA expression or protein concentration. Values are presented as means (±SEM; n=6) and expressed as TNFα:β-actin (RQ) or pg TNFα/ml.

(a). 2-way ANOVA; LPS_{effect} F(1,16)=53.73; p<0.001, $rosiglitazone_{effect}$ F(1,16)=17.04; p<0.001, $Interaction_{effect}$ F(1,16)=41.95; p<0.001.
(b). 2-way ANOVA; LPS_{effect} F(1,20)=94.82; p<0.001, $rosiglitazone_{effect}$ F(1,20)=309.60; p<0.001, $Interaction_{effect}$ F(1,20)=5.25; p<0.05.

a

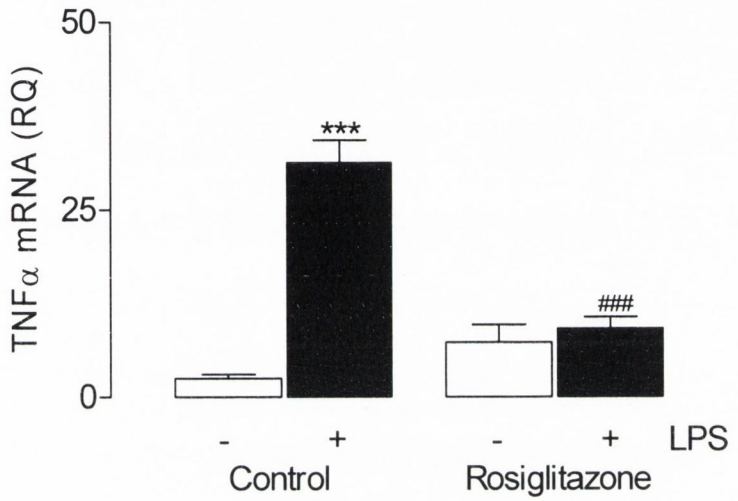
50
25
0
TNFα mRNA (RQ)
***
###
-
+
-
+
LPS
Control
Rosiglitazone

b

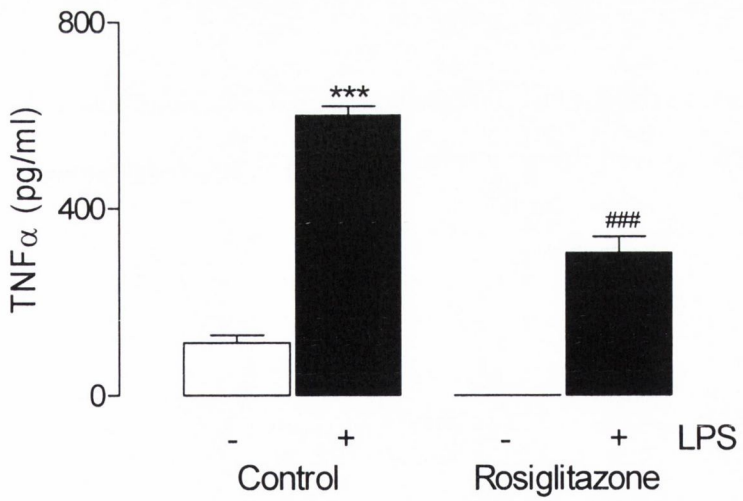
800
400
0
TNFα (pg/ml)
***
###
-
+
-
+
LPS
Control
Rosiglitazone

Figure 3.9. Rosiglitazone attenuated the LPS-induced increase in CD40 and CD11b in cultured microglia.

LPS (1μg/ml) induced a significant increase in mean CD40 and CD11b mRNA expression microglia, compared with controls (a; ***p<0.001; b; ***p<0.001; ANOVA). Pretreatment of microglia with rosiglitazone (20μM) significantly attenuated the LPS-induced increase in CD40 mRNA and CD11b mRNA (a; $^{\#}$p<0.05; b; $^{\#\#}$p<0.01; ANOVA versus LPS-treated microglia). Rosiglitazone (20μM) pretreatment did not significantly affect CD40 or CD11b mRNA expression. Values are presented as means (±SEM; n=6) and expressed as CD40:β-actin (RQ) and CD11b:βactin (RQ).

(a). 2-way ANOVA; LPS_{effect} F(1,18)=51.62; p<0.001, $rosiglitazone_{effect}$ F(1,18)=14.39; p<0.05, $Interaction_{effect}$ F(1,18)=4.11; p=0.0576.
(b). 2-way ANOVA; LPS_{effect} F(1,19)=8.77; p<0.001, $rosiglitazone_{effect}$ F(1,19)=2.09; p=0.1697, $Interaction_{effect}$. F(1,19)=36.74; p<0.01

a

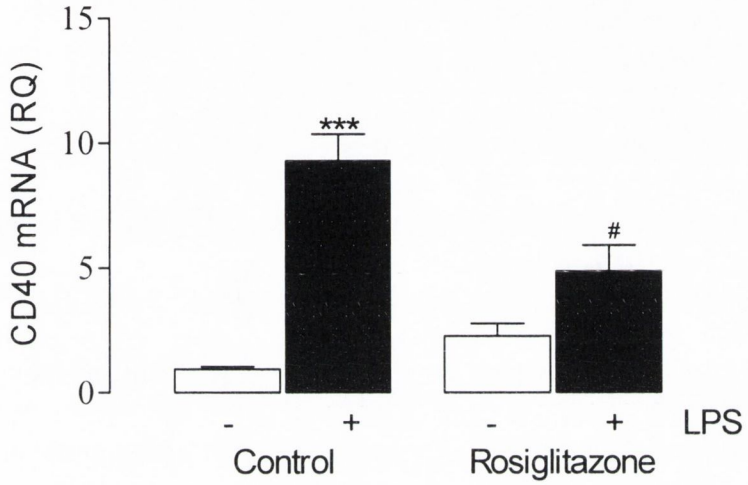
15
10
5
0
CD40 mRNA (RQ)
***
#
- + - + LPS
Control
Rosiglitazone

b

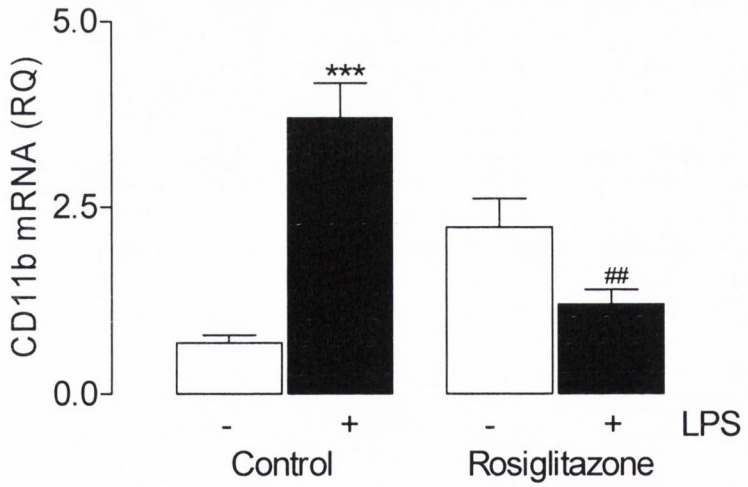
5.0
2.5
0.0
CD11b mRNA (RQ)
***
##
- + - + LPS
Control
Rosiglitazone

Figure 3.10. Rosiglitazone attenuated the LPS-induced increase in IL-1β in cultured astrocytes.

LPS (1μg/ml) induced a significant increase in mean IL-1β mRNA expression and supernatant concentration of IL-1β in astrocytes, compared with control-treated astrocytes (a; *$p<0.05$; b; ***$p<0.001$; ANOVA). Pretreatment of astrocytes with rosiglitazone (20μM) significantly attenuated the LPS-induced increase in supernatant concentration of IL-1β (b; $^{###}p<0.001$; ANOVA versus LPS-treated astrocytes) but not IL-1β mRNA concentration (a; ANOVA versus LPS-treated astrocytes). Rosiglitazone (20μM) pretreatment did not significantly affect IL-1β mRNA expression or protein concentration. Values are presented as means (±SEM; n=6) and expressed as IL-1β:β-actin (RQ) or pg IL-1β/ml.

(a). 2-way ANOVA; LPS_{effect} $F(1,14)=8.61$; $p<0.05$, $rosiglitazone_{effect}$ $F(1,14)=0.28$; $p<0.05$, $Interaction_{effect}$ $F(1,14)=0.13$; $p=0.7258$.
(b). 2-way ANOVA; LPS_{effect} $F(1,14)=263.53$; $p<0.001$, $rosiglitazone_{effect}$ $F(1,14)=37.14$; $p<0.001$, $Interaction_{effect}$ $F(1,14)=41.94$; $p<0.001$.

a

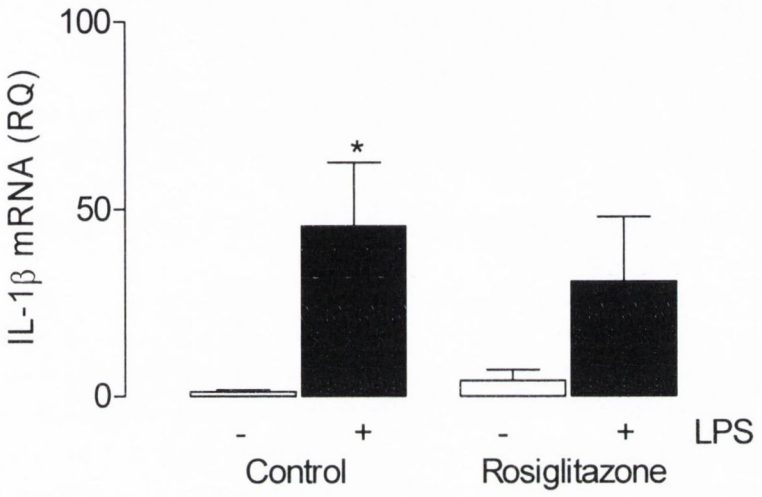
100
50
0
IL-1β mRNA (RQ)
*
- + - + LPS
Control
Rosiglitazone

b

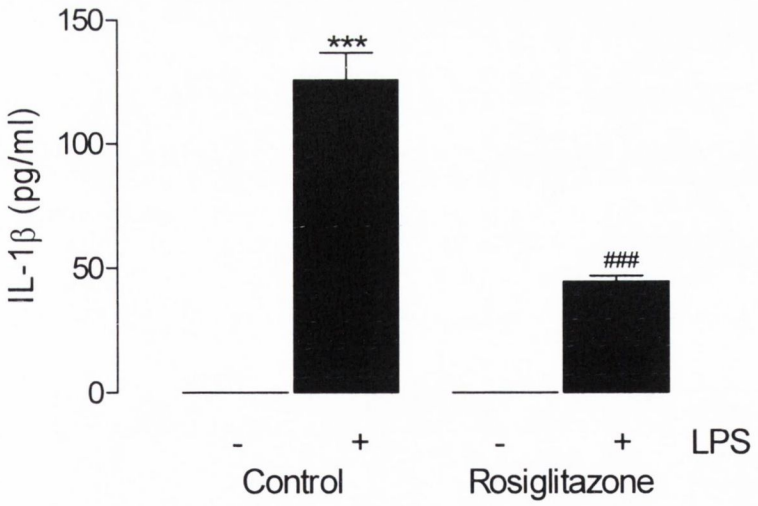
150
100
50
0
IL-1β (pg/ml)
***
###
- + - + LPS
Control
Rosiglitazone

Figure 3.11. Rosiglitazone attenuated the LPS-induced increase in IL-6 in cultured astrocytes.

LPS (1μg/ml) induced a significant increase in supernatant concentration of IL-6 in astrocytes, compared with controls (b; ***$p<0.001$; ANOVA). LPS failed to induce an increase in IL-6 mRNA expression in astrocytes (a; ANOVA). Pretreatment of astrocytes with rosiglitazone (20μM) significantly attenuated the LPS-induced increase in supernatant concentration of IL-6 (b; $^{\#}p<0.05$; ANOVA versus LPS-treated astrocytes). Rosiglitazone (20μM) pretreatment did not significantly affect IL-6 mRNA expression or supernatant concentration. Values are presented as means (±SEM; n=6) and expressed as IL-6:β-actin (RQ) or pg IL-6/ml.

(a). 2-way ANOVA; LPS_{effect} $F(1,14)=0.01$; $p=0.9379$, $rosiglitazone_{effect}$ $F(1,14)=0.20$; $p=0.8906$, $Interaction_{effect}$ $F(1,14)=0.04$; $p=0.8385$.
(b). 2-way ANOVA; LPS_{effect} $F(1,12)=97.08$; $p<0.001$, $rosiglitazone_{effect}$ $F(1,12)=8.74$; $p<0.05$, $Interaction_{effect}$ $F(1,12)=16.71$; $p<0.01$.

a

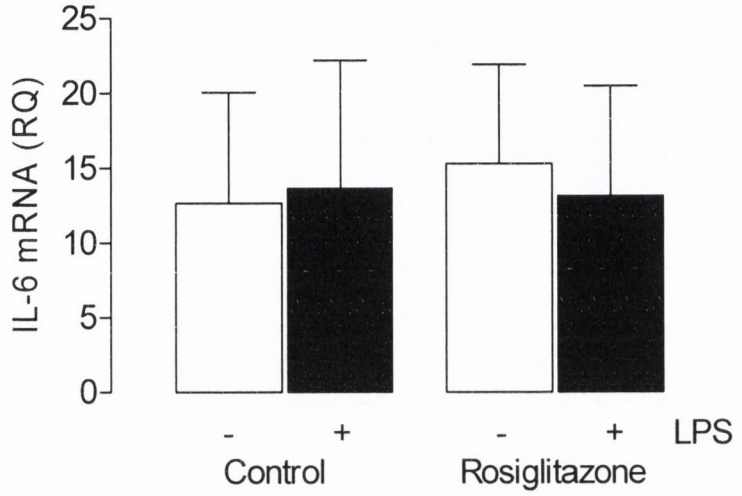
IL-6 mRNA (RQ)
25
20
15
10
5
0
-
+
-
+
LPS
Control
Rosiglitazone

b

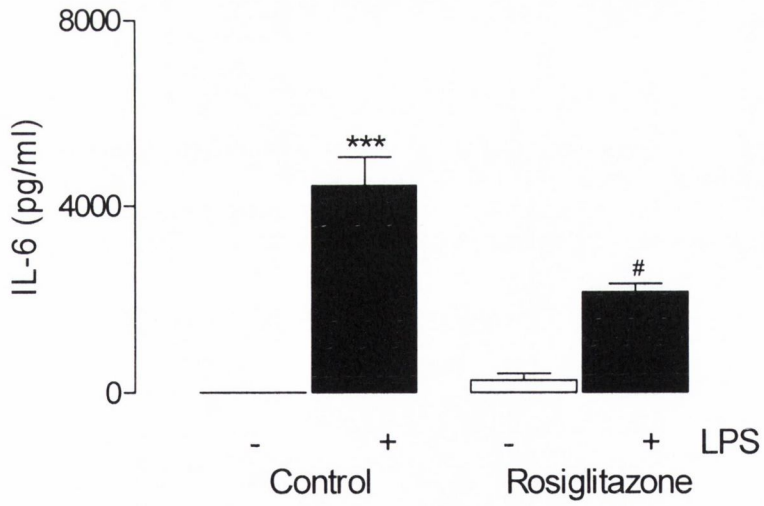
IL-6 (pg/ml)
8000
4000
0
***
#
-
+
-
+
LPS
Control
Rosiglitazone

Figure 3.12. Rosiglitazone attenuated the LPS-induced increase in TNFα in cultured astrocytes.

LPS (1μg/ml) induced a significant increase in TNFα mRNA expression and supernatant concentration of TNFα in astrocytes, compared with controls (a;***p<0.001; b; ***p<0.001; ANOVA). Pretreatment of astrocytes with rosiglitazone (20μM) significantly attenuated the LPS-induced increase in supernatant concentration of TNFα (b; $^{###}$p<0.001; ANOVA versus LPS-treated astrocytes). Rosiglitazone (20μM) pretreatment did not significantly affect TNFα mRNA expression or protein concentration. Values are presented as means (±SEM; n=6) and expressed as TNFα/β-actin (RQ) or pg TNFα/ml.

(a). 2-way ANOVA; LPS_{effect} F(1,14)=29.55; p<0.001, $rosiglitazone_{effect}$ F(1,14)=0.39; p=0.5422, $Interaction_{effect}$ F(1,14)=0.21; p=0.6544.
(b). 2-way ANOVA; LPS_{effect} F(1,14)=204.65; p<0.001, $rosiglitazone_{effect}$ F(1,14)=36.25; p<0.001, $Interaction_{effect}$ F(1,14)=35.55; p<0.001.

a

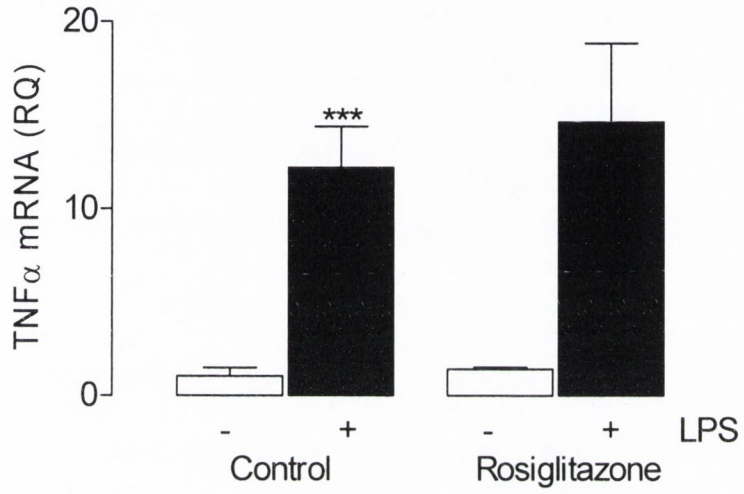
20
10
0
TNFα mRNA (RQ)
***
- + - + LPS
Control
Rosiglitazone

b

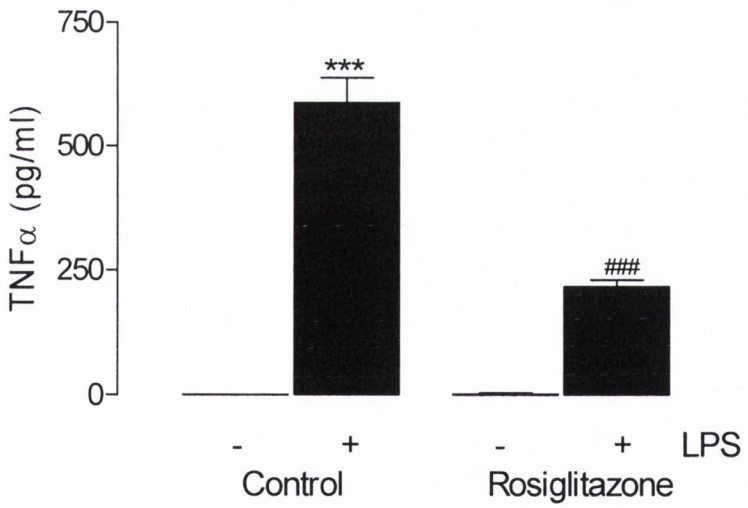
750
500
250
0
TNFα (pg/ml)
***
###
- + - + LPS
Control
Rosiglitazone

Figure 3.13. Rosiglitazone induced a significant increase in IL-4 in mixed glia and astrocytes.

Rosiglitazone (20μM) pretreatment induced a significant increase in supernatant concentration of IL-4 in mixed glia and astrocytes, compared with control-treated mixed glia and astrocytes (a; *p<0.05; b; *p<0.05; ANOVA and Student's *t* test respectively). Pretreatment of microglia with rosiglitazone (20μM) failed to increase supernatant concentration of IL-4 (c; Student's *t* test control-treated microglia). LPS (1μg/ml) treatment did not significantly affect IL-4 concentration. Values are presented as means (±SEM; n=6) and expressed as pg IL-4/ml.

(a). 2-way ANOVA; LPS_{effect} F(1,8)=0.16; p=0.6978, $rosiglitazone_{effect}$ F(1,8)=8.59 p<0.05, $Interaction_{effect}$ F(1,8)=0.01; p=0.9409.

a

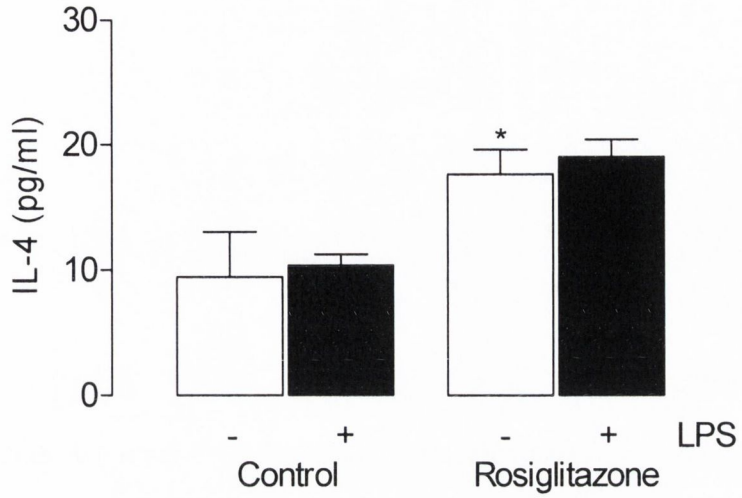
30
20
10
0
IL-4 (pg/ml)
*
- + - + LPS
Control
Rosiglitazone

b

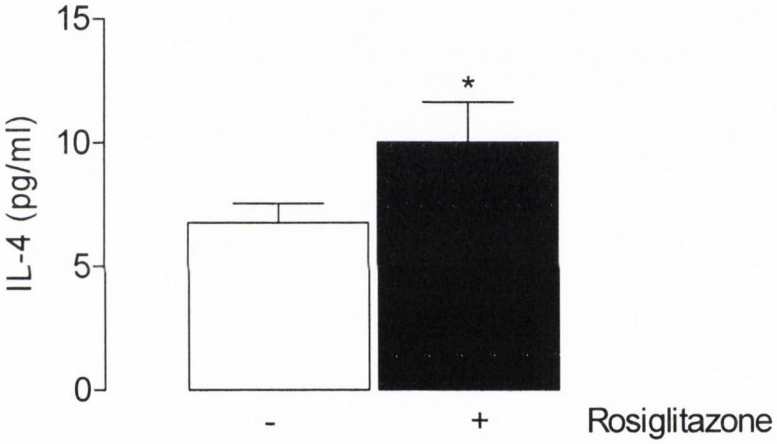
15
10
5
0
IL-4 (pg/ml)
*
- +
Rosiglitazone

c

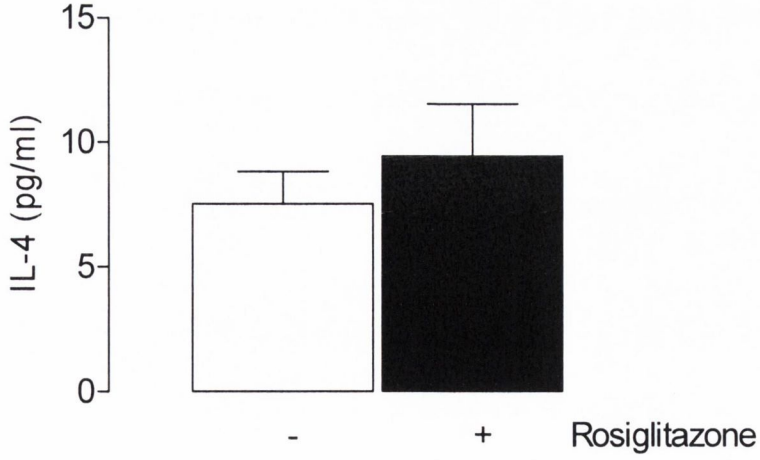
15
10
5
0
IL-4 (pg/ml)
- +
Rosiglitazone

Figure 3.14. Rosiglitazone attenuated the LPS-induced increase in IL-1β in C57BL/6 mixed glia and but not IL-4$^{-/-}$ mixed glia.

LPS (1μg/ml) induced a significant increase in mean IL-1β concentration in mixed glia, compared with control-treated glia obtained from the cortex of C57BL/6 and IL-4$^{-/-}$ mice (***$p<0.001$; ANOVA). Pretreatment of C57BL/6 mixed glia with rosiglitazone (20μM) significantly attenuated the LPS-induced increase in IL-1β ($^{\#\#}p<0.01$; ANOVA versus LPS-treated mixed glia) but rosiglitazone pretreatment failed to attenuate this increase in IL-4$^{-/-}$ mixed glia (ns; ANOVA versus LPS-treated mixed glia). Rosiglitazone (20μM) pretreatment did not significantly affect IL-1β protein concentration. Values are presented as means (±SEM; n=6) and expressed as pg IL-1β/ml.

C57BL/6, 2-way ANOVA; LPS_{effect} $F(1,29)=178.68$; $p<0.001$, $rosiglitazone_{effect}$ $F(1,29)=8.78$; $p<0.01$, $Interaction_{effect}$ $F(1,29)=9.65$; $p<0.01$.
IL-4-/-, 2-way ANOVA; LPS_{effect} $F(1,20)=10.84$; $p<0.001$, $rosiglitazone_{effect}$ $F(1,20)=0.67$; $p=0.4243$, $Interaction_{effect}$ $F(1,20)=0.99$; $p=0.3308$.

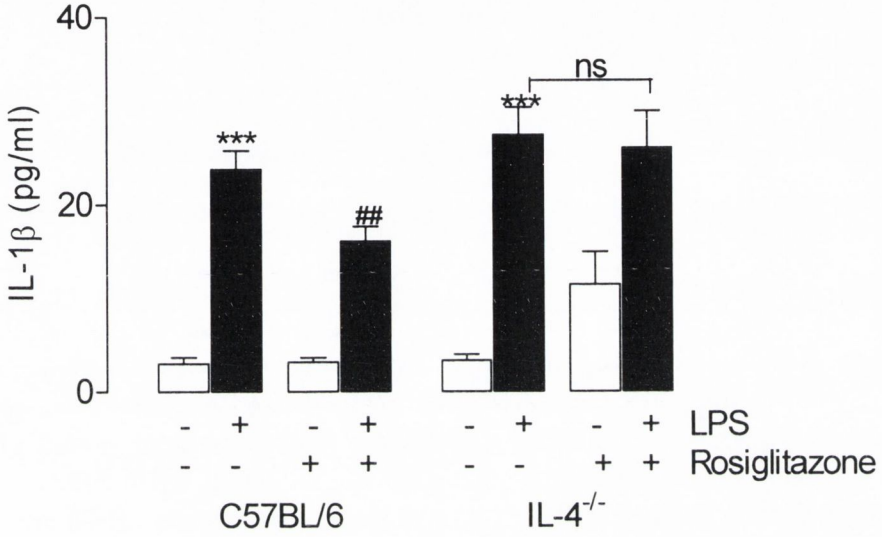
40
20
0
IL-1β (pg/ml)
***
##
ns
***
- + - + - + - + LPS
- - + + - - + + Rosiglitazone
C57BL/6
IL-4-/-

Figure 3.15. IL-4 attenuated the LPS-induced increase in IL-1β in cultured mixed glia.

LPS (1μg/ml) induced a significant increase in mean IL-1β mRNA expression and supernatant concentration of IL-1β in mixed glia, compared with control-treated mixed glia obtained from the cortex of neonatal rats (a; *p<0.05; b; ***p<0.001; ANOVA). Pretreatment of mixed glia with IL-4 (20ng/ml) significantly attenuated the LPS-induced increase in supernatant concentration of IL-1β (b; #p<0.05; ANOVA versus LPS-treated mixed glia) but not IL-1β mRNA expression (a; ANOVA versus LPS-treated mixed glia). IL-4 (20ng/ml) pretreatment did not significantly affect IL-1β mRNA expression or supernatant concentration of IL-1β. Values are presented as means (±SEM; n=6) and expressed as IL-1β:β-actin (RQ) or pg IL-1β/ml.

(a). 2-way ANOVA; LPS_{effect} F(1,20)=197.75; p<0.001, $IL\text{-}4_{effect}$ F(1,20)=4.88; p=0.067, $Interaction_{effect}$ F(1,20)=3.28; p=0.08.
(b). 2-way ANOVA; LPS_{effect} F(1,14)=5.95; p<0.05, $IL\text{-}4_{effect}$ F(1,20)=0.71; p=0.4104, $Interaction_{effect}$ F(1,20)=0.68; p=0.4188.

a

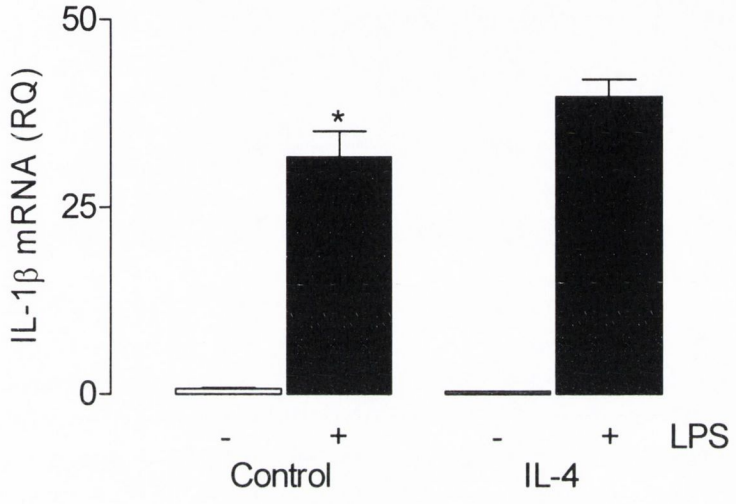
50
25
0
IL-1β mRNA (RQ)
*
- + - + LPS
Control
IL-4

b

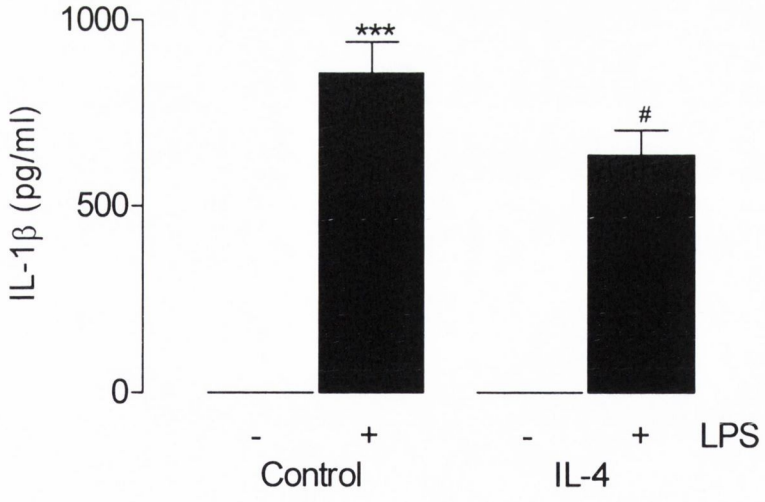
1000
500
0
IL-1β (pg/ml)
***
#
- + - + LPS
Control
IL-4

Figure 3.16. IL-4 failed to attenuate the LPS-induced increase in IL-6 in cultured mixed glia.

LPS (1μg/ml) induced a significant increase in mean IL-6 mRNA expression and supernatant concentration of IL-6 in mixed glia, compared with controls (a; *p<0.05; b; ***p<0.001; ANOVA). Pretreatment of mixed glia with IL-4 (20ng/ml) did not significantly attenuate the LPS-induced increase in IL-6 mRNA expression or supernatant concentration of IL-6 (a and b; ANOVA versus LPS-treated mixed glia). IL-4 (20ng/ml) pretreatment did not significantly affect IL-6 mRNA expression or supernatant concentration of IL-6. Values are presented as means (±SEM; n=6) and expressed as IL-6:β-actin (RQ) or pg IL-6/ml.

(a). 2-way ANOVA; LPS_{effect} F(1,20)=5.45; p<0.05, $IL\text{-}4_{effect}$ F(1,20)=0.33; p=0.5718, $Interaction_{effect}$ F(1,20)=0.77; p=0.3907.
(b). 2-way ANOVA; LPS_{effect} F(1,19)=476.40; p<0.001, $IL\text{-}4_{effect}$ F(1,19)=2.92; p=0.1039, $Interaction_{effect}$ F(1,19)=2.78; p=0.1117.

a

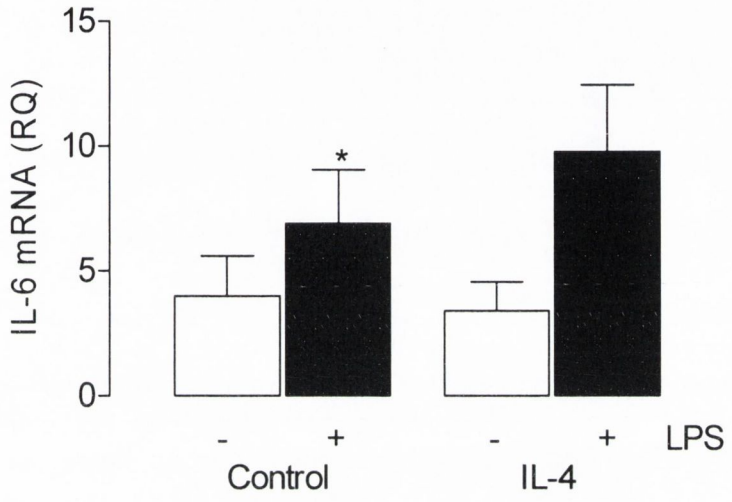
15
10
5
0
IL-6 mRNA (RQ)
*
- + - + LPS
Control
IL-4

b

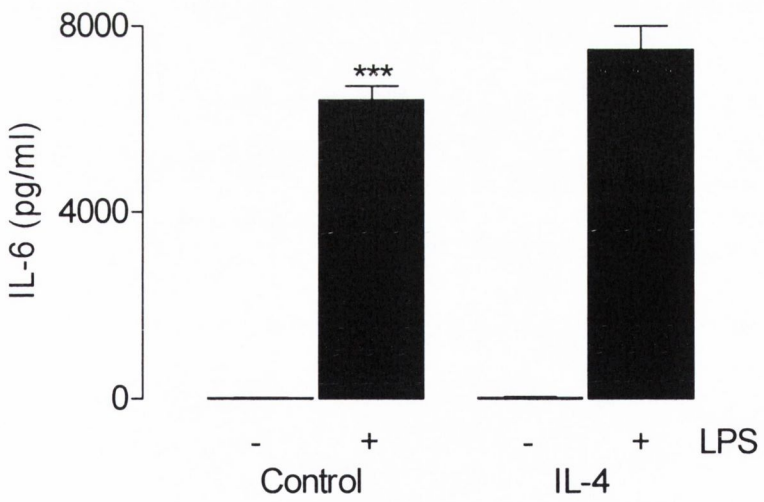
8000
4000
0
IL-6 (pg/ml)
***
- + - + LPS
Control
IL-4

Figure 3.17. IL-4 failed to attenuate the LPS-induced increase in TNFα in cultured mixed glia.

LPS (1μg/ml) induced a significant increase in mean TNFα mRNA expression and supernatant concentration of TNFα in mixed glia, compared with controls (a; *p<0.05; b; ***p<0.001; ANOVA). Pretreatment of mixed glia with IL-4 (20ng/ml) did not significantly attenuate the LPS-induced increase in TNFα mRNA expression or supernatant concetration (a and b; ANOVA versus LPS-treated mixed glia). IL-4 (20ng/ml) pretreatment did not significantly affect IL-6 mRNA expression or supernatant protein concentration. Values are presented as means (±SEM; n=6) and expressed as TNFα:β-actin (RQ) or pg TNFα/ml.

(a). 2-way ANOVA; LPS_{effect} F(1,19)=7.02; p<0.05, $IL\text{-}4_{effect}$ F(1,19)=0.27; p=0.6088, $Interaction_{effect}$ F(1,20)=0.00; p=0.9464.
(b). 2-way ANOVA; LPS_{effect} F(1,20)=211.04; p<0.001, $IL\text{-}4_{effect}$ F(1,20)=0.13; p=0.7202, $Interaction_{effect}$ F(1,20)=0.13; p=0.7202.

a

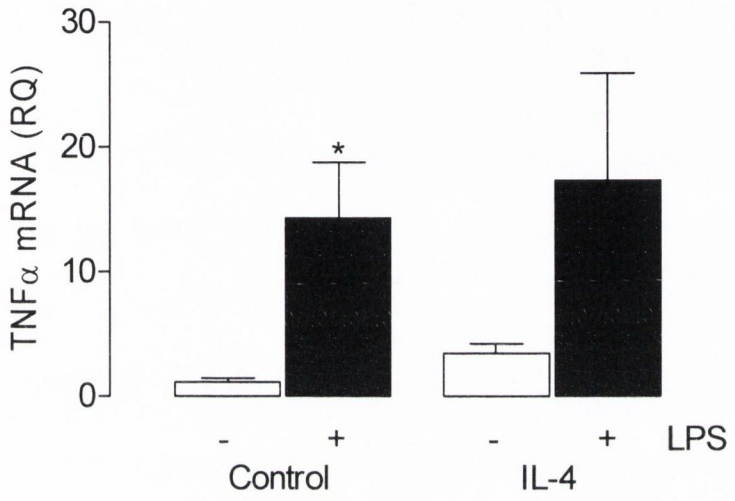
30
20
10
0
TNFα mRNA (RQ)
*
- + - + LPS
Control
IL-4

b

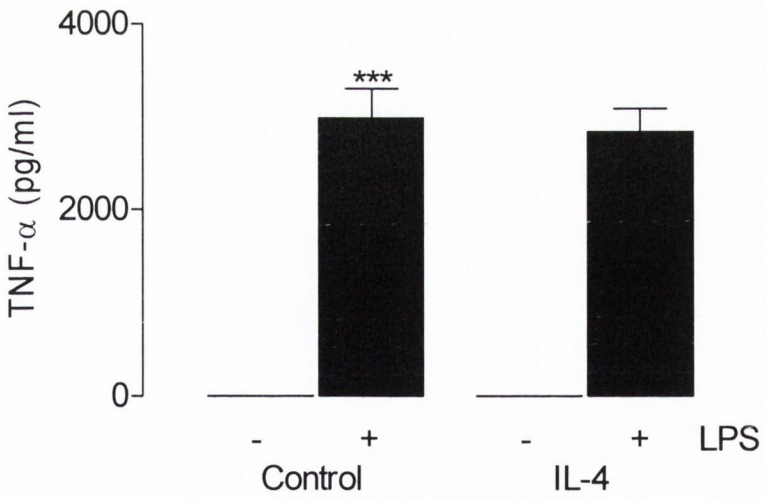
4000
2000
0
TNF-α (pg/ml)
***
- + - + LPS
Control
IL-4

Figure 3.18. IL-4 failed to attenuate the LPS-induced increase in CD40 and CD11b in cultured mixed glia.

LPS (1μg/ml) induced a significant increase in mean CD40 and CD11b mRNA expression in mixed glia, compared with controls (a; **p<0.01; b; **p<0.01; ANOVA). Pretreatment of mixed glia with IL-4 (20ng/ml) did not significantly attenuate the LPS-induced increase in CD40 or CD11b mRNA expression (a and b; ANOVA versus LPS-treated mixed glia). IL-4 (20ng/ml) pretreatment did not significantly affect CD40 or CD11b mRNA expression. Values are presented as means (±SEM; n=6) and expressed as CD40:β-actin (RQ) or CD11b:β-actin (RQ).

(a). 2-way ANOVA; LPS_{effect} F(1,19)=11.97; p<0.01, $IL\text{-}4_{effect}$ F(1,19)=4.82; p=0.0507, $Interaction_{effect}$ F(1,19)=2.39; p=0.1388.
(b). 2-way ANOVA; LPS_{effect} F(1,39)=10.27; p<0.01, $IL\text{-}4_{effect}$ F(1,39)=1.18; p=0.2841, $Interaction_{effect}$ F(1,39)=0.05; p=0.8298.

a

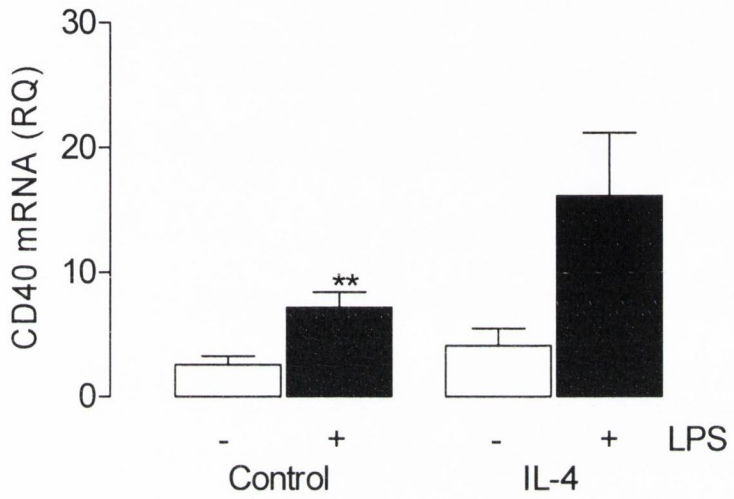
30
20
10
0
CD40 mRNA (RQ)
**
- + - + LPS
Control
IL-4

b

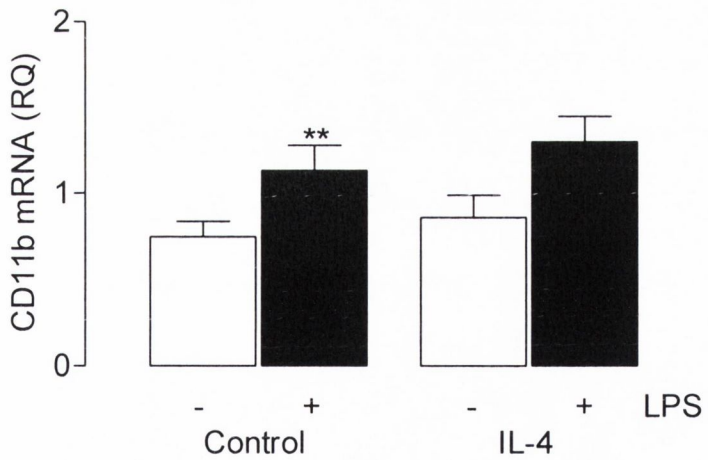
2
1
0
CD11b mRNA (RQ)
**
- + - + LPS
Control
IL-4

Chapter 4

Assessment of the anti-inflammatory properties of a novel PPARγ agonist, MDG79, on glial cells

4.1. Introduction

In the previous chapter evidence of the ability of rosiglitazone to attenuate the LPS-induced increase in pro-inflammatory cytokines *in vitro* was presented and its ability to modulate LPS-induced increases in markers of microglial activation was also demonstrated. However like all drugs PPARγ agonists have side effects, and despite the ability of rosiglitazone to modulate neuroinflammation and its success in the treatment of type II diabetes, recent reports suggest that administration of rosiglitazone is associated with an increased risk of myocardial infarction (Nissen and Wolski, 2007).

These reports have indicated the need for new PPARγ agonists that could provide the same beneficial effects in inflammation and diabetes but without the negative cardiovascular side effects. Researchers are developing and testing new drugs similar in structure to glitazones for their potential use in this area. The Molecular Design Group in Trinity College Dublin has identified a compound which is structurally different from rosiglitazone but one that also binds to PPARγ, called MDG79. In preliminary investigations using MDG79, it was shown that MDG79 modulates neuronal damage against the neurotoxin MPP^+ in dopaminergic cell lines (Davey *et al.*, unpublished).

The aim of this study was to assess whether or not the novel PPARγ agonist, MDG79, modulated LPS-induced changes in pro-inflammatory cytokines and markers of microglial activation in mixed glial cultures. An additional aim was to determine whether or not the modulatory role of MDG79 on LPS-induced changes in mixed glia was PPARγ-dependent.

4.2. Methods

Mixed glial cells were prepared from one day old Wistar rats, cultured for 10-14 days and treated with the PPARγ agonist MDG79 at four concentrations; 10, 20, 50 and 100μM in the presence and absence of LPS (1μg/ml). Analysis of supernatant cytokine concentrations were assessed by ELISA, and cytokine mRNA expression,

markers of PPARγ activity and microglial marker mRNA expression were assessed by Q-PCR (see sections 2.3., 2.4. and 2.5 for specific details).

Mixed glia were also prepared from one day old Wistar rats, cultured for 10-14 days and treated with the PPARγ antagonist GW9662 and agonist MDG79 in the presence or absence of LPS (1μg/ml). As before, analysis of supernatant cytokine concentrations were assessed by ELISA, and cytokine mRNA expression and microglial marker mRNA expression were assessed by Q-PCR (see sections 2.3., 2.4. and 2.5 for specific details).

Data are expressed as means ± standard error of the mean. Data were analysed by 1-way ANOVA and if significant changes were detected post hoc comparisons were performed using Newman Keuls test.

4.3. Results

Anti-inflammatory effects of MDG79 in vitro.

The focus continues on PPARγ agonists as potential anti-inflammatory therapeutics in neurodegenerative disease. As shown in the previous chapter rosiglitazone, a well established PPARγ agonist, has the ability to modulate LPS-induced inflammatory changes *in vitro*. More recently emphasis has been put on the development of novel and structurally-different PPARγ agonists. These agonists are designed to be more specific and to bind more tightly to the PPARγ receptor, but little is known about their ability to modulate inflammatory cytokines in the brain. The aim of this study was to establish whether MDG79, a novel PPARγ agonist, might modulate LPS-induced changes in mixed glial cells.

The ability of MDG79 to modulate LPS-induced changes in IL-1β mRNA and protein was investigated. Figure 4.1a shows that mean IL-1β mRNA expression was increased in LPS-treated glia compared with control-treated glia and this difference was statistically significant (ANOVA; $F=15.19$, $p<0.001$). Post-hoc tests after a

significant 1-way ANOVA showed that MDG79 (100μM) significantly attenuated this LPS-induced increase in IL-1β mRNA ($^{###}p<0.001$). Figure 4.1b shows that the mean supernatant concentration of IL-1β in LPS-treated glia was increased compared with control and this difference was statistically significant (ANOVA; F=12.13, $p<0.001$). Post-hoc tests following the ANOVA also showed that MDG79 alone (100μM) significantly increased IL-1β compared with control ($^{***}p<0.001$). Post-hoc analysis also showed that MDG79 pretreatment attenuated the LPS-induced increase in IL-1β in a dose-dependent manner; 10μM ($^{##}p<0.01$), 20μM ($^{###}p<0.001$), 50μM ($^{###}p<0.001$) and 100μM ($^{###}p<0.001$).

Figure 4.2 shows that LPS induced a significant increase in mean TNFα mRNA expression (a; 12.27 RQ ± 2.295; n=6) and supernatant concentration of TNFα (b; 15.53 pg/ml ± 3.295; n=6) in mixed glia, compared with controls (a; 2.078 RQ ± 0.5483; $^{***}p<0.001$; n=6; ANOVA) and (b; 0.3958 pg/ml ± 0.22; $^{*}p<0.05$; n=6; ANOVA). Pretreatment of mixed glia with MDG79 (100μM) significantly attenuated the LPS-induced increase in TNFα mRNA (a; 1.783 RQ ± 0.5882; $^{###}p<0.001$, n=6; ANOVA) and supernatant concentration of TNFα (b; 0.0608 pg/ml ± 0.032; $^{#}p<0.05$; n=6; ANOVA). Pretreatment of mixed glia with rosiglitazone (20μM) significantly attenuated the LPS-induced increase in TNFα mRNA (5.513 RQ ± 1.836; $^{#}p<0.05$; n=6; ANOVA). But did not significantly affect the LPS-induced increase in supernatant concentration of TNFα (b; 9.134 pg/ml ± 1.678; n=6; ANOVA). MDG79 (100μM) pretreatment did not significantly affect TNFα.

Figure 4.3 shows that LPS induced a significant increase in mean IL-6 mRNA expression (a; 15.78 RQ ± 2.98; n=6; ANOVA) and supernatant concentration of IL-6 (b; 376.3 pg/ml ± 66.53; n=6; ANOVA) in mixed glia, compared with controls (a; 1.406 RQ ± 0.1420; $^{***}p<0.001$; n=6; ANOVA) and (b; 90.08 pg/ml ± 34.4; $^{**}p<0.01$; n=6; ANOVA). Pretreatment of mixed glia with MDG79 (100μM) significantly attenuated the LPS-induced increase in IL-6 mRNA (a; 2.537 RQ ± 0.9750; $^{##}p<0.01$; n=6; ANOVA) and supernatant concentration of IL-6 (b; 78.46 pg/ml ± 7.831; $^{##}p<0.01$; n=6; ANOVA). Pretreatment of mixed glia with rosiglitazone (20μM) significantly attenuated the LPS-induced increase in IL-6 mRNA (a; 4.63 RQ ± 1.443; $^{##}p<0.01$; n=6; ANOVA) but not supernatant

concentration (b; 205.12 pg/ml ± 56.18; n=6; ANOVA). MDG79 (100μM) alone did not significantly affect IL-6 mRNA expression or supernatant concentration of IL-6.

Figure 4.4 shows that LPS induced a significant increase in mean CD40 mRNA (a; 6.950 RQ ± 1.2; n=6; ANOVA) and CD11b mRNA (b; 15.98 RQ ± 2.257; n=6; ANOVA) expression in mixed glia, compared with controls (a; 1.182 RQ ± 0.2841; **p<0.01; n=6; ANOVA) and (b; 0.7713 RQ ± 0.1208; ***p<0.001; n=6; ANOVA). Pretreatment of mixed glia with MDG79 (100μM) significantly attenuated the LPS-induced increase in CD40 mRNA (a; 0.44 RQ ± 0.273; $^{###}$p<0.001; n=6; ANOVA) and CD11b (b; 2.162 RQ ± 0.8210; $^{###}$p<0.001; n=6; ANOVA). Pretreatment of mixed glia with rosiglitazone (20μM) also significantly attenuated the LPS-induced increase in CD40 mRNA (a; 2.408 RQ ± 0.8984; $^{##}$p<0.01; n=6; ANOVA) and CD11b mRNA (b; 2.035 RQ ± 0.4161;$^{###}$p<0.001; n=6; ANOVA). MDG79 (100μM) alone did not significantly affect CD40 or CD11b mRNA expression.

MDG79 and PPARγ activation

The results above show that MDG79 does indeed have the ability to modulate LPS-induced inflammatory changes *in vitro* in mixed glial cells. It has the ability to attenuate mRNA expression and supernatant concentration of pro-inflammatory cytokines in a manner which is similar to rosiglitazone.

The next objective of this study was to establish if this ability to attenuate pro-inflammatory cytokines was dependent on, or independent of, PPARγ activation. Two downstream gene products of PPARγ activation were assessed, CD36 mRNA and LPL mRNA. Figure 4.5 shows that pretreatment of mixed glia with MDG79 at the three concentrations (10, 20 and 100μM) did not significantly affect CD36 mRNA (a; 0.23 RQ ± 0.11; 0.23 RQ ± 0.12; 0.23 RQ ± 0.13) or LPL mRNA (b; 0.45 RQ ± 0.08; 0.44 RQ ± 0.05; 0.46 RQ ± 0.07) expression compared with controls (a; 0.33 RQ ± 0.23; b; 0.68 RQ ± 0.10; n=6; ANOVA).

To further assess the role of PPARγ activation mixed glia were pretreated with MDG79, in the presence or absence of a PPARγ antagonist GW9662, and LPS.

Figure 4.6a shows that mean IL-1β mRNA expression was increased in LPS-treated glia compared with control-treated glia and this difference was statistically significant (ANOVA; $F=13.26$, $p<0.001$). Post-hoc tests after a significant 1-way ANOVA showed that MDG79 (100μM) significantly attenuated the LPS-induced increase in IL-1β mRNA ($^{\#}p<0.05$). Post-hoc tests showed no significant difference in IL-1β mRNA in MDG79/LPS–treated glia compared with MDG79/LPS/GW9662-treated glia, which suggested that the ability of MDG79 to attenuate the LPS-induced increase in IL-1β mRNA was not PPARγ dependent. Figure 4.6b shows that the mean supernatant concentration of IL-1β in LPS-treated glia was increased compared with control-treated glia and this difference was statistically significant (ANOVA; $F=10.26$, $p<0.001$). Post-hoc tests following the ANOVA also showed that MDG79 (100μM) significantly increased IL-1β compared with control ($^{***}p<0.001$). Post-hoc analysis also showed that MDG79 (100μM) pre-treatment significantly attenuated the LPS-induced increase in IL-1β ($^{\#\#}p<0.01$). The ability of MDG79 to attenuate this LPS-induced increase in IL-1β was found to be independent of PPARγ as post hoc tests showed no significant difference in the supernatant concentration of IL-1β in MDG79/LPS-treated glia compared with MDG79/LPS/GW9662-treated glia.

The ability of MDG79 to modulate LPS-induced changes in IL-6 mRNA and protein was investigated, and the dependence of this on PPARγ was also investigated by treating in the presence of the PPARγ antagonist GW9662. Figure 4.7a shows that mean IL-6 mRNA expression was increased in LPS-treated glia compared with control-treated glia and this difference was statistically significant (ANOVA; $F=6.645$, $p<0.01$). Post-hoc tests after a significant ANOVA showed that MDG79 (100μM) significantly attenuated the LPS-induced increase in IL-6 mRNA ($^{\#}p<0.05$). Post-hoc test showed no significant difference in IL-6 mRNA expression in MDG79/LPS-treated glia compared with MDG79/LPS/GW9662-treated glia, which suggested that the ability of MDG79 to attenuate the LPS-induced increase in IL-6 mRNA expression was not PPARγ dependent. Figure 4.7b shows that mean supernatant concentration of IL-6 in LPS-treated glia was increased compared with

control and this difference was statistically significant (ANOVA; $F=10.33$; $p<0.001$). Post-hoc tests following the ANOVA showed that MDG79 (100μM) significantly attenuated the LPS-induced increase in IL-6 ($^{###}p<0.001$). The ability of MDG79 to attenuate this LPS-induced increase in IL-6 was found to be independent of PPARγ as post hoc tests showed no significant difference in supernatant concentration IL-6 in MDG79/LPS-treated glia compared with MDG79/LPS/GW9662-treated glia

The ability of MDG79 to modulate LPS-induced changes in CD40 and CD11b mRNA expression, and whether this was dependent on PPARγ was investigated. Figure 4.8a shows that mean CD40 mRNA expression was increased in LPS-treated glia compared with control-treated glia and this difference was statistically significant (ANOVA; $F=18.52$, $p<0.001$). Post-hoc tests after a significant 1-way ANOVA showed that MDG79 (100μM) significantly attenuated this LPS-induced increase in CD40 mRNA ($^{###}p<0.001$). Post-hoc tests also showed that CD40 mRNA expression was significantly different in LPS/MDG79/GW9662-treated glia compared with MDG79/LPS-treated glia ($^{\delta\delta}p<0.01$) which suggested that MDG79 modulates CD40 mRNA expression in a PPARγ dependent manner. Figure 4.8b shows that mean CD11b mRNA expression was increased in LPS-treated glia compared with control-treated glia and this difference was statistically significant (ANOVA; $F=11.37$, $p<0.001$). Post-hoc tests after a significant 1-way ANOVA showed that MDG79 significantly attenuated this LPS-induced increase in CD11b mRNA ($^{###}p<0.001$). The ability of MDG79 to attenuate this LPS-induced increase in CD11b was found to be independent of PPARγ as post hoc tests showed no significant difference in CD11b expression in MDG79/LPS-treated glia compared with MDG79/LPS/GW9662-treated glia.

4.4. Discussion

The aims of this study were to investigate the potential of a novel PPARγ agonist, MDG79, to modulate LPS-induced increases in pro-inflammatory cytokines and markers of microglial activation in mixed glial cultures, to compare its ability to modulate these changes with that of rosiglitazone, and to investigate the dependency of any modulatory effect on PPARγ activation.

Pretreatment of mixed glia with MDG79 (100μM) significantly attenuated the LPS-induced increases in IL-1β, IL-6 and TNFα mRNA expression in a similar manner to that of rosiglitazone (20μM). The ability of MDG79 to attenuate the mRNA expression of pro-inflammatory cytokines suggests that it may act to modulate transcription of pro-inflammatory cytokines. As mentioned in the previous chapter, PPARγ agonists can modulate the transcription in both PPARγ-dependent and independent mechanisms, ultimately preventing the activation of the pro-inflammatory transcription factors NFκB and the JAK STAT signalling pathways.

Pretreatment with MDG79 attenuated the supernatant concentration of IL-1β and IL-6 at 20 and 50μM, a much lower concentration than required to attenuate the mRNA expression of both cytokines. However supernatant concentration of TNFα was significantly attenuated at a concentration of 100μM. In contrast, pretreatment with rosiglitazone did not attenuate the LPS-induced increase in the supernatant concentration of IL-6 and TNFα, confirming the data in Chapter 3. The results identify a differential effect of MDG79 at the mRNA and protein level and uncover a possible difference between MDG79 and rosiglitazone. The importance of the proteolytic cleavage of cytokines, particularly IL-1β and IL-18, as a potential mechanism in the control of inflammation has been realised in recent times (Martinon and Tschopp, 2004; Medzhitov, 2007). Inflammasomes are protein complexes that activate pro-inflammatory caspases. For example, activation of caspase 1 is required for processing two members of the IL-1 family of cytokines, IL-1β and IL-18 (Martinon and Tschopp, 2004). These cytokines are stored in an inactive form, such as pro-IL-1β, and require cleavage by caspase 1 to the active form which is subsequently secreted. The ability of MDG79 to attenuate supernatant concentration

of IL-1β suggests that it may involve an interaction with the inflammasome but further investigation is required to explore this possibility.

An increase in the supernatant concentration of IL-1β was observed in supernatants obtained from MDG79-treated, compared with control-treated, mixed glia. This was unexpected, as neither TNFα nor IL-6, nor the expression of markers of glial activation were increased with pretreatment of MDG79. Only one study in the literature presents evidence of a PPARγ agonist-induced increase in pro-inflammatory cytokines. The study was conducted in pigs where injection of rosiglitazone (3mg/kg) in combination with LPS (100μg/kg) induced a significantly greater increase in TNFα and IL-6 mRNA and protein concentration in the spleen and thymus compared with LPS-injected animals (Liu et al., 2009).

In the brain, microglia express cell surface markers and the expression of certain markers such as CD40, CD11b and MHCII can be upregulated in response to stress, age or stimuli such as LPS (Loane et al., 2009; Minagar et al., 2002; Schintu et al., 2009; Sun et al., 2008). In this study a significant increase in CD40 and CD11b mRNA in response to LPS (1μg/ml) was observed which supports the data presented in the previous chapter. Pretreatment with the highest concentration of MDG79 significantly attenuated the LPS-induced increase in the expression of both CD40 and CD11b mRNA expression. This corresponds with the ability of rosiglitazone to attenuate the expression of both CD40 and CD11b, and it is well established in the literature that PPARγ agonists modulate LPS- and IFNγ-induced increases in MHCII, CD40 and CD11b (Bernardo and Minghetti, 2006; Loane et al., 2009; Schintu et al., 2009).

MDG79 is clearly able to attenuate the LPS-induced increase in pro-inflammatory cytokines whether the anti-inflammatory action of MDG79, and indeed PPARγ agonists, is PPAR-dependent remains to be established

In this study I investigated whether MDG79 had an affect on PPARγ activation by examining changes in CD36 and LPL mRNA which are two gene products of PPARγ activation (Berger and Moller, 2002). CD36 is a class B scavenger receptor, its function is to scavenge oxidised LDL particles and take up

cholesterol into macrophages; and its expression has been shown to be dependent on PPARγ activation (Hodgkinson and Ye, 2003). Evidence in the literature shows that the PPARγ agonists; $15dPGJ_2$, ciglitazone and rosiglitazone, increase CD36 mRNA expression in macrophages and that the dependence of CD36 expression on PPARγ activation is demonstrated as treatment of J774 cells and NIH-3T3 (both cell types do not express PPARγ) with troglitazone failed to induce an increase in CD36 mRNA expression (Chawla et al., 2001; Hodgkinson and Ye, 2003).

No change in CD36 mRNA expression in response to MDG79 treatment was observed in mixed glia, which suggests that the abilty of MDG79 to modulate inflammatory cytokines in mixed glia is PPARγ independent. This is reminiscent of the findings of Loane and colleagues (2009) who reported that in the hippocampus of rosiglitazone-treated animals CD36 mRNA and protein were unaffected by rosiglitazone treatment (Loane et al., 2009). In order to further examine this LPL expression in the same mixed glia cells was assessed. LPL is a reliable marker of PPARγ activation, for example, pioglitazone has been shown to increase LPL mRNA in white adipose tissue and in adipocytes via the stimulation of PPARγ (Bogacka et al., 2004; Kageyama et al., 2003). No change in LPL mRNA expression in response to treatment of mixed glia with MDG79 was observed.

These data therefore indicate that MDG79 appears to act in a manner independent of PPARγ activation, at least if the proxy markers of two downstream gene products is an acceptable measure of activation. To further investigate and obtain confirmatory data I examined whether the PPARγ antagonist, GW9662, abrogated the modulatory effect of MDG79 on LPS-induced changes. GW9662 is a potent, selective, and irreversible antagonist of PPARγ (Leesnitzer et al., 2002). The data indicate that GW9662 failed to modulate the inhibitory effect of MDG79 on LPS-induced mRNA expression and supernatant concentration of IL-1β and IL-6 in mixed glia. This further suggests that the modulatory role of MDG79 was independent of PPARγ. Numerous reports in the literature have previously reported that the anti-inflammatory effects of PPARγ agonists are independent of PPARγ activity. Castrillo and colleagues (2001) reported that $15dPGJ_2$, and other non-thiazolidinedione PPARγ agonists, inhibited TNFα and IL-6 secretion in a murine

microglial cell line that expresses negligible PPARγ (Castrillo et al., 2001). It was shown that GW9662 failed to reverse the attenuation of the LPS-induced increase in IL-1β by rosiglitazone in mixed glia (Loane et al., 2009) and that rosiglitazone exhibited an anti-inflammatory action in the murine microglial cell line, BV2, despite undetectable levels of PPARγ transcripts (Park et al., 2003).

However GW9662 did modulate the inhibitory effect of MDG79 on LPS-induced mRNA expression of CD40 and CD11b. This suggests that MDG79 downregulates the expression of the cell surface proteins CD40 and CD11b in a PPARγ dependent mechanism and therefore it might be tentatively proposed that while expression of cell surface markers can be modulated by PPARγ activation, modulation of inflammatory cytokines can not. The ability of PPARγ agonists to attenuate the TNFα and IFNγ induced increase in CD40 mRNA expression has been demonstrated in human renal proximal tubular epithelial (HK-2) cells, and this attenuation was partly abrogated by GW9662 (Zhang et al., 2006). Bernardo and colleagues (2005) demonstrated that the attenuation in MHC II expression by microglia is PPARγ dependent, and interestingly experiments in microglia by the same authors indicate that an NSAID, a flubriprofen derivate HCT1026, attenuated NO release from activated microglia. The anti-inflammatory affect was abrogated by treatment with GW9662 but the drug itself did not alter PPARγ expression (Bernardo et al., 2005). As Landreth and colleagues note, there is no common consensus on what is the dominant mode of PPARγ action, and it is probable that PPARγ agonists act through multiple pathways to affect disease pathophysiology in both humans and animal models of disease (Landreth et al., 2008).

Chapter 4
Figures

Figure 4.1. MDG79 attenuated the LPS-induced increase in IL-1β in cultured mixed glia.

a.) Relative quantification of IL-1β mRNA in mixed glia pre-treated with MDG79 (10-100μM) in the presence or absence of LPS (1μg/ml). Data are expressed as the fold difference in IL-1β relative to control (RQ), and data are presented as means (±SEM; n=4-6). ***=p<0.001, Newman Keuls post hoc test, LPS-treated versus control. ###=p<0.001, Newman Keuls post-hoc test, LPS/MDG79 100μM treated versus LPS-treated.**b).** Supernatant concentration of IL-1β measured by ELISA in mixed glia pre-treated with MDG79 (10-100μM) in the presence or absence of LPS (1μg/ml). Data are expressed as pgIL-1β/ml and presented as means (±SEM; n=4-6). ***=p<0.001, Newman Keuls post-hoc test, control versus LPS-treated. ***=p<0.001, Newman Keuls post-hoc test, control versus MDG79-treated. ##=p<0.01, ###=p<0.001, Newman Keuls post-hoc test, LPS-treated versus LPS/MDG79-treated (10-100μM).

(a). 1-way ANOVA; LPS_{effect} F(1,39)=15.19; p<0.001,
(b). 1-way ANOVA; LPS_{effect} F(1,40)=12.13; p<0.001.

a

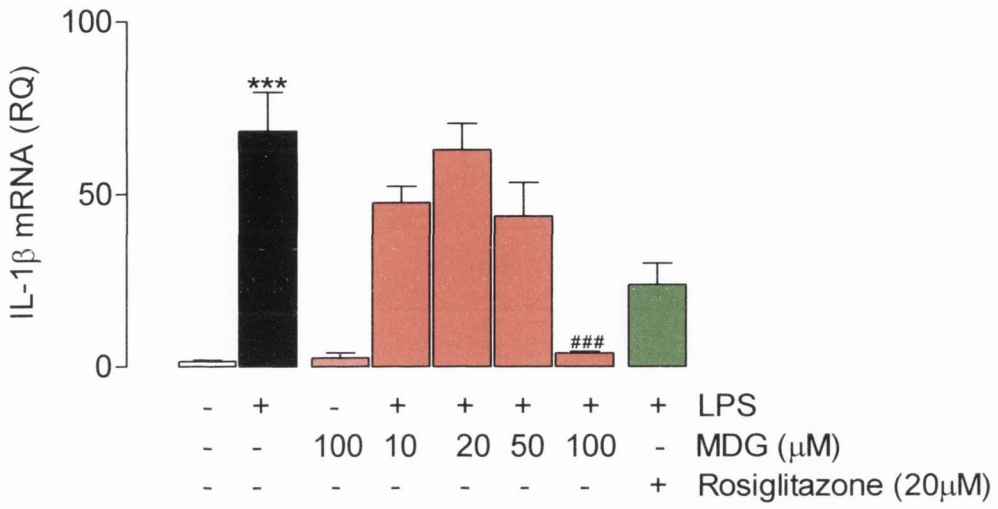
100
50
0
IL-1β mRNA (RQ)
***
###
- + - + + + + + LPS
- - 100 10 20 50 100 - MDG (μM)
- - - - - - - + Rosiglitazone (20μM)

b

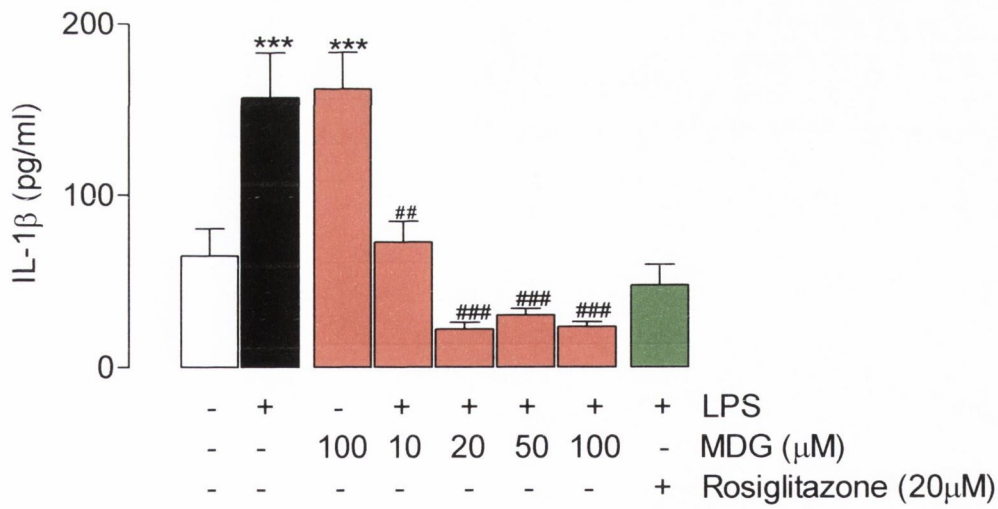
200
100
0
IL-1β (pg/ml)
***
***
##
###
###
###
- + - + + + + + LPS
- - 100 10 20 50 100 - MDG (μM)
- - - - - - - + Rosiglitazone (20μM)

Figure 4.2. MDG79 attenuated the LPS-induced increase in TNFα in cultured mixed glia.

LPS (1μg/ml) induced a significant increase in mean TNFα mRNA expression and supernatant concentration of TNFα in mixed glia, compared with controls (a; ***$p<0.001$; b; *$p<0.05$; ANOVA). Pretreatment of mixed glia with MDG79 (100μM) significantly attenuated the LPS-induced increase in TNFα mRNA and supernatant concentration (a; $^{\#\#\#}p<0.001$; b; $^{\#}p<0.05$; ANOVA versus LPS-treated mixed glia). MDG79 (100μM) pretreatment did not significantly affect TNFα mRNA expression or supernatant concentration. Values are presented as means (±SEM; n=6) and expressed as TNFα:β-actin (RQ) or pg TNFα/ml.

(a). 1-way ANOVA; LPS_{effect} $F(1,37)=6.284$; $p<0.001$,
(b). 1-way ANOVA; LPS_{effect} $F(1,37)=5.032$; $p<0.01$.

a

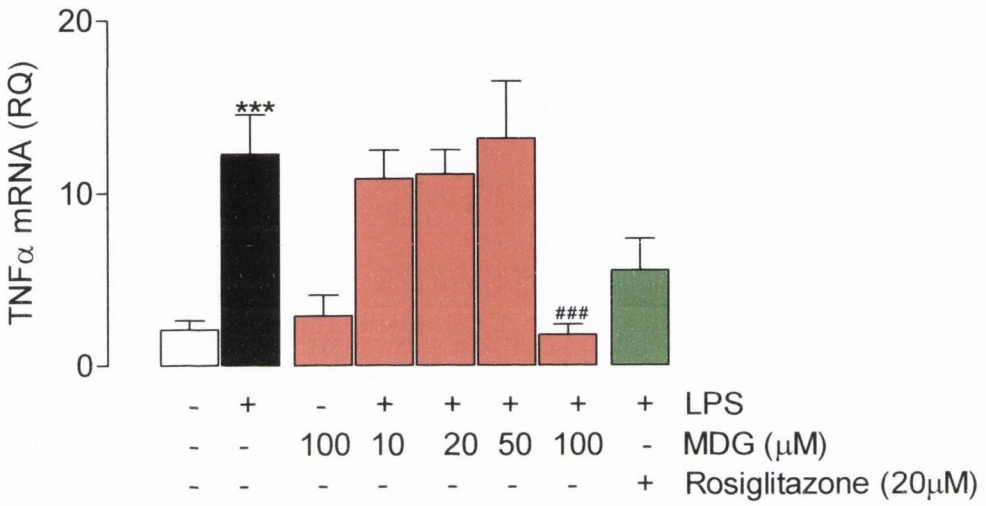
TNFα mRNA (RQ)
20
10
0
***
###
- + - + + + + + LPS
- - 100 10 20 50 100 - MDG (μM)
- - - - - - - + Rosiglitazone (20μM)

b

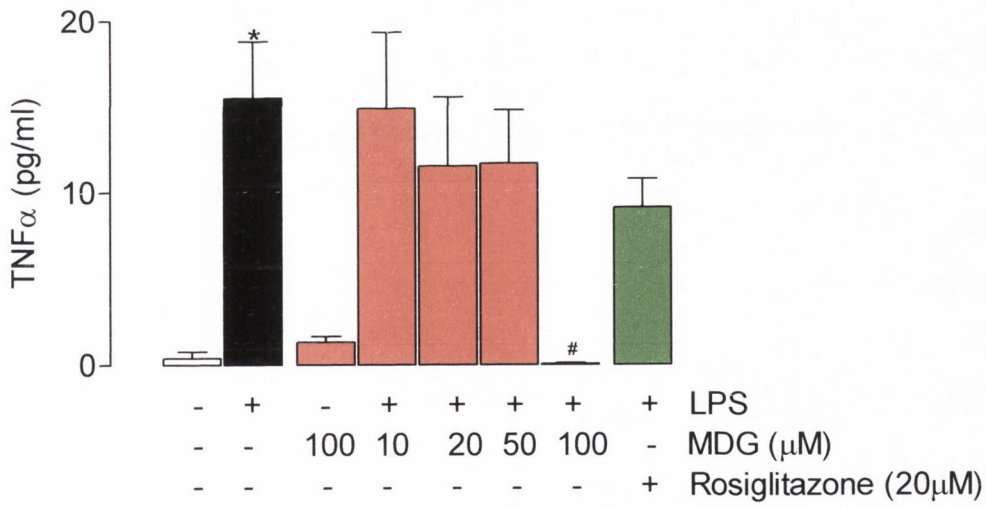
TNFα (pg/ml)
20
10
0
*
#
- + - + + + + + LPS
- - 100 10 20 50 100 - MDG (μM)
- - - - - - - + Rosiglitazone (20μM)

Figure 4.3. MDG79 attenuated the LPS-induced increase in IL-6 in cultured mixed glia.

LPS (1μg/ml) induced a significant increase in mean IL-6 mRNA expression and supernatant concentration of IL-6 in mixed glia, compared with controls (a; ***$p<0.001$; b;**$p<0.01$; ANOVA). Pretreatment of mixed glia with MDG79 (100μM) significantly attenuated the LPS-induced increase in IL-6 mRNA (a; $^{\#\#}p<0.01$) and pretreatment with MDG79 (20, 50 and 100μM) attenuated supernatant concentration of IL-6 (b; $^{\#}p<0.05$; $^{\#\#}p<0.01$; ANOVA versus LPS-treated mixed glia). MDG79 (100μM) pretreatment did not significantly affect IL-6 mRNA expression or supernatant concentration of IL-6. Values are presented as means (±SEM; n=6) and expressed as IL-6:β-actin (RQ) or pg IL-6/ml.

(a). 1-way ANOVA; LPS_{effect} $F(1,38)=8.956$; $p<0.001$,
(b). 1-way ANOVA; LPS_{effect} $F(1,37)=6.075$; $p<0.001$

a

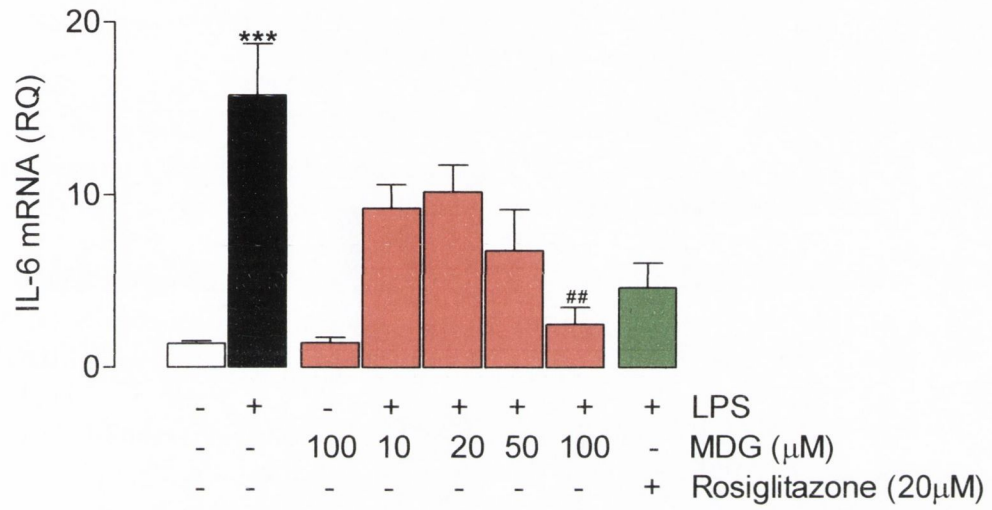
IL-6 mRNA (RQ)
20
10
0
***
##
- + - + + + + + LPS
- - 100 10 20 50 100 - MDG (μM)
- - - - - - - + Rosiglitazone (20μM)

b

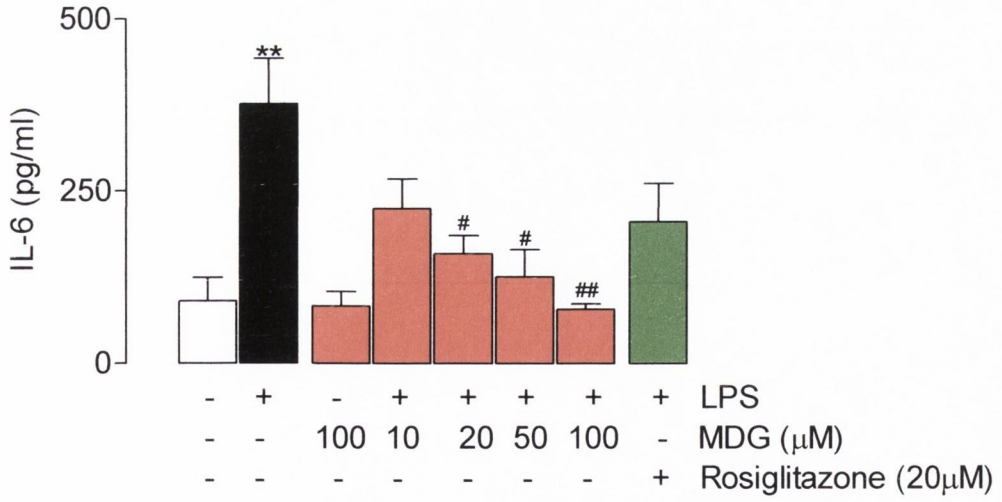
IL-6 (pg/ml)
500
250
0
**
#
#
##
- + - + + + + + LPS
- - 100 10 20 50 100 - MDG (μM)
- - - - - - - + Rosiglitazone (20μM)

Figure 4.4. MDG79 attenuated the LPS-induced increase in CD40 and CD11b in cultured mixed glia.

LPS (1μg/ml) induced a significant increase in mean CD40 and CD11b mRNA expression in mixed glia, compared with controls (a; **p<0.01; b; ***p<0.001; ANOVA). Pretreatment of mixed glia with MDG79 (100μM) significantly attenuated the LPS-induced increase in CD40 mRNA and CD11b (a; $^{###}$p<0.001; b; $^{###}$p<0.001; ANOVA versus LPS-treated mixed glia). MDG79 (100μM) pretreatment did not significantly affect CD40 or CD11b mRNA expression. Values are presented as means (±SEM; n=6) and expressed as CD40:β-actin (RQ) or CD11b:β-actin (RQ).

(a). 1-way ANOVA; LPS_{effect} F(1,31)=4.761; p<0.01,
(b). 1-way ANOVA; LPS_{effect} F(1,36)=12.12; p<0.001,

a

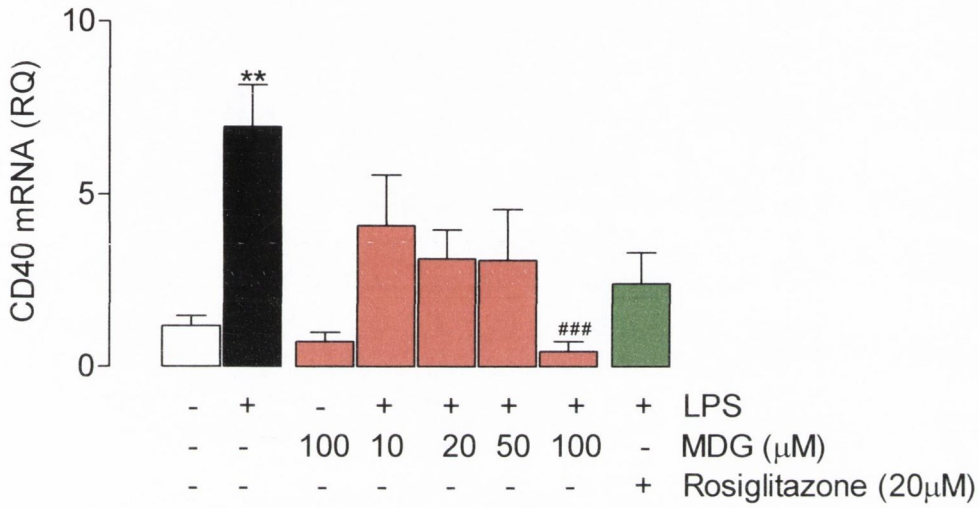
CD40 mRNA (RQ)
10
5
0
**
###
- + - + + + + + LPS
- - 100 10 20 50 100 - MDG (μM)
- - - - - - - + Rosiglitazone (20μM)

b

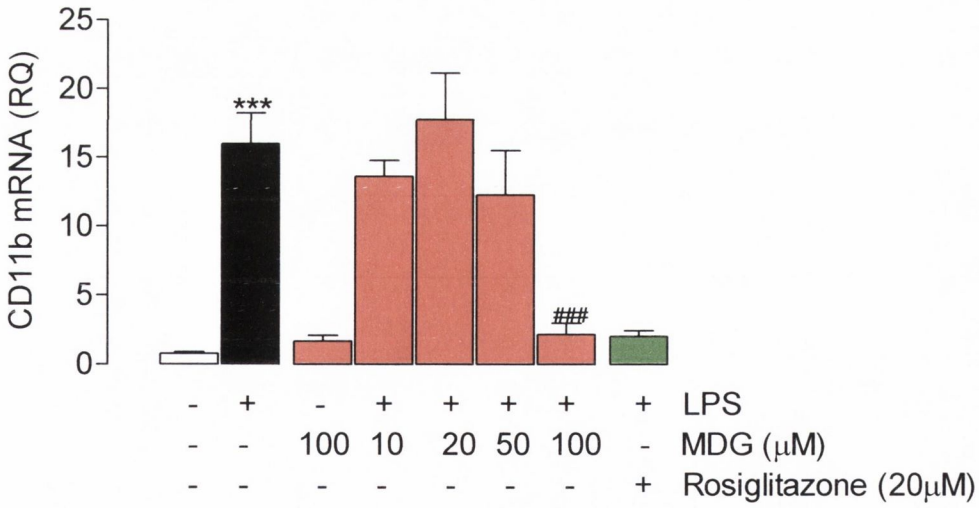
CD11b mRNA (RQ)
25
20
15
10
5
0
***
###
- + - + + + + + LPS
- - 100 10 20 50 100 - MDG (μM)
- - - - - - - + Rosiglitazone (20μM)

Figure 4.5. MDG79 treatment did not change CD36 or LPL mRNA expression in cultured mixed glia.

Treatment of mixed glia with MDG79 (10, 20 or 100μM) did not significantly change CD36 mRNA or LPL mRNA expression (a and b; ANOVA versus control-treated mixed glia). Values are presented as means (±SEM; n=6) and expressed as CD36:β-actin (RQ) or LPL:β-actin (RQ).

(a). 1-way ANOVA; MDG_{effect} F(1,14)=0.090; p=0.9640.
(b). 1-way ANOVA; MDG_{effect} F(1,19)=1.995; p=0.1553.

a

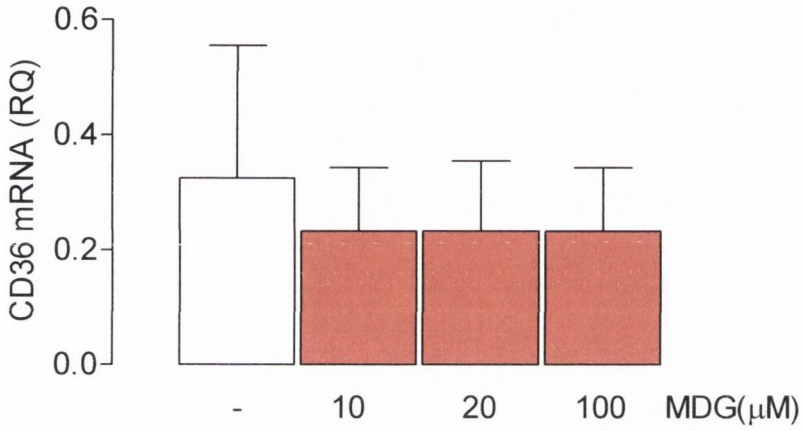
0.6
0.4
0.2
0.0
CD36 mRNA (RQ)
-
10
20
100
MDG(μM)

b

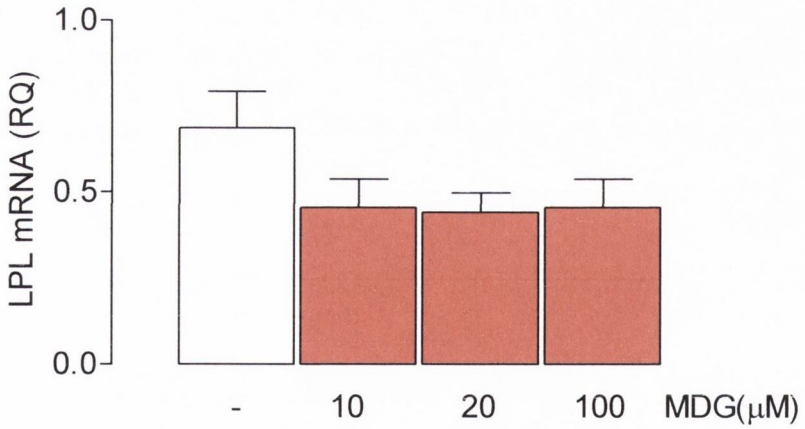
1.0
0.5
0.0
LPL mRNA (RQ)
-
10
20
100
MDG(μM)

Figure 4.6. GW9662 did not reverse the ability of MDG79 to attenuate the LPS-induced increase in IL-1β.

a).Relative quantification of IL-1β mRNA in mixed glia pre-treated with MDG79 (100μM), or MDG79 (100μM) in combination with GW9662 (20μM), in the presence or absence of LPS (1μg/ml). Data are expressed as the fold difference in IL-1β mRNA relative to control (RQ) and data are presented as means (±SEM; n=5-6). **=$p<0.01$, Newman Keuls post-hoc test, LPS-treated versus control. #=$p<0.05$, Newman Keuls post-hoc test, LPS-treated versus MDG79/LPS-treated. b). Supernatant concentration of IL-1β measured by ELISA in mixed glia pre-treated with MDG79 (100μM) or MDG79 (100μM) in combination with GW9662 (20μM), in the presence or absence of LPS (1μg/ml). Data are expressed as pgIL-1β/ml and presented as means (±SEM; n=5-6). ***=$p<0.001$, Newman Keuls post-hoc test, LPS-treated versus control. ***$p<0.001$, Newman Keuls post-hoc test, MDG79-treated versus control, ##=$p<0.01$, Newman Keuls post-hoc test, MDG79/LPS-treated versus LPS-treated.

(a). 1-way ANOVA; LPS_{effect} $F(1,18)=13.26$; $p<0.001$.
(b). 1-way ANOVA; LPS_{effect} $F(1,30)=10.26$; $p<0.001$.

a

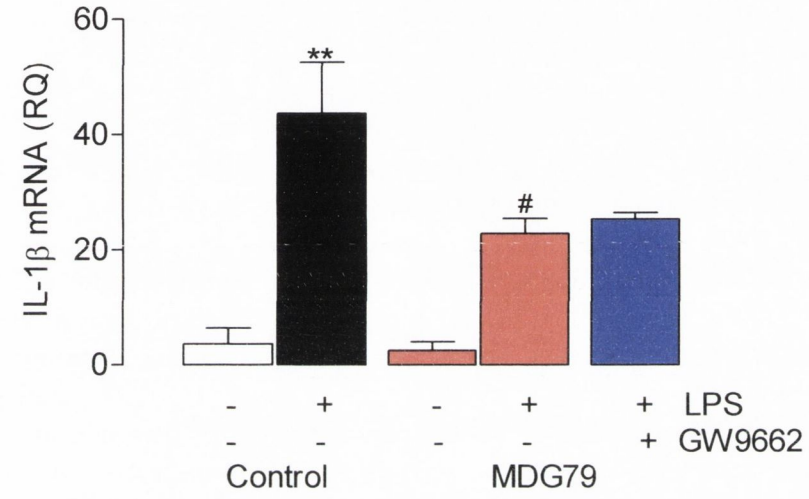
60
40
20
0
IL-1β mRNA (RQ)
**
#
- + - + + LPS
- - - - + GW9662
Control
MDG79

b

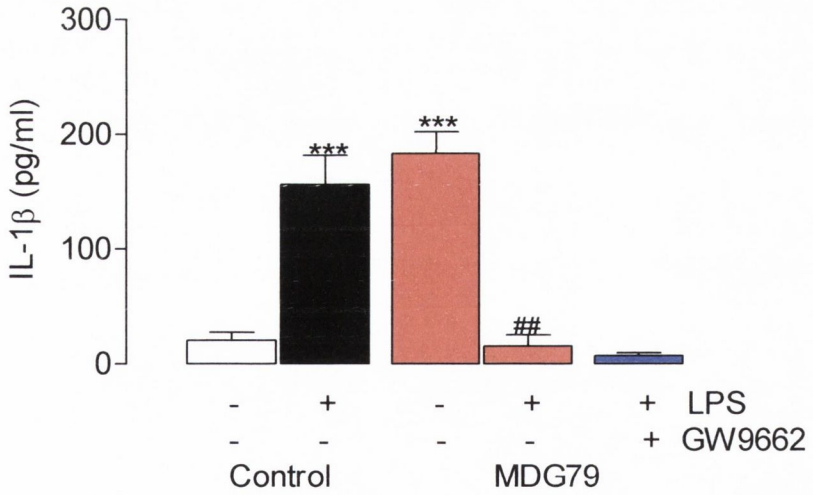
300
200
100
0
IL-1β (pg/ml)
***
***
##
- + - + + LPS
- - - - + GW9662
Control
MDG79

Figure 4.7. GW9662 did not reverse the ability of MDG79 to attenuate the LPS-induced increase in IL-6.

a). Relative quantification of IL-6 mRNA in mixed glia pre-treated with MDG79 (100μM), or MDG79 (100μM) in combination with GW9662 (20μM), in the presence or absence of LPS (1μg/ml). Data are expressed as the fold change in IL-6 mRNA relative to control (RQ) and presented as means (±SEM; n=6). **=$p<0.01$, Newman Keuls post hoc test, LPS-treated versus control. #= $p<0.05$, Newman Keuls post-hoc test, MDG79/LPS-treated versus LPS-treated. b). Supernatant concentration of IL-6 measured by ELISA in mixed glia pre-treated with MDG79 (100μM) or pre-treated with MDG79 (100 μM) in combination with GW9662 (20μM), in the presence or absence of LPS (1μg/ml). Data are expressed as pgIL-6/ml and presented as means (±SEM; n=6). ***=$p<0.001$, Newman Keuls post-hoc test LPS-treated versus control. ###=$p<0.001$, Newman Keuls post-hoc test, LPS-treated versus MDG79/LPS-treated.

(a). 1-way ANOVA; LPS_{effect} $F(1,20)= 6.645$; $p<0.01$.
(b).1-way ANOVA; LPS_{effect} $F(1,29)=10.33$; $p<0.001$.

a

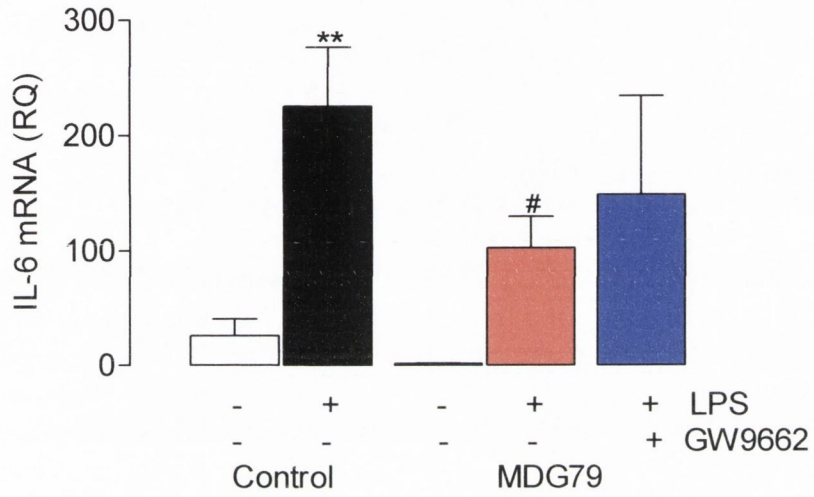
IL-6 mRNA (RQ)
300
200
100
0
**
#
- + - + + LPS
- - - - + GW9662
Control
MDG79

b

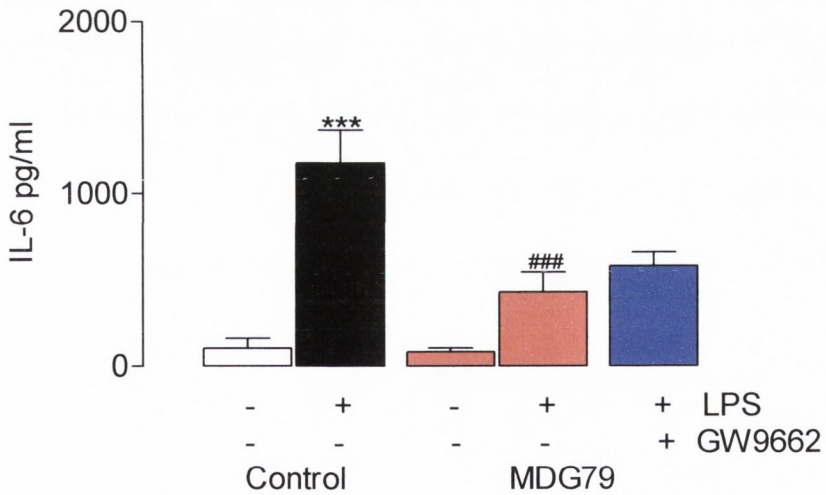
IL-6 pg/ml
2000
1000
0
***
###
- + - + + LPS
- - - - + GW9662
Control
MDG79

Figure 4.8. GW9662 did reverse the ability of MDG79 to attenuate the LPS-induced increase in CD40 and but not CD11b

a). Relative quantification of CD40 mRNA in mixed glia pre-treated with MDG79 (100μM), or pre-treated with MDG79 (100μM) in combination with GW9662 (20μM), in the presence or absence of LPS (1μg/ml). Data are expressed as the fold change in CD40 relative to control (RQ), and presented as means (±SEM; n=6). ***=$p<0.001$, Newman Keuls post-hoc test, LPS-treated versus control. ###=$p<0.001$, Newman Keuls post-hoc test LPS-treated versus MDG79/LPS-treated. δδ=$p<0.01$, Newman Keuls post-hoc test, MDG79/LPS-treated versus MDG79/GW9662/LPS-treated.

b). Relative quantification of CD11b mRNA in mixed glia pre-treated with MDG79 (100μM), or pre-treated with MDG79 (100μM) in combination with GW9662 (20μM), in the presence or absence of LPS (1μg/ml). Data are expressed as the fold change in CD11b relative to control (RQ), and presented as means (±SEM; n=6). **=$p<0.01$, Newman Keuls post-hoc test, LPS-treated versus control treated. ###=$p<0.001$, Newman Keuls post-hoc test, MDG79/LPS-treated versus LPS-treated.

(a). 1-way ANOVA; LPS_{effect} $F(1,23)=18.52$; $p<0.001$.
(b).1-way ANOVA; LPS_{effect} $F(1,21)=11.37$ $p<0.001$.

a

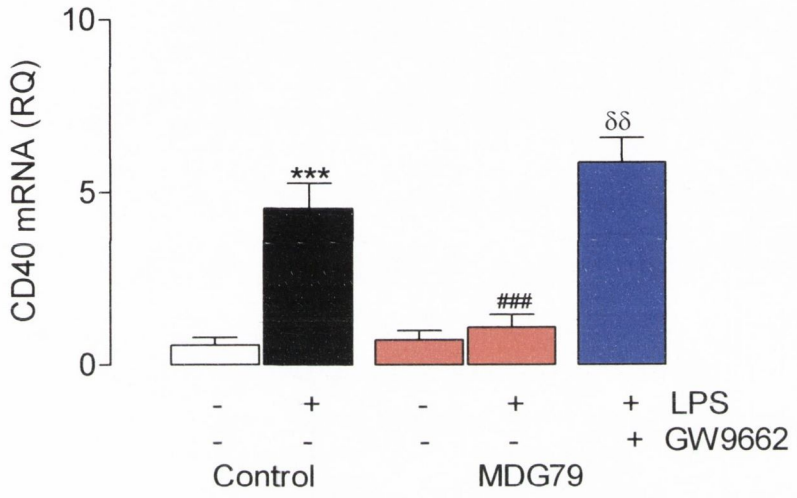
10
5
0
CD40 mRNA (RQ)
***
δδ
###
- + - + + LPS
- - - - + GW9662
Control
MDG79

b

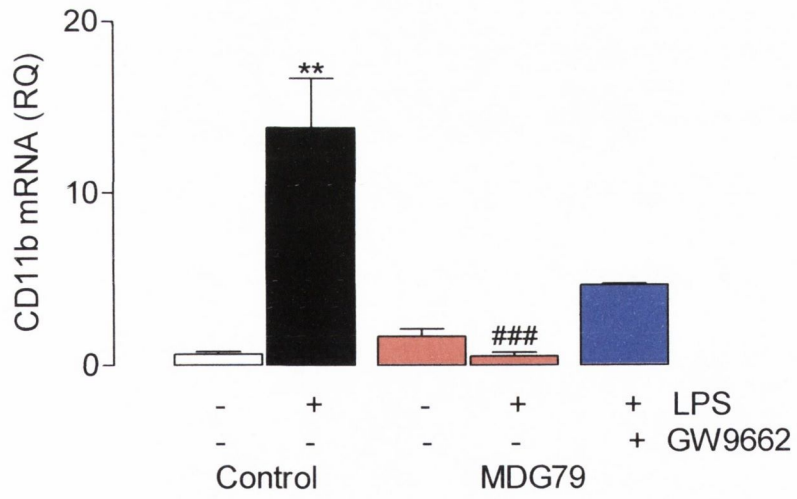
20
10
0
CD11b mRNA (RQ)
**
###
- + - + + LPS
- - - - + GW9662
Control
MDG79

Chapter 5

Microglial activation in EAE prior to and after the onset of clinical symptoms

5.1. Introduction

Multiple sclerosis (MS) and its animal model EAE are chronic demyelinating diseases of the CNS. It is generally agreed that MS and EAE begin with acute inflammatory lesions characterised by the breakdown of the BBB (McFarland and Martin, 2007). This allows the migration of $CD4^+$ T cells into the brain, the presentation of antigen to the T cells by microglia and the subsequent recruitment of B cells, macrophages, dendritic cells and microglia that amplifies the inflammatory response and the demyelination of the axons.

The antigen in EAE and MS is one of the myelin proteins that form the insulating sheath along the axon, which include MBP, PLP and MOG. The principle behind the disease model is the development of an immune response to the myelin peptide and the disease progression is enhanced by a combination of adjuvant (CFA) and mycobacterium which results in the appearance of clinical symptoms that permit the monitoring of disease progression.

It is well established that $CD4^+$ T cells, particularly Th1 and Th17 cells play an important role in EAE disease progression, both IL-6 and TNFα cytokines produced by T cells are found in the lesions of the MS brain. Importantly though, the extent of axonal damage in EAE correlates with the number of microglia/macrophage at the lesion site (Kuhlmann et al., 2002). Activated microglia contribute to disease pathology as they function not only as antigen presenting cells but also produce pro-inflammatory cytokines. Cytokines such as TNFα, and IL-1β produced by microglia have the potential to enhance inflammation in the brain and spinal cord by promoting the destruction of myelin (Martin and Near, 1995). Activated microglia have been shown to express a number of immunologically relevant molecules including CD40 (Tan et al., 1999). CD40 is a member of the TNF receptor family of cell surface proteins. Microglia expressing CD40 interact with CD40L positive T cells and the interactions play a role in the activation of cells of the monocytic lineage and contribute to the inflammatory process (Alderson et al., 1993).

Recent reports have highlighted the importance of cell-cell interactions in the regulation of microglial activation. One such system involves the CD200-CD200R

interaction. CD200, which is expressed on neurons, interacts with its receptor, which is expressed on cells of the myeloid lineage, primarily microglia. Evidence in the literature suggests that the CD200-C200R interaction exerts an inhibitory signal to microglia that suppresses their proliferation and activation and the subsequent production of NO and cytokines thus protecting neurons from the inflammatory damage that occurs in AD, MS and in EAE (Meuth et al., 2008b). Studies conducted in $CD200^{-/-}$ mice identified that EAE disease onset occurred earlier in $CD200^{-/-}$, compared with wildtype, mice and that this was accompanied by increased microglial activation (Hoek et al., 2000). Similarly experiments have shown that antibody mediated blockade of CD200R leads to an aggravated clinical course and outcome of EAE in rats and selective elevation of CD200 on CNS neurons which, in turn, resulted in diminished accumulation of macrophages and microglia in the CNS, and reduced expression of pro-inflammatory cytokines (Chitnis et al., 2007).

Cognitive decline has been reported in MS patients in particular the ability to learn and remember new information (Thornton et al., 2002). The presence of demyelinating lesions in the hippocampus of MS patients has been documented and may be the cause of the underlying cognitive decline (Geurts et al., 2007). Further evidence has shown that there is selective hippocampal atrophy in EAE in the CA1 region which is associated with deficits in memory encoding and retrieval (Sicotte et al., 2008).

The aim of this study was to monitor pro-inflammatory cytokine production in EAE both prior to and after the onset of clinical symptoms both in the spleen, spinal cord and hippocampus. A second aim was to investigate the role of CD200 in EAE and to establish whether changes in CD200 were correlated with changes in microglial activation in this condition as well as others.

5.2. Methods

Mice (C57BL/6) were injected subcutaneously with 150μg myelinoligodendrocyte glycoprotein (MOG_{35-55}), CFA and Mycobacteria tuberculosis at Day 0 and an intraperitoneal injection of PT at Day 0 and Day 2. Clinical scores

were assessed daily and disease severity was graded as follows: grade 0 – normal; grade 1 – flaccid tail; grade 2 – wobbly gait; grade 3 – hind limb weakness; grade 4 – hind limb paralysis; grade 5 – tetraparalysis/death.

Mice were sacrificed at predetermined time points to allow the disease progression to be assessed. The time points were 0.5, 3, 5, 7, 10, and 21 days post MOG injection. The spinal cord, hippocampus and spleen were removed and stored for later analysis. Analysis of microglial markers, neuronal markers and cytokine mRNA were assessed by PCR and cytokine concentrations were assessed by ELISA (see sections 2.3., 2.4. and 2.5. for specific details). Data are expressed as means ± standard error of the mean. A 1-way ANOVA was performed to determine whether significant differences existed and post-hoc comparisons using Newman Keuls post-hoc tests were performed in the event of main effects of EAE during the timecourse.

5.3. Results

EAE was induced in C57BL/6 mice and clinical symptoms were scored.

Clinical scores for EAE were assessed daily for the duration of the study. Figure 5.1 shows the appearance of clinical scores of EAE 7 days post MOG injection. Average clinical scores increased in the mice at each day post immunisation. None of the animals in the control group developed any clinical symptoms of EAE and therefore did not score above 0 throughout the study.

Glial cells and cytokine production in the spinal cord during EAE

Figure 5.2 shows that IL-1β mRNA expression was significantly increased in the spinal cord 5 days (a; 5.74 RQ ± 0.98; n=6), 10 days (a; 26.85 RQ ± 6.89; n=6) and 21 days (a; 20.51 RQ ± 3.02; n=6) post MOG injection compared with controls (a; 1.05 RQ ± 0.2; n=6; **$p<0.01$, ***$p<0.001$; ANOVA). Figure 5.2 indicates that IL-1β concentration was significantly increased in the spinal cord 10 days (b; 83.23 pg/mg ± 17.01; n=6) and 21 days (b; 71.95 pg/mg ± 8.61; n=6) post MOG injection compared with controls (b; 26.64 pg/mg ± 9.16; n=6; ***$p<0.001$; ANOVA).

Figure 5.3 shows that neither IL-6 mRNA expression (Figure 5.3a) nor IL-6 concentration (Figure 5.3b) changed significantly at any of the time points post MOG injection.

TNFα mRNA expression was investigated in the spinal cord of mice 0.5-21 days post-MOG injection. Figure 5.4a shows that TNFα mRNA was increased in EAE and this difference was statistically significant (ANOVA, $F=6.809$, $p<0.001$). Post-hoc test after a significant 1-way ANOVA showed that TNFα mRNA expression 10 days post-MOG injection was significantly different when compared with control (***$p<0.001$). Figure 5.4b shows that TNFα protein concentration was decreased in EAE and this difference was statistically significant (ANOVA, $F=3.553$, $p<0.01$). Although differences TNFα are apparent from the graph, no significant differences were detected by post hoc comparisons between control and any time point. The inability to detect significant differences by post hoc tests may be due to the high variability in of the data in the 21 day time point.

Figure 5.5 shows that CD40 mRNA expression increased over time following MOG injection. Expression was significantly increased in the spinal cord 7 days (a; 3.47 RQ ± 0.49; n=6) and 21 days (a; 6.53 RQ ± 0.24; n=6) post MOG injection compared with controls (a; 1.18 RQ ± 0.63; n=6; *$p<0.05$, ***$p<0.001$; ANOVA). Data suggests that one factor which modulates microglial activation is CD200 and interestingly Figure 5.5 also shows that CD200 mRNA expression was significantly decreased in the spinal cord 21 days (b; 0.599 RQ ± 0.119; n=6) post MOG injection compared with controls (b; 1.08 RQ; n=6; *$p<0.05$; ANOVA). This indicates that an inverse relationship between CD40 mRNA and CD200 mRNA exists.

IL-4 mRNA expression was investigated in the spinal cord of mice 0.5-21 days post-MOG injection. Figure 5.6 shows that IL-4 mRNA expression was unchanged in EAE (ANOVA; $F=1.336$, $p=0.2897$).

Glial cells and cytokine production in the hippocampus during EAE.

IL-1β mRNA expression was analysed in the hippocampus of mice 0.5-21 days post-MOG injection. Figure 5.7a shows that IL-1β mRNA expression was

increased in the hippocampus of EAE mice and this difference was statistically significant (ANOVA, $F=5.288$, $p<0.01$). Post-hoc tests after a significant 1-way ANOVA showed that IL-1β mRNA was significantly increased compared with control 5 and 7 days post-MOG injection (*$p<0.05$ and **$p<0.01$ respectively). Figure 5.7b shows that IL-1β protein concentration was decreased in the hippocampus of EAE mice and this difference was statistically significant (ANOVA, 8.624, $p<0.001$). Post-hoc tests after a significant 1-way ANOVA showed that IL-1β protein was significantly decreased compared with control, 10 and 21 days post-MOG injection (*$p<0.05$ and **$p<0.01$ respectively).

IL-6 mRNA expression and protein was investigated in the hippocampus of mice 0.5-21 days post MOG injection. Figure 5.8a shows that IL-6 mRNA increased in EAE and this difference was statistically significant (ANOVA; $F=2.573$, $p<0.05$). Post-hoc tests after a significant 1-way ANOVA showed no significant differences between specific time points and the control. Figure 5.8b shows that IL-6 protein was unchanged in EAE (ANOVA; $F=2.202$; $p=0.058$).

Figure 5.9 shows that TNFα mRNA expression was significantly increased in the hippocampus 5 days (a; 67.98 RQ ± 21.12; n=6) 10 days (a; 37.2 RQ ± 10.74; n=6) and 21 days (a; 60.79 RQ ± 7.28; n=6) post MOG injection compared with controls (a; 2.87 RQ ± 0.92; n=6; *$p<0.05$, **$p<0.01$; ANOVA). Figure 5.9 indicates that TNFα concentration was not significantly changed in the hippocampus at any time point post MOG injection compared with controls.

Figure 5.10 shows that CD40 mRNA expression was significantly increased in the hippocampus 7 days (a; 3.09 RQ ± 0.61; n=6) and 21 days (a; 2.99 RQ ± 0.45; n=6) post MOG injection compared with controls (a; 0.88 RQ ± 0.25; n=6; *$p<0.05$, ANOVA). Figure 5.10 indicates that CD200 mRNA expression was significantly decreased in the hippocampus 3 days (b; 0.25 RQ ± 0.93; n=6), 5 days (b; 0.22 RQ ± 0.14; n=6), 7 days (b; 0.29 RQ ± 0.24; n=6), 10 days (b; 0.05 RQ ± 0.03) and 21 days (b; 0.09 RQ ± 0.006; n=6) post MOG injection compared with controls (b; 0.77 RQ ± 0.08; n=6; *$p<0.05$, **$p<0.01$; ANOVA).

Figure 5.11 shows that CD11b mRNA expression was significantly increased in the hippocampus 7 days (a; 3.09 RQ ± 0.61; n=6) and 21 days (a; 1.92 RQ ± 0.11; n=6) post MOG injection compared with controls (a; 1.33 RQ ± 0.19; n=6; *p<0.05; ANOVA). It is also evident in Figure 5.11 that IL-4 mRNA expression was significantly decreased 3 days (b; 0.53 RQ ± 0.09; n=6), 5 days (b; 0.30 RQ ± 0.16; n=6), 7 days (b; 0.196 RQ ± 0.08; n=6) 10 days (b; 0.09 RQ ± 0.07; n=6) and 21 days (b; 0.06 RQ ± 0.02; n=6) post MOG injection compared with controls (0.73 RQ ± 0.27; n=6; *p<0.05; ANOVA).

Cytokines in the spleen during EAE

Figure 5.12 shows that IL-1β mRNA expression was significantly increased in the spleen 10 days (a; 133.4 RQ ± 47.03; n=6) post MOG injection compared with controls (a; 4.09 RQ ± 0.86; n=6; ***p<0.001; ANOVA). Figure 5.12 indicates that IL-1β was significantly increased in the spleen 3 days (b; 53.58 pg/mg ± 9.26; n=6) post MOG injection compared with controls (b; 3.81 pg/mg ± 8.81; n=6; *p<0.05; ANOVA). Thus the earliest change observed after MOG injection is the increase in IL-1β in the spleen.

Figure 5.13 shows that TNFα mRNA expression was significantly increased in the spleen 10 days (a; 42.49 ± RQ ± 21.3; n=6) post MOG injection compared with controls (a; 5.42 RQ ± 2.90; n=6; *p<0.05, ANOVA). Figure 5.13 indicates that TNFα concentration was not significantly changed in the spleen at any time point post MOG injection compared with controls (b; 16.61 pg/mg ± 3.68; n=6; ANOVA).

Figure 5.14 shows that IL-6 mRNA expression was unchanged in the spleen at any time point post MOG injection (a; 14.60 RQ ± 2.21; n=6) but, perhaps surprisingly, IL-6 concentration was decreased in the spleen 7 days (b; 4.67 pg/mg ± 0.46; n=6), 10 days (b; 5.51 pg/mg ± 0.94; n=6) and 21 days (b; 2.82 pg/mg ± 0.65; n=6) post MOG injection compared with controls (b; 14.60 pg/mg ± 2.21; n=6; ***p<0.001).

Figure 5.15 shows that CD11b mRNA expression was significantly increased in the spleen 10 days (a; 777.4 RQ ± 361; n=6) post MOG injection compared with

controls (a; 38.08 RQ ± 36.16; n=6; *p<0.05; ANOVA). Changes in CD40 mRNA expression paralleled these changes in CD11b mRNA but these did not reach statistical significance (b; 1.31 RQ ± 0.17; n=6; ns; ANOVA).

Discussion 5.4.

The aims of this study were to examine the expression of pro-inflammatory cytokines over the course of disease progression both in the hippocampus and spinal cord and in the spleen. The data indicates that there was an increase in the mRNA expression of the pro-inflammatory cytokines IL-1β and TNFα prior to the onset of clinical symptoms. This was accompanied by an increase in microglial activation in the spinal cord at the onset of clinical symptoms and the increase in pro-inflammatory cytokine expression and concentration was greatest at the peak of disease severity, which corresponded with a decrease in CD200 and IL-4 expression in the hippocampus.

Clinical symptoms of the disease were first observed 6-7 days post MOG injection, characterised by a limp or flaccid tail in many animals. The clinical symptoms progressed steadily with disease, with a wobbly gait observed in the majority of animals 10 days after immunisation and the disease progressed over the following days to hind limb weakness and paralysis and, at day 21 post-MOG injection, animals were sacrificed. A large number of EAE models exist making comparisons of outcomes across different protocols difficult and, even within similar models, varying doses of antigen or origin of the antigen can compound the variance. However one common time point in each EAE model is the onset of clinical symptoms and it can serve as a marker from which comparisons can be made.

Interestingly, in this study the increase in pro-inflammatory cytokine expression in the spinal cord precedes the development of clinical symptoms. Both IL-1β and TNFα mRNA expression in the spinal cord were significantly increased 5 days post-immunisation while clinical symptom onset occurred, at the earliest, at 6 days post-immunisation. Both pro-inflammatory cytokines have previously been

shown to be important in the instigation of autoimmune pathology, as blocking or removal of IL-1β and TNFα resulted in a delayed onset of disease (Jacobs et al., 1991; Murphy et al., 2002). In Lewis rats in which EAE was induced subsequent treatment for 15 consecutive days with sIL-1R, an IL-1 antagonist, significantly delayed the onset of EAE (Jacobs et al., 1991). Similarly, the onset of clinical symptoms of EAE was delayed by 5 days in $TNF^{-/-}$ mice compared with wildtype mice (Murphy et al., 2002). The origin of this early elevation in pro-inflammatory cytokines in the CNS is still debated as evidence exists for both T cell-derived and glial cell-derived cytokines.

In C57BL/6 mice in which EAE was induced increases in TNFα are associated with activated microglia in the CNS. FACS analysis revealed that 3 days prior to the onset of clinical symptoms microglia, $CD45^{low}$ $Mac1^{+}$ cells, were the primary source of the increased $Mac1^{+}$-derived TNFα. (Juedes et al., 2000). A further study documented the distribution, extent and timing of major inflammatory changes in EAE. Microglial activation and T cell infiltration, were followed by immunolabelling for Iba-1, a marker of activated microglia and CD3, a marker of T lymphocytes, in control mice and mice with EAE (Brown and Sawchenko, 2007). Examination of the CNS at various intervals both pre- and post-onset of clinical symptoms in EAE revealed consistent themes in the distribution and timing of inflammatory changes. Iba-1 positive microglia were present in the meninges, plial surfaces, olfactory bulbs and circumventricular organs prior to development of clinical symptoms. This was accompanied by increased T cell numbers throughout the brain parenchyma, though the magnitude of T cell recruitment was modest relative to microglial activation, but there was no evidence of staining in the spinal cord. At the onset of clinical symptoms there was an increase in microglial activation, in the meninges, plial surfaces, olfactory bulbs, circumventricular organs and the spinal cord; infiltration of T cells in the spinal cord was also observed (Brown and Sawchenko, 2007). The present data also indicate an increase in the marker of microglial activation, CD40 mRNA expression, in the spinal cord at onset of clinical symptoms.

It has been proposed by others though that the source of TNFα involved in the initiation of EAE is blood-borne leukocytes (Murphy et al., 2002). Experiments conducted using bone marrow chimeras from wildtype, and $TNF^{-/-}$, mice to test whether TNFα was essential for induction and development of EAE showed that greater than 99% of TNFα present was derived from blood-derived leukocytes. The authors proposed that TNFα derived from leukocytes interacts with glial cells which in turn produce chemokines that initiate accumulation of T cells and leukocytes, and initiation of disease (Murphy et al., 2002). In this study an increase in the pro-inflammatory Th1 cytokine, IL-1β, 3 days post MOG injection was observed in the spleen, but this was not accompanied by changes TNFα. The spleen is an important lymphoid organ and site of T cell activation in response to MOG_{33-35} (Juedes et al., 2000). An increase in IL-1β and TNFα mRNA expression in the spleen following the onset of clinical symptoms was also observed and this was accompanied by an increase in expression of a marker of macrophage/monocyte activation in the periphery, CD11b.

Accompanying this neuroinflammation in EAE, there is evidence that significant axonal loss occurs before clinical symptoms develop after challenge with MOG_{35-55}. Jones and colleagues (2008) reported that there was significant axonal loss in the spinal cord of mice with EAE, quantified by Toludine blue staining and manual counting, 3 days prior to the onset of clinical symptoms. They also reported that this was accompanied by an increase in both $CD3^+$ T cells and Iba-1 positive microglia. Staining for T cells and microglia was greatest at the onset of the disease and the authors noted that peak neurodegeneration or axonal loss occurred 20-30 days post MOG injection (Jones et al., 2008). Papadopoulos and colleagues (2006) focussed on the timing of axonal loss, its relationship with inflammation and demyelination, and spinal cord volume changes with regard to pathological features and neurological deficit in EAE (Papadopoulos et al., 2006). They presented evidence that showed axonal loss began early in the course of progressive EAE coinciding with the time of peak inflammation in the spinal cord. Inflammation was assessed by OX42 staining for microglia, monocytes and macrophages, and they showed that OX42 immunoreactivity exhibited a strong association with axonal loss (Papadopoulos et al., 2006). This is supported by another study in which a close association between

degree of axonal loss and microglial/macrophages activity was observed in Lewis rats. Using amyloid precursor protein (APP) immunocytochemistry as a marker of acute axonal damage, they found a correlation between APP immunoreactivity and microglial accumulation in the brain and spinal cord (Kornek et al., 2000).

EAE/MS causes widespread damage well beyond the traditionally defined white matter lesions, leading to diffuse changes in the brain as well as the spinal cord (Sicotte et al., 2008). Recent evidence suggests that in addition to the focal lesions, diffuse inflammatory and degenerative processes take place throughout the MS brain (Zeis et al., 2008). MS patients have decreased brain volumes, ventricular atrophy as well as spinal cord atrophy (Miller et al., 2002). Interestingly, little is known about the effect of MS on the hippocampus, although loss of cognition is one of the earliest manifestations of the disease (Rao et al., 1991a; Rao et al., 1991b) and demyelinating lesions and areas of signal abnormality have been identified in the hippocampus using MRI (Roosendaal et al., 2008). Experimental *in vivo* imaging studies have reported metabolic abnormalities in the MS hippocampus (Paulesu et al., 1996) and an MR spectroscopy study showed increased concentration of myo-inositial suggestive of gliosis in the MS hippocampus (Geurts et al., 2006). Importantly, volume loss in the CA1 region of the hippocampus in RRMS is associated with worsening performance in screening tests of verbal learning (Sicotte et al., 2008).

Here increases in the mRNA expression of two markers of activated microglia CD11b and CD40, in the hippocampus, 7 days post-MOG injection were demonstrated and this matches the expression of CD40 mRNA in the spinal cord from the same animals, indicating microglial activation in two CNS regions at the onset of disease symptoms. In addition to this, an increase in the mRNA expression of the pro-inflammatory cytokines IL-1β, IL-6 and TNFα was observed in the hippocampus 21 days post MOG injection. Peak concentrations of IL-1β and TNFα mRNA were recorded in the spinal cord 21 days post MOG injection, however this was not accompanied by an increase in IL-6 which is consistent with evidence by Juedes and colleagues (2000) who, using FACS analysis, did not detect any significant changes in IL-6 protein in CNS of mice with EAE (Juedes et al., 2000). This in contrast to studies showing that IL-6 is involved in the initiation of EAE

where IL-$6^{-/-}$ mice have been shown to be resistant to development of clinical symptoms of the disease (Eugster et al., 1998; Mendel et al., 1998).

In the spinal cord, the peak increase in the pro-inflammatory cytokines IL-1β and TNFα, at the peak of clinical severity of the disease corresponds with the expression of CD40 mRNA. Interestingly this is accompanied by a decrease in the expression of the CD200 mRNA.

A decrease in CD200 expression is probably a significant factor in maintenance of microglia in a quiescent state and an inverse relationship between microglial activation and CD200 expression has been reported. Lyons and colleagues (2007), reported that microglial activation in the hippocampus of aged and Aβ-treated rats was accompanied by decreased expression of neuronal CD200 (Lyons et al., 2007a). This is further emphasised in studies involving $CD200^{-/-}$ mice. Hoek and colleagues (2000) reported increased microglial activation in $CD200^{-/-}$ mice, exhibited by increased CD11b and CD45 expression, in comparison to wildtype mice, and the presence of microglial aggregation in the spinal cord which is characteristic of microglia involved in an inflammatory response (Hoek et al., 2000). In a model of EAE, onset of clinical symptoms was significantly advanced by three days in $CD200^{-/-}$ compared with wildtype mice, and this was accompanied by increased expression of CD68, which is an indicator of microglial activation (Hoek et al., 2000). Consistent with these findings it has been reported that antibody-mediated blockade of CD200R leads to enhanced EAE (Meuth et al., 2008b).

In this study a decrease in CD200 mRNA expression was also observed in the hippocampus, which, although was accompanied by an increase CD40 mRNA expression, in addition corresponded with a decrease in the expression of the anti-inflammatory cytokine IL-4 mRNA. The importance of Th2 type cytokines in controlling the progression of the disease has been highlighted before with evidence showing that IL-4 and IL-10 have the ability to downregulate EAE severity and disease progression (McCombe et al., 1998; Racke et al., 1994; Rott et al., 1994). This is strengthened by data showing that IL-$10^{-/-}$ mice are more susceptible to EAE and develop an increased disease severity. Similarly, spontaneous recovery from EAE has been associated with an increased production of IL-4 in the CNS (Khoury et al.,

1992). In this study, it is important to note that IL-4 protein was not measured due to a difficulty in detecting IL-4 protein using a standard ELISA kit

The decrease in IL-4 mRNA corresponded with the decrease in CD200 mRNA at every timepoint of the disease. Evidence from this lab has previously shown the importance of IL-4 in modulating CD200 expression and that the anti-inflammatory action of IL-4 may be mediated through CD200 (Lyons et al., 2007a). Treatment of neurons in culture with IL-4 increased CD200 mRNA expression and ICV injection of IL-4 increased CD200 staining in the hippocampus (Lyons et al., 2007a).

The data presented highlights the importance of pro-inflammatory cytokines IL-1 and TNFα in EAE prior to the onset of clinical symptoms. This was accompanied by increased expression in markers of microglial activation, CD40, at the onset of disease. At peak of disease severity both microglial activation and pro-inflammatory cytokine production were increased to maximal levels in both the spinal cord and hippocampus. The results suggest that targeting of microglia and their pro-inflammatory cytokines as a possible mechanism of control of disease progression. The increase in microglial activation was accompanied by a decrease in CD200 mRNA expression, emphasising the importance of CD200 in the regulation of microglial activation. This was accompanined by a decrease in IL-4, which supports previous work which suggests the potential of IL-4 as a modulator of CD200 expression and a potential role of targeting the microglia involved in EAE disease progession.

Chapter 5
Figures

Figure 5.1. Clinical scores of C57BL/6 mice with EAE.

Mice (C57BL/6) were injected subcutaneously with 150 μg myeinoligodendrocyte glycoprotein (MOG_{35-55}), Complete Freund's adjuvant (CFA) and Mycobacteria tuberculosis at Day 0 and an intraperitoneal injection of Pertusis Toxin (PT) at Day 0 and Day 2. Control animals were injected with saline i.p. Clinical scores were assessed daily and disease severity was graded as follows: grade 0 – normal; grade 1 – flaccid tail; grade 2 – wobbly gait; grade 3 – hind limb weakness; grade 4 – hind limb paralysis; grade 5 – tetraparalysis/death. Mice were sacrificed at the time points, day 0.5, 3, 5, 7, 10 and 21. (n=6 per time point).

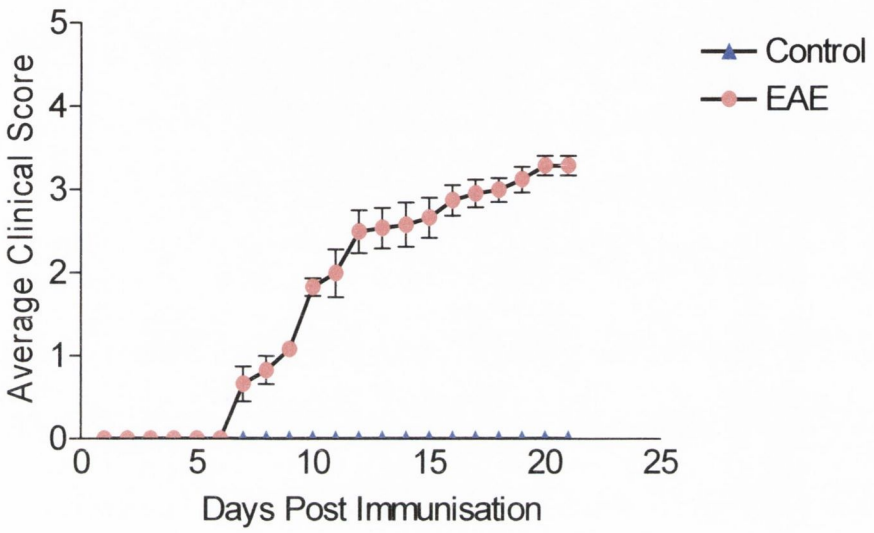
Average Clinical Score
5
4
3
2
1
0
0
5
10
15
20
25
Days Post Immunisation
Control
EAE

Figure 5.2. IL-1β was significantly increased in the spinal cord during EAE.

IL-1β mRNA expression was significantly increased in spinal cord 5, 10 and 21 days after MOG injection (a; **p<0.01;***p<0.001; ANOVA; versus control). IL-1β protein concentration was significantly increased 10 and 21 days after MOG injection (b; ***p<0.001; ANOVA; versus control). Data are presented as means (± SEM; n=6) and expressed as IL-1β:β-actin (RQ) or pg IL-1β/ml.

(a) 1-way ANOVA; EAE_{effect} F(1,36)=17.16; p<0.001
(b) 1-way ANOVA; EAE_{effect} F(1,90)=20.14; p<0.001

a

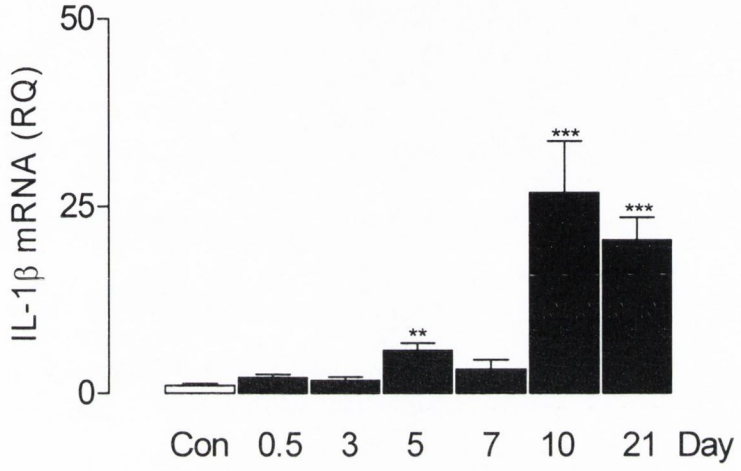
50
25
0
IL-1β mRNA (RQ)
**
***
***
Con
0.5
3
5
7
10
21
Day

b

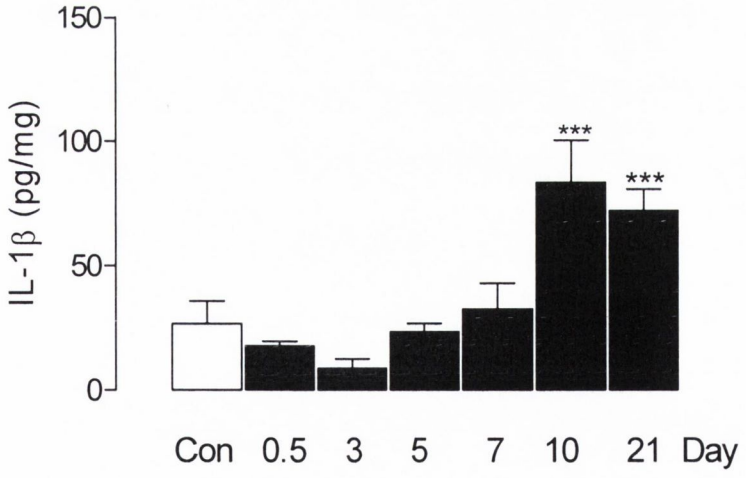
150
100
50
0
IL-1β (pg/mg)
***
***
Con
0.5
3
5
7
10
21
Day

Figure 5.3. IL-6 was not significantly changed in the spinal cord during EAE.

IL-6 mRNA expression or protein concentration were not significantly changed in spinal cord at any time point after MOG injection (a and b; ANOVA; versus control). Data are presented as means (± SEM; n=6) expressed as IL-6:β-actin (RQ) or pg IL-6/ml.

(a)1-way ANOVA; EAE_{effect} F(1,21)=0.9037; p=0.5177
(b)1-way ANOVA; EAE_{effect} F(1,36)=0.1.465; p=0.2238

a

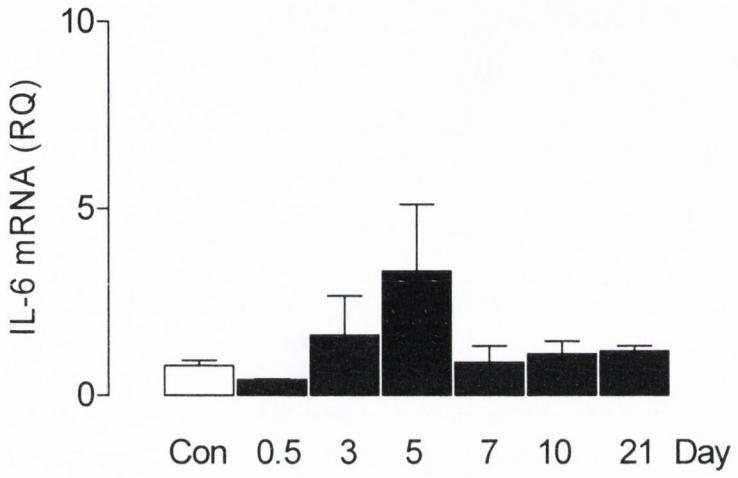
10
5
0
IL-6 mRNA (RQ)
Con
0.5
3
5
7
10
21
Day

b

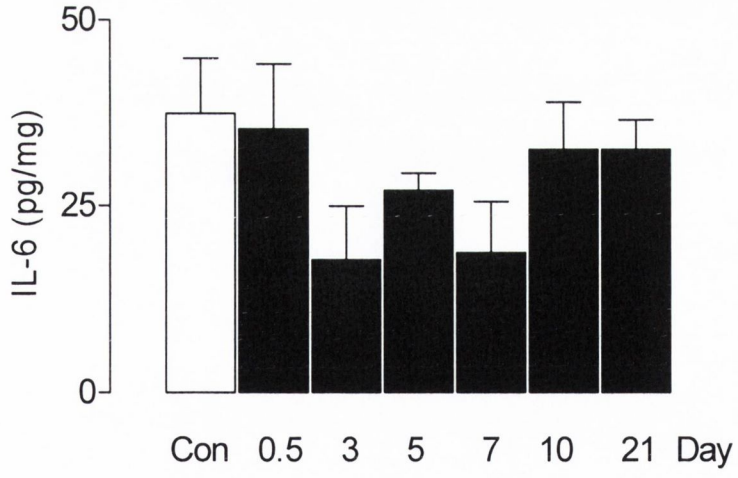
50
25
0
IL-6 (pg/mg)
Con
0.5
3
5
7
10
21
Day

Figure 5.4. TNFα in the spinal cord during EAE.

a). Relative quantification of TNFα mRNA in the spinal cord of EAE mice at 0.5-21 days post-MOG injection. Data are expressed as the fold change in TNFα relative to control (RQ) and presented as means (± SEM; n=4-6). ***=p<0.001 Newman Keuls post-hoc test, EAE day 10 versus control. **b)**.TNF protein concentration measured by ELISA in the spinal cord of EAE mice at 0.5-21 days post-MOG injection. Data are expressed as TNFα (pg/mg) and presented as means (± SEM; n=4-6).

(a)1-way ANOVA; EAE_{effect} F(1,31)=6.809; p<0.001
(b)1-way ANOVA; EAE_{effect} F(1,37)=3.553; p<0.01

a

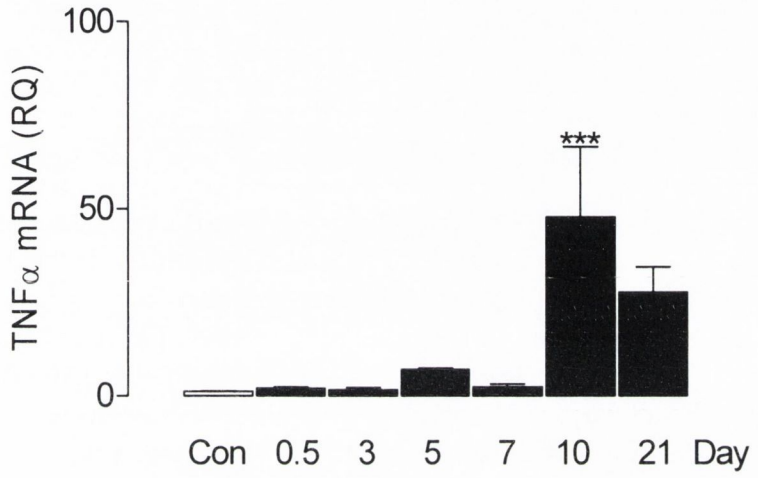
100
50
0
TNFα mRNA (RQ)
***
Con 0.5 3 5 7 10 21 Day

b

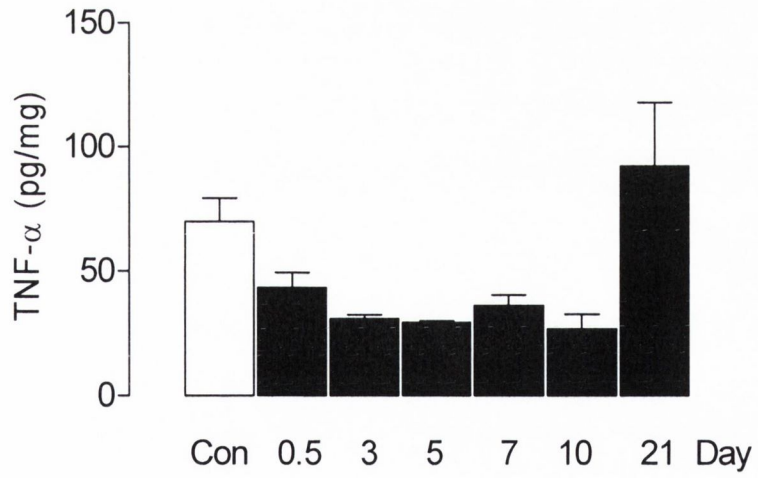
150
100
50
0
TNF-α (pg/mg)
Con 0.5 3 5 7 10 21 Day

Figure 5.5. CD40 mRNA expression was significantly increased in the spinal cord during EAE and CD200 was significantly decreased.

CD40 mRNA expression was significantly increased in spinal cord 7 and 21 days after MOG injection (a; *p<0.05; ***p<0.001; ANOVA; versus control). CD200 mRNA expression was significantly decreased in spinal cord 21 days after MOG injection (b; *p<0.05; ANOVA; versus control). Data are presented as means (± SEM; n=6) expressed as CD40:β-actin (RQ) or CD200:β-actin (RQ).

(a)1-way ANOVA; EAE_{effect} F(1,28)=2.123; p<0.05
(b)1-way ANOVA; EAE_{effect} F(1,36)=2.728; p<0.05

a

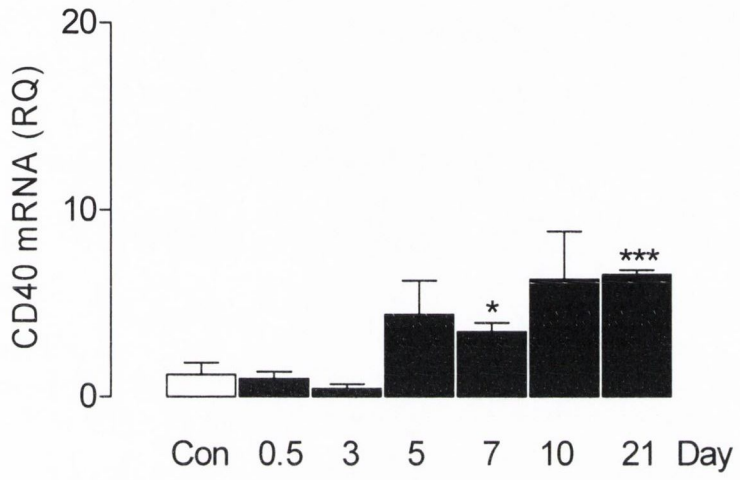
20
10
0
CD40 mRNA (RQ)
*
***
Con
0.5
3
5
7
10
21
Day

b

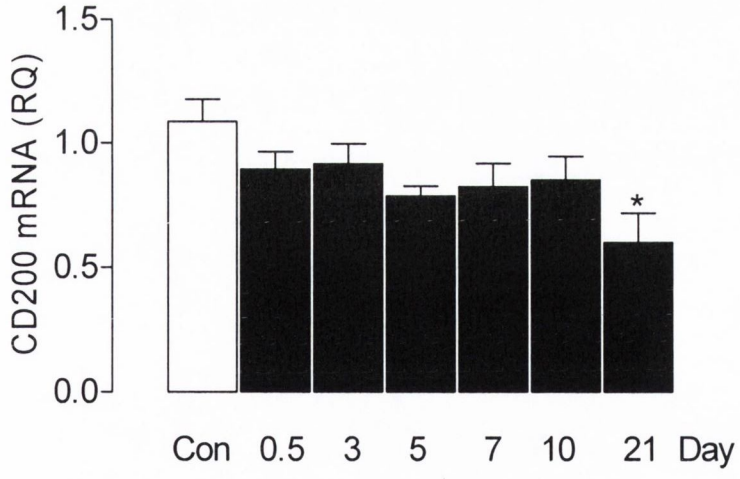
1.5
1.0
0.5
0.0
CD200 mRNA (RQ)
*
Con
0.5
3
5
7
10
21
Day

Figure 5.6. IL-4 mRNA expression was unchanged in the spinal cord during EAE.

Relative quantification of IL-4 mRNA in the spinal cord of EAE mice at 0.5-21 days post-MOG injection. Data are expressed fold change in IL-4 mRNA relative to control (RQ), and presented as means (± SEM; n=4-6).

a) 1-way ANOVA; EAE_{effect} F(1,25)=1.336; p=0.2897

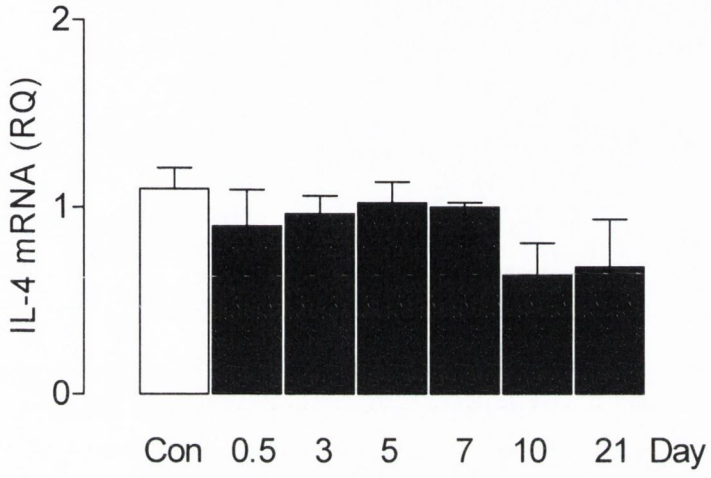
IL-4 mRNA (RQ)
2
1
0
Con
0.5
3
5
7
10
21
Day

Figure 5.7. IL-1β mRNA was significantly increased in the hippocampus, and IL-1β protein was significantly decreased during EAE.

a). Relative quantification of IL-1β mRNA in the hippocampus of EAE mice at 0.5-21 days post-MOG injection. Data are expressed as the fold change in IL-1β relative to control (RQ) and presented as means (± SEM; n=4-6). *=$p<0.05$, Newman Keuls post-hoc test, EAE day 5 post-injection versus control. **$p<0.01$, Newman Keuls post-hoc test, EAE day 7 post-injection versus control. **b).** IL-1β protein by ELISA in the hippocampus of EAE mice at 0.5-21 days post-MOG injection. Data are expressed as IL-1β (pg/mg) and presented as means (± SEM; n=6). *=$p<0.05$, Newman Keuls post-hoc test EAE day 10 post-injection versus control. **=$p<0.01$, Newman Keuls post-hoc test EAE day 21 post-injection versus control. . .

(a). 1-way ANOVA; EAE_{effect} $F(1,29)=5.288$; $p<0.01$
(b). 1-way ANOVA; EAE_{effect} $F(1,41)=8.624$; $p<0.001$

a

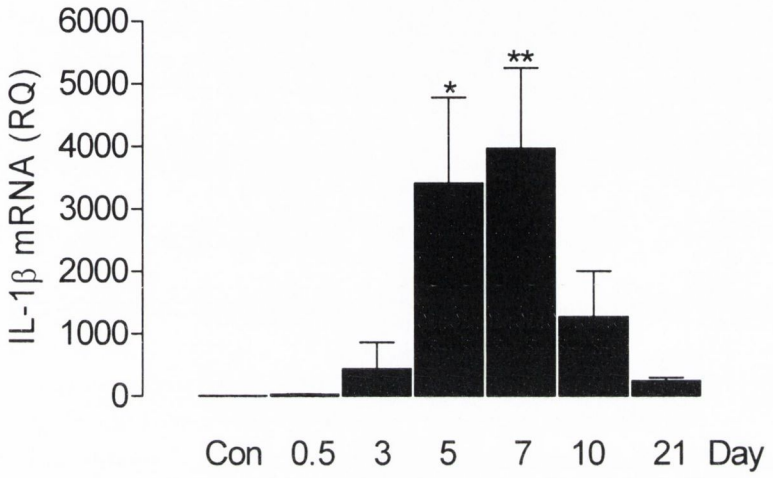
6000
5000
4000
3000
2000
1000
0
IL-1β mRNA (RQ)
*
**
Con
0.5
3
5
7
10
21
Day

b

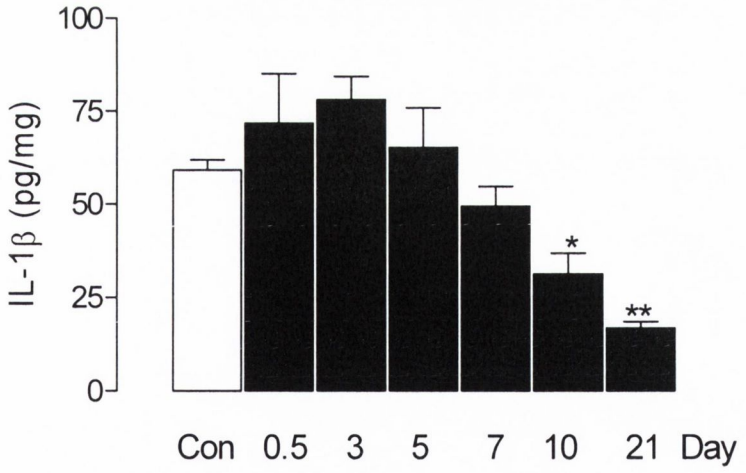
100
75
50
25
0
IL-1β (pg/mg)
*
**
Con
0.5
3
5
7
10
21
Day

Figure 5.8. IL-6 mRNA and protein in the hippocampus during EAE.

a). Relative quantification of IL-6 mRNA in the hippocampus of EAE mice at 0.5-21 days post-MOG injection. Data are expressed as the fold change in IL-6 mRNA relative to control (RQ) and presented as means (± SEM; n=4-6). b). IL-6 protein by ELISA in the hippocampus of EAE mice at 0.5-21 days post-MOG injection. Data are expressed as pgIL-6/mg and presented as means (± SEM; n=6)..

(a). 1-way ANOVA; EAE_{effect} $F(1,36)=2.573$; $p<0.05$
(b). 1-way ANOVA; EAE_{effect} $F(1,41)=2.272$; $p=0.058$

a

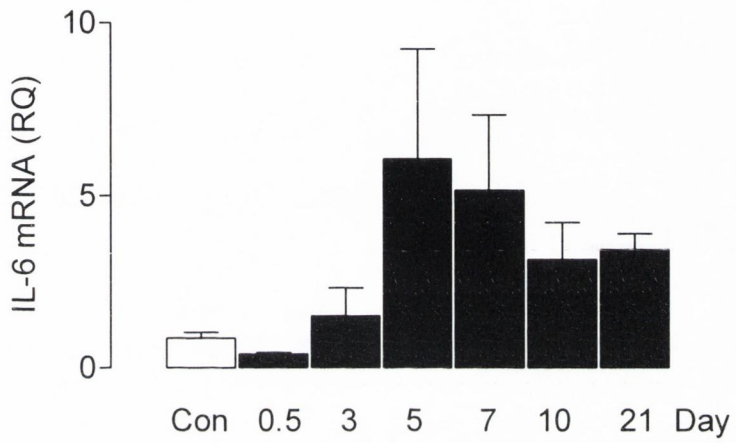
10
5
0
IL-6 mRNA (RQ)
Con
0.5
3
5
7
10
21
Day

b

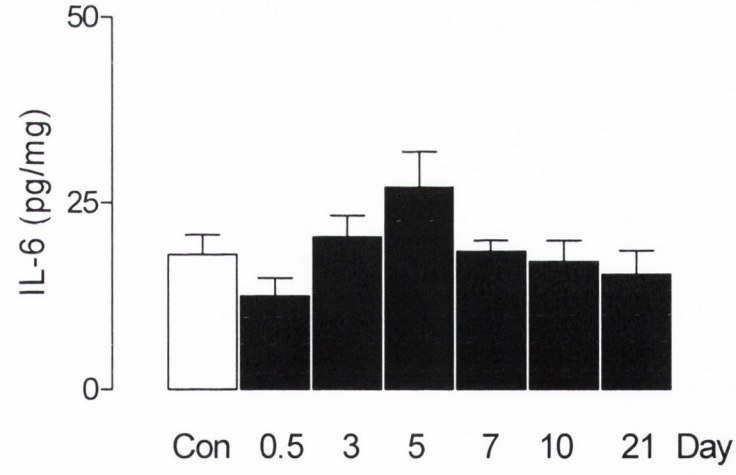
50
25
0
IL-6 (pg/mg)
Con
0.5
3
5
7
10
21
Day

Figure 5.9. TNFα mRNA was significantly increased in the hippocampus during EAE.

TNFα mRNA expression was significantly increased in hippocampus 5, 10 and 21 days after MOG injection (a; *p<0.05; **p<0.01; ANOVA; versus control). TNFα protein concentration was not significantly different at any time point after MOG injection (b; ns; ANOVA; versus control). Data are presented as means (± SEM; n=6) expressed as TNFα:β-actin (RQ) or pg TNFα/ml.

(a). 1-way ANOVA; EAE_{effect} F(1,41)=3.873; p<0.01
(b). 1-way ANOVA; EAE_{effect} F(1,41)=1.135; p=0.3630

a

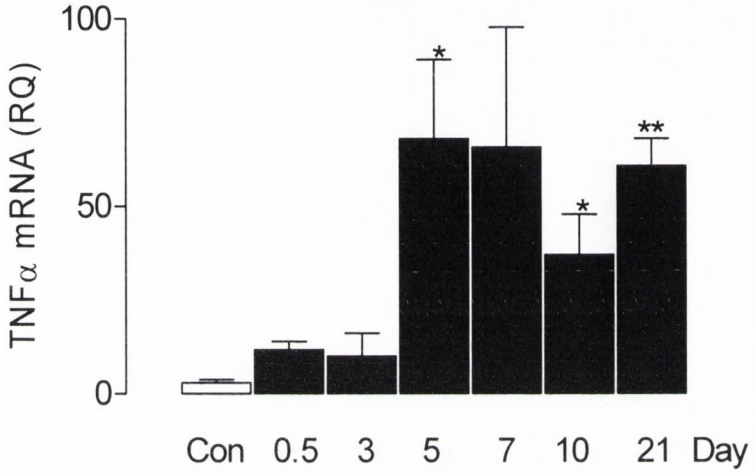
100
50
0
TNFα mRNA (RQ)
*
*
**
Con
0.5
3
5
7
10
21
Day

b

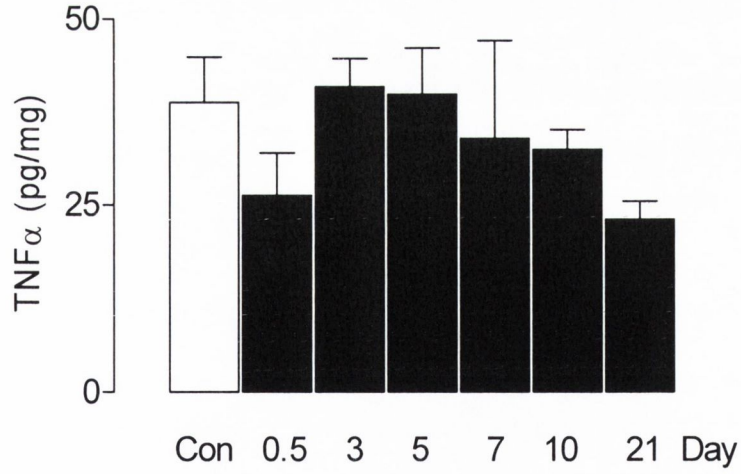
50
25
0
TNFα (pg/mg)
Con
0.5
3
5
7
10
21
Day

Figure 5.10. CD40 expression was significantly increased in the hippocampus and CD200 was significantly decreased in the hippocampus during EAE.

CD40 mRNA expression was significantly increased in hippocampus 7 and 21 days after MOG injection (a; *$p<0.05$; ANOVA; versus control). CD200 mRNA expression was significantly decreased 3, 5, 7, 10, 21 days after MOG injection (b; *$p<0.05$; **$p<0.01$; ANOVA; versus control). Data are presented as means (± SEM; n=6) expressed as CD40:β-actin (RQ) or CD200:β-actin (RQ).

(a) 1-way ANOVA; EAE_{effect} $F(1,41)=3.108$; $p<0.05$.
(b) 1-way ANOVA; EAE_{effect} $F(1,25)=6.119$; $p<0.01$.

a

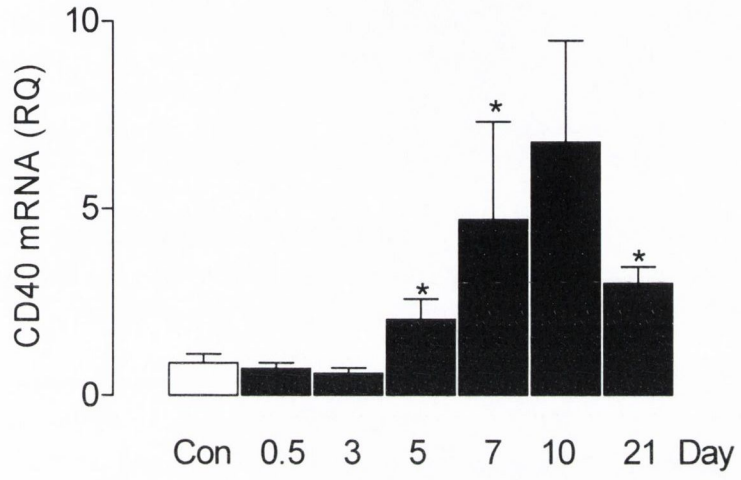
10
5
0
CD40 mRNA (RQ)
*
*
*
Con
0.5
3
5
7
10
21
Day

b

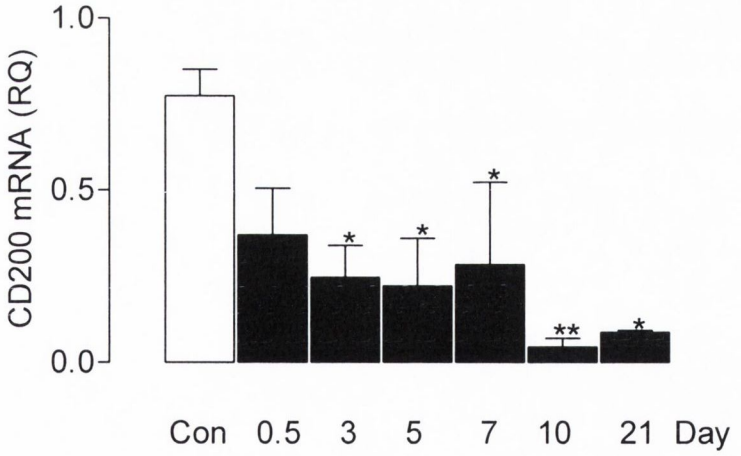
1.0
0.5
0.0
CD200 mRNA (RQ)
*
*
*
**
*
Con
0.5
3
5
7
10
21
Day

Figure 5.11. CD11b mRNA expression was significantly increased and IL-4 mRNA expression significantly decreased in the hippocampus during EAE.

CD11b mRNA expression was significantly increased in hippocampus 7 and 21 days after MOG injection (a; *p<0.05; ANOVA; versus control). IL-4 mRNA expression was decreased 3, 5, 7, 10 and 21 days after MOG injection (b; *p<0.05; ANOVA; versus control). Data are presented as means (± SEM; n=6) expressed as IL-4:β-actin (RQ) or CD11b:β-actin (RQ).

(a) 1-way ANOVA; EAE_{effect} F(1,34)=3.497; p<0.05.
(b) 1-way ANOVA; EAE_{effect} F(1,25)=5.112; p<0.01.

a

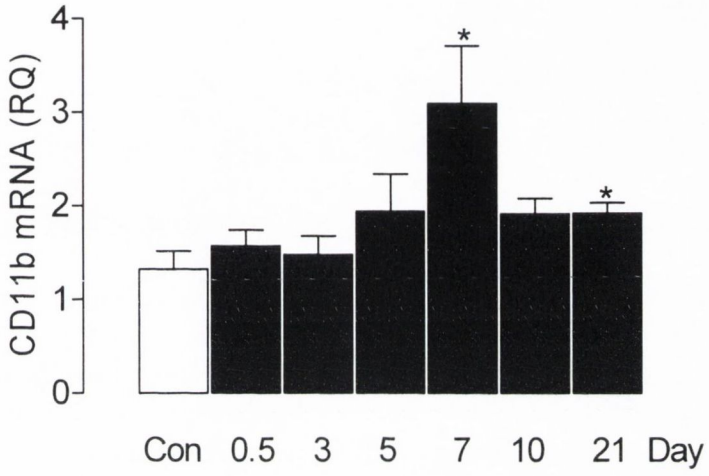
CD11b mRNA (RQ)
4
3
2
1
0
*
*
Con
0.5
3
5
7
10
21
Day

b

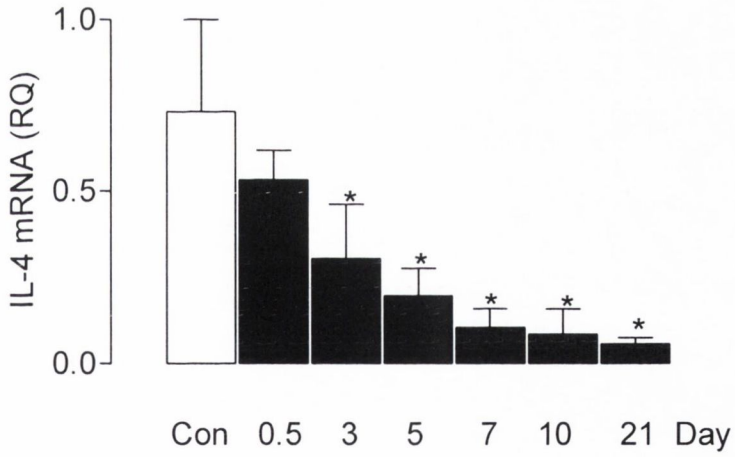
IL-4 mRNA (RQ)
1.0
0.5
0.0
*
*
*
*
*
Con
0.5
3
5
7
10
21
Day

Figure 5.12. IL-1β was significantly increased in spleen during EAE.

IL-1β mRNA expression was significantly increased in spleen 10 days after MOG injection (a; ***$p<0.001$; ANOVA; versus control). IL-1β protein concentration was increased significantly 3 days after MOG injection (b; *$p<0.05$; ANOVA; versus control). Data are presented as means (± SEM; n=6) expressed as IL-1β:β-actin (RQ) or pg IL-1β/ml.

(a). 1-way ANOVA; EAE_{effect} $F(1,39)=6.294$; $p<0.001$
(b). 1-way ANOVA; EAE_{effect} $F(1,40)=5.293$; $p<0.001$

a

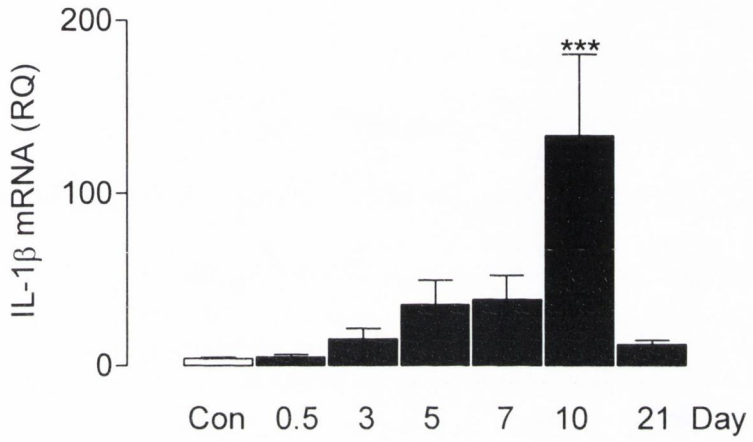
200
100
0
IL-1β mRNA (RQ)
***
Con
0.5
3
5
7
10
21
Day

b

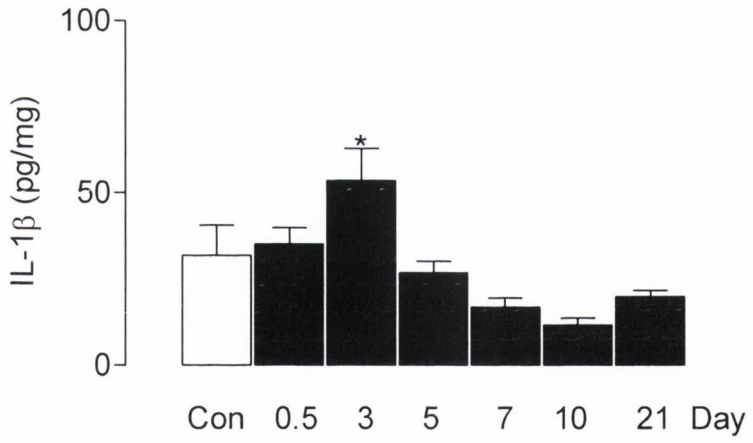
100
50
0
IL-1β (pg/mg)
*
Con
0.5
3
5
7
10
21
Day

Figure 5.13. TNFα was significantly increased in the spleen during EAE.

TNFα mRNA expression was significantly increased in the spleen 10 days after MOG injection (a; *$p<0.05$; ANOVA; versus control). TNFα protein concentration was not significantly different at any time point after MOG injection (b; ANOVA; versus control). Data are presented as means (± SEM; n=6) and expressed as TNFα:β-actin (RQ) or pg TNFα/ml.

(a). 1-way ANOVA; EAE_{effect} $F(1,38)=3.317$; $p=0.0118$
(b). 1-way ANOVA; EAE_{effect} $F(1,37)=2.204$; $p=0.0693$

a

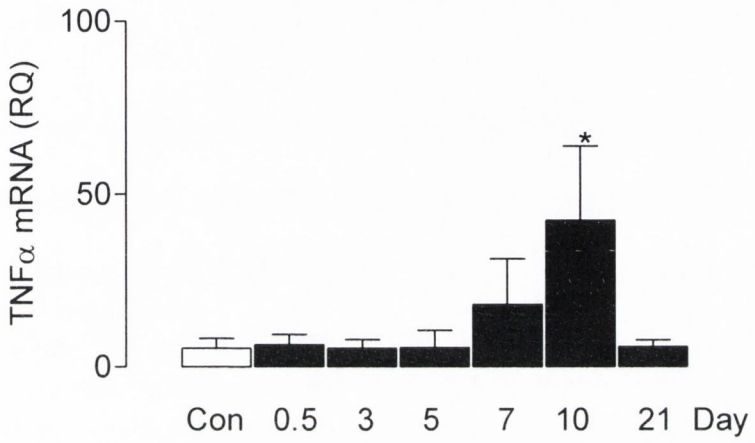
100
50
0
TNFα mRNA (RQ)
*
Con 0.5 3 5 7 10 21 Day

b

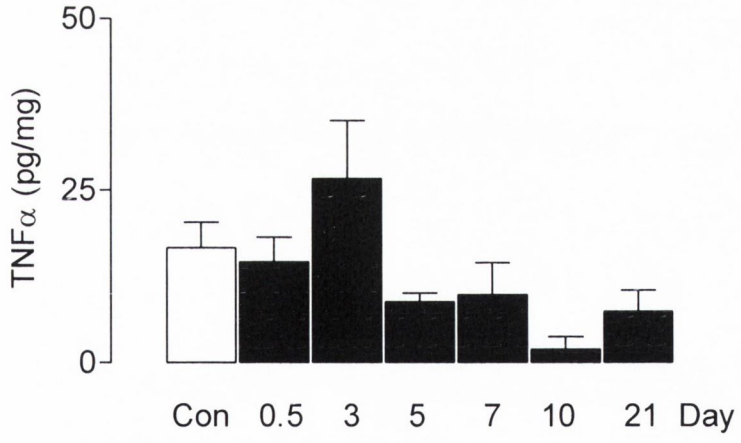
50
25
0
TNFα (pg/mg)
Con 0.5 3 5 7 10 21 Day

Figure 5.14. IL-6 was significantly decreased in the spleen during EAE.

IL-6 mRNA expression was not significantly different in the spleen at any time point after MOG injection (a; ANOVA; versus control). IL-6 protein concentration was significantly decreased 7,10 and 21 days after MOG injection (b; ***$p<0.001$; ANOVA; versus control). Data are presented as means (± SEM; n=6) and expressed as IL-6:β-actin (RQ) or pg IL-6/ml. .

(a). 1-way ANOVA; EAE_{effect} $F(1,41)=1.187$; $p=0.3349$
(b). 1-way ANOVA; EAE_{effect} $F(1,39)=10.95$; $p<0.001$

a

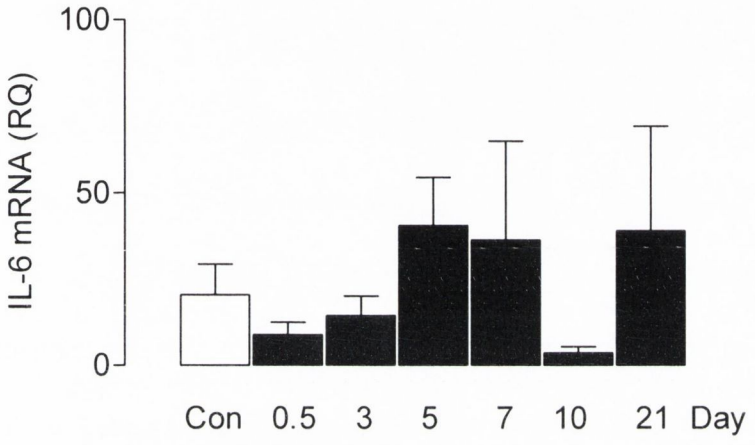
100
50
0
IL-6 mRNA (RQ)
Con
0.5
3
5
7
10
21
Day

b

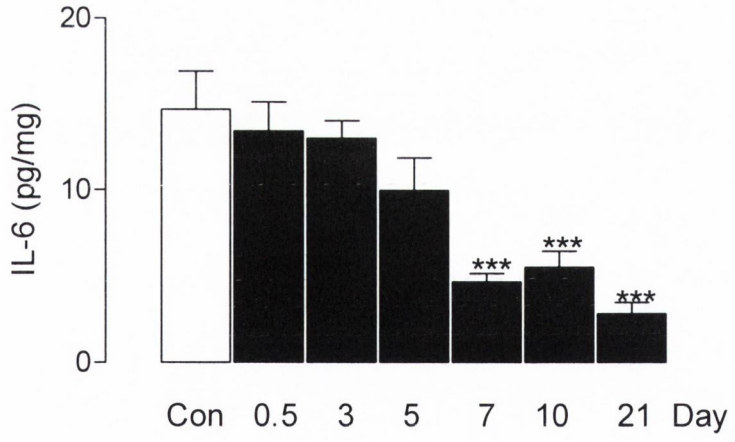
20
10
0
IL-6 (pg/mg)
***
***
***
Con
0.5
3
5
7
10
21
Day

Figure 5.15. CD11b mRNA expression was significantly increased in the spleen during EAE.

CD11b mRNA expression was significantly increased 10 days after MOG injection in the spleen (a; *$p<0.05$; ANOVA; versus control) but CD40 expression was unchanged at any time point (b; ANOVA; versus control). Data are presented as means (± SEM; n=6) and expressed as CD11b:β-actin or CD40:β-actin (RQ).

(a) **1-way ANOVA; EAE_{effect} $F(1,36)=3.034$; $p<0.05$.**
(b) 1-way ANOVA; EAE_{effect} $F(1,33)=1.568$; $p=0.1943$.

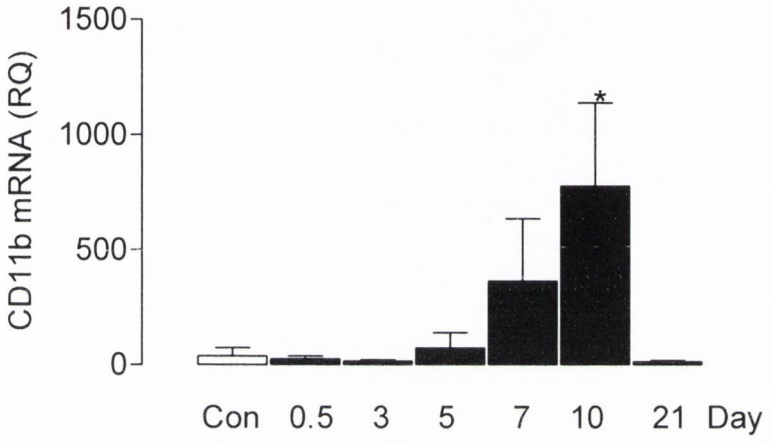
CD11b mRNA (RQ)
1500
1000
500
0
*
Con
0.5
3
5
7
10
21
Day

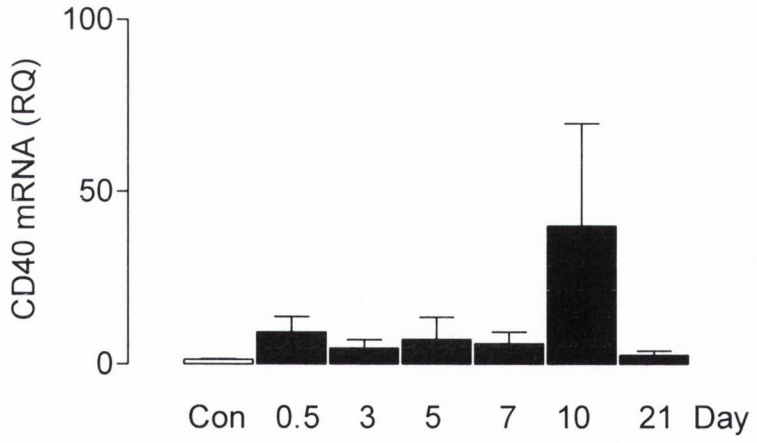
CD40 mRNA (RQ)
100
50
0
Con
0.5
3
5
7
10
21
Day

Chapter 6

Rosiglitazone and IL-4, potential modulators of microglial activation and EAE disease progression

6.1. Introduction

Although infiltration and proliferation of T cells are reported to be important in the initiation of MS and EAE, the pathological features of neurodegenerative conditions have also been attributed to activated microglia and astrocytes in the CNS. Neuroinflammation associated with disease pathology has been shown to involve the increase in pro-inflammatory cytokines IL-1β, IL-6 and TNFα accompanied by a decrease in anti-inflammatory cytokines, IL-4 and IL-10. Previous work from this lab has shown that deficits in cognitive function and inflammation in age and in response to LPS are associated with a decrease in the hippocampal concentration of IL-4, and that reversing this decrease in IL-4 abrogates the inflammation (Loane et al., 2009; Lynch et al., 2007). Recovery from EAE has been associated with increased production of IL-4 (Khoury et al., 1992) and treatment with IL-4 has been shown to suppress EAE (Racke et al., 1994). One aim of this study was to examine the role of IL-4 in CNS inflammation in EAE which was assessed using mice deficient in the IL-4 gene (IL-$4^{-/-}$).

Based on the evidence that MS and EAE are inflammatory diseases associated with activated glial cells, interventions targeting the activated glia may prove to be beneficial in the modulation of disease progression. Current drugs on the market for the treatment of MS focus on modulating the immune response, glatiramer acetate, or suppressing the immune response, mitoxantrone. As rosiglitazone has previously been shown to modulate glial cell activation, decrease pro-inflammatory cytokine production and increase IL-4, it may serve to modulate glial driven inflammation in EAE. The aim of this study was to examine the ability of rosiglitazone to modulate EAE disease progression and the subsequent microglial activation and inflammation in the CNS associated with the disease.

6.2. Methods

Mice (C57BL/6 and IL-$4^{-/-}$) were injected subcutaneously with 150μg myelinoligodendrocyte glycoprotein (MOG_{35-55}), CFA and Mycobacteria tuberculosis at Day 0 and an intraperitoneal injection of PT at Day 0 and Day 2. Clinical scores

were assessed daily and disease severity was graded as follows: grade 0 – normal; grade 1 – flaccid tail; grade 2 – wobbly gait; grade 3 – hind limb weakness; grade 4 – hind limb paralysis; grade 5 – tetraparalysis/death.

Mice were sacrificed 21 days post MOG injection and the spinal cord and hippocampus were removed. Analysis of spinal cord and hippocampal tissue for microglial markers, neuronal markers and cytokine mRNA was assessed by PCR, CD200 expression was assessed by Western Immunoblotting and cytokine concentrations were assessed by ELISA (see sections 2.3., 2.4., 2.5 and 2.6. for specific details).

Mice (C57BL/6) were pretreated orally with rosiglitazone (6mg/kg/day) for three weeks. Mice were then divided into two groups. The first group was injected subcutaneously with 150μg myelinoligodendrocyte glycoprotein (MOG_{35-55}), CFA and Mycobacteria tuberculosis at Day 0 and an intraperitoneal injection of PT at Day 0 and Day 2. The second group were injected subcutaneously with saline at Day 0 and a further intraperitoneal injection of saline at Day 0 and Day 2. Clinical scores were assessed daily and disease severity was graded as follows: grade 0 – normal; grade 1 – flaccid tail; grade 2 – wobbly gait; grade 3 – hind limb weakness; grade 4 – hind limb paralysis; grade 5 – tetraparalysis/death.

Mice were sacrificed 21 days post MOG or saline injection and the spinal cord was removed. Analysis of spinal cord for microglial markers, neuronal markers and cytokine mRNA was assessed by PCR and cytokine concentrations were assessed by ELISA (see sections 2.3, 2.4. and 2.5. for specific details).

Data are expressed as means ± standard error of the mean. A 2-way ANOVA was performed to determine whether significant differences existed between conditions and. post hoc Newman Keuls test was performed in the event of main effects of time post injection, and or rosiglitazone or strain. A 2-way repeated measures ANOVA was used in the analysis of clinical score data (Figure 6.1 and Figure 6.9), and post hoc test performed as above if required.

6.3. Results

EAE was induced in C57BL/6 and IL-4$^{-/-}$ mice, and clinical symptoms were scored.

Clinical scores were compared in wildtype (C57BL/6) and IL-4$^{-/-}$ mice. A two-way repeated measures ANOVA was performed to examine the effect of EAE, IL-4 and their interaction. Figure 6.1 shows a main effect of time (post injection with MOG) (ANOVA; $F=3.996$, $p<0.001$). There was no main effect of IL-4$^{-/-}$ (ANOVA; $F=1.107$, $p=0.3061$) but a significant interaction between IL-4$^{-/-}$ and EAE (ANOVA; $F=1.95$, $p<0.01$). Post hoc tests were performed and showed no significant differences between groups. Interpretation of the interaction from the graph, would suggest at the end of the experiment disease severity is greater in C57BL/6 compared with IL-4$^{-/-}$.

Microglial activation and cytokine production in the spinal cord during EAE

Figure 6.2 shows that IL-1β mRNA expression was significantly increased in the spinal cord of wildtype mice with EAE (a; 8.53 RQ ± 3.49; n=6) compared with control wildtype mice (a; 0.72 RQ ± 0.24; n=6; *$p<0.05$; ANOVA). IL-1β mRNA expression was significantly increased in IL-4$^{-/-}$ mice with EAE (a; 27.08 RQ ± 9.90; n=6) compared to wildtype mice with EAE (a; 8.53 RQ ± 3.49; n=6; $^{\#}p<0.05$; ANOVA).

It is also evident from Figure 6.2 that IL-1β concentration was increased in EAE (b; 919pg/mg ± 188.83; n=12) compared with wildtype mice (b; 381.55pg/mg ± 63.42; n=12; ***$p<0.001$; ANOVA). Further to this there was a significant increase in IL-1β concentration in spinal cord of IL-4$^{-/-}$ mice with EAE (b; 1164 pg/mg ± 283.2; n=6) compared with wildtype mice with EAE (b; 674 ± 94.47; n=6; $^{\#}p<0.05$; ANOVA). IL-1β concentration was decreased in control IL-4$^{-/-}$ mice (b; 234.7pg/mg ± 51.27; n=6) compared with wildtype mice (b; 528.4 ± 75.65; n=6; **$p<0.01$; ANOVA).

Figure 6.3 shows that TNFα mRNA expression was similar in spinal cord of wildtype mice (a; 0.803 RQ ± 0.104; n=6) and IL-4$^{-/-}$ mice (a; 0.5 RQ ± 0.23; n=6) and was not significantly increased in either wildtype (a; 2373 RQ ± 133.4; n=6) or IL-4$^{-/-}$ (a; 303.4 RQ ± 249.2; n=6) mice with EAE. TNFα protein concentration was also similar in both the spinal cord of wildtype mice (b; 60.81pg/mg ± 19.59; n=6) and IL-4$^{-/-}$ mice (b; 49.77pg/mg ± 23.71; n=6). As observed at the mRNA level, there was no significant change in TNFα protein concentration in the spinal cord of wildtype (b; 115.4pg/mg ± 17.18; n=6) or IL-4$^{-/-}$ (b; 34.39pg/mg ± 18.4; n=6) mice with EAE.

Figure 6.4 shows that there was a significant increase in CD40 mRNA expression in spinal cord of wildtype mice with EAE (a; 3.346 RQ ± 1.304; n=6) compared with wildtype control (a; 0.406 RQ ± 0.07; n=6; *p<0.05; ANOVA).CD200 mRNA expression was significantly decreased in the spinal cord of wildtype mice with EAE (b; 0.49 RQ ± 0.12; n=6) compared with wildtype control (1.2 RQ ± 0.08; n=6; ***p<0.001; ANOVA).

Microglial activation and cytokine production in the hippocampus during EAE.

Figure 6.5 shows that there was a significant increase in IL-1β mRNA expression in the hippocampus of wildtype mice (a; 72.66 RQ ± 33.11; n=6) with EAE compared with control (a; 4.641 RQ ± 1.154; n=6; *p<0.05; Student's *t* test).

There was a significant increase in IL-1β concentration in the hippocampus of mice with EAE (b; 25.30pg/mg ± 2.87; n=6; ***p<0.001; ANOVA) compared with wildtype mice. IL-1β concentration was similar in the hippocampus of wildtype (b; 3.78pg/mg ± 1.1; n=6) and IL-4$^{-/-}$ (b; 1.88pg/mg ± 0.26; n=6) mice,

Figure 6.6 shows that TNFα mRNA expression was significantly increased in the hippocampus of wildtype mice with EAE (a; 955.9 RQ ± 359.4; n=6) compared with control wildtype mice (a; 2.8 RQ ± 1.09; n=6; *p<0.05; ANOVA). There was no further increase in TNFα mRNA in IL-4$^{-/-}$ mice with EAE (a; 10904 RQ ± 10417; n=6; ANOVA) compared with control.

There was no significant difference in TNFα concentration in hippocampus of wildtype mice with EAE (b; 64.06pg/mg ± 7.704) and IL-4$^{-/-}$ mice with EAE (b; 146.9pg/mg ± 78.6) compared with wildtype control (b; 89.48pg/mg ± 24.45; n=6) and IL-4$^{-/-}$ control (b; 83.21pg/mg ± 26.86; n=6) mice

Figure 6.7a shows that there was a significant increase in CD40 mRNA in the hippocampus of mice with EAE (a; 1.08 RQ ± 0.24; n=12) compared with control wildtype mice (a; 0.46 RQ ± 0.08; n=6; **p<0.01; ANOVA). CD40 mRNA expression was not further increased in the hippocampus of IL-4$^{-/-}$ mice with EAE (a; 1.43 arbitrary units ± 0.36; n=6) compared with control. CD40 mRNA expression was similar in hippocampus of wildtype control (a; 0.46 RQ ± 0.08; n=6) and control IL-4$^{-/-}$ (a; 0.40 RQ ± 0.09; n=6) mice.

Figure 6.7b shows that CD200 mRNA expression was significantly decreased in the hippocampus of wildtype mice with EAE (b; 0.69 RQ ± 0.1; n=6) compared to wildtype control (b; 1.31 RQ ± 0.9; n=6, **p<0.01, ANOVA). CD200 mRNA expression was significantly decreased further in IL-4$^{-/-}$ mice with EAE (0.46 RQ ± 0.04; n=6) compared with wildtype EAE mice (b; 0.69 RQ ± 0.1; n=6; $^{\#}$p<0.05; Student's *t* test).

Figure 6.8 shows that expression of CD200 protein was decreased in hippocampus of control IL-4$^{-/-}$ mice (1.25 RQ ± 0.11; n=6) compared with control wildtype mice (2.02 RQ ± 0.47; n=6; ANOVA; **p<0.01). Expression of CD200 protein was decreased in the hippocampus of wildtype mice with EAE (1.12 RQ ± 0.12; n=6; ANOVA; **p<0.01) compared with wildtype control. There was a further decrease in expression CD200 concentration in the hippocampus of IL-4$^{-/-}$ mice with EAE (0.699 RQ ± 0.17; n=6; Students' *t* test; $^{\#}$p<0.05) compared with wildtype EAE mice.

EAE was induced in C57BL/6 mice treated with rosiglitazone

Previous evidence has indicated that rosiglitazone exerts anti-inflammatory effects and that it attenuates the age-related decrease in IL-4. The effect of rosiglitazone was investigated on EAE. Clinical scores were recorded daily post

MOG injection in mice administered control and rosiglitazone diets. A two-way repeated measures ANOVA was performed to examine effect of EAE, rosiglitazone and their interaction. Figure 6.9 shows a main effect of time (post injection with MOG) ($F=136.61$, $p<0.001$) but no effect of rosiglitazone ($F=2.17$, $p=0.17$) or no interaction of rosiglitazone with EAE ($F=1.5$, $p=0.08$).

Figure 6.10 shows that IL-1β mRNA expression (a; 18.07 RQ ± 3.67; n=6) and IL-1β protein concentration (b; 76.84 pg/mg ±6.12; n=6) were significantly increased in the spinal cord of mice with EAE compared with mRNA expression (a; 0.28 RQ ± 0.15; n=6; ANOVA; ***$p<0.001$) and protein concentration (b; 50.52 pg/mg ± 8.24; n=6; *$p<0.05$; Student's *t* test) in controls. Treatment of mice orally with rosiglitazone for 3 weeks (6mg/kg/day) significantly attenuated the EAE-induced increase in IL-1β mRNA (a; 5.55 RQ ± 1.70; n=6; Student's *t* test; $^{\#}p<0.05$) but no attenuation was observed in IL-1β concentration (b; 61.11 pg/mg ± 4.96; n=6).

Figure 6.11 shows that there was a significant increase in TNFα mRNA expression (a; 14.98 RQ ± 5.54; n=6) and protein concentration (b; 215.7 pg/mg ± 91.64; n=6) in the spinal cord of mice with EAE compared to mRNA expression (a; 0.45 RQ ± 0.12; n=6; ***$p<0.001$; ANOVA) and protein concentration (b; 66.42 pg/mg ± 14.41; n=6; *$p<0.05$; ANOVA) in spinal cord of controls. Treatment with rosiglitazone did not significantly attenuate the EAE-induced increase in TNFα mRNA (a; 10.13 RQ ± 1.47; n=6; ANOVA) or protein (b; 132 pg/mg± 9.1; n=6; ANOVA).

Figure 6.12 shows that there was a significant increase in CD40 mRNA expression in the spinal cord of mice with EAE (a; 5.92 RQ ± 2.45; n=6) compared with controls (a; 0.98 RQ ± 0.31; n=6; **$p<0.01$; ANOVA). Treatment of mice with rosiglitazone did not significantly attenuate the EAE induced increase in CD40 mRNA (a; 9.17 RQ ± 5.36; n=6; ANOVA).

Figure 6.12 also shows that CD200 mRNA expression was significantly decreased in the spinal cord of EAE mice (b; 0.81 RQ ± 0.08; n=6) compared with controls (b; 1.55 RQ ± 0.17; n=6; ***$p<0.001$; ANOVA). Treatment with rosiglitazone did not significantly attenuate the EAE-induced decrease in CD200

mRNA expression (b; 0.97 RQ ± 0.12; n=6; ANOVA). However rosiglitazone significantly increased CD200 mRNA expression in the spinal cord (b 2.04 RQ ± 0.11; n=6; *p<0.05; ANOVA) compared with control.

Figure 6.13 shows that there was no significant difference in IL-4 mRNA expression in the spinal cord of mice with EAE (0.63 RQ ± 0.19; n=6) compared with control mice (1.14 RQ ± 0.14; n=6; ns, ANOVA).Treatment with rosiglitazone did not significantly attenuate the decrease in IL-4 mRNA in mice with EAE (1.53 RQ ± 0.56; n=6; ns; ANOVA), and rosiglitazone did not significantly affect IL-4 mRNA expression (3.19 RQ ± 1.4; n=6; ns; ANOVA) in controls.

6.4. Discussion

The aim of this study was to investigate the role of IL-4 in EAE and its role in modulating the pro-inflammatory activity of microglia. As rosiglitazone modulates microglial- driven inflammation in an IL-4-dependent manner, the effect of rosiglitazone to modulate EAE was also investigated. The results indicate that there was an increase in IL-1β in the spinal cord and hippocampus of wildtype mice with EAE and this was further increased in the spinal cord of IL-$4^{-/-}$ mice with EAE. This was accompanied by a significant decrease in CD200 expression in the spinal cord and hippocampus of wildtype mice with EAE which was decreased further in the hippocampus of IL-$4^{-/-}$ mice in which EAE was induced. Rosiglitazone treatment did not significantly modulate the severity of the disease but rosiglitazone treatment did attenuate the increase in IL-1β mRNA in the spinal cord.

In vitro studies (Chapter 3) have shown the importance of maintaining the balance of pro- and anti-inflammatory cytokines in the CNS, and how IL-4 has the ability to modulate microglial activation and the associated pro-inflammatory cytokine production. Pro-inflammatory cytokines are believed to play a crucial role in this pathogenic process of EAE as they promote and sustain the development of myelin-specific T cells, and promote the recruitment of myelinotoxic monocytes and macrophages into the CNS. Blockade and regulation of the pro-inflammatory cytokines has been considered an effective therapeutic strategy for EAE. Strategies include the blockade of IFNγ/TNF by a soluble receptor or by a blocking antibody, but also regulation can be achieved by modulator cytokines such as IL-10, TGF-β and IL-4 (Falcone et al., 1998; Ho et al., 2006; Rott et al., 1994). Racke and colleagues (1994) have shown that IL-4 induced immune deviation can be used as a therapy in EAE (Racke et al., 1994), and spontaneous recovery from EAE has been associated with an increased production of IL-4 in the CNS (Khoury et al., 1992).

In this study the aim was to examine the role of IL-4 in EAE disease progression using mice deficient in the IL-4 gene. Clinical scores were recorded over the course of disease progression post MOG injection, but no significant difference between groups was observed. Falcone and colleagues (1998) reported that disease onset occurred one day earlier and was more severe in IL-$4^{-/-}$ mice with EAE,

compared with wildtype mice, in an acute bout of EAE (Falcone et al., 1998) and this is supported by evidence that EAE induced in IL-$4^{-/-}$ mice was more severe in these mice than in wildtype mice (C57BL/6), but the authors found no delay in the onset of the disease (Bettelli et al., 1998). Evidence presented by Liblau and colleagues (1997) who compared the clinical course of EAE induced by immunisation with mouse spinal cord homogenate in three mouse mutants for the IL-4 gene; IL-$4^{-/-}$, IL-$4^{+/-}$ and IL-$4^{+/+}$ mice of the PL/J background, indicated that there was no significant difference in the frequency, severity and duration of EAE between the littermates (Liblau et al., 1997). Together the results suggest that the role of this cytokine in the regulation of EAE is quite complex.

A role for IL-4 as a modulator of neuroinflammation in age, Aβ and LPS-driven inflammation has been reported (Maher et al., 2005; Nolan et al., 2005). In EAE, administration of IL-4 prior to the onset of disease, and IL-4 administration during disease progression, has been shown to modulate and even halt its progression. Systemic administration of IL-4 (1μg every 8h) to mice with EAE resulted in the amelioration of the disease, a shift towards Th2 cell proliferation and a decrease in the CNS levels of the pro-inflammatory cytokines IFNγ and TNFα (Racke et al., 1994). However, IL-4 was administered systemically which supports the argument that the effect of IL-4 was observed on the peripheral T cells rather than the resident CNS cells (Furlan et al., 2001).

Experiments conducted using viral vector administration of IL-4 showed that IL-4 can inhibit EAE through a mechanism exerted at the CNS level. Injection of a viral vector containing the IL-4 gene into the CNS of Biozzi AB/H mice after the onset of disease in a relapsing remitting model of EAE, altered the progression of the disease (Furlan et al., 2001). The alteration was characterised by a shorter duration of the first attack, a longer remission period and a decreased severity and duration of the relapse in the IL-4-treated group. Interestingly the IL-4-treated group had decreased mRNA levels of the pro-inflammatory chemokines MCP-1 and RANTES, which was accompanied by increased IL-4 and IL-10 mRNA in the spinal cord. The authors also report a trend toward a decrease of TNFα and IL-1β mRNA in spinal cord of IL-4 treated animals (Furlan et al., 2001). The authors provide further evidence of this IL-4

treatment to attenuate a mouse model of chronic progressive EAE in a separate study where IL-4 administration in a viral vector reduced demyelination and axonal loss in EAE mice, while increasing the number of infiltrating T reg cells. The authors suggested that IL-4 was involved in T reg recruitment, through the release of chemokines capable of recruiting T reg cells with suppressant functions (Butti et al., 2008). The use of chemokine inhibitors has given insight into possible mechanism of IL-4 in EAE. While chemokines recruiting T reg cells are beneficial in the control of symptoms of EAE, inhibitors of the the matrix degrading enzyme MMP has proven to be protective in a chronic relapsing disease model (Liedtke et al., 1998). MMP inhibitors decreased demyelination and glial scarring associated with the disease and downregulated TNFα mRNA expression which was accompanied by increased expression of IL-4 on microglia like cells and astrocytes (Liedtke et al., 1998).

In this study, an increase in IL-1β mRNA and protein in both the spinal cord and hippocampus of mice with EAE was observed. Interestingly, there was a further increase in IL-1β mRNA and protein in the spinal cord of IL-$4^{-/-}$ mice with EAE, which is similar to the results of Falcone and colleagues (1998) who reported an increase IL-1β mRNA expression in the spinal cord of IL-$4^{-/-}$ mice with EAE, compared with wildtype mice (Falcone et al., 1998). This supports the role of IL-4 in maintaining the balance of pro- and anti-inflammatory cytokines in the CNS and is consistent with previous reports which showed that the neuroinflammatory changes in the hippocampus of aged rats was associated with a decrease in IL-4 and an increase in IL-1β (Nolan et al., 2005).

The increase in IL-1β in EAE is coupled with an increase in the expression of CD40 mRNA in both the hippocampus and spinal cord. Increased CD40 expression, an indicator of microglial activation, has been associated with a number of CNS inflammatory diseases such as MS and AD (Calingasan et al., 2002; Gerritse et al., 1996) and CD40 deletion renders an animal resistant to EAE disease progression (Chen et al., 2006). However in this study CD40 expression was not further increased in the CNS of IL-$4^{-/-}$ mice with EAE. This concurs with the earlier work reported in chapter 3, where treatment of mixed glia with IL-4 failed to attenuate the LPS-induced increase in CD40 mRNA. Both results suggest that the ability of IL-4 to

attenuate microglial activation appears to be independent of this marker of microglia activation.

Early reports have proposed that the ability of IL-4 to attenuate microglial activation and pro-inflammatory cytokine release is mediated through its interactions with the MAPKs, in particular ERK. However it has recently been suggested that the modulatory effect of IL-4 on microglial activation is driven by its ability to increase CD200 expression (Lyons et al., 2007a). CD200 is expressed on neurons and previous work, both *in vivo* and *in vitro,* has highlighted the importance of CD200-CD200R interaction in modulating microglial activation (Lyons et al., 2007a; Lyons et al., 2009)

The results from this study indicate that the increase in CD40 mRNA expression and IL-1β both in the spinal cord and hippocampus of mice with EAE, are associated with a decrease in the expression of CD200. Interestingly in the hippocampus the decrease in CD200 mRNA and protein expression in mice with EAE was further decreased in the hippocampus of IL-$4^{-/-}$ mice with EAE, providing further evidence of a role for IL-4 in the expression of CD200.

Earlier results (Chapter 3) show the ability of PPARγ agonists to modulate inflammation. Their ability to modulate the release of both pro- and anti-inflammatory cytokines from glial cells has focussed the research on their potential role in neuroinflammatory disease. In this study, oral administration of rosiglitazone did not significantly modulate the clinical score of mice with EAE when compared to the untreated mice with EAE. Feinstein and colleagues (2002) report that treatment of mice with rosiglitazone (5-10 mg/day), 3 days prior to EAE induction and each day for the course of the disease, in a chronic monophasic model of EAE did not reduce the maximum clinical score, but reduced average clinical scores 14 days after immunisation, and this reduction was sustained until recovery (Feinstein et al., 2002). Despite the inability of rosiglitazone to attenuate clinical severity of EAE, other PPARγ agonists have shown the ability to modulate clinical symptoms. The PPARγ agonists, pioglitazone and troglitazone, have been shown to ameliorate EAE in a MOG-induced mouse model (Feinstein et al., 2002; Niino et al., 2001a). Administration of troglitazone (100mg/kg/day) 1 day prior to EAE induction and

throughout the disease significantly delayed the onset of clinical symptoms and also reduced disease severity as maximal clinical scores were significantly reduced (Niino et al., 2001a). Subsequent experiments by these authors suggested that troglitazone was most effective when administered at the onset of clinical symptoms of the disease rather than in the induction phase of the disease. Interestingly they also report that expression of the pro-inflammatory cytokines TNFα and IL-1β in the spinal cord of troglitazone-treated mice was significantly lower than in untreated animals with EAE. This corresponds with the present data which shows that the increase in IL-1β and TNFα mRNA and protein, in the spinal cord of mice with EAE and the increase in IL-1β mRNA was significantly attenuated in the rosiglitazone-treated group. Niino and colleagues (2001) suggest that amelioration in EAE was attributable to the attenuation of pro-inflammatory cytokine gene expression (Niino et al., 2001a).

Research by Natarajan and Bright (2002) using the natural PPARγ agonist $15dPGJ_2$, has highlighted further the ability of PPARγ agonists to modulate microglia and have elaborated on how microglial activation is a potential mechanism for the progression/development of EAE. Administration of $15dPGJ_2$ (100μg) or ciglitazone (100μg) to SJL/J mice in a progressive EAE model delayed the onset of the disease and reduced the maximal clinical score; they report that this corresponded with a decrease in inflammation and demyelination in the spinal cord (Natarajan and Bright, 2002). This inhibition of EAE by the PPARγ agonists was associated with a decrease in IL-12 production and differentiation of neural antigenic specific Th1 cells; IL-12 is important in the pathogenesis of EAE and it has been shown previously that inhibition of IL-12 reduces the clinical symptoms of the disease. The authors performed *in vitro* experiments which indicated that PPARγ agonists inhibited the JAK STAT signalling cascade by blocking the IL-12-induced phosphorylation of JAK thereby preventing activation of STAT3 and STAT4; this resulted in a reduction in IL-12-induced proliferation and Th1 differentiation in T cells (Natarajan and Bright, 2002). The combination of evidence suggests that PPARγ agonists may modulate EAE in part through their effect on CNS glia.

The variation in ability of PPARγ agonists to modulate EAE may, in part be due to the method of administration of the drug. In this study the drug was dissolved

to the desired concentration in vegetable oil and the pellets of lab chow were coated with the suspension dispensed, which is similar to the method used by others (Feinstein et al., 2002). However the PPARγ agonists can be administered by i.p. injection or by gavage also. As the disease progresses, the animals mobility is impaired and they display sickness behaviour and reduced food intake, which is paralleled by a decrease in body weight. Administration of drugs by i.p. injection or gavage may prove more efficient as the intake of drug in these situations is consistent. The ability of PPARγ agonists to penetrate the BBB is limited, recent reports from GlaxoSmithKline the manufacturer of *Avandia*, which is the leading rosiglitazone brand, indicated that rosiglitizone binds with high affinity to serum proteins which reduces levels of the drug crossing the BBB and this reduces the effective concentration of the drug in the CNS. It would also be interesting to repeat the experiment with a larger number of animals, as the interaction of rosiglitazone and EAE as assessed by two-way ANOVA was close to statistical significance ($p=0.08$).

There any many factors that can play a role in the modulation of microglial activation, but cell-cell interaction is a mechanism of particular interest. The CD200-CD200R interaction as described above has been highlighted in EAE recently. In this study there was a significant decrease in CD200 mRNA expression in the spinal cord of mice with EAE, which was accompanied by a significant increase in CD40 mRNA expression. Rosiglitazone treatment significantly increased CD200 mRNA in the spinal cord of control mice. This is a novel finding as no evidence has been reported before for the ability of a PPARγ agonist to modulate CD200 mRNA expression and it is suggested here that this may serve as a potential mechanism for their anti-inflammatory action. However this requires further detailed investigation. Despite the effect, rosiglitazone treatment failed to reverse the EAE-induced decrease in CD200 which was accompanied by decrease in IL-4 mRNA. Interestingly rosiglitazone treatment increased, albeit not significantly, IL-4 mRNA in the spinal cord of control-treated mice, it failed to reverse the decrease in IL-4 mRNA with EAE.

The data presented here emphasise the important link between CD200 and microglial activation. Although no significant difference in clinical symptoms was

observed in IL-4$^{-/-}$ mice with EAE, compared with controls, a particular interesting observation is that the decrease in CD200 in MOG-treated animals is exaggerated in IL-4$^{-/-}$ mice. This provides further evidence for IL-4 in the expression of CD200, a possible target for the control of microglial activation in MS and EAE.

Chapter 6
Figures

Figure 6.1. Clinical scores in EAE in IL-4 $^{-/-}$ and C57BL/6 mice.

Clinical scores assessed daily (graded as follows: grade 0 – normal; grade 1 – flaccid tail; grade 2 – wobbly gait; grade 3 – hind limb weakness; grade 4 – hind limb paralysis; grade 5 – tetraparalysis/death) in mice (C57BL/6 and IL-4$^{-/-}$) injected subcutaneously with 150μg myelinoligodendrocyte glycoprotein (MOG_{35-55}), Complete Freund's Adjuvant (CFA) and Mycobacteria tuberculosis at Day 0 and an intraperitoneal injection of Pertussis Toxin (PT) at Day 0 and Day 2. Data are expressed as clinical score and presented as means (± SEM; n=6).

2-way RM ANOVA; $Time_{effect}$ $F(1,441)=339.6$; $p<0.001$, $Strain_{effect}$ $F(1,441)=1.107$; $p=0.3061$, $Interaction_{effect}$ $F(1,441)=1.95$; $p=0.007$

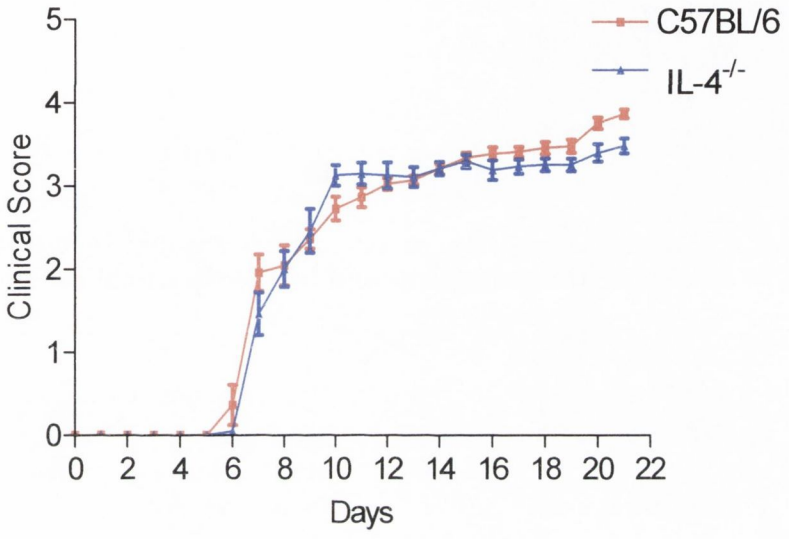
C57BL/6
IL-4-/-
Clinical Score
0
1
2
3
4
5
0 2 4 6 8 10 12 14 16 18 20 22
Days

Figure 6.2. IL-1β was increased in the spinal cord during EAE and IL-1β was significantly increased further in spinal cord of IL-4$^{-/-}$ mice with EAE.

IL-1β mRNA expression and protein concentration were significantly increased in spinal cord of EAE mice (a; *p<0.05; b;***p<0.001; ANOVA versus wildtype). IL-1β mRNA expression and protein concentration were further increased in IL-4$^{-/-}$ mice with EAE compared to wildtype EAE mice (a; $^{\#}$p<0.05; b; $^{\#}$p<0.05; ANOVA; versus wildtype EAE mice). IL-1β protein concentration was significantly decreased in IL-4$^{-/-}$ mice (b; **p<0.01; ANOVA; versus wildtype control). Data are presented as means (± SEM; n=6) and expressed as IL-1β:β-actin (RQ) or pg IL-1β/mg.

.

(a)2-way ANOVA; EAE_{effect} F(1,18)=8.19; p<0.05, $Strain_{effect}$ F(1,18)=2.27; p=0.149, $Interaction_{effect}$ F(1,18)=2.45; p=0.1347
(b)2-way ANOVA; EAE_{effect} F(1,21)=16.41; p<0.001, $Strain_{effect}$ F(1,21)=0.855; p=0.46, $Interaction_{effect}$ F(1,21)=8.72; p<0.001

a

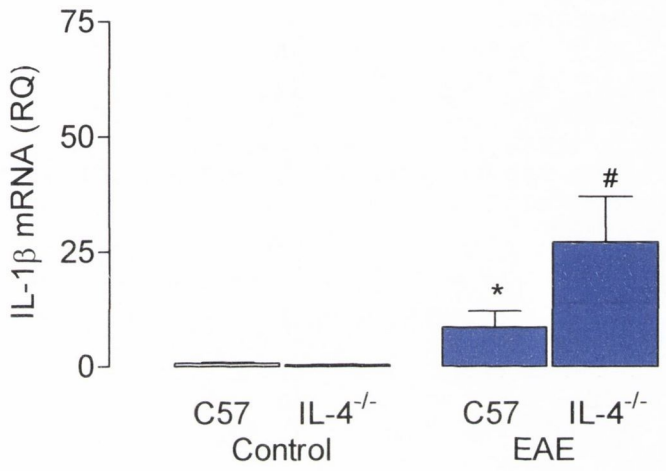
75
50
25
0
IL-1β mRNA (RQ)
*
#
C57
IL-4-/-
C57
IL-4-/-
Control
EAE

b

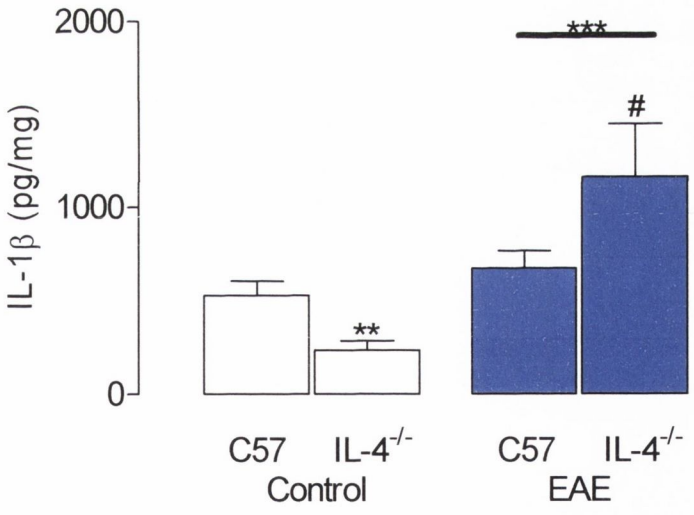
2000
1000
0
IL-1β (pg/mg)
***
#
**
C57
IL-4-/-
C57
IL-4-/-
Control
EAE

Figure 6.3. TNFα was not significantly increased in the spinal cord during EAE.

TNFα mRNA expression or protein concentration were not significantly increased in spinal cord of mice with EAE (a and b; ANOVA; versus wildtype control). TNFα mRNA expression or protein concentration were not increased in IL-$4^{-/-}$ mice with EAE (a; ANOVA; versus wildtype EAE). Data are presented as means (± SEM; n=6) and expressed as TNFα:β-actin (RQ) or pg TNFα/mg.

(a)2-way ANOVA; EAE_{effect} F(1,9)=3.35; p=0.1044, $Strain_{effect}$ F(1,9)=0.05; p=0.8283, $Interaction_{effect}$ F(1,9)=8.267; p=0.05
(b)2-way ANOVA; EAE_{effect} F(1,14)=1.66; p=0.2184, $Strain_{effect}$ F(1,14)=2.99; p=0.059, $Interaction_{effect}$ F(1,14)=1.44; p=0.2494

a

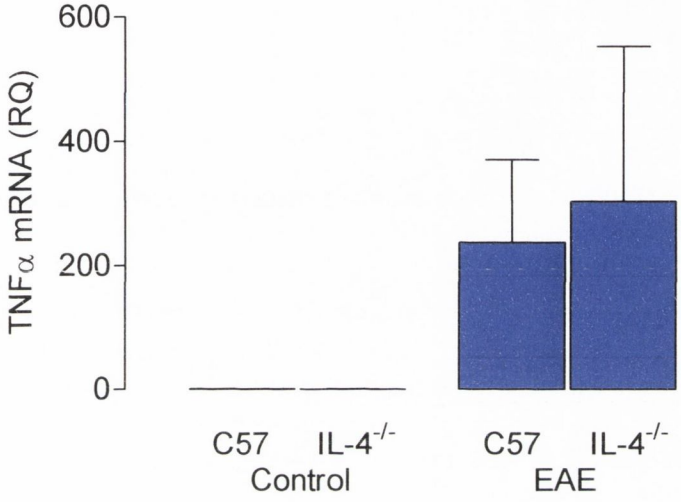
600
400
200
0
TNFα mRNA (RQ)
C57
IL-4-/-
Control
C57
IL-4-/-
EAE

b

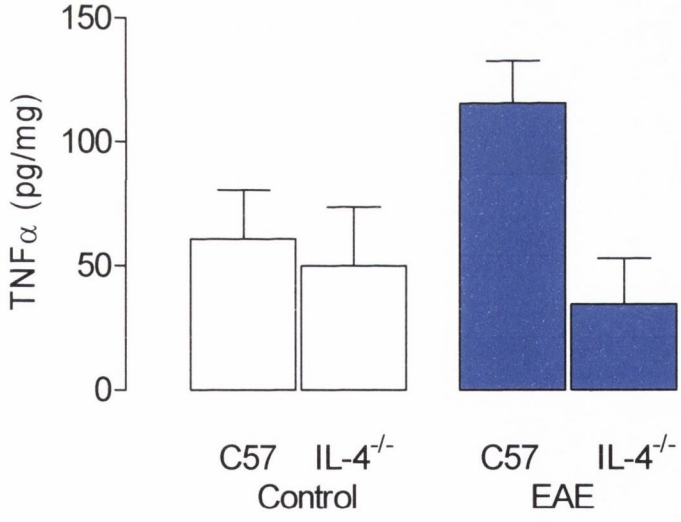
150
100
50
0
TNFα (pg/mg)
C57
IL-4-/-
Control
C57
IL-4-/-
EAE

Figure 6.4. CD200 expression was significantly decreased in the spinal cord during EAE.

CD40 mRNA expression was significantly increased in spinal cord of EAE mice (a; *p<0.05; ANOVA; versus wildtype control). CD200 mRNA expression was significantly decreased in EAE (b; ***p<0.001; ANOVA; versus wildtype control). Data are presented as means (± SEM; n=6) and expressed as CD40:β-actin (RQ) or CD200:β-actin (RQ).

(a) 2-way ANOVA; EAE_{effect} F(1,15)=4.9; p<0.05, $Strain_{effect}$ F(1,15)=3.74; p=0.0723, $Interaction_{effect}$ F(1,15)=3.63; p=0.0766.
(b) 2-way ANOVA; EAE_{effect} F(1,22)=1.59; p<0.001, $Strain_{effect}$ F(1,22)=1.09; p=0.3071, $Interaction_{effect}$ F(1,22)=0.60; p=0.4455.

a

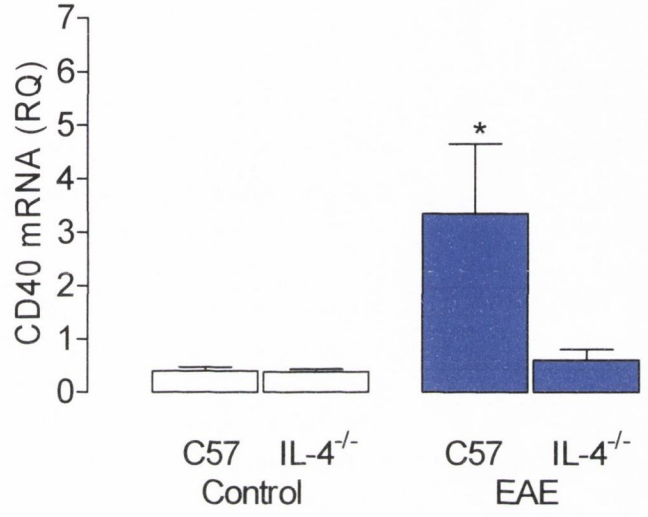
CD40 mRNA (RQ)
7
6
5
4
3
2
1
0
*
C57
IL-4-/-
Control
C57
IL-4-/-
EAE

b

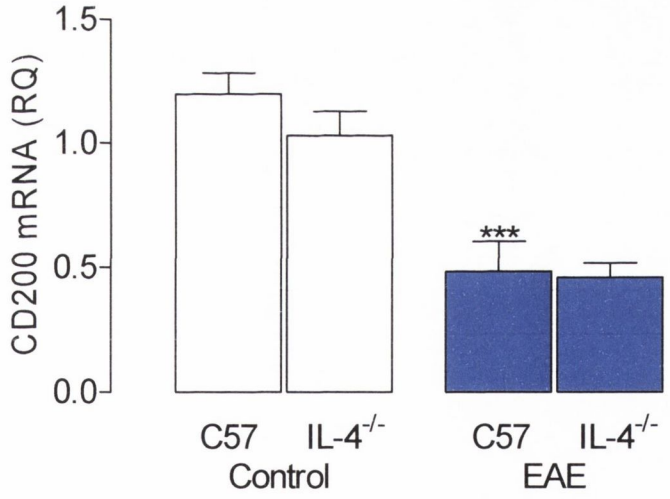
CD200 mRNA (RQ)
1.5
1.0
0.5
0.0
***
C57
IL-4-/-
Control
C57
IL-4-/-
EAE

Figure 6.5. IL-1β was significantly increased in the hippocampus during EAE.

IL-1β mRNA expression and protein concentration were significantly increased in hippocampus of EAE mice (a; *p<0.05; Student's *t* test; b; ***p<0.001; ANOVA; versus wiltype control). IL-1β mRNA expression and protein concentration were not further increased in IL-$4^{-/-}$ mice with EAE (a and b; ANOVA; versus wildtype EAE). Data are presented as means (± SEM; n=6) and expressed as IL-1β:β-actin (RQ) or pg IL-1β/mg.

(a)2-way ANOVA; EAE_{effect} F(1.36)=0.07; p=0.7876, $Strain_{effect}$ F(1,36)=3.11; p=0.862, $Interaction_{effect}$ F(1,36)=0.31; p=0.5795
(b)2-way ANOVA; EAE_{effect} F(1,26)=37.65; p<0.001, $Strain_{effect}$ F(1,26)=0.71; p=0.4073, $Interaction_{effect}$ F(1,26)=0.01; p=0.9303

a

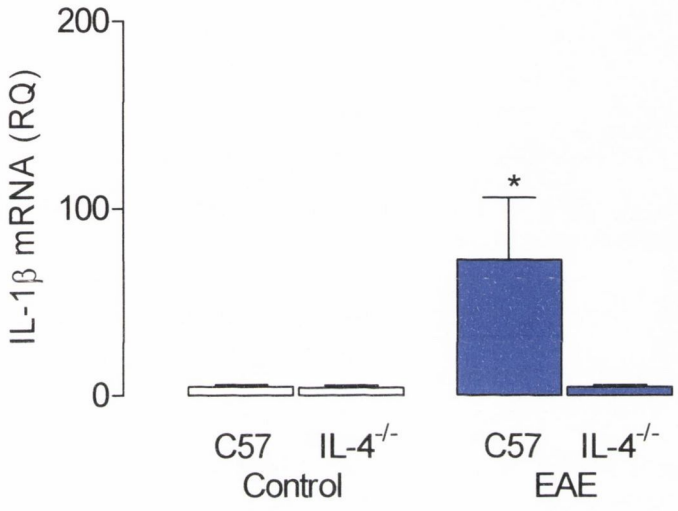
200
100
0
IL-1β mRNA (RQ)
*
C57
IL-4-/-
Control
C57
IL-4-/-
EAE

b

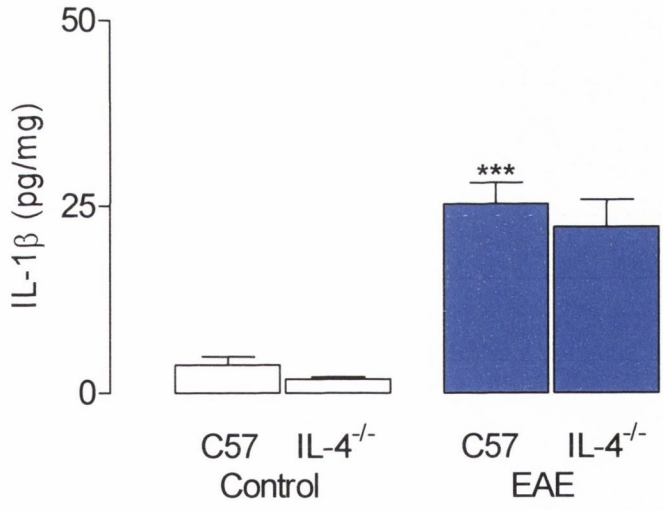
50
25
0
IL-1β (pg/mg)
***
C57
IL-4-/-
Control
C57
IL-4-/-
EAE

Figure 6.6. TNFα mRNA was significantly increased in the hippocampus during EAE.

TNFα mRNA expression was significantly increased in hippocampus of mice with EAE (a; *p<0.05; ANOVA; versus wildtype control). TNFα protein concentration did not significantly change in the hippocampus of mice with EAE (b; ANOVA; versus wildtype control). TNFα mRNA expression was not significantly increased in IL-$4^{-/-}$ mice with EAE mice (a; ANOVA; versus wildtype EAE). Data are presented as means (± SEM; n=6) or expressed as TNFα:β-actin (RQ) or pg TNFα/mg.

(a)2-way ANOVA; EAE_{effect} F(1,9)=3.35; p<0.05, $Strain_{effect}$ F(1,9)=0.05; p=0.8283, $Interaction_{effect}$ F(1,9)=8.267; p=0.05
(b)2-way ANOVA; EAE_{effect} F(1,14)=1.66; p=0.2184, $Strain_{effect}$ F(1,14)=2.99; p=0.059, $Interaction_{effect}$ F(1,14)=1.44; p<0.2494

a

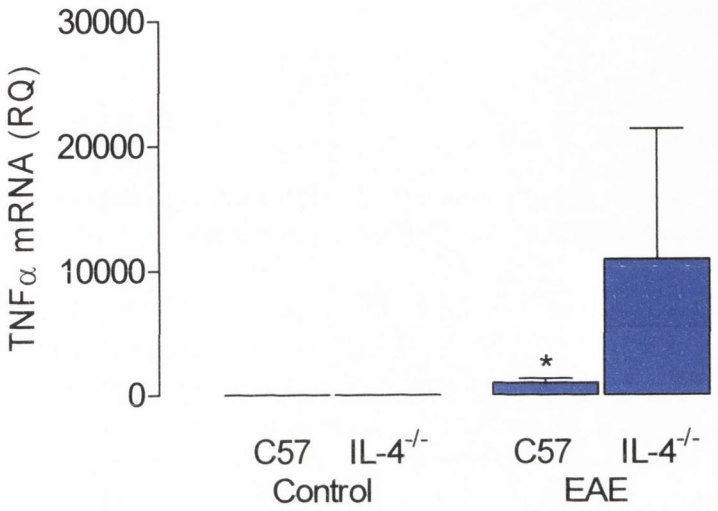
30000
20000
10000
0
TNFα mRNA (RQ)
*
C57
IL-4-/-
C57
IL-4-/-
Control
EAE

b

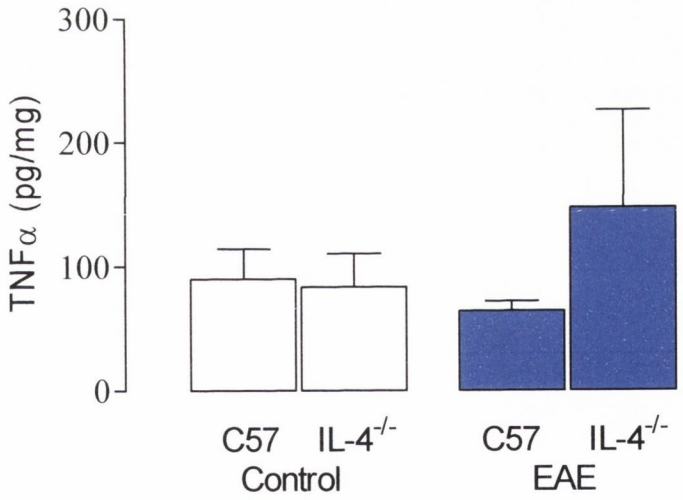
300
200
100
0
TNFα (pg/mg)
C57
IL-4-/-
C57
IL-4-/-
Control
EAE

Figure 6.7. CD40 expression was significantly increased in the hippocampus during EAE and CD200 expression was decreased.

CD40 mRNA expression was significantly increased in hippocampus mice with EAE (a; **p<0.01; ANOVA; versus wildtype control). CD200 mRNA expression was significantly decreased in EAE (b; **p<0.01; ANOVA; versus wildtype control) and further decreased in IL-$4^{-/-}$ mice (b; $^{\#}$p<0.05; Student's *t* test; versus wildtype EAE). Data are presented as means (± SEM; n=6) and expressed as CD40:β-actin (RQ) or CD200:β-actin.

(a)2-way ANOVA; EAE_{effect} F(1,20)=7.78; p<0.05, $Strain_{effect}$ F(1,20)=0.197; p=0.1753, $Interaction_{effect}$ F(1,20)=2.7; p=0.1158.
(b)2-way ANOVA; EAE_{effect} F(1,14)=73.91; p<0.001, $Strain_{effect}$ F(1,14)=6.04; p<0.05, $Interaction_{effect}$ F(1,14)=0.21; p=0.6543.

a

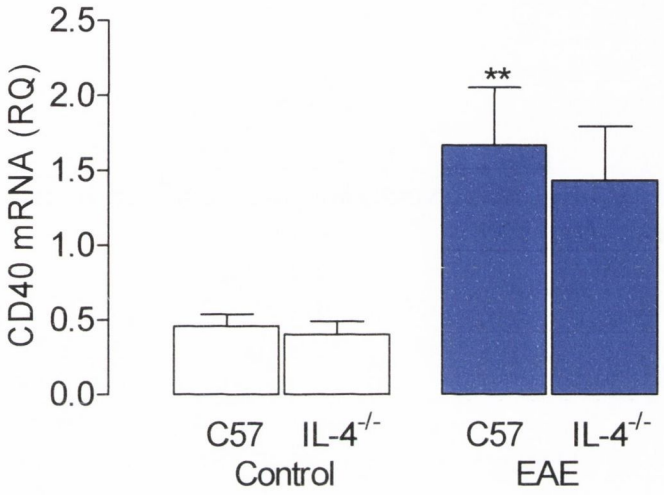
CD40 mRNA (RQ)
2.5
2.0
1.5
1.0
0.5
0.0
**
C57
IL-4-/-
Control
C57
IL-4-/-
EAE

b

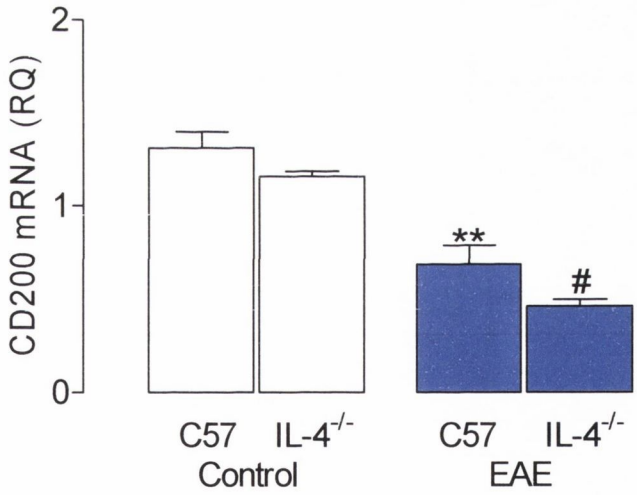
CD200 mRNA (RQ)
2
1
0
**
#
C57
IL-4-/-
Control
C57
IL-4-/-
EAE

Figure 6.8. CD200 protein expression was significantly decreased in the hippocampus during EAE.

A representative western immunoblot for CD200 proten expression (a). CD200 protein expression was significantly decreased in hippocampus in IL-$4^{-/-}$ mice (b;**$p<0.01$; ANOVA; versus control). CD200 protein expression was decreased in C57 mice with EAE (b; **$p<0.01$; ANOVA; versus control) . CD200 protein expression was further decreased in IL-$4^{-/-}$ with EAE (b; $^{\#}p<0.05$; Student's *t* test; versus wildtype EAE). Data are presented as means (± SEM; n=6) and expressed as CD200/actin (arbitrary units).

2-way ANOVA; EAE_{effect} $F(1,20)=8.887$; $p<0.01$, $Strain_{effect}$ $F(1,20)=5.899$; $p<0.05$, $Interaction_{effect}$ $F(1,20)=0.52$; $p=0.4792$.

a

CD200

C57 IL-4$^{-/-}$ C57 IL-4$^{-/-}$
Control EAE

b

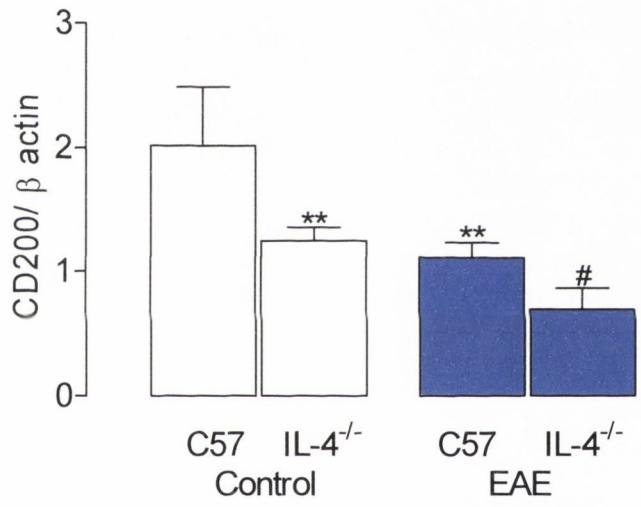

Figure 6.9. Clinical scores of C57BL/6 mice with EAE treated with rosiglitazone.

Clinical scores were assessed daily (graded as follows: grade 0 – normal; grade 1 – flaccid tail; grade 2 – wobbly gait; grade 3 – hind limb weakness; grade 4 – hind limb paralysis; grade 5 – tetraparalysis/death) in C57BL/6 mice treated orally with or without rosiglitazone for three weeks (rosiglitazone; 6mg/kg/day) and subsequently both groups were injected subcutaneously with 150 μg myelinoligodendrocyte glycoprotein (MOG_{35-55}), Complete Freund's Adjuvant (CFA) and Mycobacteria tuberculosis at Day 0 and an intraperitoneal injection of Pertusis Toxin (PT) at Day 0 and Day 2. Data are expressed as clinical scores and presented as means (± SEM; n=6).

2-way ANOVA; $Time_{effect}$ $F(1,210)=136.61$; $p<0.001$, $Rosiglitazone_{effect}$ $F(1,210)=2.17$; $p=0.1711$, $Interaction_{effect}$ $F(1,210)=1.5$; $p=0.0802$.

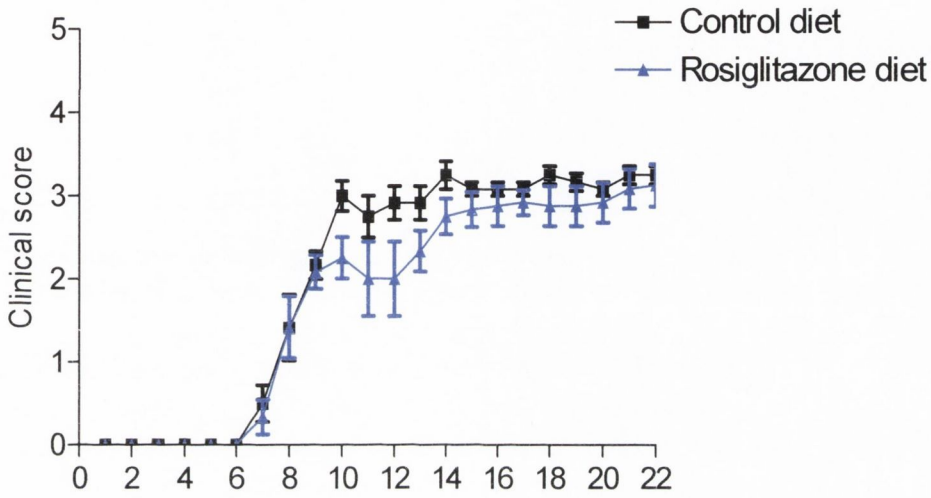
Control diet
Rosiglitazone diet
Clinical score
0
1
2
3
4
5
0 2 4 6 8 10 12 14 16 18 20 22

Figure 6.10. Pretreatment with rosiglitazone significantly attenuated the increase in IL-1β mRNA in the spinal cord of mice with EAE.

IL-1β mRNA expression and protein concentration were significantly increased in spinal cord of EAE mice (a; ***p<0.001; ANOVA; b; *p<0.05; Student's *t* test; ANOVA; versus wildtype control). IL-1β mRNA expression was attenuated by rosiglitazone (6mg/kg/day) pretreatment (a; $^{\#}$p<0.05; Student's *t* test; versus EAE). Pretreatment with rosiglitazone (6mg/kg/day) failed to attenuate the increase in IL-1β protein (b; ANOVA; versus EAE). Data are presented as means (± SEM; n=6) and expressed as IL-1β:β-actin (RQ) or pg IL-1β/mg. .

(a)2-way ANOVA; EAE_{effect} F(1,22)=11.98; p<0.001, $Rosiglitazone_{effect}$ F(1,22)=3.13; p=0.09, $Interaction_{effect}$ F(1,22)=2.94; p=0.11066.
(b)2-way ANOVA; EAE_{effect} F(1,18)=1.81; p=0.1952, $Rosiglitazone_{effect}$ F(1,18)=0.00; p=0.9960, $Interaction_{effect}$ F(1,18)=4.05; p=0.0593.

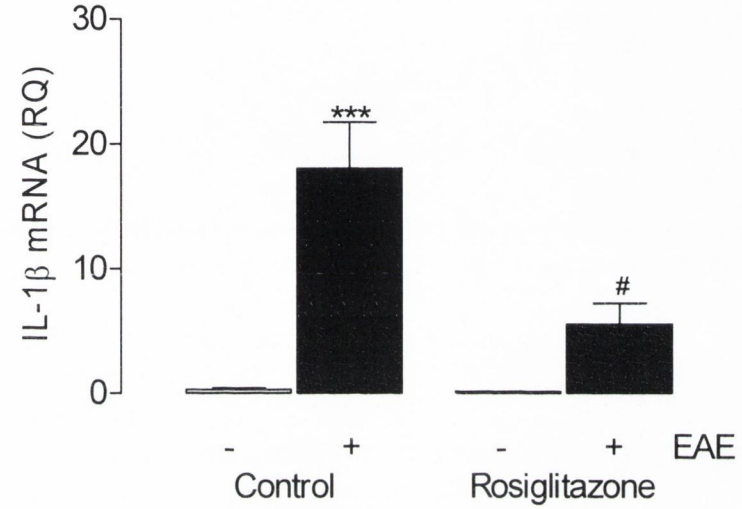
30
20
10
0
IL-1β mRNA (RQ)
***
#
-
+
-
+
EAE
Control
Rosiglitazone

b

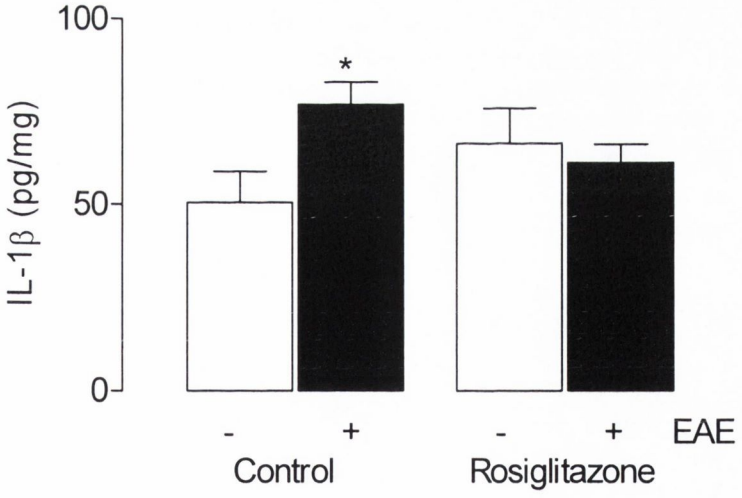
100
50
0
IL-1β (pg/mg)
*
-
+
-
+
EAE
Control
Rosiglitazone

Figure 6.11. TNFα was increased in the spinal cord during EAE and rosiglitazone treatment did not attenuate this increase.

TNFα mRNA expression and protein concentration were significantly increased in spinal cord of EAE mice (a; ***p<0.001; b; *p<0.05; ANOVA; versus control). Pretreatment with rosiglitazone (6mg/kg/day) failed to attenuate the increase in TNFα mRNA expression and protein concentration (a and b; ANOVA; versus EAE mice). Data are presented as means (± SEM; n=6) and expressed as TNFα:β-actin (RQ) or pg TNFα/mg. .

(a)2-way ANOVA; EAE_{effect} F(1,19)=22.95; p<0.001, $Rosiglitazone_{effect}$ F(1,19)=0.85; p=0.3677, $Interaction_{effect}$ F(1,19)=0.93; p=0.3467
(b) 2-way ANOVA; EAE_{effect} F(1,18)=6.05; p<0.05, $Rosiglitazone_{effect}$ F(1,18)=0.31; p=0.5843, $Interaction_{effect}$ F(1,18)=3.5; p=0.0778.

a

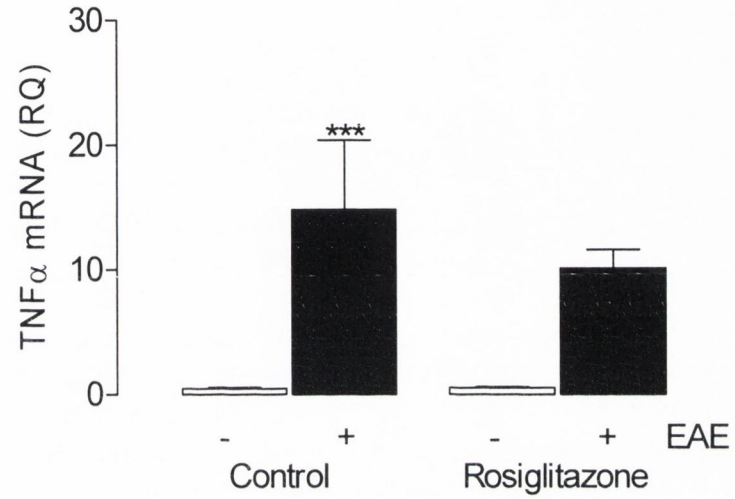
30
20
10
0
TNFα mRNA (RQ)
***
- + - + EAE
Control
Rosiglitazone

b

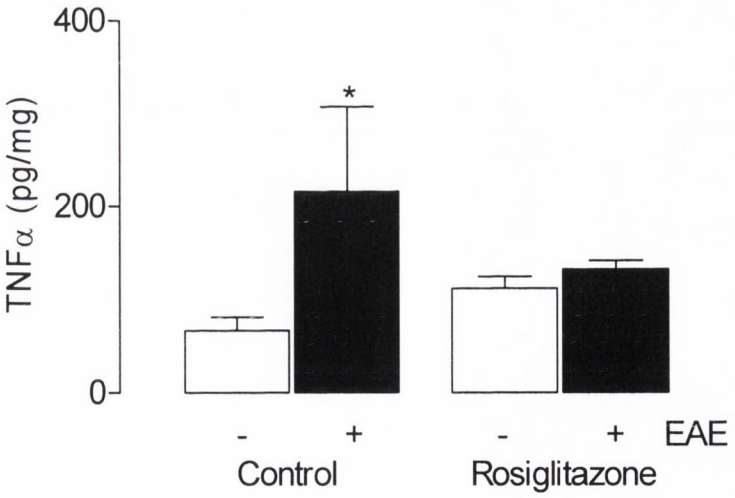
400
200
0
TNFα (pg/mg)
*
- + - + EAE
Control
Rosiglitazone

Figure 6.12. CD40 was significantly increased in the spinal cord and CD200 was decreased in spinal cord during EAE.

CD40 mRNA expression was significantly increased in spinal cord of mice with EAE (a; **p<0.01; ANOVA; versus control). CD40 mRNA expression was not attenuated by rosiglitazone (6mg/kg/day) pretreatment (a; ANOVA; versus EAE). CD200 mRNA expression was significantly decreased in EAE (b; ***p<0.001; ANOVA; versus control). Pretreatment with rosiglitazone (6mg/kg/day) significantly increased CD200 mRNA expression (b; *p<0.05; ANOVA; versus control). Data are presented as means (± SEM; n=6) and expressed as CD40:β-actin (RQ) or CD200:β-actin.

(a)2-way ANOVA; EAE_{effect} F(1,23)=1.78; p<0.01, $Rosiglitazone_{effect}$ F(1,23)=0.85; p=0.3706, $Interaction_{effect}$ F(1,23)=0.31; p=0.5683

(b)2-way ANOVA; EAE_{effect} F(1,18)=51.78; p<0.001, $Rosiglitazone_{effect}$ F(1,18)=6.72; p<0.05, $Interaction_{effect}$ F(1,18)=1.76; p=0.2013.

a

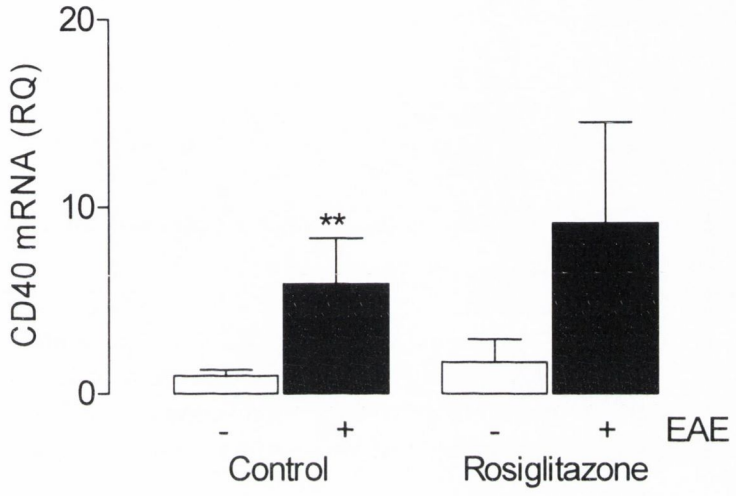
20
10
0
CD40 mRNA (RQ)
**
- + - + EAE
Control
Rosiglitazone

b

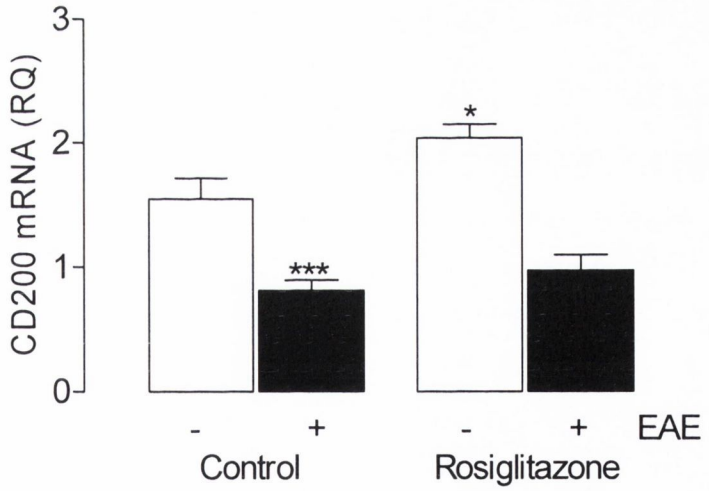
3
2
1
0
CD200 mRNA (RQ)
***
*
- + - + EAE
Control
Rosiglitazone

Figure 6.13. IL-4 was not significantly decreased in the spinal cord during EAE.

IL-4 mRNA expression was significantly decreased in spinal cord of mice with EAE (ns; ANOVA; versus control). IL-4 protein concentration was not significantly changed by rosiglitazone pretreatment (ns; ANOVA; versus control). Data are presented as means (± SEM; n=6)and expressed as pg IL-4/mg.

2-way ANOVA; EAE_{effect} F(1,15)=1.43; p=0..2499, $Rosiglitazone_{effect}$ F(1,15)=2.62; p=0.1261, $Interaction_{effect}$ F(1,15)=0.40; p=0.5347.

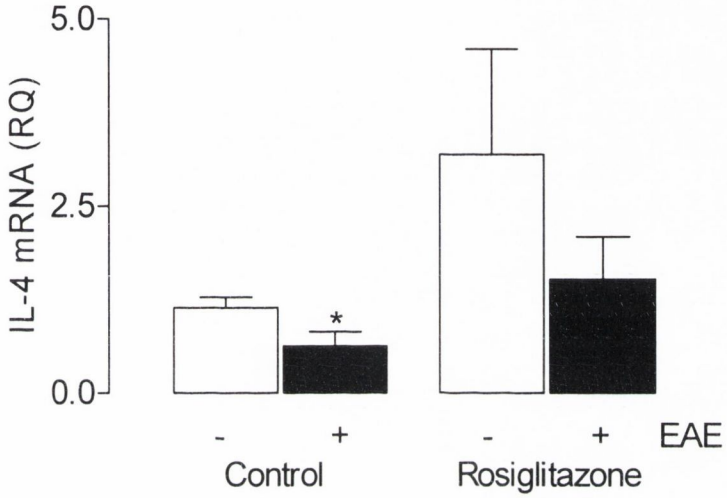
5.0
2.5
0.0
IL-4 mRNA (RQ)
*
- + - + EAE
Control
Rosiglitazone

Chapter 7

General Discussion

7.1. General Discussion

The overall objective of this study was to understand the mechanism by which microglial activation can be modulated as this is believed to play an important role in the pathogenesis of neurodegenerative diseases. This study focussed on the role of rosiglitazone as an anti-inflammatory agent and analysis was carried out to evaluate its effect *in vitro* and *in vivo*. The specific mechanism by which rosiglitazone might exert its effect was investigated and its effect on different glial cell types was also assessed.

The data show that rosiglitazone has the ability to modulate inflammation in mixed glial cells. LPS, which exerts a profound neuroinflammatory effect, induced a significant increase in IL-1β in mixed glia and pretreatment of mixed glia with rosiglitazone attenuated both the LPS-induced increase in the mRNA expression of IL-1β and the release of IL-1β. Activated glial cells also release other pro-inflammatory cytokines such as TNFα and IL-6 and the data show that pretreatment of mixed glia with rosiglitazone attenuated the LPS-induced increase in IL-6 and TNFα mRNA. Significantly it also inhibited the LPS-induced increase in expression of two markers of microglial activation CD40 and CD11b.

The ability of PPARγ agonists to modulate inflammation in the CNS has been demonstrated both *in vitro* and *in vivo*, but the exact mechanism by which the modulation occurs is debated. Studies in mixed glia, microglia and astrocytes have shown that PPARγ agonists can modulate the expression of pro-inflammatory cytokines, and this has been demonstrated to be mediated through PPARγ-dependent or PPARγ-independent mechanisms; in the latter case interaction with the transcription factors NFκB, AP1 and the JAK STAT pathway have been hypothesised.

As well as attenuating the mRNA expression of inflammatory cytokines including IL-1β, rosiglitazone attenuated the LPS-induced increase in IL-1β release from cultured glia. This corresponds with previous reports both *in vitro* and *in vivo* of the ability of rosiglitazone to modulate cytokine concentrations (Loane et al., 2009). Thus PPARγ agonists not only modulate pro-inflammatory cytokine transcriptional

activity but also the translation or release of pro-inflammatory cytokines. Recent research has focussed on the role of caspase 1 in the cleavage of pro-IL-1β to form IL-1β (Ferrari et al., 2006). The data presented here may indicate a possible modulatory role of rosiglitazone on caspase 1 or perhaps up-stream of this at the level of the inflammasome. Recent work has shown the importance of P2X7 receptor activation on caspase-1 activity. P2X7, a purinergic receptor and ligand gated ion channel, is activated by ATP and elicits both cleavage of mature IL-1β through a caspase-1 dependent process and its subsequent release. It is possible to measure P2X7 receptor expression by western immunoblotting or flow cytometry and would be interesting to identify if rosiglitazone had any effect on the expression of this receptor. The activity of the receptor could be monitored by measuring the activity of downstream products of P2X7 receptor activation such as MAPK, PLA_2 and phospholipase D. It would be interesting in future experiments also, to investigate whether rosiglitazone alters caspase-1 activity which can be assessed by a caspase 1 immunoassay.

As a mixed glial cell population contains both astrocytes and microglia, the ability of rosiglitazone to modulate LPS-induced changes in both individual cell types was examined. In astrocytes, pretreatment with rosiglitazone attenuated the LPS-induced increase in the supernatant concentration of IL-1β, which mirrors the result obtained in mixed glial cells, however in isolated microglia, rosiglitazone pretreatment failed to attenuate the LPS-induced increase in IL-1β. This identifies a cell associated differential effect of rosiglitazone and it can be concluded that the ability of rosiglitazone to inhibit IL-1β release from mixed glia can be attributed to its action on astrocytes.

However pretreatment with rosiglitazone attenuated the LPS-induced increase in TNFα and IL-6 in both astrocytes and microglia, but no attenuation was reported in mixed glia cells, which matches data in the literature in astrocytes and microglia (Bernardo et al., 2000; Giri et al., 2004). The distinct differences in the ability of rosiglitazone to attenuate the pro-inflammatory cytokines in isolated microglia and astrocytes compared with mixed glial cultures suggests that the isolation of cell types may result in changes in the phenotype of the cells, a loss of cell-cell communication

that may alter their response to rosiglitazone. One possible conclusion is that the study of mixed glial cells is more relevant than the study of individual cell types.

Previous work has shown that the age, Aβ and LPS-induced increases IL-1β were associated with a decrease in the anti-inflammatory cytokines IL-4 and IL-10 (Clarke et al., 2008; Kavanagh et al., 2004; Loane et al., 2009). It has been reported that maintaining the balance of pro-inflammatory and anti-inflammatory cytokines is important, as reversing the age- and Aβ-related decrease in IL-4, attenuated the increase in IL-1β (Loane et al., 2009; Nolan et al., 2005). In this study, rosiglitazone induced an increase in the supernatant concentration of IL-4 in mixed glia and astrocytes, however it did not increase IL-4 in microglia. This suggests that the possible modulatory role of rosiglitazone, on pro-inflammatory cytokine secretion, in particular IL-1β, may be mediated by increased IL-4, and that the source of the IL-4 is astrocytes. Recently published data confirms the ability of astrocytes to produce IL-4 (Park et al., 2009). It is noted that the levels of IL-4 in both microglia and astrocytes are quite low, and would be strengthened by knowledge of the specificity of the IL-4 ELISA assay. This could be achieved by measuring IL-4 concentration in supernatant of mixed glia from IL-$4^{-/-}$ mice, a result that would strengthen the conclusions of the current work and of future studies.

The potential importance of IL-4 in mediating the modulatory effect of rosiglitazone was investigated further in mixed glia obtained from wildtype mice and mice deficient in IL-4. The data show that rosiglitazone attenuated the LPS-induced increase in IL-1β in mixed glia obtained from wildtype mice, but no attenuation was observed in mixed glia from IL-$4^{-/-}$ mice, emphasising the role for IL-4 in mediating the action of rosiglitazone. If this is true, it would be expected that treatment of mixed glia directly with IL-4 would mimic the modulatory effect of rosiglitazone. The results of this study show that treatment of mixed glia with IL-4 did attenuate the LPS-induced increase in IL-1β, which mirror the results obtained for rosiglitazone treatment. While the use of glial cells from IL-$4^{-/-}$ mice is useful, treatment of mixed glia with antibodies for IL-4 or IL-4 receptor blocking antibodies would provide further insight into the ability of rosiglitazone to modulate inflammation in an IL-4 dependent manner, and is something that would merit further investigation.

Rosiglitazone attenuated the LPS-induced increase in the expression of the markers of microglial activation CD40 and CD11b, in both mixed glia and isolated microglia. However treatment of mixed glia with IL-4 did not attenuate the increase in CD40 and CD11b expression. This means that the modulation of pro-inflammatory cytokines by rosiglitazone occurs by a different mechanism to that responsible for the modulation of cell surface expression of CD40 and CD11b. Previous reports have shown the ability of IL-4 to inhibit IFNγ-induced increases in CD40 expression. The authors reported that the inhibition occurred at the transcriptional level whereby IL-4 activated the transcription factor STAT-6 which bound to CD40 promoter inhibiting its expression (Nguyen and Benveniste, 2000). Although LPS, not IFNγ, was the inflammatory stimulus in this study, this mechanism may underlie the change in CD40 described here. An alternative possibility is that NFκB activation may play a role since Qin and colleagues (2005) report that LPS induced CD40 expression in microglia through the activation of the transcription factors NFκB and STAT-1α. Previous evidence from this lab has shown the ability of rosiglitazone to attenuate the age-related increase in pro-inflammatory cytokines and markers of microglial activation. It would be interesting to compare the ability of rosiglitazone to attenuate inflammatory markers *in vitro*, as demonstrated here, directly with the ability of rosiglitazone to modulate LPS-induced inflammation *in vivo*. Administration of LPS intracerebrally to animals treated orally with rosiglitazone or IL-4 may provide insight into the mechanism by which rosiglitazone mediates its anti-inflammatory properties in *vivo*.

Evidence has emerged that although rosiglitazone has the ability to function well in the treatment of diabetes and demonstrates anti-inflammatory properties in the brain, it has been associated with an increased risk of myocardial infarction in patients. These initial reports have led to the search for novel PPARγ agonists that can exert similar effects to rosiglitazone without the cardiotoxicity. In this study a novel PPARγ agonist MDG79 was investigated for its ability to modulate LPS-induced changes in mixed glial cells. MDG79, which is probably BBB permeable, was required at a higher concentration than rosiglitazone to attenuate the LPS-induced increase in TNFα and IL-6 and the expression of the markers of microglial activation CD40 and CD11b. However MDG79 attenuated the LPS-induced increase

in IL-1β at a concentration similar to rosiglitazone. To examine whether its actions are PPARγ-dependent the effect of MDG79 on CD36 and LPL expression was assessed; these are two gene products of PPARγ activation. MDG79 did not increase the expression of either, which suggested that the modulatory role of MDG79 was independent of PPARγ activation. To further assess this, a PPARγ antagonist GW9662 was used. Interestingly GW9662 failed to reverse the ability of MDG79 to attenuate the LPS-induced increase in pro-inflammatory cytokines, suggesting that MDG79 operates independent of PPARγ, but GW9662 did reverse the ability of MDG79 to attenuate the LPS-induced increase in CD40 and CD11b mRNA expression. This raises the issue of whether PPARγ agonists can in fact modulate the expression of cell surface proteins and pro-inflammatory cytokines in two different ways. Previous work has shown that the attenuation in expression of CD40 by rosiglitazone was PPARγ-dependent. Sun and colleagues (2008) showed that rosiglitazone attenuated the increase in CD40 expression in the hippocampus of mice in a model of epilepsy and that treatment with PPARγ antagonists T0070907 reversed the rosiglitazone-induced attenuation (Sun et al., 2008). This raises the issue, as pointed out by Landreth, that there is no common consensus on what is the dominant mode of PPARγ action. Although rosiglitazone attenuated the pro-inflammatory cytokine expression and release in a PPARγ-independent manner, possibly mediated by IL-4, it appears that the ability of PPARγ agonists to modulate the expression of cell surface markers of microglial activation is PPARγ-dependent.

Inflammation, microglial activation and increased pro-inflammatory cytokines are associated with neuroinflammation and neurodegenerative disease. One such disease is MS, and much of our understanding of the inflammatory process associated with MS comes from research using the animal model of MS, EAE. In this study, microglial activation and pro-inflammatory cytokine production were examined in the CNS prior to, and following, onset of clinical symptoms of the disease. The data showed an increase in the IL-1β and TNFα mRNA expression in the spinal cord prior to the onset of clinical symptoms, which was accompanied by an increase in CD40 mRNA expression at the onset of symptoms. Both pro-inflammatory cytokines have been shown to be important in the onset of disease as blocking or removal of these

pro-inflammatory cytokines delayed the onset of disease (Jacobs et al., 1991; Murphy et al., 2002). Pro-inflammatory cytokine expression and concentration of cytokines were increased in the spinal cord at the peak of disease. The origin of the source of these cytokines involved in the onset of EAE is still debated as evidence for both glial cell-derived and T cell-derived cytokines is suggested. Here we show an increase in a marker of microglial activation, CD40, which is consistent with cytokines being glial cell-derived, however future experiments would benefit greatly from the use of double-labelling experiments, using confocal microscopy or light microscopy, for these cytokines and their colocalisation with markers of microglial activation such as CD40, CD11b and MHC II, which would provide a cell specific indication of the cells responsible for cytokine production in EAE.

Loss of cognition is one of the earliest manifestations of MS, but little research has focussed on the effect of MS on the hippocampus. In this study analysis of changes in the hippocampus was included and an increase in the mRNA expression of two markers of microglial activation, CD40 and CD11b are reported at the onset of clinical symptoms. This corresponds with the increase in CD40 mRNA in the spinal cord at the same time point, indicating microglial activation in two distinct regions of the CNS at the onset of clinical symptoms. This study also showed an increase in the expression of the pro-inflammatory cytokines, TNFα, IL-6 and IL-1β, in the hippocampus at the peak of disease severity, which was associated with the increase in CD40 mRNA expression.

Cell-cell interactions play an important role in the maintenance of microglia in a quiescent state. One protein expressed on neurons that interacts with microglia is CD200. Its interaction with CD200 receptor which is expressed on microglia has been shown to decrease microglial activation (Hoek et al., 2000; Lyons et al., 2007a). In this study the data indicate a decrease in CD200 expression in the spinal cord and hippocampus over the course of EAE which was associated with the increase in CD40 mRNA expression. Previous work by Hoek and colleagues (2000) has shown the importance of CD200 in EAE, where onset of clinical symptoms of EAE occurred earlier in $CD200^{-/-}$, compared with wildtype, mice and that this was accompanied by an increase in the expression of CD68, a marker of microglial activation (Hoek et al.,

2000). Interestingly in this study, the decrease in CD200 in the hippocampus was associated with a decrease in anti-inflammatory cytokine IL-4 at every time point of the disease. Evidence in the literature shows the importance of IL-4 in modulating CD200 expression and that the anti-inflammatory action of IL-4 may be mediated through CD200 (Lyons et al., 2007a; Lyons et al., 2009). Therefore any potential therapeutic benefit of IL-4 in MS may be associated with CD200 expression and this may be an additional, more specific target.

With respect to the importance of the anti-inflammatory cytokines in maintaining the balance of pro- and anti-inflammatory cytokines in the brain the current data showed that IL-4 mRNA expression was decreased in the hippocampus over the course of EAE disease progression, which corresponded with the increase in pro-inflammatory cytokines and markers of microglial activation. This suggests that a potential target for the treatment of inflammation associated with EAE may be to address the deficit in IL-4.

To further investigate the role of IL-4 in EAE, we assessed the direct effect of IL-4 on EAE by inducing EAE in mice deficient in the IL-4 gene. The data shows no significant differences in clinical symptoms were recorded between IL-$4^{-/-}$ mice and wildtype mice with EAE. There are disparities in the literature on the role of IL-4 in EAE. It has been reported that disease occurred earlier (Falcone et al., 1998) and was more severe in IL-$4^{-/-}$ mice (Bettelli et al., 1998; Falcone et al., 1998), however Liblau and colleagues (1997) reported no difference in the frequency, severity, and duration of EAE in IL-$4^{-/-}$, IL-$4^{+/-}$ and IL-$4^{+/+}$ mice (Liblau et al., 1997). Here, the data show that there was an increase in IL-1β expression and protein in the spinal cord and hippocampus with EAE, which was increased further in the spinal cord obtained from IL-$4^{-/-}$ mice. This emphasised the role of IL-4 in modulating the pro-inflammatory cytokine IL-1β which has been demonstrated previously in the literature. However it is important to note that this further increase in expression was not observed for other cytokines or glial markers measured in IL-$4^{-/-}$ mice with EAE which suggests that careful consideration of all cytokines must be considered for therapies, as not all inflammatory markers are modulated in a similar manner.

This study also confirmed that there was an increase in CD40 mRNA expression in mice with EAE, and this was associated with a decrease in the expression of CD200. Interestingly, in the hippocampus the decrease in CD200mRNA and protein expression in mice with EAE was further decreased in the hippocampus of IL-$4^{-/-}$ mice with EAE, providing further evidence of a role for IL-4 in the expression of CD200, and a possible target for the control of microglial driven inflammation in MS and EAE.

As rosiglitazone has been shown to increase IL-4 in mixed glia, and *in vivo* it has reversed the age related deficit in IL-4 (Loane et al., 2009), the ability of rosiglitazone to modulate EAE was investigated. Rosiglitazone was administered to mice for three weeks prior to MOG injection, and as the disease progressed. Interestingly, mice with EAE that were treated with rosiglitazone were not significantly different in clinical score than non-treated mice with EAE. Feinstein and colleagues (2002) have previously found that the PPARγ agonist pioglitazone ameliorated clinical symptoms in a mouse model of EAE and this is supported by another study which demonstrated that troglitazone delayed the onset of EAE and significantly reduced maximal clinical scores of the disease (Niino et al., 2001a). The apparent variation in the ability of different PPARγ agonists to modulate EAE may be, in part, due to the method of administration of the drug. In the current study, the drug was administered in a similar method to Feinstein and colleagues (2002) where it was dissolved in vegetable oil and the food pellets were coated with the suspension. However this method does not guarantee that all of the drug is consumed by the animal, especially in late disease when voluntary intake of food is lower. Administration of the drug by gavage or i.p. injection is clearly more efficient as the intake of the drug in these situations is consistent. There is also debate over the ability of these drugs to penetrate the BBB. In EAE the BBB barrier is compromised but a drug, such as MDG79, with similar anti-inflammatory effects to rosiglitazone but one which is more BBB permeable may be of greater benefit in the treatment of EAE. Although no significant difference was observed in the clinical score rosiglitazone treatment did attenuate the increase in IL-1β in the spinal cord of mice with EAE, which reiterates the ability of rosiglitazone to modulate IL-1β in an inflammatory environment. Interestingly, rosiglitazone treatment also increased the expression of

CD200 in the spinal cord, which is the first report in the literature of this, but rosiglitazone treatment failed to reverse the decrease in CD200 in mice with EAE.

The most important findings of this study are that the PPARγ agonists rosiglitazone and MDG79 can modulate microglial activation *in vitro* and that. The data suggest that the ability of rosiglitazone to increase IL-4 may be an important contributory factor in the mechanism of action of rosiglitazone, although other mechanisms cannot be ruled out. Additional experiments are required to uncover the precise mechanisms by which rosiglitazone acts in the brain and to provide an understanding of its potential benefit, and the benefit of other PPARγ agonists, in conditions like MS.

References

References

Abbas, N., Bednar, I., Mix, E., Marie, S., Paterson, D., Ljungberg, A., Morris, C., Winblad, B., Nordberg, A., Zhu, J., 2002. Up-regulation of the inflammatory cytokines IFN-gamma and IL-12 and down-regulation of IL-4 in cerebral cortex regions of APP(SWE) transgenic mice. J Neuroimmunol 126, 50-57.

Abbott, N.J., Ronnback, L., Hansson, E., 2006. Astrocyte-endothelial interactions at the blood-brain barrier. Nat Rev Neurosci 7, 41-53.

Adams, S., van der Laan, L.J., Vernon-Wilson, E., Renardel de Lavalette, C., Dopp, E.A., Dijkstra, C.D., Simmons, D.L., van den Berg, T.K., 1998. Signal-regulatory protein is selectively expressed by myeloid and neuronal cells. J Immunol 161, 1853-1859.

Aharoni, R., Arnon, R., Eilam, R., 2005. Neurogenesis and neuroprotection induced by peripheral immunomodulatory treatment of experimental autoimmune encephalomyelitis. J Neurosci 25, 8217-8228.

Albrecht, P.J., Dahl, J.P., Stoltzfus, O.K., Levenson, R., Levison, S.W., 2002. Ciliary neurotrophic factor activates spinal cord astrocytes, stimulating their production and release of fibroblast growth factor-2, to increase motor neuron survival. Exp Neurol 173, 46-62.

Alderson, M.R., Armitage, R.J., Tough, T.W., Strockbine, L., Fanslow, W.C., Spriggs, M.K., 1993. CD40 expression by human monocytes: regulation by cytokines and activation of monocytes by the ligand for CD40. J Exp Med 178, 669-674.

Allan, S.M., Tyrrell, P.J., Rothwell, N.J., 2005. Interleukin-1 and neuronal injury. Nat Rev Immunol 5, 629-640.

Aloisi, A.M., Casamenti, F., Scali, C., Pepeu, G., Carli, G., 1997. Effects of novelty, pain and stress on hippocampal extracellular acetylcholine levels in male rats. Brain Res 748, 219-226.

Aloisi, F., 2001. Immune function of microglia. Glia 36, 165-179.

Aloisi, F., De Simone, R., Columba-Cabezas, S., Penna, G., Adorini, L., 2000. Functional maturation of adult mouse resting microglia into an APC is promoted by granulocyte-macrophage colony-stimulating factor and interaction with Th1 cells. J Immunol 164, 1705-1712.

Aloisi, F., Penna, G., Polazzi, E., Minghetti, L., Adorini, L., 1999. CD40-CD154 interaction and IFN-gamma are required for IL-12 but not prostaglandin E2 secretion by microglia during antigen presentation to Th1 cells. J Immunol 162, 1384-1391.

Araque, A., Parpura, V., Sanzgiri, R.P., Haydon, P.G., 1998a. Glutamate-dependent astrocyte modulation of synaptic transmission between cultured hippocampal neurons. Eur J Neurosci 10, 2129-2142.

Araque, A., Sanzgiri, R.P., Parpura, V., Haydon, P.G., 1998b. Calcium elevation in astrocytes causes an NMDA receptor-dependent increase in the frequency of miniature synaptic currents in cultured hippocampal neurons. J Neurosci 18, 6822-6829.

Argaw, A.T., Zhang, Y., Snyder, B.J., Zhao, M.L., Kopp, N., Lee, S.C., Raine, C.S., Brosnan, C.F., John, G.R., 2006. IL-1beta regulates blood-brain barrier permeability via reactivation of the hypoxia-angiogenesis program. J Immunol 177, 5574-5584.

Armitage, R.J., Fanslow, W.C., Strockbine, L., Sato, T.A., Clifford, K.N., Macduff, B.M., Anderson, D.M., Gimpel, S.D., Davis-Smith, T., Maliszewski, C.R., et al., 1992. Molecular and biological characterization of a murine ligand for CD40. Nature 357, 80-82.

Atalar, K., Afzali, B., Lord, G., Lombardi, G., 2009. Relative roles of Th1 and Th17 effector cells in allograft rejection. Curr Opin Organ Transplant 14, 23-29.

Babcock, A.A., Kuziel, W.A., Rivest, S., Owens, T., 2003. Chemokine expression by glial cells directs leukocytes to sites of axonal injury in the CNS. J Neurosci 23, 7922-7930.

Bailey, S.L., Schreiner, B., McMahon, E.J., Miller, S.D., 2007. CNS myeloid DCs presenting endogenous myelin peptides 'preferentially' polarize CD4+ T(H)-17 cells in relapsing EAE. Nat Immunol 8, 172-180.

Banerjee, D., Dick, A.D., 2004. Blocking CD200-CD200 receptor axis augments NOS-2 expression and aggravates experimental autoimmune uveoretinitis in Lewis rats. Ocul Immunol Inflamm 12, 115-125.

Barclay, A.N., 1981. Different reticular elements in rat lymphoid tissue identified by localization of Ia, Thy-1 and MRC OX 2 antigens. Immunology 44, 727-736.

Barron, K.D., 1995. The microglial cell. A historical review. J Neurol Sci 134 Suppl, 57-68.

Bauer, J., Sminia, T., Wouterlood, F.G., Dijkstra, C.D., 1994. Phagocytic activity of macrophages and microglial cells during the course of acute and chronic relapsing experimental autoimmune encephalomyelitis. J Neurosci Res 38, 365-375.

Baxter, A.G., 2007. The origin and application of experimental autoimmune encephalomyelitis. Nat Rev Immunol 7, 904-912.

Beck, J., Rondot, P., Catinot, L., Falcoff, E., Kirchner, H., Wietzerbin, J., 1988. Increased production of interferon gamma and tumor necrosis factor precedes clinical manifestation in multiple sclerosis: do cytokines trigger off exacerbations? Acta Neurol Scand 78, 318-323.

Benveniste, E.N., 1997. Role of macrophages/microglia in multiple sclerosis and experimental allergic encephalomyelitis. J Mol Med 75, 165-173.

Benveniste, E.N., 1998. Cytokine actions in the central nervous system. Cytokine Growth Factor Rev 9, 259-275.

Benveniste, E.N., Sparacio, S.M., Norris, J.G., Grenett, H.E., Fuller, G.M., 1990. Induction and regulation of interleukin-6 gene expression in rat astrocytes. J Neuroimmunol 30, 201-212.

Berger, J., Moller, D.E., 2002. The mechanisms of action of PPARs. Annu Rev Med 53, 409-435.

Bernard, C.C., Carnegie, P.R., 1975. Experimental autoimmune encephalomyelitis in mice: immunologic response to mouse spinal cord and myelin basic proteins. J Immunol 114, 1537-1540.

Bernardo, A., Ajmone-Cat, M.A., Gasparini, L., Ongini, E., Minghetti, L., 2005. Nuclear receptor peroxisome proliferator-activated receptor-gamma is activated in rat microglial cells by the anti-inflammatory drug HCT1026, a derivative of flurbiprofen. J Neurochem 92, 895-903.

Bernardo, A., Levi, G., Minghetti, L., 2000. Role of the peroxisome proliferator-activated receptor-gamma (PPAR-gamma) and its natural ligand 15-deoxy-Delta12, 14-prostaglandin J2 in the regulation of microglial functions. Eur J Neurosci 12, 2215-2223.

Bernardo, A., Minghetti, L., 2006. PPAR-gamma agonists as regulators of microglial activation and brain inflammation. Curr Pharm Des 12, 93-109.

Bettelli, E., Das, M.P., Howard, E.D., Weiner, H.L., Sobel, R.A., Kuchroo, V.K., 1998. IL-10 is critical in the regulation of autoimmune encephalomyelitis as demonstrated by studies of IL-10- and IL-4-deficient and transgenic mice. J Immunol 161, 3299-3306.

Bezzi, P., Carmignoto, G., Pasti, L., Vesce, S., Rossi, D., Rizzini, B.L., Pozzan, T., Volterra, A., 1998. Prostaglandins stimulate calcium-dependent glutamate release in astrocytes. Nature 391, 281-285.

Black, R.A., Rauch, C.T., Kozlosky, C.J., Peschon, J.J., Slack, J.L., Wolfson, M.F., Castner, B.J., Stocking, K.L., Reddy, P., Srinivasan, S., Nelson, N., Boiani, N., Schooley, K.A., Gerhart, M., Davis, R., Fitzner, J.N., Johnson, R.S., Paxton, R.J., March, C.J., Cerretti, D.P., 1997. A metalloproteinase disintegrin that releases tumour-necrosis factor-alpha from cells. Nature 385, 729-733.

Block, M.L., Hong, J.S., 2005. Microglia and inflammation-mediated neurodegeneration: multiple triggers with a common mechanism. Prog Neurobiol 76, 77-98.

Boado, R.J., Pardridge, W.M., 2002. Glucose deprivation and hypoxia increase the expression of the GLUT1 glucose transporter via a specific mRNA cis-acting regulatory element. J Neurochem 80, 552-554.

Bogacka, I., Xie, H., Bray, G.A., Smith, S.R., 2004. The effect of pioglitazone on peroxisome proliferator-activated receptor-gamma target genes related to lipid storage in vivo. Diabetes Care 27, 1660-1667.

Brodie, C., Goldreich, N., Haiman, T., Kazimirsky, G., 1998. Functional IL-4 receptors on mouse astrocytes: IL-4 inhibits astrocyte activation and induces NGF secretion. J Neuroimmunol 81, 20-30.

Brok, H.P., van Meurs, M., Blezer, E., Schantz, A., Peritt, D., Treacy, G., Laman, J.D., Bauer, J., t Hart, B.A., 2002. Prevention of experimental autoimmune encephalomyelitis in common marmosets using an anti-IL-12p40 monoclonal antibody. J Immunol 169, 6554-6563.

Brosnan, C.F., Cannella, B., Battistini, L., Raine, C.S., 1995. Cytokine localization in multiple sclerosis lesions: correlation with adhesion molecule expression and reactive nitrogen species. Neurology 45, S16-21.

Brown, D.A., Sawchenko, P.E., 2007. Time course and distribution of inflammatory and neurodegenerative events suggest structural bases for the pathogenesis of experimental autoimmune encephalomyelitis. J Comp Neurol 502, 236-260.

Bruno, V., Battaglia, G., Copani, A., D'Onofrio, M., Di Iorio, P., De Blasi, A., Melchiorri, D., Flor, P.J., Nicoletti, F., 2001. Metabotropic glutamate receptor subtypes as targets for neuroprotective drugs. J Cereb Blood Flow Metab 21, 1013-1033.

Bukovsky, A., Presl, J., Zidovsky, J., Mancal, P., 1983. The localization of Thy-1.1, MRC OX 2 and Ia antigens in the rat ovary and fallopian tube. Immunology 48, 587-596.

Bush, T.G., Puvanachandra, N., Horner, C.H., Polito, A., Ostenfeld, T., Svendsen, C.N., Mucke, L., Johnson, M.H., Sofroniew, M.V., 1999. Leukocyte infiltration, neuronal degeneration, and neurite outgrowth after ablation of scar-forming, reactive astrocytes in adult transgenic mice. Neuron 23, 297-308.

Butti, E., Bergami, A., Recchia, A., Brambilla, E., Del Carro, U., Amadio, S., Cattalini, A., Esposito, M., Stornaiuolo, A., Comi, G., Pluchino, S., Mavilio, F., Martino, G., Furlan, R., 2008. IL4 gene delivery to the CNS recruits regulatory T cells and induces clinical recovery in mouse models of multiple sclerosis. Gene Ther 15, 504-515.

Calingasan, N.Y., Erdely, H.A., Altar, C.A., 2002. Identification of CD40 ligand in Alzheimer's disease and in animal models of Alzheimer's disease and brain injury. Neurobiol Aging 23, 31-39.

Cannella, B., Raine, C.S., 1995. The adhesion molecule and cytokine profile of multiple sclerosis lesions. Ann Neurol 37, 424-435.

Cao, Z., Henzel, W.J., Gao, X., 1996. IRAK: a kinase associated with the interleukin-1 receptor. Science 271, 1128-1131.

Carswell, E.A., Old, L.J., Kassel, R.L., Green, S., Fiore, N., Williamson, B., 1975. An endotoxin-induced serum factor that causes necrosis of tumors. Proc Natl Acad Sci U S A 72, 3666-3670.

Castrillo, A., Mojena, M., Hortelano, S., Bosca, L., 2001. Peroxisome proliferator-activated receptor-gamma-independent inhibition of macrophage activation by the non-thiazolidinedione agonist L-796,449. Comparison with the effects of 15-deoxy-delta(12,14)-prostaglandin J(2). J Biol Chem 276, 34082-34088.

Chao, C.C., Molitor, T.W., Hu, S., 1993. Neuroprotective role of IL-4 against activated microglia. J Immunol 151, 1473-1481.

Chawla, A., Barak, Y., Nagy, L., Liao, D., Tontonoz, P., Evans, R.M., 2001. PPAR-gamma dependent and independent effects on macrophage-gene expression in lipid metabolism and inflammation. Nat Med 7, 48-52.

Chen, K., Huang, J., Gong, W., Zhang, L., Yu, P., Wang, J.M., 2006. CD40/CD40L dyad in the inflammatory and immune responses in the central nervous system. Cell Mol Immunol 3, 163-169.

Chitnis, T., Imitola, J., Wang, Y., Elyaman, W., Chawla, P., Sharuk, M., Raddassi, K., Bronson, R.T., Khoury, S.J., 2007. Elevated neuronal expression of CD200 protects Wlds mice from inflammation-mediated neurodegeneration. Am J Pathol 170, 1695-1712.

Clark, R.B., 2002. The role of PPARs in inflammation and immunity. J Leukoc Biol 71, 388-400.

Clarke, R.M., Lyons, A., O'Connell, F., Deighan, B.F., Barry, C.E., Anyakoha, N.G., Nicolaou, A., Lynch, M.A., 2008. A pivotal role for interleukin-4 in atorvastatin-associated neuroprotection in rat brain. J Biol Chem 283, 1808-1817.

Combs, C.K., Johnson, D.E., Karlo, J.C., Cannady, S.B., Landreth, G.E., 2000. Inflammatory mechanisms in Alzheimer's disease: inhibition of beta-amyloid-stimulated proinflammatory responses and neurotoxicity by PPARgamma agonists. J Neurosci 20, 558-567.

Copland, D.A., Calder, C.J., Raveney, B.J., Nicholson, L.B., Phillips, J., Cherwinski, H., Jenmalm, M., Sedgwick, J.D., Dick, A.D., 2007. Monoclonal antibody-mediated CD200 receptor signaling suppresses macrophage activation and tissue damage in experimental autoimmune uveoretinitis. Am J Pathol 171, 580-588.

Corbin, J.G., Kelly, D., Rath, E.M., Baerwald, K.D., Suzuki, K., Popko, B., 1996. Targeted CNS expression of interferon-gamma in transgenic mice leads to hypomyelination, reactive gliosis, and abnormal cerebellar development. Mol Cell Neurosci 7, 354-370.

D'Aversa, T.G., Weidenheim, K.M., Berman, J.W., 2002. CD40-CD40L interactions induce chemokine expression by human microglia: implications for human immunodeficiency virus encephalitis and multiple sclerosis. Am J Pathol 160, 559-567.

Darnell, J.E., Jr., Kerr, I.M., Stark, G.R., 1994. Jak-STAT pathways and transcriptional activation in response to IFNs and other extracellular signaling proteins. Science 264, 1415-1421.

Davson, H., Oldendorf, W.H., 1967. Symposium on membrane transport. Transport in the central nervous system. Proc R Soc Med 60, 326-329.

De Vos, P., Lefebvre, A.M., Miller, S.G., Guerre-Millo, M., Wong, K., Saladin, R., Hamann, L.G., Staels, B., Briggs, M.R., Auwerx, J., 1996. Thiazolidinediones repress ob gene expression in rodents via activation of peroxisome proliferator-activated receptor gamma. J Clin Invest 98, 1004-1009.

Diab, A., Deng, C., Smith, J.D., Hussain, R.Z., Phanavanh, B., Lovett-Racke, A.E., Drew, P.D., Racke, M.K., 2002. Peroxisome proliferator-activated receptor-gamma agonist 15-deoxy-Delta(12,14)-prostaglandin J(2) ameliorates experimental autoimmune encephalomyelitis. J Immunol 168, 2508-2515.

Dickson, D.W., 1997. The pathogenesis of senile plaques. J Neuropathol Exp Neurol 56, 321-339.

Dickson, D.W., Lee, S.C., Mattiace, L.A., Yen, S.H., Brosnan, C., 1993. Microglia and cytokines in neurological disease, with special reference to AIDS and Alzheimer's disease. Glia 7, 75-83.

Didier, N., Romero, I.A., Creminon, C., Wijkhuisen, A., Grassi, J., Mabondzo, A., 2003. Secretion of interleukin-1beta by astrocytes mediates endothelin-1 and tumour necrosis factor-alpha effects on human brain microvascular endothelial cell permeability. J Neurochem 86, 246-254.

Dong, Y., Benveniste, E.N., 2001. Immune function of astrocytes. Glia 36, 180-190.

Drew, P.D., Xu, J., Storer, P.D., Chavis, J.A., Racke, M.K., 2006. Peroxisome proliferator-activated receptor agonist regulation of glial activation: relevance to CNS inflammatory disorders. Neurochem Int 49, 183-189.

Duda, P.W., Schmied, M.C., Cook, S.L., Krieger, J.I., Hafler, D.A., 2000. Glatiramer acetate (Copaxone) induces degenerate, Th2-polarized immune responses in patients with multiple sclerosis. J Clin Invest 105, 967-976.

Dziennis, S., Van Etten, R.A., Pahl, H.L., Morris, D.L., Rothstein, T.L., Blosch, C.M., Perlmutter, R.M., Tenen, D.G., 1995. The CD11b promoter directs high-level expression of reporter genes in macrophages in transgenic mice. Blood 85, 319-329.

Ebers, G.C., Dyment, D.A., 1998. Genetics of multiple sclerosis. Semin Neurol 18, 295-299.

Egeler, R.M., Favara, B.E., Laman, J.D., Claassen, E., 2000. Abundant expression of CD40 and CD40-ligand (CD154) in paediatric Langerhans cell histiocytosis lesions. Eur J Cancer 36, 2105-2110.

Eugster, H.P., Frei, K., Kopf, M., Lassmann, H., Fontana, A., 1998. IL-6-deficient mice resist myelin oligodendrocyte glycoprotein-induced autoimmune encephalomyelitis. Eur J Immunol 28, 2178-2187.

Falcone, M., Rajan, A.J., Bloom, B.R., Brosnan, C.F., 1998. A critical role for IL-4 in regulating disease severity in experimental allergic encephalomyelitis as demonstrated in IL-4-deficient C57BL/6 mice and BALB/c mice. J Immunol 160, 4822-4830.

Farina, C., Aloisi, F., Meinl, E., 2007. Astrocytes are active players in cerebral innate immunity. Trends Immunol 28, 138-145.

Feinstein, D.L., Galea, E., Gavrilyuk, V., Brosnan, C.F., Whitacre, C.C., Dumitrescu-Ozimek, L., Landreth, G.E., Pershadsingh, H.A., Weinberg, G., Heneka, M.T., 2002. Peroxisome proliferator-activated receptor-gamma agonists prevent experimental autoimmune encephalomyelitis. Ann Neurol 51, 694-702.

Ferrari, D., Pizzirani, C., Adinolfi, E., Lemoli, R.M., Curti, A., Idzko, M., Panther, E., Di Virgilio, F., 2006. The P2X7 receptor: a key player in IL-1 processing and release. J Immunol 176, 3877-3883.

Fesik, S.W., 2000. Insights into programmed cell death through structural biology. Cell 103, 273-282.

Frank, M.G., Barrientos, R.M., Biedenkapp, J.C., Rudy, J.W., Watkins, L.R., Maier, S.F., 2006. mRNA up-regulation of MHC II and pivotal pro-inflammatory genes in normal brain aging. Neurobiol Aging 27, 717-722.

Fridkis-Hareli, M., Teitelbaum, D., Pecht, I., Arnon, R., Sela, M., 1997. Binding of copolymer 1 and myelin basic protein leads to clustering of class II MHC molecules on antigen-presenting cells. Int Immunol 9, 925-934.

Furlan, R., Poliani, P.L., Marconi, P.C., Bergami, A., Ruffini, F., Adorini, L., Glorioso, J.C., Comi, G., Martino, G., 2001. Central nervous system gene therapy with interleukin-4 inhibits progression of ongoing relapsing-remitting autoimmune encephalomyelitis in Biozzi AB/H mice. Gene Ther 8, 13-19.

Gadient, R.A., Otten, U., 1993. Differential expression of interleukin-6 (IL-6) and interleukin-6 receptor (IL-6R) mRNAs in rat hypothalamus. Neurosci Lett 153, 13-16.

Gerritse, K., Laman, J.D., Noelle, R.J., Aruffo, A., Ledbetter, J.A., Boersma, W.J., Claassen, E., 1996. CD40-CD40 ligand interactions in experimental allergic encephalomyelitis and multiple sclerosis. Proc Natl Acad Sci U S A 93, 2499-2504.

Geurts, J.J., Bo, L., Roosendaal, S.D., Hazes, T., Daniels, R., Barkhof, F., Witter, M.P., Huitinga, I., van der Valk, P., 2007. Extensive hippocampal demyelination in multiple sclerosis. J Neuropathol Exp Neurol 66, 819-827.

Geurts, J.J., Reuling, I.E., Vrenken, H., Uitdehaag, B.M., Polman, C.H., Castelijns, J.A., Barkhof, F., Pouwels, P.J., 2006. MR spectroscopic evidence for thalamic and hippocampal, but not cortical, damage in multiple sclerosis. Magn Reson Med 55, 478-483.

Ghirnikar, R.S., Lee, Y.L., Eng, L.F., 1998. Inflammation in traumatic brain injury: role of cytokines and chemokines. Neurochem Res 23, 329-340.

Giri, S., Rattan, R., Singh, A.K., Singh, I., 2004. The 15-deoxy-delta12,14-prostaglandin J2 inhibits the inflammatory response in primary rat astrocytes via down-regulating multiple steps in phosphatidylinositol 3-kinase-Akt-NF-kappaB-p300 pathway independent of peroxisome proliferator-activated receptor gamma. J Immunol 173, 5196-5208.

Giulian, D., Woodward, J., Young, D.G., Krebs, J.F., Lachman, L.B., 1988. Interleukin-1 injected into mammalian brain stimulates astrogliosis and neovascularization. J Neurosci 8, 2485-2490.

Gold, R., Linington, C., Lassmann, H., 2006. Understanding pathogenesis and therapy of multiple sclerosis via animal models: 70 years of merits and culprits in experimental autoimmune encephalomyelitis research. Brain 129, 1953-1971.

Gorczynski, R.M., Chen, Z., Yu, K., Hu, J., 2001. CD200 immunoadhesin suppresses collagen-induced arthritis in mice. Clin Immunol 101, 328-334.

Grange, R.A., Hawkins, T.D., Samuel, J.R., 1969. Influence of carbon dioxide tension othe angiographic appearance of intracranial tumours. Acta Radiol Diagn (Stockh) 9, 292-299.

Greenfeder, S.A., Nunes, P., Kwee, L., Labow, M., Chizzonite, R.A., Ju, G., 1995. Molecular cloning and characterization of a second subunit of the interleukin 1 receptor complex. J Biol Chem 270, 13757-13765.

Griffin, W.S., 2006. Inflammation and neurodegenerative diseases. Am J Clin Nutr 83, 470S-474S.

Haegeman, G., Content, J., Volckaert, G., Derynck, R., Tavernier, J., Fiers, W., 1986. Structural analysis of the sequence coding for an inducible 26-kDa protein in human fibroblasts. Eur J Biochem 159, 625-632.

Haque, S.J., Harbor, P., Tabrizi, M., Yi, T., Williams, B.R., 1998. Protein-tyrosine phosphatase Shp-1 is a negative regulator of IL-4- and IL-13-dependent signal transduction. J Biol Chem 273, 33893-33896.

Hashimoto, C., Hudson, K.L., Anderson, K.V., 1988. The Toll gene of Drosophila, required for dorsal-ventral embryonic polarity, appears to encode a transmembrane protein. Cell 52, 269-279.

Hauser, S.L., Doolittle, T.H., Lincoln, R., Brown, R.H., Dinarello, C.A., 1990. Cytokine accumulations in CSF of multiple sclerosis patients: frequent detection of interleukin-1 and tumor necrosis factor but not interleukin-6. Neurology 40, 1735-1739.

Hawkins, B.T., Davis, T.P., 2005. The blood-brain barrier/neurovascular unit in health and disease. Pharmacol Rev 57, 173-185.

Herx, L.M., Yong, V.W., 2001. Interleukin-1 beta is required for the early evolution of reactive astrogliosis following CNS lesion. J Neuropathol Exp Neurol 60, 961-971.

Ho, S.H., Lee, H.J., Kim, D.S., Jeong, J.G., Kim, S., Yu, S.S., Jin, Z., Kim, J.M., 2006. Intrasplenic electro-transfer of IL-4 encoding plasmid DNA efficiently inhibits rat experimental allergic encephalomyelitis. Biochem Biophys Res Commun 343, 816-824.

Hodgkinson, C.P., Ye, S., 2003. Microarray analysis of peroxisome proliferator-activated receptor-gamma induced changes in gene expression in macrophages. Biochem Biophys Res Commun 308, 505-510.

Hoek, R.M., Ruuls, S.R., Murphy, C.A., Wright, G.J., Goddard, R., Zurawski, S.M., Blom, B., Homola, M.E., Streit, W.J., Brown, M.H., Barclay, A.N., Sedgwick, J.D., 2000. Down-regulation of the macrophage lineage through interaction with OX2 (CD200). Science 290, 1768-1771.

Hofmann, C., Lorenz, K., Braithwaite, S.S., Colca, J.R., Palazuk, B.J., Hotamisligil, G.S., Spiegelman, B.M., 1994. Altered gene expression for tumor necrosis factor-alpha and its receptors during drug and dietary modulation of insulin resistance. Endocrinology 134, 264-270.

Holley, J.E., Gveric, D., Newcombe, J., Cuzner, M.L., Gutowski, N.J., 2003. Astrocyte characterization in the multiple sclerosis glial scar. Neuropathol Appl Neurobiol 29, 434-444.

Hua, L.L., Lee, S.C., 2000. Distinct patterns of stimulus-inducible chemokine mRNA accumulation in human fetal astrocytes and microglia. Glia 30, 74-81.

Hulshof, S., Montagne, L., De Groot, C.J., Van Der Valk, P., 2002. Cellular localization and expression patterns of interleukin-10, interleukin-4, and their receptors in multiple sclerosis lesions. Glia 38, 24-35.

Igarashi, Y., Utsumi, H., Chiba, H., Yamada-Sasamori, Y., Tobioka, H., Kamimura, Y., Furuuchi, K., Kokai, Y., Nakagawa, T., Mori, M., Sawada, N., 1999. Glial cell line-derived neurotrophic factor induces barrier function of endothelial cells forming the blood-brain barrier. Biochem Biophys Res Commun 261, 108-112.

Jacobs, C.A., Baker, P.E., Roux, E.R., Picha, K.S., Toivola, B., Waugh, S., Kennedy, M.K., 1991. Experimental autoimmune encephalomyelitis is exacerbated by IL-1 alpha and suppressed by soluble IL-1 receptor. J Immunol 146, 2983-2989.

Jenmalm, M.C., Cherwinski, H., Bowman, E.P., Phillips, J.H., Sedgwick, J.D., 2006. Regulation of myeloid cell function through the CD200 receptor. J Immunol 176, 191-199.

Jepsen, K., Rosenfeld, M.G., 2002. Biological roles and mechanistic actions of co-repressor complexes. J Cell Sci 115, 689-698.

Jiang, C., Ting, A.T., Seed, B., 1998. PPAR-gamma agonists inhibit production of monocyte inflammatory cytokines. Nature 391, 82-86.

Jones, M.V., Nguyen, T.T., Deboy, C.A., Griffin, J.W., Whartenby, K.A., Kerr, D.A., Calabresi, P.A., 2008. Behavioral and pathological outcomes in MOG 35-55 experimental autoimmune encephalomyelitis. J Neuroimmunol 199, 83-93.

Juedes, A.E., Hjelmstrom, P., Bergman, C.M., Neild, A.L., Ruddle, N.H., 2000. Kinetics and cellular origin of cytokines in the central nervous system: insight into mechanisms of myelin oligodendrocyte glycoprotein-induced experimental autoimmune encephalomyelitis. J Immunol 164, 419-426.

Kabat, E.A., Wolf, A., Bezer, A.E., Murray, J.P., 1951. Studies on acute disseminated encephalomyelitis produced experimentally in rhesus monkeys. J Exp Med 93, 615-633.

Kageyama, H., Hirano, T., Okada, K., Ebara, T., Kageyama, A., Murakami, T., Shioda, S., Adachi, M., 2003. Lipoprotein lipase mRNA in white adipose tissue but not in

skeletal muscle is increased by pioglitazone through PPAR-gamma. Biochem Biophys Res Commun 305, 22-27.

Kallen, C.B., Lazar, M.A., 1996. Antidiabetic thiazolidinediones inhibit leptin (ob) gene expression in 3T3-L1 adipocytes. Proc Natl Acad Sci U S A 93, 5793-5796.

Kaneko, S., Wang, J., Kaneko, M., Yiu, G., Hurrell, J.M., Chitnis, T., Khoury, S.J., He, Z., 2006. Protecting axonal degeneration by increasing nicotinamide adenine dinucleotide levels in experimental autoimmune encephalomyelitis models. J Neurosci 26, 9794-9804.

Kang, J., Jiang, L., Goldman, S.A., Nedergaard, M., 1998. Astrocyte-mediated potentiation of inhibitory synaptic transmission. Nat Neurosci 1, 683-692.

Kapadia, R., Yi, J.H., Vemuganti, R., 2008. Mechanisms of anti-inflammatory and neuroprotective actions of PPAR-gamma agonists. Front Biosci 13, 1813-1826.

Kavanagh, T., Lonergan, P.E., Lynch, M.A., 2004. Eicosapentaenoic acid and gamma-linolenic acid increase hippocampal concentrations of IL-4 and IL-10 and abrogate lipopolysaccharide-induced inhibition of long-term potentiation. Prostaglandins Leukot Essent Fatty Acids 70, 391-397.

Kennedy, K.J., Karpus, W.J., 1999. Role of chemokines in the regulation of Th1/Th2 and autoimmune encephalomyelitis. J Clin Immunol 19, 273-279.

Kersten, S., Desvergne, B., Wahli, W., 2000. Roles of PPARs in health and disease. Nature 405, 421-424.

Khoury, S.J., Hancock, W.W., Weiner, H.L., 1992. Oral tolerance to myelin basic protein and natural recovery from experimental autoimmune encephalomyelitis are associated with downregulation of inflammatory cytokines and differential upregulation of transforming growth factor beta, interleukin 4, and prostaglandin E expression in the brain. J Exp Med 176, 1355-1364.

Kim, S.H., Smith, C.J., Van Eldik, L.J., 2004. Importance of MAPK pathways for microglial pro-inflammatory cytokine IL-1 beta production. Neurobiol Aging 25, 431-439.

Kluger, M.J., Kozak, W., Leon, L.R., Conn, C.A., 1998. The use of knockout mice to understand the role of cytokines in fever. Clin Exp Pharmacol Physiol 25, 141-144.

Koenders, M.I., Lubberts, E., van de Loo, F.A., Oppers-Walgreen, B., van den Bersselaar, L., Helsen, M.M., Kolls, J.K., Di Padova, F.E., Joosten, L.A., van den Berg, W.B., 2006. Interleukin-17 acts independently of TNF-alpha under arthritic conditions. J Immunol 176, 6262-6269.

Koritschoner, R., Schweinburg, F., 1925. Klinisch und experimentelle beobachtungen uber lahmungen nach Wutschutzimpfung. Z. Immunitats Forsh 42, 217-283.

Kornek, B., Storch, M.K., Weissert, R., Wallstroem, E., Stefferl, A., Olsson, T., Linington, C., Schmidbauer, M., Lassmann, H., 2000. Multiple sclerosis and chronic autoimmune encephalomyelitis: a comparative quantitative study of axonal injury in active, inactive, and remyelinated lesions. Am J Pathol 157, 267-276.

Kreutzberg, G.W., 1996. Microglia: a sensor for pathological events in the CNS. Trends Neurosci 19, 312-318.

Krueger, J.M., Fang, J., Taishi, P., Chen, Z., Kushikata, T., Gardi, J., 1998. Sleep. A physiologic role for IL-1 beta and TNF-alpha. Ann N Y Acad Sci 856, 148-159.

Kuhlmann, T., Wendling, U., Nolte, C., Zipp, F., Maruschak, B., Stadelmann, C., Siebert, H., Bruck, W., 2002. Differential regulation of myelin phagocytosis by macrophages/microglia, involvement of target myelin, Fc receptors and activation by intravenous immunoglobulins. J Neurosci Res 67, 185-190.

Lacosta, S., Merali, Z., Anisman, H., 1999. Behavioral and neurochemical consequences of lipopolysaccharide in mice: anxiogenic-like effects. Brain Res 818, 291-303.

Landreth, G., Jiang, Q., Mandrekar, S., Heneka, M., 2008. PPARgamma agonists as therapeutics for the treatment of Alzheimer's disease. Neurotherapeutics 5, 481-489.

Lawrence, C.B., Allan, S.M., Rothwell, N.J., 1998. Interleukin-1beta and the interleukin-1 receptor antagonist act in the striatum to modify excitotoxic brain damage in the rat. Eur J Neurosci 10, 1188-1195.

Ledeboer, A., Breve, J.J., Poole, S., Tilders, F.J., Van Dam, A.M., 2000. Interleukin-10, interleukin-4, and transforming growth factor-beta differentially regulate lipopolysaccharide-induced production of pro-inflammatory cytokines and nitric oxide in co-cultures of rat astroglial and microglial cells. Glia 30, 134-142.

Lee, S.C., Dickson, D.W., Liu, W., Brosnan, C.F., 1993a. Induction of nitric oxide synthase activity in human astrocytes by interleukin-1 beta and interferon-gamma. J Neuroimmunol 46, 19-24.

Lee, S.C., Liu, W., Dickson, D.W., Brosnan, C.F., Berman, J.W., 1993b. Cytokine production by human fetal microglia and astrocytes. Differential induction by lipopolysaccharide and IL-1 beta. J Immunol 150, 2659-2667.

Lee, S.C., Moore, G.R., Golenwsky, G., Raine, C.S., 1990. Multiple sclerosis: a role for astroglia in active demyelination suggested by class II MHC expression and ultrastructural study. J Neuropathol Exp Neurol 49, 122-136.

Lee, S.W., Kim, W.J., Choi, Y.K., Song, H.S., Son, M.J., Gelman, I.H., Kim, Y.J., Kim, K.W., 2003. SSeCKS regulates angiogenesis and tight junction formation in blood-brain barrier. Nat Med 9, 900-906.

Leesnitzer, L.M., Parks, D.J., Bledsoe, R.K., Cobb, J.E., Collins, J.L., Consler, T.G., Davis, R.G., Hull-Ryde, E.A., Lenhard, J.M., Patel, L., Plunket, K.D., Shenk, J.L., Stimmel, J.B., Therapontos, C., Willson, T.M., Blanchard, S.G., 2002. Functional consequences of cysteine modification in the ligand binding sites of peroxisome proliferator activated receptors by GW9662. Biochemistry 41, 6640-6650.

Lehn, M., Weiser, W.Y., Engelhorn, S., Gillis, S., Remold, H.G., 1989. IL-4 inhibits H2O2 production and antileishmanial capacity of human cultured monocytes mediated by IFN-gamma. J Immunol 143, 3020-3024.

Liblau, R., Steinman, L., Brocke, S., 1997. Experimental autoimmune encephalomyelitis in IL-4-deficient mice. Int Immunol 9, 799-803.

Liedtke, W., Cannella, B., Mazzaccaro, R.J., Clements, J.M., Miller, K.M., Wucherpfennig, K.W., Gearing, A.J., Raine, C.S., 1998. Effective treatment of models of multiple sclerosis by matrix metalloproteinase inhibitors. Ann Neurol 44, 35-46.

Liu, B., Hong, J.S., 2003. Role of microglia in inflammation-mediated neurodegenerative diseases: mechanisms and strategies for therapeutic intervention. J Pharmacol Exp Ther 304, 1-7.

Liu, Y., Shi, J., Lu, J., Meng, G., Zhu, H., Hou, Y., Yin, Y., Zhao, S., Ding, B., 2009. Activation of peroxisome proliferator-activated receptor-gamma potentiates pro-inflammatory cytokine production, and adrenal and somatotropic changes of weaned pigs after Escherichia coli lipopolysaccharide challenge. Innate Immun 15, 169-178.

Loane, D.J., Deighan, B.F., Clarke, R.M., Griffin, R.J., Lynch, A.M., Lynch, M.A., 2007. Interleukin-4 mediates the neuroprotective effects of rosiglitazone in the aged brain. Neurobiol Aging.

Loane, D.J., Deighan, B.F., Clarke, R.M., Griffin, R.J., Lynch, A.M., Lynch, M.A., 2009. Interleukin-4 mediates the neuroprotective effects of rosiglitazone in the aged brain. Neurobiol Aging 30, 920-931.

Locksley, R.M., Killeen, N., Lenardo, M.J., 2001. The TNF and TNF receptor superfamilies: integrating mammalian biology. Cell 104, 487-501.

Lorenzo, M., Fernandez-Veledo, S., Vila-Bedmar, R., Garcia-Guerra, L., De Alvaro, C., Nieto-Vazquez, I., 2008. Insulin resistance induced by tumor necrosis factor-alpha in myocytes and brown adipocytes. J Anim Sci 86, E94-104.

Lucas, S.M., Rothwell, N.J., Gibson, R.M., 2006. The role of inflammation in CNS injury and disease. Br J Pharmacol 147 Suppl 1, S232-240.

Luna-Medina, R., Cortes-Canteli, M., Alonso, M., Santos, A., Martinez, A., Perez-Castillo, A., 2005. Regulation of inflammatory response in neural cells in vitro by thiadiazolidinones derivatives through peroxisome proliferator-activated receptor gamma activation. J Biol Chem 280, 21453-21462.

Lund, S., Christensen, K.V., Hedtjarn, M., Mortensen, A.L., Hagberg, H., Falsig, J., Hasseldam, H., Schrattenholz, A., Porzgen, P., Leist, M., 2006. The dynamics of the LPS triggered inflammatory response of murine microglia under different culture and in vivo conditions. J Neuroimmunol 180, 71-87.

Lynch, A.M., Loane, D.J., Minogue, A.M., Clarke, R.M., Kilroy, D., Nally, R.E., Roche, O.J., O'Connell, F., Lynch, M.A., 2007. Eicosapentaenoic acid confers neuroprotection in the amyloid-beta challenged aged hippocampus. Neurobiol Aging 28, 845-855.

Lyons, A., Downer, E.J., Crotty, S., Nolan, Y.M., Mills, K.H., Lynch, M.A., 2007a. CD200 ligand receptor interaction modulates microglial activation in vivo and in vitro: a role for IL-4. J Neurosci 27, 8309-8313.

Lyons, A., Griffin, R.J., Costelloe, C.E., Clarke, R.M., Lynch, M.A., 2007b. IL-4 attenuates the neuroinflammation induced by amyloid-beta in vivo and in vitro. J Neurochem 101, 771-781.

Lyons, A., McQuillan, K., Deighan, B.F., O'Reilly, J.A., Downer, E.J., Murphy, A.C., Watson, M., Piazza, A., O'Connell, F., Griffin, R., Mills, K.H., Lynch, M.A., 2009. Decreased neuronal CD200 expression in IL-4-deficient mice results in increased neuroinflammation in response to lipopolysaccharide. Brain Behav Immun.

Magnus, T., Rao, M.S., 2005. Neural stem cells in inflammatory CNS diseases: mechanisms and therapy. J Cell Mol Med 9, 303-319.

Maher, F.O., Nolan, Y., Lynch, M.A., 2005. Downregulation of IL-4-induced signalling in hippocampus contributes to deficits in LTP in the aged rat. Neurobiol Aging 26, 717-728.

Martin, D., Near, S.L., 1995. Protective effect of the interleukin-1 receptor antagonist (IL-1ra) on experimental allergic encephalomyelitis in rats. J Neuroimmunol 61, 241-245.

Martinon, F., Tschopp, J., 2004. Inflammatory caspases: linking an intracellular innate immune system to autoinflammatory diseases. Cell 117, 561-574.

McCombe, P.A., Nickson, I., Pender, M.P., 1998. Cytokine expression by inflammatory cells obtained from the spinal cords of Lewis rats with experimental autoimmune encephalomyelitis induced by inoculation with myelin basic protein and adjuvants. J Neuroimmunol 88, 30-38.

McCoy, M.K., Tansey, M.G., 2008. TNF signaling inhibition in the CNS: implications for normal brain function and neurodegenerative disease. J Neuroinflammation 5, 45.

McFarland, H.F., Martin, R., 2007. Multiple sclerosis: a complicated picture of autoimmunity. Nat Immunol 8, 913-919.

McGeer, P.L., Kawamata, T., Walker, D.G., Akiyama, H., Tooyama, I., McGeer, E.G., 1993. Microglia in degenerative neurological disease. Glia 7, 84-92.

McKenzie, B.S., Kastelein, R.A., Cua, D.J., 2006. Understanding the IL-23-IL-17 immune pathway. Trends Immunol 27, 17-23.

McMenamin, P.G., 1999. Distribution and phenotype of dendritic cells and resident tissue macrophages in the dura mater, leptomeninges, and choroid plexus of the rat brain as demonstrated in wholemount preparations. J Comp Neurol 405, 553-562.

Mebius, R.E., Kraal, G., 2005. Structure and function of the spleen. Nat Rev Immunol 5, 606-616.

Medzhitov, R., 2007. Recognition of microorganisms and activation of the immune response. Nature 449, 819-826.

Mendel, I., Katz, A., Kozak, N., Ben-Nun, A., Revel, M., 1998. Interleukin-6 functions in autoimmune encephalomyelitis: a study in gene-targeted mice. Eur J Immunol 28, 1727-1737.

Merrill, J.E., 1992. Proinflammatory and antiinflammatory cytokines in multiple sclerosis and central nervous system acquired immunodeficiency syndrome. J Immunother (1991) 12, 167-170.

Meuth, S.G., Kanyshkov, T., Melzer, N., Bittner, S., Kieseier, B.C., Budde, T., Wiendl, H., 2008a. Altered neuronal expression of TASK1 and TASK3 potassium channels in rodent and human autoimmune CNS inflammation. Neurosci Lett 446, 133-138.

Meuth, S.G., Simon, O.J., Grimm, A., Melzer, N., Herrmann, A.M., Spitzer, P., Landgraf, P., Wiendl, H., 2008b. CNS inflammation and neuronal degeneration is aggravated by impaired CD200-CD200R-mediated macrophage silencing. J Neuroimmunol 194, 62-69.

Miles, P.D., Romeo, O.M., Higo, K., Cohen, A., Rafaat, K., Olefsky, J.M., 1997. TNF-alpha-induced insulin resistance in vivo and its prevention by troglitazone. Diabetes 46, 1678-1683.

Miller, D.H., Barkhof, F., Frank, J.A., Parker, G.J., Thompson, A.J., 2002. Measurement of atrophy in multiple sclerosis: pathological basis, methodological aspects and clinical relevance. Brain 125, 1676-1695.

Minagar, A., Shapshak, P., Fujimura, R., Ownby, R., Heyes, M., Eisdorfer, C., 2002. The role of macrophage/microglia and astrocytes in the pathogenesis of three neurologic disorders: HIV-associated dementia, Alzheimer disease, and multiple sclerosis. J Neurol Sci 202, 13-23.

Mizuta, I., Ohta, M., Ohta, K., Nishimura, M., Mizuta, E., Kuno, S., 2001. Riluzole stimulates nerve growth factor, brain-derived neurotrophic factor and glial cell line-derived neurotrophic factor synthesis in cultured mouse astrocytes. Neurosci Lett 310, 117-120.

Mogi, M., Harada, M., Riederer, P., Narabayashi, H., Fujita, K., Nagatsu, T., 1994. Tumor necrosis factor-alpha (TNF-alpha) increases both in the brain and in the cerebrospinal fluid from parkinsonian patients. Neurosci Lett 165, 208-210.

Moynagh, P.N., 2005. The interleukin-1 signalling pathway in astrocytes: a key contributor to inflammation in the brain. J Anat 207, 265-269.

Moynagh, P.N., Williams, D.C., O'Neill, L.A., 1994. Activation of NF-kappa B and induction of vascular cell adhesion molecule-1 and intracellular adhesion molecule-1 expression in human glial cells by IL-1. Modulation by antioxidants. J Immunol 153, 2681-2690.

Mrak, R.E., Griffin, W.S., 2001. Interleukin-1, neuroinflammation, and Alzheimer's disease. Neurobiol Aging 22, 903-908.

Murphy, Travers, Walport, 2008. Janeway's Immunobiology Taylor and Francis Group, New York.

Murphy, C.A., Hoek, R.M., Wiekowski, M.T., Lira, S.A., Sedgwick, J.D., 2002. Interactions between hemopoietically derived TNF and central nervous system-resident glial chemokines underlie initiation of autoimmune inflammation in the brain. J Immunol 169, 7054-7062.

Murray, T.J., 2009. The history of multiple sclerosis: the changing frame of the disease over the centuries. J Neurol Sci 277 Suppl 1, S3-8.

Muzio, M., Ni, J., Feng, P., Dixit, V.M., 1997. IRAK (Pelle) family member IRAK-2 and MyD88 as proximal mediators of IL-1 signaling. Science 278, 1612-1615.

Natarajan, C., Bright, J.J., 2002. Peroxisome proliferator-activated receptor-gamma agonists inhibit experimental allergic encephalomyelitis by blocking IL-12 production, IL-12 signaling and Th1 differentiation. Genes Immun 3, 59-70.

Navikas, V., Matusevicius, D., Soderstrom, M., Fredrikson, S., Kivisakk, P., Ljungdahl, A., Hojeberg, B., Link, H., 1996. Increased interleukin-6 mRNA expression in blood and cerebrospinal fluid mononuclear cells in multiple sclerosis. J Neuroimmunol 64, 63-69.

Nelms, K., Keegan, A.D., Zamorano, J., Ryan, J.J., Paul, W.E., 1999. The IL-4 receptor: signaling mechanisms and biologic functions. Annu Rev Immunol 17, 701-738.

Neumann, H., Misgeld, T., Matsumuro, K., Wekerle, H., 1998. Neurotrophins inhibit major histocompatibility class II inducibility of microglia: involvement of the p75 neurotrophin receptor. Proc Natl Acad Sci U S A 95, 5779-5784.

Newman, E.A., 2003. New roles for astrocytes: regulation of synaptic transmission. Trends Neurosci 26, 536-542.

Nguyen, V.T., Benveniste, E.N., 2000. IL-4-activated STAT-6 inhibits IFN-gamma-induced CD40 gene expression in macrophages/microglia. J Immunol 165, 6235-6243.

Niino, M., Iwabuchi, K., Kikuchi, S., Ato, M., Morohashi, T., Ogata, A., Tashiro, K., Onoe, K., 2001a. Amelioration of experimental autoimmune encephalomyelitis in C57BL/6 mice by an agonist of peroxisome proliferator-activated receptor-gamma. J Neuroimmunol 116, 40-48.

Niino, M., Kikuchi, S., Fukazawa, T., Yabe, I., Sasaki, H., Tashiro, K., 2001b. Genetic polymorphisms of IL-1beta and IL-1 receptor antagonist in association with multiple sclerosis in Japanese patients. J Neuroimmunol 118, 295-299.

Nissen, S.E., Wolski, K., 2007. Effect of rosiglitazone on the risk of myocardial infarction and death from cardiovascular causes. N Engl J Med 356, 2457-2471.

Nolan, Y., Maher, F.O., Martin, D.S., Clarke, R.M., Brady, M.T., Bolton, A.E., Mills, K.H., Lynch, M.A., 2005. Role of interleukin-4 in regulation of age-related inflammatory changes in the hippocampus. J Biol Chem 280, 9354-9362.

Nolte, R.T., Wisely, G.B., Westin, S., Cobb, J.E., Lambert, M.H., Kurokawa, R., Rosenfeld, M.G., Willson, T.M., Glass, C.K., Milburn, M.V., 1998. Ligand binding and co-activator assembly of the peroxisome proliferator-activated receptor-gamma. Nature 395, 137-143.

Oksenberg, J.R., Barcellos, L.F., 2005. Multiple sclerosis genetics: leaving no stone unturned. Genes Immun 6, 375-387.

Panek, R.B., Lee, Y.J., Itoh-Lindstrom, Y., Ting, J.P., Benveniste, E.N., 1994. Characterization of astrocyte nuclear proteins involved in IFN-gamma- and TNF-alpha-mediated class II MHC gene expression. J Immunol 153, 4555-4564.

Papadopoulos, D., Pham-Dinh, D., Reynolds, R., 2006. Axon loss is responsible for chronic neurological deficit following inflammatory demyelination in the rat. Exp Neurol 197, 373-385.

Park, E.J., Park, S.Y., Joe, E.H., Jou, I., 2003. 15d-PGJ2 and rosiglitazone suppress Janus kinase-STAT inflammatory signaling through induction of suppressor of cytokine signaling 1 (SOCS1) and SOCS3 in glia. J Biol Chem 278, 14747-14752.

Park, K.W., Lee, D.Y., Joe, E.H., Kim, S.U., Jin, B.K., 2005. Neuroprotective role of microglia expressing interleukin-4. J Neurosci Res 81, 397-402.

Park, M.H., Lee, Y.K., Lee, Y.H., Kim, Y.B., Yun, Y.W., Nam, S.Y., Hwang, S.J., Han, S.B., Kim, S.U., Hong, J.T., 2009. Chemokines released from astrocytes promote chemokine receptor 5-mediated neuronal cell differentiation. Exp Cell Res 315, 2715-2726.

Pascual, G., Fong, A.L., Ogawa, S., Gamliel, A., Li, A.C., Perissi, V., Rose, D.W., Willson, T.M., Rosenfeld, M.G., Glass, C.K., 2005. A SUMOylation-dependent pathway mediates transrepression of inflammatory response genes by PPAR-gamma. Nature 437, 759-763.

Pasti, L., Volterra, A., Pozzan, T., Carmignoto, G., 1997. Intracellular calcium oscillations in astrocytes: a highly plastic, bidirectional form of communication between neurons and astrocytes in situ. J Neurosci 17, 7817-7830.

Pasti, L., Zonta, M., Pozzan, T., Vicini, S., Carmignoto, G., 2001. Cytosolic calcium oscillations in astrocytes may regulate exocytotic release of glutamate. J Neurosci 21, 477-484.

Paulesu, E., Perani, D., Fazio, F., Comi, G., Pozzilli, C., Martinelli, V., Filippi, M., Bettinardi, V., Sirabian, G., Passafiume, D., Anzini, A., Lenzi, G.L., Canal, N., Fieschi, C., 1996. Functional basis of memory impairment in multiple sclerosis: a[18F]FDG PET study. Neuroimage 4, 87-96.

Pernis, A.B., 2009. Th17 cells in rheumatoid arthritis and systemic lupus erythematosus. J Intern Med 265, 644-652.

Perry, V.H., Brown, M.C., Lunn, E.R., 1991. Very Slow Retrograde and Wallerian Degeneration in the CNS of C57BL/Ola Mice. Eur J Neurosci 3, 102-105.

Petrova, T.V., Akama, K.T., Van Eldik, L.J., 1999. Cyclopentenone prostaglandins suppress activation of microglia: down-regulation of inducible nitric-oxide synthase by 15-deoxy-Delta12,14-prostaglandin J2. Proc Natl Acad Sci U S A 96, 4668-4673.

Peyser, J.M., Rao, S.M., LaRocca, N.G., Kaplan, E., 1990. Guidelines for neuropsychological research in multiple sclerosis. Arch Neurol 47, 94-97.

Porter, J.T., McCarthy, K.D., 1996. Hippocampal astrocytes in situ respond to glutamate released from synaptic terminals. J Neurosci 16, 5073-5081.

Poser, C.M., Brinar, V.V., 2004. Diagnostic criteria for multiple sclerosis: an historical review. Clin Neurol Neurosurg 106, 147-158.

Prat, A., Biernacki, K., Wosik, K., Antel, J.P., 2001. Glial cell influence on the human blood-brain barrier. Glia 36, 145-155.

Preston, S., Wright, G.J., Starr, K., Barclay, A.N., Brown, M.H., 1997. The leukocyte/neuron cell surface antigen OX2 binds to a ligand on macrophages. Eur J Immunol 27, 1911-1918.

Probert, L., Akassoglou, K., Pasparakis, M., Kontogeorgos, G., Kollias, G., 1995. Spontaneous inflammatory demyelinating disease in transgenic mice showing central nervous system-specific expression of tumor necrosis factor alpha. Proc Natl Acad Sci U S A 92, 11294-11298.

Qin, H., Wilson, C.A., Lee, S.J., Zhao, X., Benveniste, E.N., 2005. LPS induces CD40 gene expression through the activation of NF-kappaB and STAT-1alpha in macrophages and microglia. Blood 106, 3114-3122.

Racke, M.K., Bonomo, A., Scott, D.E., Cannella, B., Levine, A., Raine, C.S., Shevach, E.M., Rocken, M., 1994. Cytokine-induced immune deviation as a therapy for inflammatory autoimmune disease. J Exp Med 180, 1961-1966.

Ralevic, V., Burnstock, G., 1998. Receptors for purines and pyrimidines. Pharmacol Rev 50, 413-492.

Ramagopalan, S.V., Ebers, G.C., 2008. Genes for multiple sclerosis. Lancet 371, 283-285.

Rao, S.M., Leo, G.J., Bernardin, L., Unverzagt, F., 1991a. Cognitive dysfunction in multiple sclerosis. I. Frequency, patterns, and prediction. Neurology 41, 685-691.

Rao, S.M., Leo, G.J., Ellington, L., Nauertz, T., Bernardin, L., Unverzagt, F., 1991b. Cognitive dysfunction in multiple sclerosis. II. Impact on employment and social functioning. Neurology 41, 692-696.

Rapoport, S.I., 2001. Advances in osmotic opening of the blood-brain barrier to enhance CNS chemotherapy. Expert Opin Investig Drugs 10, 1809-1818.

Relton, J.K., Rothwell, N.J., 1992. Interleukin-1 receptor antagonist inhibits ischaemic and excitotoxic neuronal damage in the rat. Brain Res Bull 29, 243-246.

Ricote, M., Li, A.C., Willson, T.M., Kelly, C.J., Glass, C.K., 1998. The peroxisome proliferator-activated receptor-gamma is a negative regulator of macrophage activation. Nature 391, 79-82.

Rivers, T.M., Schwentker, F., 1935. Encephalomyelitis accompanied by myelin destruction experimentally produced by monkeys. Journal of Experimental Medicine 61, 689-702.

Rivers, T.M., Sprunt, D.M., Berry, G.P., 1933. Observations on attempts to promote acute disseminated encephalomyelitis in monkeys. Journal of Experimental Medicine 58, 39-53.

Roosendaal, S.D., Moraal, B., Vrenken, H., Castelijns, J.A., Pouwels, P.J., Barkhof, F., Geurts, J.J., 2008. In vivo MR imaging of hippocampal lesions in multiple sclerosis. J Magn Reson Imaging 27, 726-731.

Rosenman, S.J., Shrikant, P., Dubb, L., Benveniste, E.N., Ransohoff, R.M., 1995. Cytokine-induced expression of vascular cell adhesion molecule-1 (VCAM-1) by astrocytes and astrocytoma cell lines. J Immunol 154, 1888-1899.

Rothwell, N.J., Luheshi, G.N., 2000. Interleukin 1 in the brain: biology, pathology and therapeutic target. Trends Neurosci 23, 618-625.

Rott, O., Fleischer, B., Cash, E., 1994. Interleukin-10 prevents experimental allergic encephalomyelitis in rats. Eur J Immunol 24, 1434-1440.

Roy, A., Fung, Y.K., Liu, X., Pahan, K., 2006. Up-regulation of microglial CD11b expression by nitric oxide. J Biol Chem 281, 14971-14980.

Roy, A., Jana, A., Yatish, K., Freidt, M.B., Fung, Y.K., Martinson, J.A., Pahan, K., 2008. Reactive oxygen species up-regulate CD11b in microglia via nitric oxide: Implications for neurodegenerative diseases. Free Radic Biol Med 45, 686-699.

Ruiz, P.J., DeVoss, J.J., Nguyen, L.V., Fontoura, P.P., Hirschberg, D.L., Mitchell, D.J., Garcia, K.C., Steinman, L., 2001. Immunomodulation of experimental autoimmune encephalomyelitis with ordered peptides based on MHC-TCR binding motifs. J Immunol 167, 2688-2693.

Sajad, M., Zargan, J., Chawla, R., Umar, S., Sadaqat, M., Khan, H.A., 2009. Hippocampal neurodegeneration in experimental autoimmune encephalomyelitis (EAE): potential role of inflammation activated myeloperoxidase. Mol Cell Biochem 328, 183-188.

Samoilova, E.B., Horton, J.L., Hilliard, B., Liu, T.S., Chen, Y., 1998. IL-6-deficient mice are resistant to experimental autoimmune encephalomyelitis: roles of IL-6 in the activation and differentiation of autoreactive T cells. J Immunol 161, 6480-6486.

Sanz, J.M., Di Virgilio, F., 2000. Kinetics and mechanism of ATP-dependent IL-1 beta release from microglial cells. J Immunol 164, 4893-4898.

Sawada, M., Suzumura, A., Marunouchi, T., 1992. TNF alpha induces IL-6 production by astrocytes but not by microglia. Brain Res 583, 296-299.

Scheller, J., Rose-John, S., 2006. Interleukin-6 and its receptor: from bench to bedside. Med Microbiol Immunol 195, 173-183.

Schintu, N., Frau, L., Ibba, M., Caboni, P., Garau, A., Carboni, E., Carta, A.R., 2009. PPAR-gamma-mediated neuroprotection in a chronic mouse model of Parkinson's disease. Eur J Neurosci 29, 954-963.

Schobitz, B., de Kloet, E.R., Sutanto, W., Holsboer, F., 1993. Cellular localization of interleukin 6 mRNA and interleukin 6 receptor mRNA in rat brain. Eur J Neurosci 5, 1426-1435.

Schwaninger, M., Sallmann, S., Petersen, N., Schneider, A., Prinz, S., Libermann, T.A., Spranger, M., 1999. Bradykinin induces interleukin-6 expression in astrocytes through activation of nuclear factor-kappaB. J Neurochem 73, 1461-1466.

Seder, R.A., Paul, W.E., 1994. Acquisition of lymphokine-producing phenotype by CD4+ T cells. Annu Rev Immunol 12, 635-673.

Sela, M., 1999. The concept of specific immune treatment against autoimmune diseases. Int Rev Immunol 18, 201-216.

Selmaj, K., Raine, C.S., Cross, A.H., 1991. Anti-tumor necrosis factor therapy abrogates autoimmune demyelination. Ann Neurol 30, 694-700.

Sharief, M.K., Hentges, R., 1991. Association between tumor necrosis factor-alpha and disease progression in patients with multiple sclerosis. N Engl J Med 325, 467-472.

Shimazu, R., Akashi, S., Ogata, H., Nagai, Y., Fukudome, K., Miyake, K., Kimoto, M., 1999. MD-2, a molecule that confers lipopolysaccharide responsiveness on Toll-like receptor 4. J Exp Med 189, 1777-1782.

Sholi-Franco, A., da Silva, A.G., Adao-Novaes, J., 2009. Interleukin-4 as a neuromodulatory cytokine: roles and signaling in the nervous system. Ann N Y Acad Sci 1153, 65-75.

Shrikant, P., Chung, I.Y., Ballestas, M.E., Benveniste, E.N., 1994. Regulation of intercellular adhesion molecule-1 gene expression by tumor necrosis factor-alpha, interleukin-1 beta, and interferon-gamma in astrocytes. J Neuroimmunol 51, 209-220.

Sicotte, N.L., Kern, K.C., Giesser, B.S., Arshanapalli, A., Schultz, A., Montag, M., Wang, H., Bookheimer, S.Y., 2008. Regional hippocampal atrophy in multiple sclerosis. Brain 131, 1134-1141.

Simi, A., Lerouet, D., Pinteaux, E., Brough, D., 2007a. Mechanisms of regulation for interleukin-1beta in neurodegenerative disease. Neuropharmacology 52, 1563-1569.

Simi, A., Tsakiri, N., Wang, P., Rothwell, N.J., 2007b. Interleukin-1 and inflammatory neurodegeneration. Biochem Soc Trans 35, 1122-1126.

Simpson, J.E., Newcombe, J., Cuzner, M.L., Woodroofe, M.N., 1998. Expression of monocyte chemoattractant protein-1 and other beta-chemokines by resident glia and inflammatory cells in multiple sclerosis lesions. J Neuroimmunol 84, 238-249.

Sims, J.E., Gayle, M.A., Slack, J.L., Alderson, M.R., Bird, T.A., Giri, J.G., Colotta, F., Re, F., Mantovani, A., Shanebeck, K., et al., 1993. Interleukin 1 signaling occurs exclusively via the type I receptor. Proc Natl Acad Sci U S A 90, 6155-6159.

Sorensen, T.L., Tani, M., Jensen, J., Pierce, V., Lucchinetti, C., Folcik, V.A., Qin, S., Rottman, J., Sellebjerg, F., Strieter, R.M., Frederiksen, J.L., Ransohoff, R.M., 1999. Expression of specific chemokines and chemokine receptors in the central nervous system of multiple sclerosis patients. J Clin Invest 103, 807-815.

Sriram, S., Steiner, I., 2005. Experimental allergic encephalomyelitis: a misleading model of multiple sclerosis. Ann Neurol 58, 939-945.

Steeghs, L., de Cock, H., Evers, E., Zomer, B., Tommassen, J., van der Ley, P., 2001. Outer membrane composition of a lipopolysaccharide-deficient Neisseria meningitidis mutant. EMBO J 20, 6937-6945.

Steinman, L., Zamvil, S.S., 2006. How to successfully apply animal studies in experimental allergic encephalomyelitis to research on multiple sclerosis. Ann Neurol 60, 12-21.

Steward, O., Trimmer, P.A., 1997. Genetic influences on cellular reactions to CNS injury: the reactive response of astrocytes in denervated neuropil regions in mice carrying a

mutation (Wld(S)) that causes delayed Wallerian degeneration. J Comp Neurol 380, 70-81.

Stone, L.A., Smith, M.E., Albert, P.S., Bash, C.N., Maloni, H., Frank, J.A., McFarland, H.F., 1995. Blood-brain barrier disruption on contrast-enhanced MRI in patients with mild relapsing-remitting multiple sclerosis: relationship to course, gender, and age. Neurology 45, 1122-1126.

Storer, P.D., Xu, J., Chavis, J., Drew, P.D., 2005. Peroxisome proliferator-activated receptor-gamma agonists inhibit the activation of microglia and astrocytes: implications for multiple sclerosis. J Neuroimmunol 161, 113-122.

Streit, W.J., Mrak, R.E., Griffin, W.S., 2004. Microglia and neuroinflammation: a pathological perspective. J Neuroinflammation 1, 14.

Strijbos, P.J., Rothwell, N.J., 1995. Interleukin-1 beta attenuates excitatory amino acid-induced neurodegeneration in vitro: involvement of nerve growth factor. J Neurosci 15, 3468-3474.

Sun, H., Huang, Y., Yu, X., Li, Y., Yang, J., Li, R., Deng, Y., Zhao, G., 2008. Peroxisome proliferator-activated receptor gamma agonist, rosiglitazone, suppresses CD40 expression and attenuates inflammatory responses after lithium pilocarpine-induced status epilepticus in rats. Int J Dev Neurosci 26, 505-515.

Sundararajan, S., Jiang, Q., Heneka, M., Landreth, G., 2006. PPARgamma as a therapeutic target in central nervous system diseases. Neurochem Int 49, 136-144.

Suzumura, A., Sawada, M., Itoh, Y., Marunouchi, T., 1994. Interleukin-4 induces proliferation and activation of microglia but suppresses their induction of class II major histocompatibility complex antigen expression. J Neuroimmunol 53, 209-218.

Swanborg, R.H., 1995. Experimental autoimmune encephalomyelitis in rodents as a model for human demyelinating disease. Clin Immunol Immunopathol 77, 4-13.

Taga, T., Kishimoto, T., 1997. Gp130 and the interleukin-6 family of cytokines. Annu Rev Immunol 15, 797-819.

Takeuchi, O., Akira, S., 2001. Toll-like receptors; their physiological role and signal transduction system. Int Immunopharmacol 1, 625-635.

Takuma, K., Baba, A., Matsuda, T., 2004. Astrocyte apoptosis: implications for neuroprotection. Prog Neurobiol 72, 111-127.

Tan, J., Town, T., Saxe, M., Paris, D., Wu, Y., Mullan, M., 1999. Ligation of microglial CD40 results in p44/42 mitogen-activated protein kinase-dependent TNF-alpha production that is opposed by TGF-beta 1 and IL-10. J Immunol 163, 6614-6621.

Tanaka, J., Toku, K., Zhang, B., Ishihara, K., Sakanaka, M., Maeda, N., 1999. Astrocytes prevent neuronal death induced by reactive oxygen and nitrogen species. Glia 28, 85-96.

Tehranian, R., Andell-Jonsson, S., Beni, S.M., Yatsiv, I., Shohami, E., Bartfai, T., Lundkvist, J., Iverfeldt, K., 2002. Improved recovery and delayed cytokine induction after closed head injury in mice with central overexpression of the secreted isoform of the interleukin-1 receptor antagonist. J Neurotrauma 19, 939-951.

Teitlebaum, S.L., Moore, K.E., Shieber, W., 1971. Parafollicular cells in the normal human thyroid. Nature 230, 334-335.

Tetsuka, T., Baier, L.D., Morrison, A.R., 1996. Antioxidants inhibit interleukin-1-induced cyclooxygenase and nitric-oxide synthase expression in rat mesangial cells. Evidence for post-transcriptional regulation. J Biol Chem 271, 11689-11693.

Thornberry, N.A., Bull, H.G., Calaycay, J.R., Chapman, K.T., Howard, A.D., Kostura, M.J., Miller, D.K., Molineaux, S.M., Weidner, J.R., Aunins, J., et al., 1992. A novel heterodimeric cysteine protease is required for interleukin-1 beta processing in monocytes. Nature 356, 768-774.

Thornton, A.E., Raz, N., Tucke, K.A., 2002. Memory in multiple sclerosis: contextual encoding deficits. J Int Neuropsychol Soc 8, 395-409.

Thornton, P., Pinteaux, E., Gibson, R.M., Allan, S.M., Rothwell, N.J., 2006. Interleukin-1-induced neurotoxicity is mediated by glia and requires caspase activation and free radical release. J Neurochem 98, 258-266.

Togo, T., Akiyama, H., Kondo, H., Ikeda, K., Kato, M., Iseki, E., Kosaka, K., 2000. Expression of CD40 in the brain of Alzheimer's disease and other neurological diseases. Brain Res 885, 117-121.

Touzani, O., Boutin, H., Chuquet, J., Rothwell, N., 1999. Potential mechanisms of interleukin-1 involvement in cerebral ischaemia. J Neuroimmunol 100, 203-215.

Veldhoen, M., Hocking, R.J., Atkins, C.J., Locksley, R.M., Stockinger, B., 2006. TGFbeta in the context of an inflammatory cytokine milieu supports de novo differentiation of IL-17-producing T cells. Immunity 24, 179-189.

Vercellino, M., Plano, F., Votta, B., Mutani, R., Giordana, M.T., Cavalla, P., 2005. Grey matter pathology in multiple sclerosis. J Neuropathol Exp Neurol 64, 1101-1107.

Vilhardt, F., 2005. Microglia: phagocyte and glia cell. Int J Biochem Cell Biol 37, 17-21.

Vincent, A.M., Mohammad, Y., Ahmad, I., Greenberg, R., Maiese, K., 1997. Metabotropic glutamate receptors prevent nitric oxide-induced programmed cell death. J Neurosci Res 50, 549-564.

Vincent, B., Beaudet, A., Dauch, P., Vincent, J.P., Checler, F., 1996. Distinct properties of neuronal and astrocytic endopeptidase 3.4.24.16: a study on differentiation, subcellular distribution, and secretion processes. J Neurosci 16, 5049-5059.

Viviani, B., Bartesaghi, S., Gardoni, F., Vezzani, A., Behrens, M.M., Bartfai, T., Binaglia, M., Corsini, E., Di Luca, M., Galli, C.L., Marinovich, M., 2003. Interleukin-1beta enhances NMDA receptor-mediated intracellular calcium increase through activation of the Src family of kinases. J Neurosci 23, 8692-8700.

Walker, D.G., Dalsing-Hernandez, J.E., Campbell, N.A., Lue, L.F., 2009. Decreased expression of CD200 and CD200 receptor in Alzheimer's disease: a potential mechanism leading to chronic inflammation. Exp Neurol 215, 5-19.

Wang, M., Wu, Y., Culver, D.G., Glass, J.D., 2001. The gene for slow Wallerian degeneration (Wld(s)) is also protective against vincristine neuropathy. Neurobiol Dis 8, 155-161.

Ward, C., Dransfield, I., Murray, J., Farrow, S.N., Haslett, C., Rossi, A.G., 2002. Prostaglandin D2 and its metabolites induce caspase-dependent granulocyte apoptosis that is mediated via inhibition of I kappa B alpha degradation using a peroxisome proliferator-activated receptor-gamma-independent mechanism. J Immunol 168, 6232-6243.

Wesche, H., Korherr, C., Kracht, M., Falk, W., Resch, K., Martin, M.U., 1997. The interleukin-1 receptor accessory protein (IL-1RAcP) is essential for IL-1-induced activation of interleukin-1 receptor-associated kinase (IRAK) and stress-activated protein kinases (SAP kinases). J Biol Chem 272, 7727-7731.

Williams, K., Alvarez, X., Lackner, A.A., 2001. Central nervous system perivascular cells are immunoregulatory cells that connect the CNS with the peripheral immune system. Glia 36, 156-164.

Wolburg, H., Lippoldt, A., 2002. Tight junctions of the blood-brain barrier: development, composition and regulation. Vascul Pharmacol 38, 323-337.

Wong, G.H., Bartlett, P.F., Clark-Lewis, I., Battye, F., Schrader, J.W., 1984. Inducible expression of H-2 and Ia antigens on brain cells. Nature 310, 688-691.

Woodroofe, M.N., Sarna, G.S., Wadhwa, M., Hayes, G.M., Loughlin, A.J., Tinker, A., Cuzner, M.L., 1991. Detection of interleukin-1 and interleukin-6 in adult rat brain, following

mechanical injury, by in vivo microdialysis: evidence of a role for microglia in cytokine production. J Neuroimmunol 33, 227-236.

Woster, A.P., Combs, C.K., 2007. Differential ability of a thiazolidinedione PPARgamma agonist to attenuate cytokine secretion in primary microglia and macrophage-like cells. J Neurochem 103, 67-76.

Wright, G.J., Puklavec, M.J., Willis, A.C., Hoek, R.M., Sedgwick, J.D., Brown, M.H., Barclay, A.N., 2000. Lymphoid/neuronal cell surface OX2 glycoprotein recognizes a novel receptor on macrophages implicated in the control of their function. Immunity 13, 233-242.

Wu, V.W., Schwartz, J.P., 1998. Cell culture models for reactive gliosis: new perspectives. J Neurosci Res 51, 675-681.

Yamasaki, Y., Matsuura, N., Shozuhara, H., Onodera, H., Itoyama, Y., Kogure, K., 1995. Interleukin-1 as a pathogenetic mediator of ischemic brain damage in rats. Stroke 26, 676-680; discussion 681.

Yan, H.Q., Banos, M.A., Herregodts, P., Hooghe, R., Hooghe-Peters, E.L., 1992. Expression of interleukin (IL)-1 beta, IL-6 and their respective receptors in the normal rat brain and after injury. Eur J Immunol 22, 2963-2971.

Yang, X.Y., Wang, L.H., Mihalic, K., Xiao, W., Chen, T., Li, P., Wahl, L.M., Farrar, W.L., 2002. Interleukin (IL)-4 indirectly suppresses IL-2 production by human T lymphocytes via peroxisome proliferator-activated receptor gamma activated by macrophage-derived 12/15-lipoxygenase ligands. J Biol Chem 277, 3973-3978.

Yasuda, T., Tsumita, T., Nagai, Y., Mitsuzawa, E., Ohtani, S., 1975. Experimental allergic encephalomyelitis (EAE) in mice. I. Induction of EAE with mouse spinal cord homogenate and myelin basic protein. Jpn J Exp Med 45, 423-427.

Yednock, T.A., Cannon, C., Fritz, L.C., Sanchez-Madrid, F., Steinman, L., Karin, N., 1992. Prevention of experimental autoimmune encephalomyelitis by antibodies against alpha 4 beta 1 integrin. Nature 356, 63-66.

Yong, V.W., Moumdjian, R., Yong, F.P., Ruijs, T.C., Freedman, M.S., Cashman, N., Antel, J.P., 1991. Gamma-interferon promotes proliferation of adult human astrocytes in vitro and reactive gliosis in the adult mouse brain in vivo. Proc Natl Acad Sci U S A 88, 7016-7020.

Yu, A.S., McCarthy, K.M., Francis, S.A., McCormack, J.M., Lai, J., Rogers, R.A., Lynch, R.D., Schneeberger, E.E., 2005. Knockdown of occludin expression leads to diverse phenotypic alterations in epithelial cells. Am J Physiol Cell Physiol 288, C1231-1241.

Zamvil, S., Nelson, P., Trotter, J., Mitchell, D., Knobler, R., Fritz, R., Steinman, L., 1985. T-cell clones specific for myelin basic protein induce chronic relapsing paralysis and demyelination. Nature 317, 355-358.

Zeinstra, E., Wilczak, N., De Keyser, J., 2003. Reactive astrocytes in chronic active lesions of multiple sclerosis express co-stimulatory molecules B7-1 and B7-2. J Neuroimmunol 135, 166-171.

Zeis, T., Kinter, J., Herrero-Herranz, E., Weissert, R., Schaeren-Wiemers, N., 2008. Gene expression analysis of normal appearing brain tissue in an animal model for multiple sclerosis revealed grey matter alterations, but only minor white matter changes. J Neuroimmunol 205, 10-19.

Zhang, S., Cherwinski, H., Sedgwick, J.D., Phillips, J.H., 2004. Molecular mechanisms of CD200 inhibition of mast cell activation. J Immunol 173, 6786-6793.

Zhang, Y.J., Yang, X., Kong, Q.Y., Zhang, Y.F., Chen, W.Y., Dong, X.Q., Li, X.Y., Yu, X.Q., 2006. Effect of 15d-PGJ2 on the expression of CD40 and RANTES induced by IFN-gamma and TNF-alpha on renal tubular epithelial cells (HK-2). Am J Nephrol 26, 356-362.

Appendix

Appendix I: Tables

Table 1

Elisa antibody concentrations

Species	Cytokine	Diluent	Capture Antibody	Standards	Detection Antibody
Rat	IL-1β	1%BSA	Goat anti-rat 0.8μg/ml in PBS	0-2000pg/ml	Biotinylated anti-rat 350ng/ml in diluents
Rat	IL-6	1% BSA	Mouse anti-rat 4.0μg/ml in coating buffer	0-4000pg/ml	Anti-rat 400ng/ml in diluents
Rat	TNFα	1% BSA	Mouse anti-rat 4.0μg/ml in coating buffer	0-4000pg/ml	Anti-rat 100ng/ml in diluent
Rat	IL-4	1% BSA	Mouse anti-rat 2μg/ml in PBS	0-1000pg/ml	Anti-rat 50ng/ml in diluent
Mouse	IL-1β	1% BSA	Rat anti-mouse 4μg/ml in Diluent	0-1000pg/ml	Anti-mouse 600ng/ml in diluents
Mouse	IL-6	1% BSA	Rat anti-mouse 2μg/ml in PBS	0-1000pg/ml	Anti-mouse 200ng/ml in diluents
Mouse	TNFα	1%BSA	Goat anti-mouse 0.8μg/ml in PBS	0-2000pg/ml	Goat anti-mouse 200ng/ml in diluents

Table 2

PCR Primers

Species	Gene Name	Gene Description	Taqman Gene Expression Assay Number
Rat	IL-1β	Interleukin-1 beta	Rn00580432_m1
Rat	IL-6	Interleukin-6	Rn00561420_m1
Rat	TNFα	Tumour necrosis factor α	Rn99999017_m1
Rat	CD11b	CD11b	Rn00709342_m1
Rat	CD40	CD40	Rn01423583_m1
Mouse	IL-1β	Interleukin-1 beta	Mm00434228_m1
Mouse	IL-6	Interleukin-6	Mm00434228_m1
Mouse	TNFα	Tumour necrosis factor α	Mm00443258_m1
Mouse	IL-4	Interleukin-4	Mm00445259_m1
Mouse	CD11b	CD11b	Mm01271265_m1
Mouse	CD40	CD40	Mm00441891_m1
Mouse	CD200L	CD200 ligand	Mm00487740_m1

Appendix II: Mean Data

Variable Units	Rat Mixed Glial Cells				
	Control	LPS			
			Rosiglitazone 5μM	Rosiglitazone 20μM	Rosiglitazone 100μM
IL-1β (pg/ml)	136.6±46.45	111±174.3	921.2±209.9	436.4±110.4	100.5±30.40

Table I Raw data from dose response curve, LPS and rosiglitazone-treated rat mixed glia. Values are expressed a means ± SEM.

Variable Units	Rat Mixed Glial Cells			
	Control	LPS	Rosiglitazone	Rosiglitazone + LPS
IL-1β mRNA (RQ)	1.486±0.3869	67.04±14.40	1.008±0.4327	23.85±3.221
IL-1β (pg/ml)	7.402±1.968	106.2±28.91	2.918±1.191	11.84±4.834
IL-6 mRNA (RQ)	1.406±0.1420	15.78±2.98	0.9106±0.2358	4.643±1.448
IL-6 (pg/ml)	24.08±16.19	2934±784.1	65.81±22.28	3304±913.5
TNFα (RQ)	2.078±0.5483	12.27±2.295	1.000±0.422	5.513±1.836
TNFα (pg/ml)	111.7±14.18	441.6±112.4	64.90±8.595	402±75.96
CD11b (RQ)	0.9345±0.04542	2.317±0.1892	1.873±0.3411	1.274±0.08646
CD40 (RQ)	1.182±0.2841	6.950±1.2	1.03±0.021	2.408±0.8989

Table II Raw data from LPS and rosiglitazone treated mixed glia. Values are expressed as means± SEM

Variable Units	Rat Microglia			
	Control	LPS	Rosiglitazone	Rosiglitazone + LPS
IL-1β mRNA (RQ)	5.342±2.111	279.8+26.55	17.61±7.498	76.32±6.109
IL-1β (pg/ml)	2.927±0.423	62.78±12.46	0.161±0.031	101.1±34.15
IL-6 mRNA (RQ)	2.575±1.018	3.575±1.450	4.487±1.796	4.284±1.806
IL-6 (pg/ml)	290.2±25.65	595.7±27.13	260.1±34.33	464.9±33.58
TNFα (RQ)	2.457±0.5974	31.25±3.046	7.307±2.342	9.148±1.540
TNFα (pg/ml)	112.8±16.59	598.9±20.19	59.06±12.05	304.9±34.56
CD11b (RQ)	0.6843±0.0099	3.696±0.4716	2.231±0.3816	1.196±0.1943
CD40 (RQ)	0.9462±0.1093	9.282±1.067	2.287±-0.4990	4.862±1.055

Table III Raw data from LPS and rosiglitazone-treated rat microglia. Values are expressed as means ± SEM.

Variable Units	Rat Astrocytes			
	Control	LPS	Rosiglitazone	Rosiglitazone + LPS
IL-1β mRNA (RQ)	1.235±0.5928	45.57±16.98	4.204±2.950	30.91±17.22
IL-1β (pg/ml)	0.056±0.012	125.55±11.07	1.03±0.06	44.44±2.323
IL-6 mRNA (RQ)	12.68±7.382	13.65±8.571	15.29±6.643	13.14±7.361
IL-6 (pg/ml)	0.068±0.023	4435±609.8	263.9±140.8	2141±177.8
TNFα (RQ)	1.049±0.4365	12.19±2.194	1.414±0.1059	14.62±4.2
TNFα (pg/ml)	1.03±0.07	587.3±50.82	1.894±1.9	217.2±12.73
CD11b (RQ)	0.7668±0.1231	4.246±0.8724	1.114±0.3313	5.4±1.798
CD40 (RQ)	0.7720±0.2345	1.717±0.6574	1.107±0.2960	1.548±0.3485

Table IV Raw data from LPS and rosiglitazone-treated rat astrocytes. Values are expressed as means ± SEM.

Variable Units	Rat Mixed Glia			
	Control	LPS	IL-4	IL-4 + LPS
IL-1β mRNA (RQ)	0.7415±0.09247	31.76±3.399	0.3722±0.0437	39.77±2.339
IL-1β (pg/ml)	0.056±0.021	855.8±85.30	0.211±0.14	636.9±66.52
IL-6 mRNA (RQ)	3.991±1.604	6.881±2.158	3.391±1.164	9.761±2.672
IL-6 (pg/ml)	7.572±7.572	6404±299.2	20.35±4.56	7476±524
TNFα (RQ)	1.116±0.3101	14.28±4.451	3.422±0.7824	17.28±8.581
TNFα (pg/ml)	0.871±0.263	2979±316.4	2.56±1.28	2833±244.8
CD11b (RQ)	0.747±0.08894	1.132±0.1475	0.8589±0.1287	1.299±0.1480
CD40 (RQ)	2.566±0.6970	7.168±1.259	4.132±1.358	16.17±5.051

Table V Raw data from LPS and IL-4-treated rat mixed glia. Values are expressed as means ± SEM.

Variable Units	Rat Mixed Glia			
	Control	LPS	Rosiglitazone	Rosiglitazone+LPS
IL-4 (pg/ml)	9.451±3.584	10.39±0.8857	17.64±1.975	19.02±1.375
	Rat Microglia		Rat Astrocytes	
	Control	Rosiglitazone	Control	Rosiglitazone
IL-4 (pg/ml)	7.526±1.297	9.462±2.074	6.768±0.7821	10.02±1.630

Table VI Raw data from LPS and rosiglitazone-treated mixed glia, microglia and astrocytes. Values are expressed as means ± SEM.

Variable Units	Mouse Mixed Glia							
	C57BL/6				IL-4$^{-/-}$			
	Control	LPS	Rosi	Rosi +LPS	Control	LPS	Rosi	Rosi +LPS
IL-1β (pg/ml)	2.968± 0.7172	23.75± 1.99	3.149± 0.509	16.09±1.5	3.300±1.990	27.38±2.930	11.42±3.475	26.00±3.912

Table VII Raw data from LPS and rosiglitazone-treated C57BL/6 and IL-4$^{-/-}$ mice. Values are expressed as means ± SEM.

Variable Units	Rat Mixed Glia						
	Control	LPS	MDG79	MDG79 10μM LPS	MDG79 20μM LPS	MDG79 50μM LPS	MDG79 100μM LPS
IL-1β mRNA (RQ)	1.49±0.39	67.07±14.4	2.5±1.5	45.3±6.3	63±7.6	46.2±7.3	3.6±0.76
IL-1β (pg/ml)	60.6±18.3	127.1±22.7	183±20.9	68.7±16.1	23.5±5.19	27.68±5.36	47.5±12
IL-6 mRNA (RQ)	1.41±0.14	15.8±3.0	1.5±0.32	9.2±1.4	10.2±1.6	6.8±2.4	2.5±0.98
IL-6 (pg/ml)	90.1±34.4	376.3±66.5	83.1±20.6	224.1±43.6	159.1±26.06	125.5±39.3	78.5±7.83
TNFα (RQ)	2.08±0.55	12.3±2.3	2.9±1.2	10.9±1.7	11.1±1.4	13.2±3.3	1.8±0.59
TNFα (pg/ml)	0.40±0.35	15.5±3.3	1.33±0.33	14.9±4.5	11.6±4.02	11.7±3.1	0.08±0.002
CD11b (RQ)	0.77±0.12	15.98±2.3	1.7±0.42	13.6±1.16	17.7±3.4	12.3±3.2	2.2±0.82
CD40 (RQ)	1.2±0.28	6.95±1.2	0.72±0.27	4.09±1.47	3.13±0.84	3.09±1.48	0.44±0.29

Table VIII Raw data from LPS and MDG79-treated rat mixed glia. Values are expressed as means ± SEM.

Variable Units	Rat Mixed Glia			
	Control	MDG79 (20μM)	MDG79 (50μM)	MDG79 (100μM)
LPL (RQ)	0.325±0.23	0.233±0.11	0.233±0.12	0.232±0.11
CD36 (RQ)	0.69±0.105	0.45±0.085	0.44±0.057	0.454±0.083

Table IX Raw data from MDG79-treated rat mixed glia. Values are expressed as means ± SEM.

Rat Mixed Glia					
Variable Units	Control	LPS	MDG79	MDG79/LPS	MDG79/GW9662/LPS
IL-1β (RQ)	3.64 ± 2.78	43.69 ± 8.9	2.54 ± 1.46	24.49 ± 3.65	26.93 ± 0.63
IL-1β (pg/ml)	20.39 ± 6.95	155.9 ± 25.31	179.5 ± 35.71	15.37 ± 9.82	7.14 ± 2.51
IL-6 (RQ)	25.98 ± 14.44	225 ± 51.64	1.46 ± 0.314	1023 ± 27.41	148.8 ± 85.23
IL-6 (pg/ml)	103.5 ± 56.38	1176 ± 191.4	83.14 ± 20.59	429.9 ± 114.2	578.8 ± 80.03
CD40 (RQ)	0.488 ± 0.28	4.543 ± 0.73	0.722 ± 0.274	1.32 ± 0.558	6.315 ± 1.511
CD11b (RQ)	0.6343 ± 0.158	13.8 ± 2.86	1.68 ± 0.419	0.53 ± 0.39	4.56 ± 0.14

Table X Raw data from LPS, MDG79 and GW9662-treated rat mixed glia. Values are expressed as means ± SEM.

Spinal Cord of C57BL/6 mice with EAE							
Variable Units	Control	Time post MOG injection (days)					
		0.5	3	5	7	10	21
IL-1β mRNA (RQ)	1.051±0.2038	2.106±0.3953	1.715±0.4986	5.740±0.9841	3.201±1.307	26.85±6.893	20.513.021
IL-1β (pg/ml)	26.64±9.157	17.76±1.823	8.792±3.782	23.38±3.337	32.52±10.26	83.23±17.01	71.95±8.610
IL-6 mRNA (RQ)	0.8023±0.1327	0.4245±0.0185	1.609±1.049	3.320±1.783	0.8833±0.4348	1.110±0.3383	1.178±0.1460
IL-6 (pg/ml)	37.25±7.447	35.27±8.75	17.78±7.156	27.03±2.314	18.67±6.862	32.49±6.359	32.5±3.961
TNFα (RQ)	1.657±0.5361	2.117±0.3248	1.656±0.6303	5.345±1.080	2.413±0.8003	47.89±18.69	27.85±6.782
TNFα (pg/ml)	75.86±7.415	43.23±6.056	30.85±1.876	29.24±0.664	36.89±5.278	26.73±5.883	85.78±18.68
CD200 (RQ)	1.085 ± 0.09	0.8937 ± 0.07	0.915 ± 0.08	0.785 ± 0.04	0.823 ± 0.09	0.85 ± 0.09	0.598 ± 0.12
CD40 (RQ)	1.177±0.6258	0.9530±0.3891	0.4394±0.2330	4.399±1.807	3.470±0.4852	6.275±2.567	6.530±0.2360

Table XI Raw data from spinal cord of C57BL/6 mice induced with EAE. Values are expressed as means ± SEM.

Hippocampus of C57BL/6 mice with EAE							
Variable Units	Control	Time post MOG injection (days)					
		0.5	3	5	7	10	21
IL-1β mRNA (RQ)	6.917± 3.448	28.91±11. 119	443.1±420. 6	3417±1366	8247±5748	1693±847.7	248.7±46.4
IL-1β (pg/ml)	59.16± 2.75	71.69±13. 36	78.05±6.23 8	65.09±10.6 5	49.36±5.27 5	31.23±5.58 3	16.81±1.676
IL-6 mRNA (RQ)	0.8653 ±0.170 1	0.4040±0. 0439	1.517±0.81 27	6.069±3.18 0	5.161±2.17 3	3.149±1.07 8	3.441±0.459 6
IL-6 (pg/ml)	18.03± 2.646	12.47±2.4 01	20.41±2.86 0	27.01±4.78 1	18.40±1.53 8	17.08±2.79 6	15.35±3.152
TNFα (RQ)	2.873± 0.9213	11.72±2.2 32	10.05±6.08 5	67.98±21.1 2	65.76±31.9 5	37.2±10.74	60.79±7.282
TNFα (pg/ml)	38.72± 6.142	26.29±5.6 08	40.81±3.79 8	39.71±6.24 6	33.88±13.1 4	32.38±2.65 5	23.02±2.422
CD200 (RQ)	0.7735 ±0.077 22	0.3698±0. 1352	0.2464±0.0 9318	0.2213±0.1 386	0.2836±0.2 395	0.04489±0. 02536	0.08735±0.0 06075
CD40 (RQ)	0.8833 ±0.246 2	0.7165±0. 1481	0.5840±0.1 493	2.035±0.54 68	4.710±2.60 9	6.780±2.70 7	2.991±0.451 5
CD11b (RQ)	1.325± 0.1931	1.572±0.1 723	1.480±0.19 69	1.940±0.39 83	3.091±0.61 34	1.914±0.16 11	1.921±0.110 9
IL-4 (RQ)	0.7307 ±0.269 3	0.5328±0. 0853	0.3038±0.1 581	0.1962±0.0 7908	0.1038±0.0 5492	0.08504±0. 07270	0.05666±0.0 1790

Table XII Raw data from the hippocampus of C57BL/6 mice induced with EAE. Values are expressed as means ± SEM.

Spleen of C57BL/6 mice with EAE							
Variable Units	Control	Time post MOG injection (days)					
		0.5	3	5	7	10	21
IL-1β mRNA (RQ)	4.090±0.85721	5.159±1.417	15.46±6.069	35.50±14.08	38.51±13.76	133.4±47.03	12.4±2.270
IL-1β (pg/ml)	3.81±8.818	35.12±4.748	53.58±9.260	26.82±3.296	16.78±2.742	11.62±2.013	19.90±1.745
IL-6 mRNA (RQ)	20.54±8.887	8.964±3.596	14.31±5.602	40.60±13.87	36.46±28.53	3.664±1.794	39.16±30.18
IL-6 (pg/ml)	14.60±2.214	13.42±1.694	12.99±1.027	9.952±1.895	4.667±0.4638	5.505±0.9377	2.824±0.6543
TNFα (RQ)	5.421±2.904	6.425±2.573	5.402±2.474	5.573±5.069	18.09±13.23	42.49±21.36	5.862±1.935
TNFα (pg/ml)	16.61±3.675	14.56±3.556	26.64±8.409	8.781±8.409	9.796±4.328	1.934±1.807	7.384±3.076
CD11b (RQ)	38.08±36.16	25.24±12.27	15.48±5.686	73.07±66.83	365.1±270.4	777.4±361	13.88±5.191
CD40 (RQ)	1.312±0.1723	9.324±4.412	4.641±2.4	7.150±6.375	5.942±3.380	40.09±29.68	2.607±1.202

Table XIII Raw data from spleen of C57BL/6 mice with EAE. Values are expressed as means ± SEM.

Appendix III: List of Company Addresses

AGB Scientific Ltd
Dublin Industrial Estate
Finglas
Dublin 11

Alcan
Alcan International Network UK Limited
Pechiney House - the Grove
Slough – Berkshire SL1 1QF
UK

Alexis Corporation (UK) Ltd
P.O. Box 6757
Bingham,

Nottingham NG13 8LS
UK

Applied Biosystems,
Frankfurter Street 129b
Biosciences

64293 Darmstadt
Germany

BD Biosciences

Bio-Rad Laboratories Ltd
2350 Qume Drive,
Maylands Avenue,
San Jose
CA

USA

Cambridge BioScience Ltd

24-25 Signet Court
Newmarket Road
Cambridge CB5 8LA
United Kingdom

DIFCO
The Danby Building
Edmund Halley Road
Oxford Science Park, Oxford OX4 4DQ
England

Gibco
Gibco Ltd.,
3 Fountain Drive,
Linchinnnan Drive,
Paisley PA4 9RF
Scotland

GE Healthcare Life Sciences
Amersham Place
Little Chalfont
Buckinghamshire
HP7 9NA, UK

Harlan UK
Bicester
Olac
UK

HYCOR
An Agilent Technologies Division
Pentlands Science Park
Bush Loan, Penicuik
Edinburgh EH26 0PL
United Kingdom

Invitrogen
Invitrogen Ltd
3 Fountain Drive,
Linchinnnan Drive,
Paisley PA4 9RF
Scotland

Jencons, a VWR Division
Unit 15, The Birches
Willard Way
Imberhorne Industrial Estate
East Grinstead
West Sussex RH19 1XZ
UK

Kaketsuken
1-6-1 Okubo,
Kumamoto-shi,
Kumamoto 860-8568,
Japan

Macherey-Nagel
Labquip (Ireland)Ltd.,
12 The Business Centre,
Fonthill Industrial Park
Clondalkin
Dublin 22

Nanodrop Technologies Inc
3411 Silverside Rd,
Bancroft Bldg,
Willmington,
Delaware, USA

NUNC

Thermo Fisher Scientific,

Kamstrupvej 90,
Postbox 280,
DK-4000,
Roskilde,
Denmark

Pall Corporation Ltd

Rosanna Rd

Tipperary Town
Co Tipperary
Ireland

Pierce

Pierce Biotechnologies

3747 N. Meridian Road

P.O. Box 117

Rockford IL 61105

USA

Promega,

Promega,

2800 Woods Hollow Road

Madison WI 53711

USA

R&D Systems,

R&D Systems,
614 McKinley Place NE
Minneapolis
MN 55413
USA

Sigma

Sigma-Aldrich Company Ltd.
Fancy Road,
Poole,
Dorset BH12 4GH
UK

Sarstedt

Starstedt Ltd.,

Sinnottstown Lane,

Drinagh,

Wexford,

Ireland.

Whatman

Whatman Plc

Whatman House,

St. Leonard's Road,

Maidstone,

Kent ME16 0LS

Appendix IV: List of Solutions

Cell culture media

Dulbecco's Modified Eagles Medium (DMEM) (GIBCO, UK) was supplemented with 10% heat activated (56°C for 60min) Foetal Calf Serum (FCS), 100mM L-Glutamine (Gibco, UK), 100µg/ml penicillin/streptomycin (Gibco, UK).
Neurobasal medium (NBM) was supplemented with 10% heat activated (56°C for 60min) FCS, 100mM L-Glutamine (Gibco, UK), 100µg/ml penicillin/streptomycin (Gibco, UK).

Phosphate-buffered saline (PBS) 20X

320g Sodium chloride (NaCl, 1.4M, Sigma, UK)

46g di-Sodium hydrogen phosphate (Na_2HPO_4, 0.08M, Sigma, UK)

8g Potassium dihydrogen phosphate (KH_2PO_4, 0.01M, Sigma, UK)

8g Potassium chloride (KCl, 0.03M, Sigma, UK)

Dissolved in 2L dH_2O, pH 7.0

ELISA Assay diluent

100ml 1X PBS

1g Bovine Serum Albumin (Sigma, UK)

ELISA wash buffer

500ml 20X PBS

9.5L dH_2O

5ml Tween 20

ELISA substrate solution

5ml colour reagent A; stabilized peroxide solution (R&D Systems, UK)

5ml colour reagent B; stabilized chromogen solution (R&D Systems, UK)

ELISA stopping solution (1M)

26.6ml 18.8M (H_2SO_4)

473.4ml dH_2O

Krebs solution containing calcium

Krebs solution

3.975g NaCl

0.095g KCl

0.08g KH_2PO_4

0.135g $MgSO_4$

0.67g $NaHCO_3$

0.9g Glucose

Make up to 500ml with dH_2O and pH to 7.3

Calcium (stock)

2.94g $CaCl_2$ in 20ml dH_2O

Store at 4°C

Krebs solution containing calcium

Add 200µl $CaCl_2$ to 100ml Krebs solution (1:500 dilution) just before use, for washing or short term storage.

For long term storage, add 10% DMSO to Krebs/$CaCl_2$, snap freeze tissue in liquid N_2 and store at -80°C.

Cell Lysis Buffer

10mM Tris-HCl,
50mM sodium chloride (NaCl),
10mM sodium pyrophosphate ($Na_4P_2O_7$),
50mM sodium fluoride (NaF),
dissolved and filtered in 1L dH_2O, pH 7.4.
+
1% IGEPAL (NP-40),
1mM sodium orthovanadate (Na_3VO_4),
1mM phenylmethylsulphonyl fluoride (PMSF),
1mM protease inhibitor cocktail.

Tris-buffered saline (TBS)

31.52g 20mM Tris-HCl; pH 7.5,
87.66g 150mM NaCl,
dissolved in 1L dH_2O (10X) or 10L dH_2O (1X), pH 7.6.

TBS-Tween (TBS-T)

TBS Buffer (1X) with 0.05% Tween.

ELSEVIER

Neurobiology of Aging 30 (2009) 920–931

NEUROBIOLOGY OF AGING

www.elsevier.com/locate/neuaging

Interleukin-4 mediates the neuroprotective effects of rosiglitazone in the aged brain

David J. Loane [1], Brian F. Deighan, Rachael M. Clarke, Rebecca J. Griffin, Aileen M. Lynch, Marina A. Lynch *

Trinity College Institute for Neuroscience and Physiology Department, Trinity College, Dublin 2, Ireland

Received 16 May 2007; received in revised form 4 September 2007; accepted 5 September 2007
Available online 22 October 2007

Abstract

Increased expression of proinflammatory cytokines, like interleukin-1β (IL-1β), is a feature of the aged brain and it is generally accepted that the primary cell source of these cytokines is activated microglia. In hippocampus of aged rats, the increase in IL-1β is accompanied by microglial activation and impaired long-term potentiation (LTP). Peroxisome proliferator-activated receptors (PPARs) possess anti-inflammatory properties that target microglia. In this study the PPARγ agonist, rosiglitazone, was orally administered to young and aged rats, and we report that the age-related increases in NO and IL-1β production were attenuated in hippocampus of rosiglitazone-treated aged rats and that this was associated with a restoration of LTP. In addition, treatment with rosiglitazone increased interleukin-4 (IL-4) mRNA and reversed the age-related decrease in hippocampal IL-4 concentration. Significantly, while rosiglitazone attenuated the LPS-induced increase in MHCII and IL-1β concentration in glia prepared from wildtype mice, it failed to exert an effect in glia prepared from IL-4$^{-/-}$ mice, thereby suggesting that the anti-inflammatory actions of rosiglitazone are mediated by its ability to increase IL-4 expression.

Keywords: Age; Hippocampus; Microglia; Interleukin-1β (IL-1β); Interleukin-4 (IL-4); Long-term potentiation (LTP); Peroxisome proliferator-activated receptor gamma (PPARγ); Rosiglitazone

1. Introduction

Aged animals exhibit an inflammatory phenotype with evidence of an impaired capacity of aged mice to elicit a functional T helper type 2 cell response (Smith et al., 2001). The evidence suggests that the inflammatory phenotype extends to the brain; thus an age-related increase in hippocampal concentration of proinflammatory cytokines, accompanied by decrease in anti-inflammatory cytokines has been described (Maher et al., 2005; Martin et al., 2002; Nolan et al., 2005). This apparent imbalance in pro- and anti-inflammatory cytokines contributes to the deficit in LTP, because restoring the balance, for example by eicosapentaenoic acid (EPA) (Lynch et al., 2007; Martin et al., 2002), leads to an improved ability of aged rats to sustain LTP. A key contributor to the age-related deficit in LTP is the increase in IL-1β concentration (Lynch and Lynch, 2002) and consistent with the evidence that IL-1β is derived largely from activated microglia (Davies et al., 1999; Li et al., 1997; Minogue et al., 2003), an age-related increase in microglial activation has been documented (Griffin et al., 2006).

Peroxisome proliferator-activated receptors (PPARs) are ligand-activated nuclear receptors, which are key regulators of lipid and glucose metabolism, energy homeostasis and adipocyte and macrophage differentiation (Kliewer et al., 1999). One subtype, PPARγ, is expressed particularly in hippocampus and entorhinal cortex (Berger and Moller, 2002; Kainu et al., 1994) and its expression in neurons and glia has been described *in vitro* and *in vivo* (Bernardo et al., 2003; Cristiano et al., 2001; Inestrosa et al., 2005; Moreno et al., 2004; Park et al., 2004). There is now compelling evidence to

* Corresponding author. Tel.: +353 1 8968531; fax: +353 1 6793545.
E-mail address: lynchma@tcd.ie (M.A. Lynch).
[1] Present address: Department of Neuroscience, Georgetown University Medical Center, Washington, DC 20057, USA.

0197-4580/$ – see front matter © 2007 Elsevier Inc. All rights reserved.
doi:10.1016/j.neurobiolaging.2007.09.001

indicate that PPARγ activation modulates brain inflammation (Bernardo and Minghetti, 2006); thus the endogenous ligand 15-deoxy-Δ^{12-14}-prostaglandin J_2 (15d-PGJ_2) and synthetic thiazolidinediones inhibit LPS-induced microglial activation (Bernardo et al., 2000) and reduce LPS-induced iNOS activation (Kim et al., 2002; Petrova et al., 1999) and COX-2 expression (Petrova et al., 1999) while protecting neurones against LPS- and Aβ-induced cell death *in vitro* and *in vivo* (Heneka et al., 2000). Similarly activation of PPARγ attenuates Aβ-stimulated activation of microglia (Combs et al., 2000) and the secretion of inflammatory cytokines from monocytes and microglia (Combs et al., 2001, 2000).

In addition to these effects, PPARγ activation has been shown to inhibit the up-regulation of stress-activated kinases, JNK and p38, which occur as a result of ischemic stress (Khandoudi et al., 2002; Lennon et al., 2002). Significantly, activation of JNK and p38 have a negative impact on LTP (Barry et al., 2005; Kelly et al., 2003); thus the age-related impairment in LTP is associated with increased JNK activation (Nolan et al., 2005) while the Aβ- and LPS-induced impairment of LTP is attenuated by inhibition of JNK (Minogue et al., 2003; Wang et al., 2004). In contrast, the PPARγ agonists rosiglitazone and pioglitazone activate ERK (Wada et al., 2006) which has been shown to be a key factor in triggering LTP (Bozon et al., 2003; Gooney and Lynch, 2001; McGahon et al., 1999). Therefore, it could be predicted that PPARγ activation might attenuate Aβ-induced and age-dependent deficits in LTP, and the evidence indicates that troglitazone, ciglitazone and 15d-PGJ_2 attenuated the Aβ-mediated decrease in LTP in CA1 *in vitro* (Costello et al., 2005).

This study set out to assess whether treatment of aged rats with rosiglitazone might affect LTP, and to examine whether this treatment modulates the age-related neuroinflammatory changes we have previously identified. The evidence indicates that rosiglitazone attenuated the increase in IL-1β concentration in hippocampus of aged rats and that this was not a consequence of any change in PPARγ activation but was probably due to its ability to increase hippocampal IL-4, which down-regulates IL-1β expression *in vivo* and *in vitro*.

2. Methods

2.1. Animals

Male Wistar rats (BioResources Unit, Trinity College, Dublin, Ireland) of mean age 4 months (250–350 g) or 22 months (450–550 g) were used in these experiments. Animals were housed in pairs (22-month-old rats) or groups of four to six (4-month-old rats) under a 12 h light schedule, ambient temperature was controlled between 22 and 23 °C and rats were maintained under veterinary supervision throughout the study. These experiments were performed under a license issued by the Department of Health (Ireland) and in accordance with the guidelines laid down by the local ethical committee.

Food intake was measured for 2 weeks prior to the period of experimental treatment to establish daily food intake. At the end of this period, young and aged rats were randomly assigned to control groups which received normal laboratory chow (Red Mills, Ireland) or experimental groups to which rosiglitazone maleate (3 mg/rat/day; Alexis Biochemicals Ltd., UK) was added. Treatment continued for 8 weeks. Food was freshly prepared and rats were offered their full daily requirement each day.

In a separate study 4-month-old rats (250–350 g) were randomly assigned to a group that received 3 mg/rat per day rosiglitazone for 3 weeks or laboratory chow (control treatment). At the end of the treatment period, rats were further subdivided into control- and LPS-treated groups. Rats were anaesthetized with urethane (1.5 g/kg) and injected intraperitoneally with 5 μl saline or LPS (100 μg/kg; Sigma, UK) and 3 h later the ability of rats to sustain LTP in perforant path–granule cell synapse was assessed (see below).

In a final study, a group of 4-month-old rats were anaesthetized and subdivided into those that were injected intracerebroventricularly (2.5 mm posterior and 0.5 mm lateral to Bregma) with 5 μl of saline or recombinant IL-4 (20 μg/ml; R&D Systems, UK). Three hours after treatment rats were killed by cervical dislocation and decapitation. The brains were rapidly removed, hemisected, and stored in Krebs buffer (118 mM NaCl, 4.7 mM KCl, 1.2 mM KH_2PO_4, 1.2 mM $MgSO_4$, 4.2 mM $NaHCO_3$, 2 mM $CaCl_2$, 10 mM glucose; pH 7.4) containing 10% dimethyl sulfoxide (DMSO) at −80 °C until required for analysis as previously described (Minogue et al., 2003).

2.2. Induction of LTP in vivo

On the day of the experiment, rats were anaesthetized by intraperitoneal injection of urethane (1.5 g/kg); the absence of a pedal reflex was considered to be an indicator of deep anaesthesia. The ability of rats to sustain LTP in perforant path–granule cell synapses, in response to tetanic stimulation of the perforant path was assessed as previously described (Clarke et al., 2007). In brief, rats were placed in a stereotaxic frame, a bipolar stimulating electrode was positioned in the perforant path (4.4 mm lateral to lambda) and a unipolar recording electrode was positioned in the dorsal cell body region of the dentate gyrus (2.5 mm lateral and 3.9 mm posterior to Bregma). Test shocks were delivered at 30 s intervals, and after a stabilization period, responses were recorded for 15 min before, and 45 min after, tetanic stimulation (three trains of stimuli; 250 Hz for 200 ms; 30 s intertrain interval). The stimulus intensity required to induce a spike was similar in all treatment groups (0.5–1 mA) and the same stimulus strength was used during delivery of the tetanic stimulation. Responses were assessed by measuring the slope of the excitatory postsynaptic potential (epsp) in the middle one-third of the rising phase of the epsp and mean and S.E.M. values

for each treatment group in 30 s bins were calculated and are presented. At the end of the experiment, rats were killed by cervical dislocation and tissue was stored as described (Minogue et al., 2003).

2.3. Preparation of primary glial cultures

Mixed glial cultures were prepared from the cortices of 1-day-old Wistar rats, C57/BL6 (wildtype) mice and IL-$4^{-/-}$ back crossed onto C57/BL6 mice (Kuhn et al., 1991) (BioResources Unit, Trinity College, Dublin, Ireland), as previously described (Nolan et al., 2005). Briefly, dissected tissue was roughly chopped and added to pre-warmed Dulbecco's modified Eagle medium (DMEM) containing fetal bovine serum, penicillin (100 U/ml) and streptomycin (100 U/ml) (all Gibco BRL, Ireland). Tissue was triturated, the suspension was filtered through a sterile mesh filter (40 μm), centrifuged at 2000 × *g* for 3 min at 20 °C and the pellet resuspended in warmed DMEM. Resuspended cells were plated in 24-well plates at a density of 2.5×10^5 cells and incubated for 2 h before addition of warmed DMEM. Cells were grown at 37 °C in a humidified 5% CO_2:95% air environment and media was changed every 3 days. Fourteen days after preparation, the mixed glial cells were pre-treated with either rosiglitazone (20 μM) or GW9662 (20 μM; Sigma, UK). The concentration of GW9662 used in this study was chosen because we have previously shown that this concentration blocks the protective effects of EPA, which is a natural PPARγ ligand, in mixed glial cells (Minogue et al., 2007), and that similar concentrations attenuate the protective effects of TZD agonists (Luna-Medina et al., 2005). The following day the cells were incubated in the presence or absence of LPS (1 μg/ml; Sigma, UK), and incubated for a further 24 h. The supernatant was removed and stored for analysis of IL-1β concentration, and the cells were harvested in either RA1 lysis buffer (Macherey-Nagel Inc., Germany) for assessment of mRNA expression, or lysis buffer (10 mM Tris–HCl, 50 mM NaCl, 10 mM $Na_4P_2O_7 \cdot 10H_2O$, 50 mM NaF, 1 mM PMSF, 1 mM Na_3VO_4, 5 μg/ml pepstatin A, 2 μg/ml leupeptin, 2 μg/ml aprotinin; pH 7.4, containing 1% NP-40) for assessment of protein expression. In other experiments, mixed glial cells were treated with recombinant IL-4 (200 ng/ml) or control media and were harvested in RA1 lysis buffer after 24 h. This mixed glial cell preparation contained approximately 63% astrocytes.

2.4. Analysis of IL-1β and IL-4 concentration

The concentrations of IL-1β and IL-4 were assessed in supernatant obtained from glial cultures as well as in hippocampal homogenates. Analysis was carried out by enzyme-linked immunosorbent assay (R&D Systems, UK) as per manufacturer's instructions and as previously described (Nolan et al., 2005). Absorbance was read at 450 nm, values were expressed as pg/ml (supernatant) and in the case of homogenates, values were corrected for protein concentration and expressed as pg/mg protein.

2.5. Analysis of total NO

A colorimetric kit (Assay Designs Inc., USA) was used to determine total nitric oxide (NO) levels in hippocampal homogenates, as per manufacturer's instructions. Values were corrected for protein and final NO concentrations were expressed as nM/mg protein.

2.6. Analysis of mRNA expression

RNA was extracted from snap-frozen hippocampal tissue and harvested mixed glial cells using a NucleoSpin RNAII isolation kit (Macherey-Nagel Inc., Germany). cDNA synthesis was performed on 1–3 μg total RNA using a High Capacity cDNA RT kit (Applied Biosystems, USA) as per manufacturer's instructions. Equal concentrations of cDNA were used for RT-PCR amplification. The primer pairs listed in Table 1 were used to measure target rat and mouse gene expression.

The PCR cycling conditions were as follows: 96 °C for 5 min followed by 32–40 cycles of 94 °C for 1 min, T_A (°C) for 1 min, and 72 °C for 2 min. The reaction was stopped by final extension for 10 min at 72 °C. To measure rat IL-4 mRNA expression a rat IL-4/18S gene Dual-PCR kit (Maxim Biotech. Ltd., USA) was used and PCR was performed as per manufacturer's instructions. PCR product (10 μl) from

Table 1
RT-PCR primer properties

Target gene	Primer sequence	T_A (°C)
Rat		
MHCII	S: 5′-CAG TCA CAG AAG GCG TTT ATG-3′; A: 5′-GAT CGC AGG CCT TGA ATG ATG-3′	58
IL-1β	S: 5′-GCA CCT TCT TTT CCT TCA TC-3′; A: 5′-CTG ATG TAC CAG TTG GGG AA-3′	59
PPARγ	S: 5′-TCA GCT CTG TGG ACC TCT CTG TGA T-3′; A: 5′-CAA GGC ACT TCT GAA ACC GAC AGT A-3′	62
LPL	S: 5′-CCT AAG GAC CCC TGA AGA CA-3′; A: 5′-GAA TTA CTG GCT TGG ATC CAG C-3′	58
CD36	S: 5′-GCC TGG TTG AGA TGG TCT TAC TTG-3′; A: 5′-CTA TAA ATG AAA GGG CCA CCC CAG-3′	61
β-Actin	S: 5′-AGA AGA GCT ATG AGC TGC CTG ACG-3′; A: 5′-CTT CTG CAT CCT GTC AGC GAT GC-3′	65
Mouse		
MHCII	S: 5′-CCA ATG TCG TCA TCT CCC TG-3′; A: 5′-CTG GAC TGG CAG TCA GGA ATT C-3′	58

S = sense primer; A = anti-sense primer; T_A = annealing temperature.

each sample was loaded onto 1.5% agarose gels, bands were separated by application of 90 V, photographed under UV light and quantified using densitometry (Labworks, UVP BioImaging Systems, UK). The target gene was normalized to mRNA expression of the β-actin or 18S endogenous control genes. There were no observable changes in endogenous control mRNA expression in any treatment group.

2.7. Western immunoblot analysis

Rat hippocampal tissue was homogenized in lysis buffer (see above) and assessed for expression of iNOS and CD36 protein by gel electrophoresis and immunoblotting. To assess PPARγ expression a nuclear fraction was prepared from rat hippocampal tissue using a ProteoExtract® Subcellular Proteome Extraction kit (Merck Biosciences, UK) as per manufacturer's instructions. Tissue samples were equalized for protein concentration and 10 μg was added to NuPAGE LDL sample buffer (Invitrogen, UK) containing NuPAGE reducing agent, heated at 70 °C for 10 min, and loaded onto 10% NuPAGE Novex Bis-Tris gels. Proteins were separated by application of 200 V constant, wet-transferred (XCell II Blot module; Invitrogen, UK) onto nitrocellulose membrane (30 V constant) and incubated overnight in blocking buffer (5% bovine serum albumin (BSA) in Tris buffered saline (100 mM Tris–Cl, 150 mM NaCl; pH 7.5) containing 0.05% Tween-20 (TBS-T)).

Membranes were incubated with antibodies for iNOS (1:1000; BD Transduction Laboratories, UK), CD36 (1:1000; Cayman Chemicals, USA), PPARγ (1:10,000; Merck Biosciences, UK) or actin (1:10,000; Sigma, UK) in TBS-T containing 2% BSA for 2 h at room temperature. Membranes were washed (4 × 15 min in TBS-T), incubated in the appropriate horseradish peroxidase conjugated secondary antibodies (anti-mouse IgG or anti-rabbit IgG, 1:1000; Sigma, UK) for 1 h at room temperature. Membranes were washed (4 × 15 min) and protein complexes were visualized using SuperSignalWest Dura Extended Duration Substrate (Pierce, USA). Immunoblots were exposed to film (Amersham Biosciences, UK) and processed using a Fuji X-ray processor. Protein bands were quantitated by densitometric analysis using Labworks software (UVP BioImaging Systems, UK). Labworks provides a single value (in arbitrary units) representing the density of protein bands, and the data presented represents the density of target protein divided by the density of the endogenous actin in each sample.

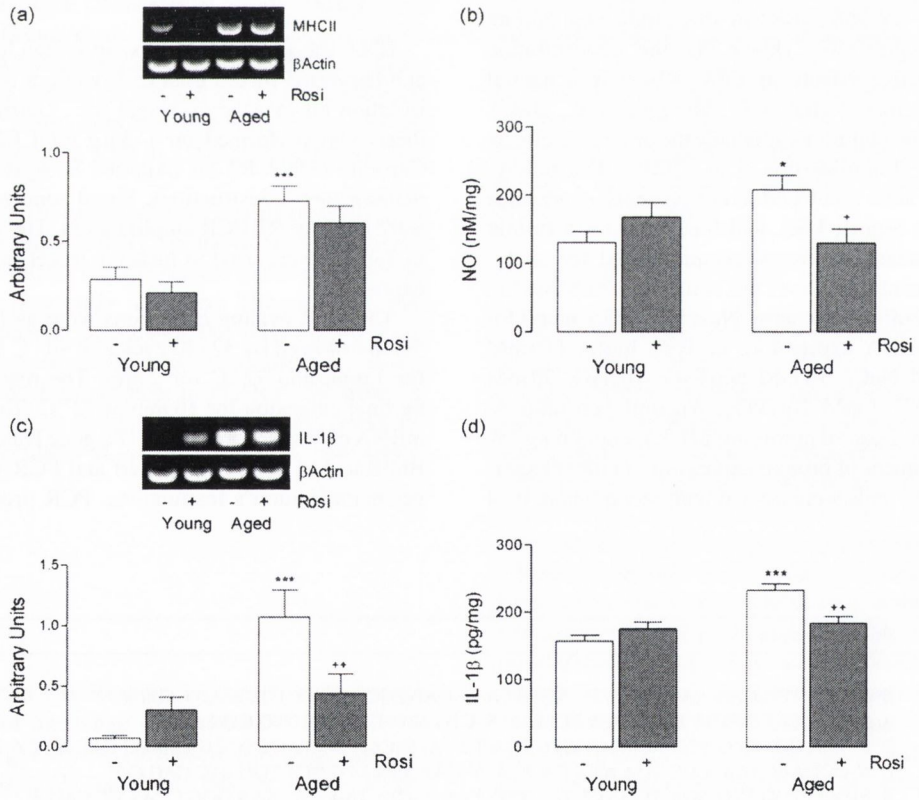

Fig. 1. Rosiglitazone attenuates the age-related increase in proinflammatory mediators in the rat hippocampus. MHCII mRNA expression (a), NO concentration (b), IL-β mRNA expression (c) and IL-1β concentration (d) were significantly increased in hippocampal tissue prepared from aged, compared with young, rats ($^{*}p < 0.05$; $^{***}p < 0.001$; ANOVA); with the exception of MHCII mRNA, these changes were significantly attenuated in tissue prepared from aged rats which were treated with rosiglitazone ($^{+}p < 0.05$; $^{++}p < 0.01$; ANOVA). Data are expressed as means ± S.E.M. of at least six observations. Sample micrographs are shown in (a) and (c).

2.8. Statistical analysis

Data were analyzed using either Student's *t*-test for independent means or a one-way analysis of variance (ANOVA) followed by post hoc Student Newman–Keuls test to determine which conditions were significantly different from each other. Data are expressed as means with standard errors and deemed statistically significant when $p < 0.05$.

3. Results

We analysed microglial activation in hippocampal tissue prepared from control-treated and rosiglitazone-treated young and aged rats by assessing MHCII mRNA, total NO production and IL-1β expression. The representative micrograph shown in Fig. 1a indicates that there was an age-related increase in MHCII mRNA (compare lanes 1 and 2 (control and rosiglitazone-treated; young) with lanes 3 and 4 (control and rosiglitazone-treated; aged)). Analysis of the mean data obtained from densitometric analysis indicated that mean MHCII mRNA expression was significantly increased in hippocampal tissue prepared from aged, compared with young, control-treated rats (***$p < 0.001$; ANOVA); this age-related change was not significantly affected by rosiglitazone treatment.

We demonstrate that the significant age-related increase in MHCII mRNA was accompanied by parallel changes in NO production (*$p < 0.05$; ANOVA; Fig. 1b), IL-1β mRNA (***$p < 0.001$; ANOVA; Fig. 1c) and IL-1β protein (***$p < 0.001$; ANOVA; Fig. 1d). However, in contrast with MHCII mRNA, the data showed that the increases in each of these measures were significantly attenuated in tissue prepared from aged rats, which were treated with rosiglitazone ($^{+}p < 0.05$; $^{++}p < 0.01$; ANOVA; tissue prepared from aged control-treated vs. aged rosiglitazone-treated rats).

Previous evidence has indicated that LTP is depressed in perforant path–granule cell synapses of aged rats; interestingly the decline in excitatory postsynaptic potential (epsp) slope was greater in the last 15 min of the recording period. The data presented here (Fig. 2a) confirms this and shows that rosiglitazone attenuated the age-related decrease in LTP. Analysis of the mean changes at 45 min post-tetanic stimulation revealed a significant decrease in epsp slope in aged control-treated rats (95.38 ± 6.67) compared with the other three groups (young control-treated 128.44 ± 5.61, young rosiglitazone-treated 129.84 ± 4.95, aged rosiglitazone-treated 118.65 ± 3.73, mean ± S.E.M.; ***$p < 0.001$; ANOVA). This age-related impairment in LTP was significantly attenuated in rosiglitazone-treated aged rats ($^{+++}p < 0.001$; ANOVA).

We demonstrate that intraperitoneal injection of LPS resulted in a deficit in LTP in 4-month-old rats (as previously shown (Barry et al., 2005)) and rosiglitazone treatment attenuated this LPS-induced impairment in LTP (Fig. 2b); although there was some evidence of a modest decline in epsp slope for the duration of the experiment. Analysis of the mean changes at 45 min post-tetanic stimulation revealed a significant decrease in epsp slope in LPS control-treated rats (84.41 ± 7.82) compared with the other three groups (saline control-treated 121.74 ± 11.06, saline rosiglitazone-treated 122.48 ± 19.58, LPS rosiglitazone-treated 126.91 ± 7.04, mean ± S.E.M.; ***$p < 0.001$; ANOVA). This LPS-related impairment in LTP was significantly attenuated in LPS-injected rats that had been rosiglitazone-treated ($^{+++}p < 0.001$; ANOVA).

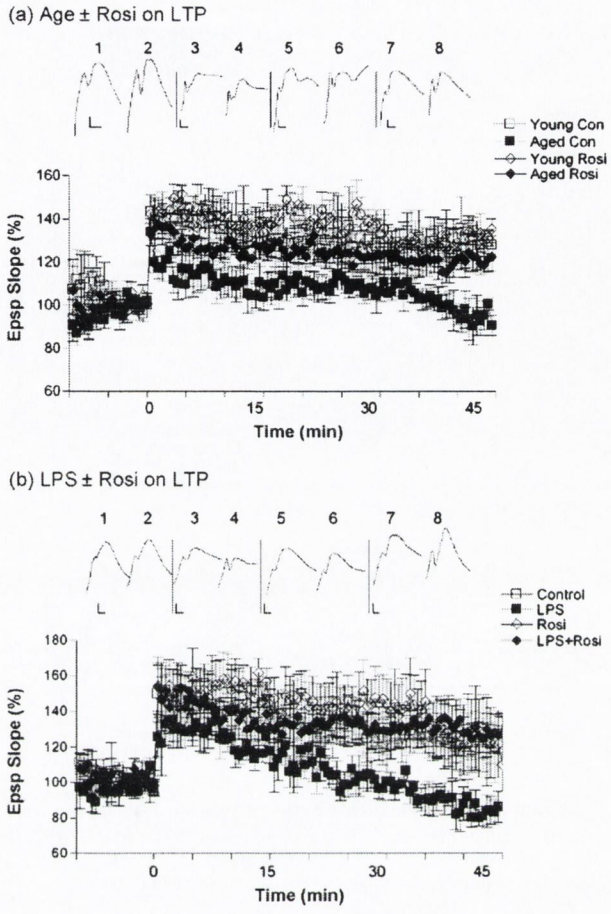

Fig. 2. Rosiglitazone attenuates the age-related and LPS-induced deficits in LTP in perforant path–granule cell synapses. Tetanic stimulation (time 0) resulted in an immediate and sustained increase in the mean population excitatory postsynaptic potential (epsp) slope in young control-treated and young rosiglitazone-treated rats in both experiments (a and b). The responses to tetanic stimulation was attenuated in aged (a) and LPS-treated (b) rats, but aged and LPS-treated rats, which received rosiglitazone sustained LTP in a manner similar to the control-treated animals. Sample epsp recordings for (a). Pre- (5 min before; 1, 3, 5, 7) and post- (after 40 min; 2, 4, 6, 8) tetanic stimulation traces are presented for rats that were control-treated (1–4) or rosiglitazone-treated (5–8), and were young (1, 2, 5, 6) or aged (3, 4, 7, 8). Sample epsp recordings for (b). Pre- (1, 3, 5, 7) and post- (2, 4, 6, 8) tetanic stimulation traces are presented for rats that were control-treated (1–4) or rosiglitazone-treated (5–8), and those which received saline (1, 2, 5, 6) or LPS (3, 4, 7, 8) ICV injection. The scale bars represent 0.1 mV and 5 ms.

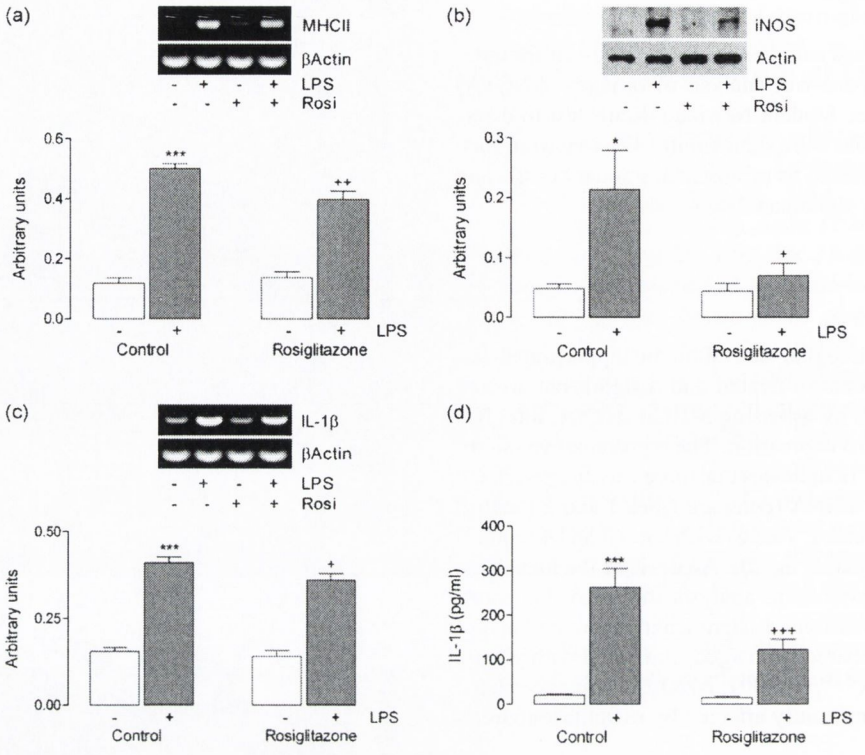

Fig. 3. Rosiglitazone attenuates LPS-induced changes in mixed glial cells. MHCII mRNA expression (a), iNOS protein expression (b), IL-1β mRNA expression (c) and IL-1β concentration (d) in mixed glial cells were significantly increased by LPS (1 μg/ml; $^{*}p<0.05$; $^{***}p<0.001$; ANOVA); these changes were significantly attenuated in cells pre-treated with rosiglitazone (20 μM; $^{+}p<0.05$; $^{++}p<0.01$; $^{+++}p<0.001$; ANOVA). Data are expressed as means ± S.E.M. of at least six observations. Sample micrographs are shown in (a)–(c).

We assessed the effects of rosiglitazone in cultured glial cells and show that incubation of cells in the presence of LPS increased MHCII expression (compare lanes 1 and 2 of sample micrograph; Fig. 3a) and that rosiglitazone partially attenuated the LPS-induced change (lane 4), without exerting any marked effect when included in the incubation medium alone (lane 3). The mean data indicate that the LPS-induced increase in MHCII mRNA was statistically significant ($^{***}p<0.001$; ANOVA; Fig. 3a) and that rosiglitazone partially but significantly attenuated the LPS-induced change ($^{++}p<0.01$; ANOVA). LPS similarly increased iNOS protein expression and IL-1β mRNA (Fig. 3b and c, respectively) and, as in the case of MHCII mRNA, rosiglitazone partially attenuated this increase. Analysis of mean data indicated a significant LPS-induced increase in both markers ($^{*}p<0.05$; $^{***}p<0.001$; ANOVA) and show that coincubation in the presence of rosiglitazone significantly attenuated the LPS-induced changes ($^{+}p<0.05$; ANOVA). IL-1β concentration in supernatant prepared from LPS-treated cells (263.60 ± 41.22 pg/ml) was significantly greater than control-treated cells (20.88 ± 2.16 pg/ml, $^{***}p<0.001$; ANOVA; Fig. 3d) and we show that this effect was significantly attenuated in cells pre-treated with rosiglitazone (123.83 ± 23.33 pg/ml, mean ± S.E.M., $n=18$, $^{+++}p<0.001$; ANOVA).

Analysis of PPARγ mRNA expression in hippocampal tissue prepared from young and aged control-treated and rosiglitazone-treated rats revealed no treatment-related changes (Fig. 4a), but analysis of PPARγ protein expression indicated that, while there were no age-related changes in hippocampal samples prepared from control-treated rats (compare lanes 1 and 3 of sample micrograph; Fig. 4b), expression was significantly increased in samples prepared from aged rats which received rosiglitazone (lane 4; $^{+}p<0.05$; ANOVA; Fig. 4b). We investigated expression of proxy markers of PPARγ activation, lipoprotein lipase (LPL) mRNA expression, and CD36 mRNA and protein expression. The data indicate that expression of these were unaffected by age or rosiglitazone treatment (Fig. 4c–e, respectively). These data suggest that the action of rosiglitazone was independent of its ability to modulate PPARγ and to explore this we analyzed the effect of rosiglitazone on the LPS-induced increase in IL-1β in cultured mixed glia in the presence and absence of the PPARγ antagonist, GW9662. Fig. 4f shows that IL-1β was significantly increased in supernatant prepared from LPS-treated cells (135.74 ± 20.74 pg/ml, $^{***}p<0.001$; ANOVA) and that this was significantly attenuated in cells pre-treated with rosiglitazone (48.02 ± 4.68 pg/ml, $^{+++}p<0.001$; ANOVA). However, the presence of the PPARγ antago-

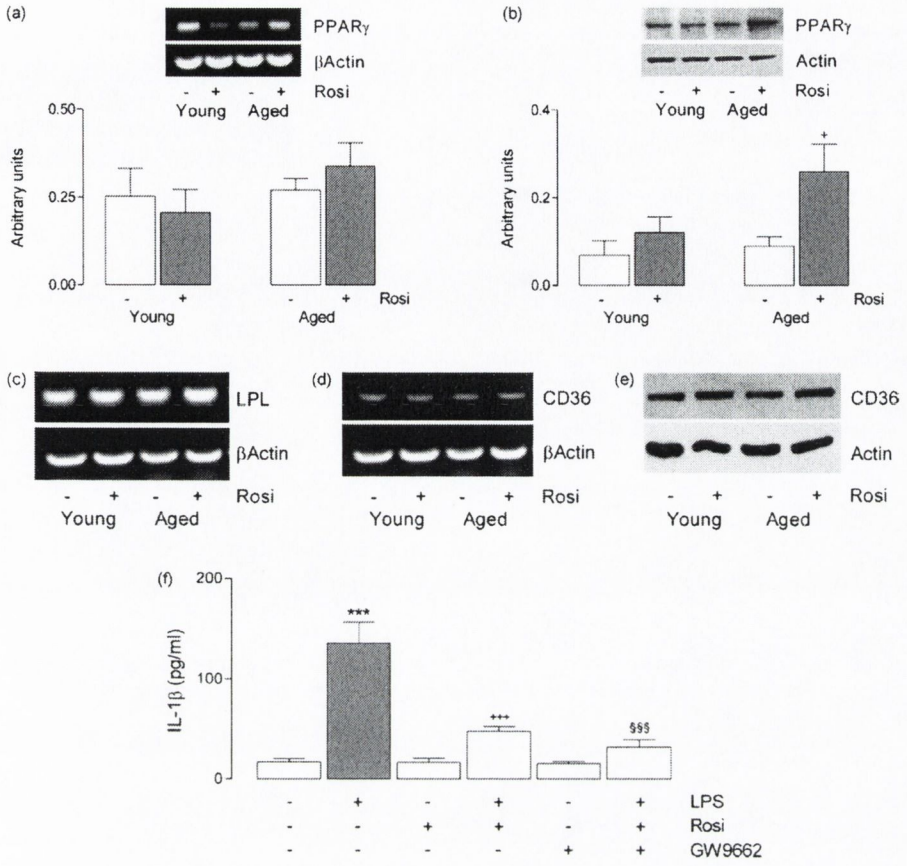

Fig. 4. The effect of rosiglitazone in the hippocampus is PPARγ-independent. There was no evidence of age-associated changes in PPARγ mRNA expression (a), PPARγ protein (b) or in the proxy markers of PPARγ activation, lipoprotein lipase (LPL) mRNA expression (c), CD36 mRNA (d) and CD36 protein (e). Rosiglitazone exerted no significant effect on these measures although PPARγ protein was significantly increased in hippocampal tissue prepared from aged, rosiglitazone-treated, compared with aged control-treated, rats ($^{+}p<0.05$; ANOVA). (f) The LPS-induced increase in mean IL-1β concentration in mixed glial cells ($^{***}p<0.001$; ANOVA) was significantly attenuated in cells pre-treated with rosiglitazone ($^{+++}p<0.001$; ANOVA) but coincubation with the PPARγ antagonist, GW9662, did not affect the rosiglitazone-mediated change. Data in (a), (b) and (f) are expressed as means ± S.E.M. of at least six observations.

nist, GW9662, in the incubation medium failed to affect the rosiglitazone-mediated attenuation in IL-1β concentration (32.12 ± 7.35 pg/ml, mean ± S.E.M., $n=12$), suggesting that the protective effect of rosiglitazone is independent of its ability to modulate PPARγ activity.

In an effort to explore the possible mechanism by which rosiglitazone exerts its neuroprotective effects, and in the context of our previous observation that IL-4 appears to exert significant anti-inflammatory effects in the brain, we assessed the effect of rosiglitazone on IL-4. The data show that, whereas IL-4 mRNA expression was similar in tissue prepared from young and aged control-treated and young rosiglitazone-treated rats, it was significantly increased in tissue prepared from aged rosiglitazone-treated, compared with aged control-treated animals ($^{+}p<0.05$; ANOVA; Fig. 5a). Analysis of IL-4 concentration revealed a significant age-related decrease in hippocampal tissue prepared from aged, compared with young, rats (33.12 ± 3.04 and 49.09 ± 6.02 pg/mg, respectively, $^{*}p<0.05$; ANOVA; Fig. 5b); the data indicate that the age-related decrease in IL-4 protein concentration was significantly attenuated by rosiglitazone treatment (57.33 ± 1.73 pg/mg, mean ± S.E.M., $n=6$, $^{+}p<0.05$; ANOVA), so that mean IL-4 concentration in hippocampus of aged, rosiglitazone-treated rats was similar to that in tissue obtained from young animals.

We considered that the age-related decrease in IL-4 may contribute to the increase in IL-1β mRNA and protein and consistent with this, we report that IL-1β mRNA was significantly decreased in hippocampal tissue prepared from rats which received an intracerebroventricular injection of IL-4 ($^{*}p<0.05$; Student's *t*-test for independent means; Fig. 5c), while addition of IL-4 to mixed glial cells also significantly decreased IL-1β mRNA ($^{*}p<0.05$; Student's *t*-test for independent means; Fig. 5d). These data suggest that IL-4 may mediate the effect of rosiglitazone, and to address this, cultured glial cells were prepared from wildtype and IL-$4^{-/-}$ mice and treated with LPS in the presence and absence of rosiglitazone. The data presented in Fig. 6a indicate that treatment with LPS significantly increased

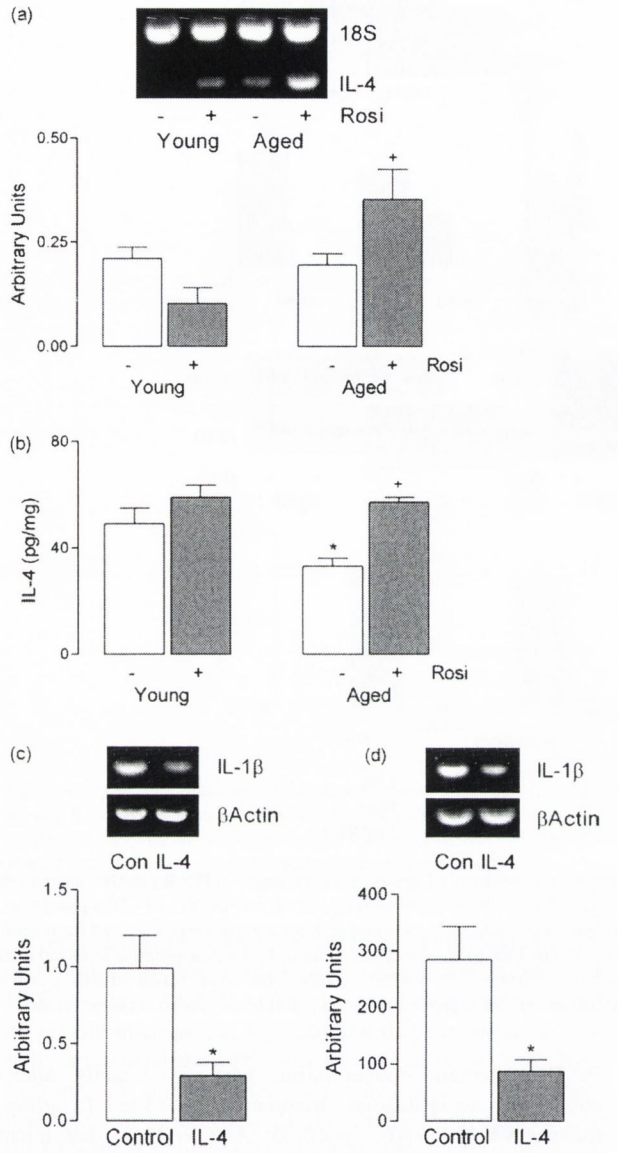

Fig. 5. Rosiglitazone increases IL-4 expression. IL-4 mRNA expression (a) was unaffected, but IL-4 concentration (b) was significantly decreased in hippocampal tissue prepared from aged rats. Treatment of aged rats with rosiglitazone significantly increased IL-4 mRNA expression and significantly reversed the age-related decrease in IL-4 concentration ($^{+}p < 0.05$; ANOVA). (c) Intracerebroventricular injection of IL-4 (20 μg/ml) significantly reduced IL-1β mRNA expression compared to saline-injected rats ($^{*}p < 0.05$; Student's *t*-test for independent means). (d) Treatment of mixed glial cells with IL-4 (200 ng/ml) also significantly decreased IL-1β mRNA ($^{*}p < 0.05$; Student's *t*-test for independent means). Data are expressed as means ± S.E.M. of at least five observations. Sample micrographs are shown in (a), (c) and (d).

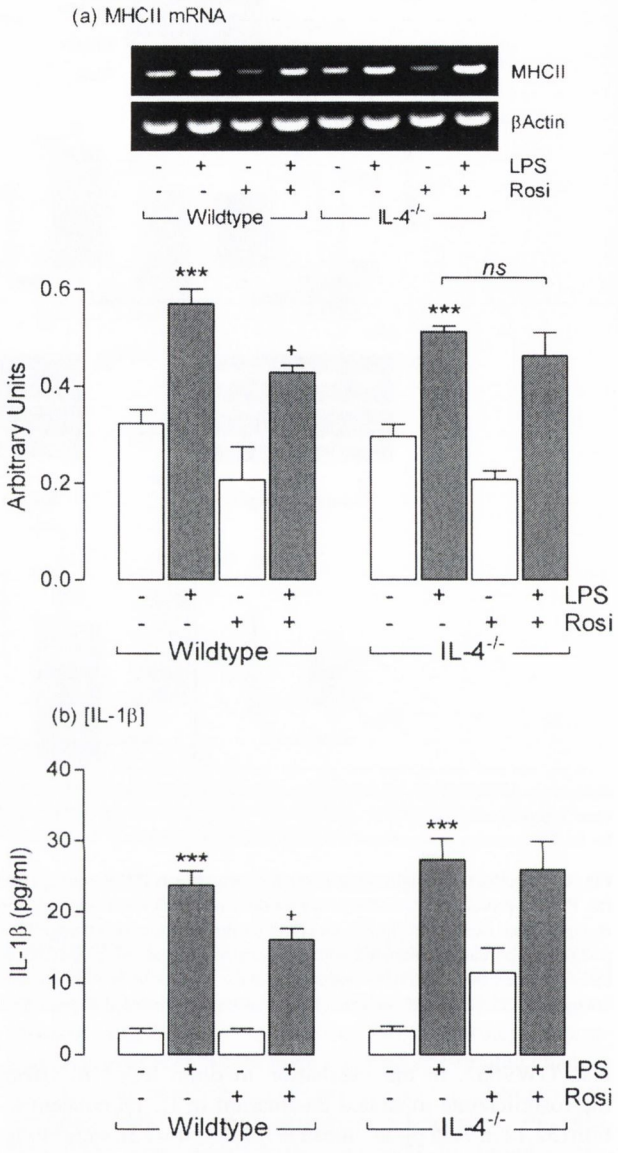

Fig. 6. Rosiglitazone attenuates the LPS-induced increases in MHCII mRNA expression and IL-1β production in mixed glial cells prepared from wildtype, but not in IL-4$^{-/-}$ mice. Treatment of mixed glial cells prepared from wildtype and IL-4$^{-/-}$ mice with LPS (1 μg/ml) significantly increased MHCII mRNA expression (a; $^{***}p < 0.001$; ANOVA) and IL-1β concentration (b; $^{***}p < 0.001$; ANOVA). Pre-treatment with rosiglitazone (20 μM) significantly attenuated these changes in cell prepared from wildtype ($^{+}p < 0.05$; ANOVA), but not IL-4$^{-/-}$ mice ($^{ns}p > 0.05$; ANOVA). Data are expressed as means ± S.E.M. of at least six observations. A sample micrograph is shown in (a).

MHCII mRNA expression in cells prepared from wildtype and IL-4$^{-/-}$ mice ($^{***}p < 0.001$; ANOVA; Fig. 6a). Pre-treatment of cells with rosiglitazone significantly attenuated the LPS-induced change in cells prepared from wildtype mice ($^{+}p < 0.05$; ANOVA). In contrast, rosiglitazone treatment failed to exert any significant effect on the LPS-induced increase in MHCII mRNA in cells prepared from IL-4$^{-/-}$ mice. In parallel, we report that treatment of cells from both wildtype and IL-4$^{-/-}$ mice with LPS significantly increased IL-1β concentration ($^{***}p < 0.001$; ANOVA; Fig. 6b), and that whereas pre-treatment with rosiglitazone significantly attenuated this effect in cells prepared from wildtype mice

($^{+}p < 0.05$; ANOVA), there was no effect of rosiglitazone on the LPS-induced change in cells prepared from IL-$4^{-/-}$ mice.

4. Discussion

We set out to investigate whether rosiglitazone exerted anti-inflammatory effects in the hippocampus of the aged rat and to assess whether treatment with rosiglitazone might restore LTP, which has been shown to be impaired in perforant path–granule cell synapses of aged rats. We report that rosiglitazone attenuates the age-related increase in IL-1β and that this is accompanied by a partial restoration of LTP. The evidence suggests that this effect is mediated by a rosiglitazone-induced increase in IL-4.

The data presented show that treatment of rats with rosiglitazone attenuated the age-related increases in IL-1β mRNA and protein and the associated increase in NO production in hippocampus, suggesting that rosiglitazone down-regulates microglial activation, the primary cell source of IL-1β and NO. In contrast, rosiglitazone treatment did not affect the age-related increase in expression of the cell surface marker MHCII, which is considered to be a reliable indicator of microglial activation. This suggests that the action of rosiglitazone is to target transcription of inflammatory genes which supports the proposal that modulation of inflammatory gene expression mediates the ability of PPARγ agonists like pioglitazone to reduce the severity of EAE (Feinstein et al., 2002). In addition to its neuroprotective effects in EAE, there is a wealth of evidence indicating that PPARγ agonists reduce infarct volume in models of ischemia (Allahtavakoli et al., 2006; Luo et al., 2006; Zhao et al., 2006) and this has been coupled with their ability to reduce microglial activation and therefore inflammation (Sundararajan et al., 2005). The ability of rosiglitazone to attenuate the age-related increase in NO described here is consistent with previous reports indicating that central injection of PPARγ agonists inhibited the LPS-induced and IFNγ-induced iNOS expression (Heneka et al., 2000), while oral administration decreased microglial activation and iNOS mRNA in hippocampus of 10-month-old APPV717I mice (Heneka et al., 2005).

Until recently the evidence for rosiglitazone's ability to cross the blood–brain barrier (BBB) was limited and the question of how it exerts its central protective effects in aged brain were not understood. Data from a number of groups indicated age-related changes in BBB permeability; for example it has been shown that permeability is increased in aged, compared with young, rats (Bake and Sohrabji, 2004) and that a similar increase occurs in mice, with more profound changes observed in ApoE$^{-/-}$ mice (Hafezi-Moghadam et al., 2007) and earlier permeability changes (i.e. at 4–10 months of age) observed in Tg2576 mice (Ujiie et al., 2003). These data suggest that access of rosiglitazone to the brain in aged rats might be increased due to increased BBB permeability. In fact, Strum et al. (2007) recently detected rosiglitazone in the CNS of 21-month-old mice at sufficiently high concentrations to cause transactivation of the mouse PPARγ receptor (Strum et al., 2007). This is the first demonstration that rosiglitazone penetrates the CNS where it exerts its protective effects.

One of the most significant findings of this study is that rosiglitazone treatment attenuates the age-related and LPS-induced inhibition of LTP. The age-related increase in IL-1β and deficit in LTP, are consistent with the previously described observation of an inverse relationship between hippocampal IL-1β concentration and LTP (Griffin et al., 2006; Martin et al., 2002) and support the evidence. This association has been underscored in other experimental conditions; for example in rats treated with LPS (Lonergan et al., 2004), or amyloid-$\beta_{(1-40)}$ (Minogue et al., 2003) and in rats exposed to irradiation (Lynch et al., 2003), and is further emphasized by the finding that rosiglitazone treatment decreases the age-related increase in IL-1β and, in parallel, restores LTP. Interestingly bath application of troglitazone, ciglitazone and 15d-PGJ_2 have been shown to attenuate the Aβ-induced inhibition of LTP in area CA1 *in vitro*, although 15d-PGJ_2, but not troglitazone or ciglitazone, reduced LTP (Costello et al., 2005). LTP is considered to be a biological substrate for learning and memory in rats and the restorative action of rosiglitazone observed here is consistent with the finding that rosiglitazone attenuates the deficits in spatial working and reference memory observed in middle-aged mice which overexpress human amyloid precursor protein (Pedersen et al., 2006). These data suggest that rosiglitazone may be important therapeutically in age-associated neurodegenerative diseases such as Alzheimer's disease. Consistently emerging evidence from clinical trials demonstrates that rosiglitazone may attenuate cognitive decline in patients with early-onset Alzheimer's disease (Risner et al., 2006; Watson et al., 2005).

We observed that the LPS-induced increases in IL-1β mRNA and protein, and also the increase in iNOS expression, in glia, were attenuated by rosiglitazone. The data show that rosiglitazone also attenuated the LPS-induced increase in MHCII mRNA *in vitro*, which contrasts with its lack of effect on this measure *in vivo*. These data are consistent with an extensive literature indicating that PPARγ agonists inhibit LPS and/or IFNγ-induced proinflammatory cytokine expression *in vitro*. For example, rosiglitazone (Luo et al., 2006) and the PPARγ agonist, NCX 2216 (Bernardo et al., 2006), both attenuate the LPS-induced increases in TNFα and IL-1β in microglial cultures, while 15d-PGJ_2 inhibits LPS-induced iNOS mRNA and protein in BV2 cells (Petrova et al., 1999). Similar findings were reported in macrophages where the evidence suggested that the PPARγ-induced effects result from inhibition of genes involved in the inflammatory response including AP1, STAT-1 and NFκB (Ricote et al., 1998). Consistent with our observation, PPARγ activation by 15d-PGJ_2, has been shown to attenuate IFNγ-induced MHCII expression (assessed by OX6 staining) in cultured rat microglia, while the increase in iNOS induced by both LPS and IFNγ was also attenuated (Bernardo et al., 2000). However, it is

unclear whether endogenous PGJ_2 concentrations are likely to reach biologically significant concentrations *in vivo*.

Our data shows that neither age nor rosiglitazone affected PPARγ mRNA expression and similarly we observed no age-related change in protein expression although rosiglitazone increased PPARγ in hippocampal tissue prepared from aged rats. We investigated PPARγ activation by assessing changes in CD36 and LPL expression. CD36 is a class B scavenger receptor, one function of which is to scavenge oxidized LDL particles. Its expression has been shown to be dependent on PPARγ activation (Hodgkinson and Ye, 2003); thus while troglitazone did not up-regulate CD36 mRNA in control J774 cells and NIH-3T3 cells (which do not express PPARγ) it significantly increased it in PPARγ-transfected cells. Similarly, rosiglitazone increased CD36 in wildtype but not PPARγ-deficient macrophages (Chawla et al., 2001). The data presented here indicate that CD36 mRNA and protein were unaffected by rosiglitazone treatment suggesting that the actions of rosiglitazone in hippocampus which we describe here are independent of PPARγ activation. This is supported by the finding that rosiglitazone treatment also failed to exert any effect on LPL mRNA expression, although it has been shown to be reliably up-regulated by PPARγ activation (Bogacka et al., 2004; Kageyama et al., 2003) and is PPARγ-dependent, since troglitazone-induced expression of the LPL gene (and CD36) was minimally induced in peritoneal macrophages prepared from PPARγ conditional gene knockout mouse (Akiyama et al., 2002).

The present data suggest that rosiglitazone acts in a manner, which is independent of PPARγ activation; to obtain confirmatory data, we examined whether the PPARγ antagonist, GW9662, abrogated the effect of rosiglitazone *in vitro*. The data indicate that it failed to modulate the inhibitory effect of rosiglitazone on LPS-induced IL-1β in glia. A number of studies have identified actions of PPARγ agonists which are independent of PPARγ activation; for example it was shown that 15d-PGJ_2, troglitazone and ciglitazone attenuated LPS-induced and IFNγ-induced increases in proinflammatory cytokines and iNOS and COX2 expression to a similar extent in wildtype and PPARγ-deficient macrophages (Chawla et al., 2001), and that the inhibitory effect of 15d-PGJ_2 on LPS-induced changes in BV2 cells was independent of PPARγ activation, but due to modulation of NFκB activation (Petrova et al., 1999). Others have suggested that 15d-PGJ_2- and rosiglitazone-induced transcription of suppressor of cytokine signalling (SOCS) 1 and 3 and the subsequent reduction in phosphorylation of JAK1, JAK2, STAT1 and STAT3 in glia are responsible for their anti-inflammatory effects (Park et al., 2003). However, expression of SOCS1 and SOCS3 mRNA was assessed in this study but rosiglitazone treatment had no effect on either (data not shown).

Previous evidence from this laboratory highlights the importance of IL-4 as a regulator of inflammation in brain, particularly hippocampus and we have reported that IL-4 down-regulates IL-1β protein in tissue prepared from aged rats (Lynch et al., 2007). We considered that rosiglitazone might exert its anti-inflammatory effects in hippocampus by up-regulating IL-4 and the evidence presented here is consistent with this proposal. First IL-4 mRNA, although unchanged with age, was increased in tissue prepared from aged, rosiglitazone-treated rats and second, the age-related decrease in IL-4 concentration in hippocampus, which confirms previous data (Lynch et al., 2007; Maher et al., 2005) was reversed in tissue prepared from rosiglitazone-treated rats. Consistent with previous findings, we demonstrate that injection of rats with IL-4 decreased IL-1β mRNA, while treatment of glia with IL-4 exerted a similar effect (Lynch et al., 2007). Although this is the first report indicating that PPARγ activation stimulated an increase in IL-4 in brain tissue, ciglitazone has been reported to increase IL-4 concentration in spleen (Gelinas et al., 2005) and pioglitazone to exert a similar effect in heart (Hasegawa et al., 2005).

In an effort to consolidate the finding that the action of rosiglitazone is mediated by IL-4, we investigated the modulatory effect of rosiglitazone on LPS-induced changes in glia prepared from wildtype and IL-$4^{-/-}$ mice. We demonstrate that while rosiglitazone attenuated the LPS-induced increases in MHCII mRNA and IL-1β concentration in cells prepared from wildtype mice, this effect was absent in cells prepared from IL-$4^{-/-}$ mice. The data presented here demonstrate that rosiglitazone exerts a powerful anti-inflammatory effect in brain of aged rats and that, associated with this there is a restoration of LTP. We suggest that the rosiglitazone-induced increase in IL-4 together with the finding that the anti-inflammatory effect of rosiglitazone was absent in IL-$4^{-/-}$ mice provides strong evidence of a pivotal role for IL-4 in mediating the effect of rosiglitazone.

Conflict of interest

Authors have no conflict of interest to disclose, financial, personal or otherwise with people or organizations within 3 years of beginning the work submitted that could inappropriately influence this study.

Disclosure

The use of Wistar rats and all procedures performed in this study were approved under a license issued by the Department of Health (Ireland) and in accordance with the guidelines laid down by the local ethical committee.

Acknowledgements

We are very grateful to our collaborator, Professor Kingston Mills, School of Biochemistry and Immunology, Trinity College, Dublin, for providing us with tissue from IL-4 knockout mice. We thank Anne-Marie Miller for tech-

nical assistance. Rachael. M. Clarke is a recipient of a Trinity College Ussher Fellowship. This study was funded by Science Foundation Ireland, The Higher Education Authority Ireland (PRTLI), and Enterprise Ireland.

References

Akiyama, T.E., Sakai, S., Lambert, G., Nicol, C.J., Matsusue, K., Pimprale, S., Lee, Y.H., Ricote, M., Glass, C.K., Brewer Jr., H.B., Gonzalez, F.J., 2002. Conditional disruption of the peroxisome proliferator-activated receptor gamma gene in mice results in lowered expression of ABCA1, ABCG1, and apoE in macrophages and reduced cholesterol efflux. Mol. Cell. Biol. 22, 2607–2619.

Allahtavakoli, M., Shabanzadeh, A.P., Sadr, S.S., Parviz, M., Djahanguiri, B., 2006. Rosiglitazone, a peroxisome proliferator-activated receptor-gamma ligand, reduces infarction volume and neurological deficits in an embolic model of stroke. Clin. Exp. Pharmacol. Physiol. 33, 1052–1058.

Bake, S., Sohrabji, F., 2004. 17Beta-estradiol differentially regulates blood–brain barrier permeability in young and aging female rats. Endocrinology 145, 5471–5475.

Barry, C.E., Nolan, Y., Clarke, R.M., Lynch, A., Lynch, M.A., 2005. Activation of c-Jun-N-terminal kinase is critical in mediating lipopolysaccharide-induced changes in the rat hippocampus. J. Neurochem. 93, 221–231.

Berger, J., Moller, D.E., 2002. The mechanisms of action of PPARs. Annu. Rev. Med. 53, 409–435.

Bernardo, A., Minghetti, L., 2006. PPAR-gamma agonists as regulators of microglial activation and brain inflammation. Curr. Pharm. Des. 12, 93–109.

Bernardo, A., Levi, G., Minghetti, L., 2000. Role of the peroxisome proliferator-activated receptor-gamma (PPAR-gamma) and its natural ligand 15-deoxy-Delta12,14-prostaglandin J2 in the regulation of microglial functions. Eur. J. Neurosci. 12, 2215–2223.

Bernardo, A., Ajmone-Cat, M.A., Levi, G., Minghetti, L., 2003. 15-Deoxy-delta12,14-prostaglandin J2 regulates the functional state and the survival of microglial cells through multiple molecular mechanisms. J. Neurochem. 87, 742–751.

Bernardo, A., Gasparini, L., Ongini, E., Minghetti, L., 2006. Dynamic regulation of microglial functions by the non-steroidal anti-inflammatory drug NCX 2216 implications for chronic treatments of neurodegenerative diseases. Neurobiol. Dis. 22, 25–32.

Bogacka, I., Xie, H., Bray, G.A., Smith, S.R., 2004. The effect of pioglitazone on peroxisome proliferator-activated receptor-gamma target genes related to lipid storage in vivo. Diabates Care 27, 1660–1667.

Bozon, B., Kelly, A., Josselyn, S.A., Silva, A.J., Davis, S., Laroche, S., 2003. MAPK CREB and zif268 are all required for the consolidation of recognition memory. Philos. Trans. R. Soc. Lond. B: Biol. Sci. 358, 805–814.

Chawla, A., Barak, Y., Nagy, L., Liao, D., Tontonoz, P., Evans, R.M., 2001. PPAR-gamma dependent and independent effects on macrophage-gene expression in lipid metabolism and inflammation. Nat. Med. 7, 48–52.

Clarke, R.M., O'Connell, F., Lyons, A., Lynch, M.A., 2007. The HMG-CoA reductase inhibitor, atorvastatin, attenuates the effects of acute administration of amyloid-beta1-42 in the rat hippocampus in vivo. Neuropharmacology 52, 136–145.

Combs, C.K., Johnson, D.E., Karlo, J.C., Cannady, S.B., Landreth, G.E., 2000. Inflammatory mechanisms in Alzheimer's disease: inhibition of beta-amyloid-stimulated proinflammatory responses and neurotoxicity by PPARgamma agonists. J. Neurosci. 20, 558–567.

Combs, C.K., Bates, P., Karlo, J.C., Landreth, G.E., 2001. Regulation of beta-amyloid stimulated proinflammatory responses by peroxisome proliferator-activated receptor alpha. Neurochem. Int. 39, 449–457.

Costello, D.A., O'Leary, D.M., Herron, C.E., 2005. Agonists of peroxisome proliferator-activated receptor-gamma attenuate the Abeta-mediated impairment of LTP in the hippocampus in vitro. Neuropharmacology 49, 359–366.

Cristiano, L., Bernardo, A., Ceru, M.P., 2001. Peroxisome proliferator-activated receptors (PPARs) and peroxisomes in rat cortical and cerebellar astrocytes. J. Neurocytol. 30, 671–683.

Davies, C.A., Loddick, S.A., Toulmond, S., Stroemer, R.P., Hunt, J., Rothwell, N.J., 1999. The progression and topographic distribution of interleukin-1beta expression after permanent middle cerebral artery occlusion in the rat. J. Cereb. Blood Flow Metab. 19, 87–98.

Feinstein, D.L., Galea, E., Gavrilyuk, V., Brosnan, C.F., Whitacre, C.C., Dumitrescu-Ozimek, L., Landreth, G.E., Pershadsingh, H.A., Weinberg, G., Heneka, M.T., 2002. Peroxisome proliferator-activated receptor-gamma agonists prevent experimental autoimmune encephalomyelitis. Ann. Neurol. 51, 694–702.

Gelinas, D.S., Lambermon, M.H., McLaurin, J., 2005. Ciglitazone increases basal cytokine expression in the central nervous system of adult rats. Brain Res. 1034, 139–146.

Gooney, M., Lynch, M.A., 2001. Long-term potentiation in the dentate gyrus of the rat hippocampus is accompanied by brain-derived neurotrophic factor-induced activation of TrkB. J. Neurochem. 77, 1198–1207.

Griffin, R., Nally, R., Nolan, Y., McCartney, Y., Linden, J., Lynch, M.A., 2006. The age-related attenuation in long-term potentiation is associated with microglial activation. J. Neurochem. 99, 1263–1272.

Hafezi-Moghadam, A., Thomas, K.L., Wagner, D.D., 2007. ApoE-deficiency leads to a progressive age-dependent blood–brain barrier leakage. Am. J. Physiol. Cell Physiol. 292, C1256–C1262.

Hasegawa, H., Takano, H., Zou, Y., Qin, Y., Hizukuri, K., Odaka, K., Toyozaki, T., Komuro, I., 2005. Pioglitazone, a peroxisome proliferator-activated receptor gamma activator, ameliorates experimental autoimmune myocarditis by modulating Th1/Th2 balance. J. Mol. Cell. Cardiol. 38, 257–265.

Heneka, M.T., Klockgether, T., Feinstein, D.L., 2000. Peroxisome proliferator-activated receptor-gamma ligands reduce neuronal inducible nitric oxide synthase expression and cell death in vivo. J. Neurosci. 20, 6862–6867.

Heneka, M.T., Sastre, M., Dumitrescu-Ozimek, L., Hanke, A., Dewachter, I., Kuiperi, C., O'Banion, K., Klockgether, T., Van Leuven, F., Landreth, G.E., 2005. Acute treatment with the PPARgamma agonist pioglitazone and ibuprofen reduces glial inflammation and Abeta1-42 levels in APPV717I transgenic mice. Brain 128, 1442–1453.

Hodgkinson, C.P., Ye, S., 2003. Microarray analysis of peroxisome proliferator-activated receptor-gamma induced changes in gene expression in macrophages. Biochem. Biophys. Res. Commun. 308, 505–510.

Inestrosa, N.C., Godoy, J.A., Quintanilla, R.A., Koenig, C.S., Bronfman, M., 2005. Peroxisome proliferator-activated receptor gamma is expressed in hippocampal neurons and its activation prevents beta-amyloid neurodegeneration: role of Wnt signaling. Exp. Cell Res. 304, 91–104.

Kageyama, H., Hirano, T., Okada, K., Ebara, T., Kageyama, A., Murakami, T., Shioda, S., Adachi, M., 2003. Lipoprotein lipase mRNA in white adipose tissue but not in skeletal muscle is increased by pioglitazone through PPAR-gamma. Biochem. Biophys. Res. Commun. 305, 22–27.

Kainu, T., Wikstrom, A.C., Gustafsson, J.A., Pelto-Huikko, M., 1994. Localization of the peroxisome proliferator-activated receptor in the brain. Neuroreport 5, 2481–2485.

Kelly, A., Vereker, E., Nolan, Y., Brady, M., Barry, C., Loscher, C.E., Mills, K.H., Lynch, M.A., 2003. Activation of p38 plays a pivotal role in the inhibitory effect of lipopolysaccharide and interleukin-1 beta on long-term potentiation in rat dentate gyrus. J. Biol. Chem. 278, 19453–19462.

Khandoudi, N., Delerive, P., Berrebi-Bertrand, I., Buckingham, R.E., Staels, B., Bril, A., 2002. Rosiglitazone, a peroxisome proliferator-activated receptor-gamma, inhibits the Jun NH(2)-terminal kinase/activating protein 1 pathway and protects the heart from ischemia/reperfusion injury. Diabetes 51, 1507–1514.

Kim, E.J., Kwon, K.J., Park, J.Y., Lee, S.H., Moon, C.H., Baik, E.J., 2002. Effects of peroxisome proliferator-activated receptor agonists on LPS-induced neuronal death in mixed cortical neurons: associated with iNOS and COX-2. Brain Res. 941, 1–10.

Kliewer, S.A., Lehmann, J.M., Milburn, M.V., Willson, T.M., 1999. The PPARs and PXRs: nuclear xenobiotic receptors that define novel hormone signaling pathways. Recent Prog. Horm. Res. 54, 345-L367 (Discussion 67–68).

Kuhn, R., Rajewsky, K., Muller, W., 1991. Generation and analysis of interleukin-4 deficient mice. Science 254, 707–710.

Lennon, A.M., Ramauge, M., Dessouroux, A., Pierre, M., 2002. MAP kinase cascades are activated in astrocytes and preadipocytes by 15-deoxy-Delta(12-14)-prostaglandin J(2) and the thiazolidinedione ciglitazone through peroxisome proliferator activator receptor gamma-independent mechanisms involving reactive oxygenated species. J. Biol. Chem. 277, 29681–29685.

Li, A.J., Katafuchi, T., Oda, S., Hori, T., Oomura, Y., 1997. Interleukin-6 inhibits long-term potentiation in rat hippocampal slices. Brain Res. 748, 30–38.

Lonergan, P.E., Martin, D.S., Horrobin, D.F., Lynch, M.A., 2004. Neuroprotective actions of eicosapentaenoic acid on lipopolysaccharide-induced dysfunction in rat hippocampus. J. Neurochem. 91, 20–29.

Luna-Medina, R., Cortes-Canteli, M., Alonso, M., Santos, A., Martinez, A., Perez-Castillo, A., 2005. Regulation of inflammatory response in neural cells in vitro by thiadiazolidinones derivatives through peroxisome proliferator-activated receptor gamma activation. J. Biol. Chem. 280, 21453–21462.

Luo, Y., Yin, W., Signore, A.P., Zhang, F., Hong, Z., Wang, S., Graham, S.H., Chen, J., 2006. Neuroprotection against focal ischemic brain injury by the peroxisome proliferator-activated receptor-gamma agonist rosiglitazone. J. Neurochem. 97, 435–448.

Lynch, A.M., Lynch, M.A., 2002. The age-related increase in IL-1 type I receptor in rat hippocampus is coupled with an increase in caspase-3 activation. Eur. J. Neurosci. 15, 1779–1788.

Lynch, A.M., Moore, M., Craig, S., Lonergan, P.E., Martin, D.S., Lynch, M.A., 2003. Analysis of interleukin-1 beta-induced cell signaling activation in rat hippocampus following exposure to gamma irradiation. Protective effect of eicosapentaenoic acid. J. Biol. Chem. 278, 51075–51084.

Lynch, A.M., Loane, D.J., Minogue, A.M., Clarke, R.M., Kilroy, D., Nally, R.E., Roche, O.J., O'Connell, F., Lynch, M.A., 2007. Eicosapentaenoic acid confers neuroprotection in the amyloid-beta challenged aged hippocampus. Neurobiol. Aging 28, 845–855.

Maher, F.O., Nolan, Y., Lynch, M.A., 2005. Down-regulation of IL-4-induced signalling in hippocampus contributes to deficits in LTP in the aged rat. Neurobiol. Aging 26, 717–728.

Martin, D.S., Lonergan, P.E., Boland, B., Fogarty, M.P., Brady, M., Horrobin, D.F., Campbell, V.A., Lynch, M.A., 2002. Apoptotic changes in the aged brain are triggered by interleukin-1beta-induced activation of p38 and reversed by treatment with eicosapentaenoic acid. J. Biol. Chem. 277, 34239–34246.

McGahon, B., Maguire, C., Kelly, A., Lynch, M.A., 1999. Activation of p42 mitogen-activated protein kinase by arachidonic acid and *trans*-1-amino-cyclopentyl-1,3-dicarboxylate impacts on long-term potentiation in the dentate gyrus in the rat: analysis of age-related changes. Neuroscience 90, 1167–1175.

Minogue, A.M., Schmid, A.W., Fogarty, M.P., Moore, A.C., Campbell, V.A., Herron, C.E., Lynch, M.A., 2003. Activation of the c-Jun N-terminal kinase signaling cascade mediates the effect of amyloid-beta on long-term potentiation and cell death in hippocampus: a role for interleukin-1beta? J. Biol. Chem. 278, 27971–27980.

Minogue, A.M., Lynch, A.M., Loane, D.J., Herron, C.E., Lynch, M.A., 2007. Modulation of amyloid-beta-induced and age associated changes in rat hippocampus by eicosapentaenoic acid. J. Neurochem., in press.

Moreno, S., Farioli-Vecchioli, S., Ceru, M.P., 2004. Immunolocalization of peroxisome proliferator-activated receptors and retinoid X receptors in the adult rat CNS. Neuroscience 123, 131–145.

Nolan, Y., Maher, F.O., Martin, D.S., Clarke, R.M., Brady, M.T., Bolton, A.E., Mills, K.H., Lynch, M.A., 2005. Role of interleukin-4 in regulation of age-related inflammatory changes in the hippocampus. J. Biol. Chem. 280, 9354–9362.

Park, E.J., Park, S.Y., Joe, E.H., Jou, I., 2003. 15d-PGJ2 and rosiglitazone suppress Janus kinase-STAT inflammatory signaling through induction of suppressor of cytokine signaling 1 (SOCS1) and SOCS3 in glia. J. Biol. Chem. 278, 14747–14752.

Park, K.S., Lee, R.D., Kang, S.K., Han, S.Y., Park, K.L., Yang, K.H., Song, Y.S., Park, H.J., Lee, Y.M., Yun, Y.P., Oh, K.W., Kim, D.J., Yun, Y.W., Hwang, S.J., Lee, S.E., Hong, J.T., 2004. Neuronal differentiation of embryonic midbrain cells by upregulation of peroxisome proliferator-activated receptor-gamma via the JNK-dependent pathway. Exp. Cell Res. 297, 424–433.

Pedersen, W.A., McMillan, P.J., Kulstad, J.J., Leverenz, J.B., Craft, S., Haynatzki, G.R., 2006. Rosiglitazone attenuates learning and memory deficits in Tg2576 Alzheimer mice. Exp. Neurol. 199, 265–273.

Petrova, T.V., Akama, K.T., Van Eldik, L.J., 1999. Cyclopentenone prostaglandins suppress activation of microglia: down-regulation of inducible nitric-oxide synthase by 15-deoxy-Delta12,14-prostaglandin J2. Proc. Natl. Acad. Sci. U.S.A. 96, 4668–4673.

Ricote, M., Li, A.C., Willson, T.M., Kelly, C.J., Glass, C.K., 1998. The peroxisome proliferator-activated receptor-gamma is a negative regulator of macrophage activation. Nature 391, 79–82.

Risner, M.E., Saunders, A.M., Altman, J.F., Ormandy, G.C., Craft, S., Foley, I.M., Zvartau-Hind, M.E., Hosford, D.A., Roses, A.D., 2006. Efficacy of rosiglitazone in a genetically defined population with mild-to-moderate Alzheimer's disease. Pharmacogenom. J. 6, 246–254.

Smith, P., Dunne, D.W., Fallon, P.G., 2001. Defective in vivo induction of functional type 2 cytokine responses in aged mice. Eur. J. Immunol. 31, 1495–1502.

Strum, J.C., Shehee, R., Virley, D., Richardson, J., Mattie, M., Selley, P., Ghosh, S., Nock, C., Saunders, A., Roses, A., 2007. Rosiglitazone induces mitochondrial biogenesis in mouse brain. J. Alzheimer's Dis. 11, 45–51.

Sundararajan, S., Gamboa, J.L., Victor, N.A., Wanderi, E.W., Lust, W.D., Landreth, G.E., 2005. Peroxisome proliferator-activated receptor-gamma ligands reduce inflammation and infarction size in transient focal ischemia. Neuroscience 130, 685–696.

Ujiie, M., Dickstein, D.L., Carlow, D.A., Jefferies, W.A., 2003. Blood–brain barrier permeability precedes senile plaque formation in an Alzheimer disease model. Microcirculation 10, 463–470.

Wada, K., Nakajima, A., Katayama, K., Kudo, C., Shibuya, A., Kubota, N., Terauchi, Y., Tachibana, M., Miyoshi, H., Kamisaki, Y., Mayumi, T., Kadowaki, T., Blumberg, R.S., 2006. Peroxisome proliferator-activated receptor gamma-mediated regulation of neural stem cell proliferation and differentiation. J. Biol. Chem. 281, 12673–12681.

Wang, Q., Walsh, D.M., Rowan, M.J., Selkoe, D.J., Anwyl, R., 2004. Block of long-term potentiation by naturally secreted and synthetic amyloid beta-peptide in hippocampal slices is mediated via activation of the kinases c-Jun N-terminal kinase, cyclin-dependent kinase 5, and p38 mitogen-activated protein kinase as well as metabotropic glutamate receptor type 5. J. Neurosci. 24, 3370–3378.

Watson, G.S., Cholerton, B.A., Reger, M.A., Baker, L.D., Plymate, S.R., Asthana, S., Fishel, M.A., Kulstad, J.J., Green, P.S., Cook, D.G., Kahn, S.E., Keeling, M.L., Craft, S., 2005. Preserved cognition in patients with early Alzheimer's disease and amnestic mild cognitive impairment during treatment with rosiglitazone: a preliminary study. Am. J. Geriatr. Psychiatry 13, 950–958.

Zhao, Y., Patzer, A., Herdegen, T., Gohlke, P., Culman, J., 2006. Activation of cerebral peroxisome proliferator-activated receptors gamma promotes neuroprotection by attenuation of neuronal cyclooxygenase-2 overexpression after focal cerebral ischemia in rats. FASEB J. 20, 1162–1175.

Brain, Behavior, and Immunity 23 (2009) 1020–1027

Contents lists available at ScienceDirect

Brain, Behavior, and Immunity

journal homepage: www.elsevier.com/locate/ybrbi

Decreased neuronal CD200 expression in IL-4-deficient mice results in increased neuroinflammation in response to lipopolysaccharide

Anthony Lyons [a,*], Keith McQuillan [a,b], Brian F. Deighan [a], Julie-Ann O'Reilly [a], Eric J. Downer [a,1], Aine C. Murphy [a,b], Melanie Watson [a], Alessia Piazza [a], Florence O'Connell [a], Rebecca Griffin [a], Kingston H.G. Mills [b], Marina A. Lynch [a]

[a] Trinity College Institute for Neuroscience, Trinity College, Dublin 2, Ireland
[b] School of Biochemistry and Immunology, Trinity College, Dublin 2, Ireland

ARTICLE INFO

Article history:
Received 26 February 2009
Received in revised form 19 May 2009
Accepted 30 May 2009
Available online 6 June 2009

Keywords:
IL-4
IL-1β
IL-6
CD200
Microglial activation
CD40
Sickness behaviour

ABSTRACT

Maintenance of the balance between pro- and anti-inflammatory cytokines in the brain, which is affected by the activation state of microglia, is important for maintenance of neuronal function. Evidence has suggested that IL-4 plays an important neuromodulatory role and has the ability to decrease lipopolysaccharide-induced microglial activation and the production of IL-1β. We have also demonstrated that CD200–CD200R interaction is involved in immune homeostasis in the brain. Here, we investigated the anti-inflammatory role of IL-4 and, using *in vitro* and *in vivo* analysis, established that the effect of lipopolysaccharide was more profound in IL-4$^{-/-}$, compared with wildtype, mice. Intraperitoneal injection of lipopolysaccharide exerted a greater inhibitory effect on exploratory behaviour in IL-4$^{-/-}$, compared with wildtype, mice and this was associated with evidence of microglial activation. We demonstrate that the increase in microglial activation is inversely related to CD200 expression. Furthermore, CD200 was decreased in neurons prepared from IL-4$^{-/-}$ mice, whereas stimulation with IL-4 enhanced CD200 expression. Importantly, neurons prepared from wildtype, but not from IL-4$^{-/-}$, mice attenuated the lipopolysaccharide-induced increase in pro-inflammatory cytokine production by glia. These findings suggest that the neuromodulatory effect of IL-4, and in particular its capacity to maintain microglia in a quiescent state, may result from its ability to upregulate CD200 expression on neurons.

1. Introduction

Neuroinflammatory changes, characterized by microglial activation and increased production of pro-inflammatory mediators, have been reported in the brain of aged animals (Lynch et al., 2007; Lyons et al., 2007b) and in animal models of Alzheimer's disease and Parkinson's disease (Chen et al., 2005; McGeer and McGeer, 1998). Similar changes occur following treatment of rats with amyloid-β (Aβ) or lipopolysaccharide (LPS; Clarke et al., 2007; Lyons et al., 2007b; Nolan et al., 2005) and in these experimental conditions, there is a deterioration in neuronal function with specific evidence of an inverse correlation between hippocampal concentration of the pro-inflammatory cytokine, interleukin-1β (IL-1β), and ability of rats to sustain long-term potentiation (LTP) (Maher et al., 2005).

In aged rodents, the reported increase in hippocampal concentration of IL-1β is accompanied by a decrease in IL-4 (Lynch et al., 2007; Maher et al., 2005) and, similarly, the age-related increase in IL-6 (Ye and Johnson, 1999) is accompanied by a decrease in release of the anti-inflammatory cytokine IL-10 from brain slices (Ye and Johnson, 2001). While IL-10 suppresses synthesis of pro-inflammatory cytokines in brain (Strle et al., 2001), IL-4 decreases IL-1β mRNA synthesis and IL-1β release from glia (Loane et al., 2009; Lynch et al., 2007). IL-4 also attenuates the Aβ-induced increase in markers of microglia, MHC class II, CD86 and ICAM expression and hippocampal concentrations of IL-1β and TNFα (Clarke et al., 2007; Lyons et al., 2007b). These data are consistent with the demonstration that IL-4 modulates microglial activation (Benveniste et al., 2004), whether stimulated by LPS or TNFα (Iribarren et al., 2005; Kitamura et al., 2000; Zhao et al., 2006). The inhibitory effects of IL-4 on TNFα-induced expression in microglial cells have been attributed to its stimulating effect on ERK (Iribarren et al., 2005), however, our findings suggest that the modulatory effect of IL-4 on microglial activation is driven by its ability to increase in CD200 expression (Lyons et al., 2007a). CD200 is a glycoprotein that is expressed on the surface of neurons and other cells and interacts with its receptor, CD200R, which is

* Corresponding author. Address: Trinity College Institute for Neuroscience, Trinity College, Physiology Department, College Green, Dublin 2, Ireland. Fax: +353 1 8963183.
E-mail address: lyonsan@tcd.ie (A. Lyons).
[1] Present address: Institute of Immunology, Department of Biology, National University of Ireland, Maynooth, Maynooth, Co. Kildare, Ireland.

0889-1591/$ - see front matter © 2009 Elsevier Inc. All rights reserved.
doi:10.1016/j.bbi.2009.05.060

expressed on cells of the myeloid lineage, including microglia (Barclay et al., 2002). Engagement of CD200R has been shown to contribute to the maintenance of microglia in a quiescent state (Lyons et al., 2007a). Consistent with this, an activated macrophage/microglial phenotype was observed in CD200$^{-/-}$ mice following facial nerve transection, in collagen-induced arthritis (Hoek et al., 2000) and in experimental autoimmune uveoretinitis (Broderick et al., 2002).

Since there are significant anti-inflammatory roles for CD200 and IL-4 in the central nervous system, we sought to further explore these roles. We investigated the effect of LPS on glia prepared from wildtype and IL-4$^{-/-}$ mice and compared the effects of intraperitoneal administration of LPS on inflammatory responses in hippocampus of wildtype and IL-4$^{-/-}$ mice. We found that the effect of LPS *in vitro* and *in vivo* was more profound in IL-4$^{-/-}$ mice and that exploratory behaviour was affected to a greater extent in IL-4$^{-/-}$ mice. The findings, coupled with evidence of microglial activation in the hippocampus of IL-4$^{-/-}$ mice, suggest that the effect of IL-4 may be attributed to the decrease in expression of CD200.

2. Materials and methods

2.1. Animals

C57BL/6 mice (6–7 weeks old) were purchased from Harlan UK Ltd. IL-4-defective (IL-4$^{-/-}$) mice were originally purchased from B&K Universal, UK and were bred under SPF conditions. Animals had free access to food and water, were housed in groups of 3–6 in a controlled environment (temperature: 20–22 °C; 12:12 h light/dark cycle) and maintained under veterinary supervision for the duration of the experiment. For *in vitro* experiments, one-day-old rats or mice were used. All experiments were carried out under a licence from the Department of Health and Children (Ireland) and with ethical approval from Trinity College Ethical Committee.

In one series of experiments, wildtype and IL-4$^{-/-}$ mice were injected intraperitoneally (i.p.) with LPS (50 μg/mouse) and after 4 h animals were killed, the brains were rapidly removed and hippocampus and cortex dissected free and stored as described for later analysis (Lyons et al., 2007a). In a parallel study, LPS-treated and control-treated animals were assessed for evidence of sickness behaviour and for exploratory behaviour in the open field.

2.2. Preparation of cells

Primary cortical glial cells and neurons were prepared from one-day-old C57BL/6 and IL-4$^{-/-}$ mice or from one-day-old rats as previously described (Lyons et al., 2007a). Briefly, cortical tissue was chopped, incubated for 5 min in 5% CO_2 at 37 °C in warm filter-sterilized Dulbecco's Modified Eagle Medium (DMEM; Sigma–Aldrich, UK) supplemented with penicillin (100 μl/ml; Gibco, UK), streptomycin (100 μl/ml; Gibco, UK) and FBS (10% w/v; Gibco, UK). A single cell suspension was prepared by triturating tissue, filtering though a 50 μl sterile nylon mesh filter (BD Biosciences, USA), centrifuging at 2000*g* for 3 min at 20 °C, and resuspending the pellet 1 ml warm filter-sterilized culture media. Tissue was triturated and resuspended glia were counted, equal numbers of cells were plated onto poly-L-lysine-coated coverslips and incubated for 2 h in 5% CO_2 at 37 °C to allow the cells to adhere. After 2 h the cells were flooded with 400 μl warm filter-sterilized culture media and incubated for 3 days in 5% CO_2 at 37 °C. Culture media was replaced with fresh culture media every 3 days for 12–14 days until cells were ready for treatments. In this mixed glial culture, between 70% and 80% of cells were astrocytes and the remainder were microglia which is consistent with previous reports (Cao et al., 2007).

To prepare neurons, cortices were incubated in PBS containing trypsin (0.25%, Gibco, UK) for 20 min at 37 °C, tissue was triturated in PBS containing Trypsin inhibitor (0.1%, Sigma, UK) and DNase (0.2 mg/ml, Sigma, UK), filtered though a sterile mesh filter and centrifuged (2000*g* for 5 min at 20 °C). The pellet was resuspended in neurobasal medium (NBM) supplemented with heat-inactivated horse serum (10% v/v, Sigma, UK), penicillin (100 μl/ml, Gibco, UK), streptomycin (100 μl/ml, Gibco, UK), glutamax (2 mM; Sigma, UK) and the anti-oxidant B27 (1% w/v; Gibco, UK) and cells (1.5×10^6) were plated in T25 flasks and incubated in a humidified atmosphere containing 5% CO_2 at 37 °C for 2 h prior to being flooded with pre-warmed NBM. After 48 h, cytosine arabinofuranoside (5 ng/ml; Sigma, UK) was included in the cell medium to prevent the proliferation of non-neuronal cells. Culture media was exchanged every 3 days and cells were grown in culture for about 12 days.

In one series of experiments, rat glial cells were co-treated with neurons and LPS (100 ng/ml); primary neuronal cells were added in suspension in DMEM in a ratio of 1:8 neurons:glia and after 24 h, supernatant was taken and frozen for later analysis. In another series of experiments, we assessed the effect of blocking CD200 ligand:receptor interaction by including a blocking CD200 antibody (5 μg/ml, Serotec); neurons were incubated in the presence or absence of an anti-CD200 or an isotype control (5 μg/ml, Santa Cruz) for 4 h and then added to glia in a co-treatment regime in the presence or absence of LPS. After 24 h, supernatant was taken and frozen for later analysis.

In another series of experiments, mouse glial cells were incubated with or without LPS (100 ng/ml), and in the presence of neurons prepared from wildtype mice or neurons prepared from IL-4$^{-/-}$ mice; neurons were added in suspension in DMEM at a ratio of 1:8 neurons:glia, and after 24 h, supernatant was taken and frozen for later analysis.

2.3. Analysis of cytokines by ELISA

The concentrations of IL-1β, IL-6 and TNFα were assessed in samples of supernatant prepared from cultured glia and in samples of hippocampal homogenate prepared from control-treated and LPS-treated wildtype and IL-4$^{-/-}$ mice; the methods used have been described in detail elsewhere (Lyons et al., 2007a). Briefly, stored hippocampal slices were thawed, rinsed, homogenized in ice-cold Krebs solution and equalized for protein concentrations (Bradford, 1976). Standards or samples (100 μl) of this homogenate and of supernatant prepared from cultured cells were added to 96-well plates. Plates were coated with goat anti-rat IL-1β antibody, (100 μl; 1 μg/ml in PBS containing 1% BSA, pH 7.3; R&D Systems), rat anti-mouse IL-1β antibody (100 μl; 4 μg/ml in PBS containing 0.1% BSA, pH 7.3; R&D Systems), rat anti-mouse TNFα and rat anti-mouse IL-6 (100 μl; 0.8 μg/ml for TNFα, 1 μg/ml for IL-6 (BD Pharmigen, USA), incubated overnight, washed and incubated for 1 h with assay diluent (300 μl; PBS containing 1% BSA, and 0.05% NaN_3, or PBS containing 10% FBS for IL-6 and TNFα). After washing in PBS, triplicate samples and standards (100 μl; 0–1000 pg/nl, recombinant rat IL-1β and recombinant mouse IL-1β, or 0–2000 pg/ml recombinant mouse TNFα, or 0–5000 pg/ml recombinant mouse IL-6) were added, incubation proceeded for 2 h and samples were washed and incubated for 2 h in the presence of detection antibody (100 μl; 350 ng/ml biotinylated goat anti-rat IL-1β in PBS containing 1% BSA, 400 ng/ml biotinylated rat anti-mouse IL-1β in PBS containing 0.1% BSA, 150 ng/ml biotinylated rat anti-mouse TNF-α or 1 μg/ml biotinylated rat anti-mouse IL-6 diluted in 1% BSA). Detection reagent (100 μl; HRP conjugated streptavidin; 1:200 dilution in PBS containing 1% BSA for anti-rat IL-1β, 1:200 dilution in PBS containing 0.1% BSA for anti-mouse IL-1β or 1:250 dilution assay diluent for IL-6 and TNFα) was added,

incubation continued for 20 min, samples were washed and substrate solution (100 µl; 1:1 mixture of H_2O_2 and tetramethylbenzidine) was added. Samples were incubated in the dark for 20–30 min and the reaction was stopped using 50 µl 1 M H_2SO_4. Plates were read at 450 nm and cytokine concentrations were estimated from the appropriate standard curve and expressed as pg/mg protein for homogenate and pg/ml for supernatants.

2.4. Analysis of IL-1β, CD40 and CD200 mRNA

To assess IL-1β, CD40 and CD200 mRNA expression, a PCR mastermix was prepared containing Taqman Universal PCR Mastermix (Applied Biosystems, Darmstadt, Germany), mouse β-actin RNA and rat β-actin as the endogenous controls (Applied Biosystems, Darmstadt, Germany) and specific primers for the target genes (TaqMan® Gene Expression Assays, Applied Biosystems, Darmstadt, Germany; IL-1β, Mm00434228_m1; CD200 Mm004877 40_m1; CD40, Mm0041895_m1; IL-1β Rn00580432_m1). cDNA was diluted (2 µl cDNA and 8 µl RNA-free H_20) and added in triplicate to wells in a 96-well plate. Mastermix for the target genes (15 µl) was added to each well giving a total reaction volume of (25 µl/well) and concentration of cDNA as (200 pg/well). Plates were centrifuged at 2000g for 1 min and real-time PCR was performed. The PCR consisted of 40 cycles with the following conditions: 2 min at 50 °C, 10 min at 95 °C and for each cycle 15 s at 95 °C for denaturation and 1 min at 60 °C for transcription and to ensure complete extension of the PCR product (7300 real-time PCR system, Applied Biosystems, US). IL-1β, CD40 and CD200 mRNA was determined using the efficiency-corrected comparative CT method and compared with β-actin, the values were normalized to an endogenous control and the relative differences between samples were expressed as a ratio. Values are expressed as relative quantities of specific genes (7300 real-time PCR software, Applied Biosystems, US).

2.5. Analysis of behaviour

Wildtype and IL-4$^{-/-}$ mice were either injected i.p. with LPS (200 µl, 50 µg/ml) or sterile saline (200 µl) and were assessed for clinical signs of sickness behaviour prior to, and 3 h after, LPS injection (Kentner et al., 2007; Nemzek et al., 2004). In brief sickness behaviour was evaluated according to signs which include animal appearance, food and water intake, natural behaviour and provoked behaviour. Mice were removed from the home cage and assessed before and after saline or LPS administration. A score of 0 was assigned to animals which exhibited 'normal' behaviour and a score of 3 to animals exhibiting a substantial deviation from normal behaviour (Kentner et al., 2007; Nemzek et al., 2004). If a score of 3 was attained more than once, an extra point was allotted. In this study, a maximum score of 20 could be attained and an overall score of 0–4 indicated normal behaviour; 5–9 required careful monitoring and possible analgesic treatment; 10–14 indicated suffering; 15–20 indicated severe distress; the maximum mean score in this study was <10.

To determine exploratory behaviour, mice were released into the same side of the outer corner of a square (60 cm width × 60 cm length × 43 cm height; marked in a 5 × 5 grid) open field arena for 3 min in a noise-, light- and temperature-controlled room. Individual mice were videotaped with a camera mounted on the ceiling circa 2 m above the centre of the floor of the open field. Activity was recorded using a video camera and advanced motion-recognition software package (Mediacruise Software, Canopus Corporation, UK). The total distance moved and the time spent in the 16 border squares compared with the nine centre zone squares was analysed. A single trial was carried out prior to saline or LPS administration and two further trials were carried out 2 and 4 h after injection.

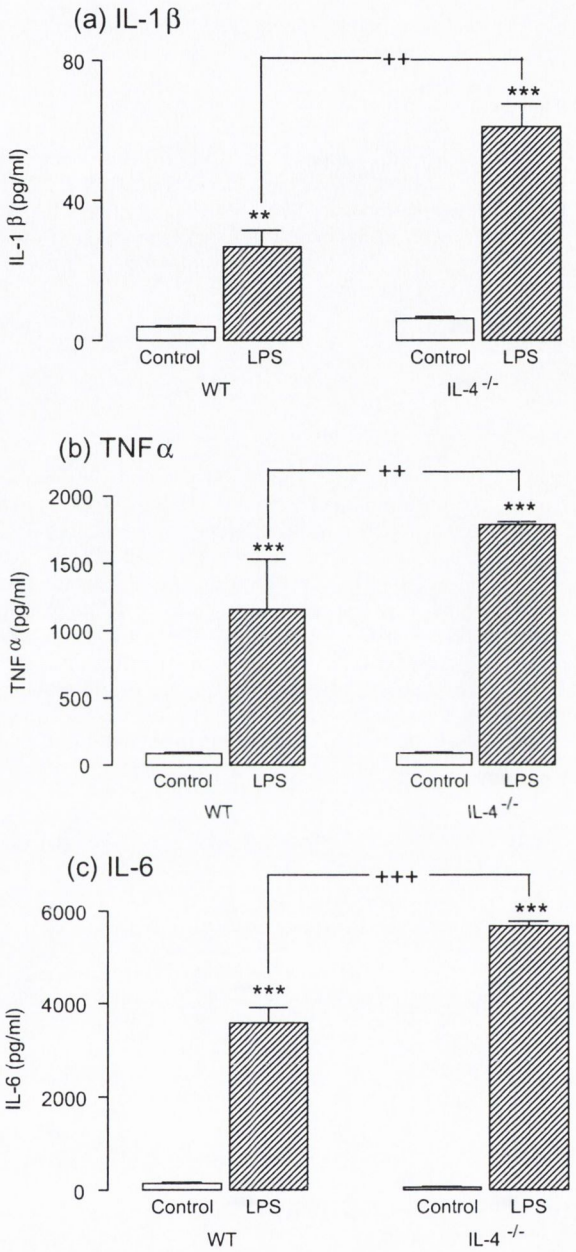

Fig. 1. IL-4$^{-/-}$ mice exhibit enhanced LPS-induced inflammatory cytokine production *in vitro*. LPS (1 µg/ml) significantly increased IL-1β (a), TNFα (b) and IL-6 (c) in mixed glia prepared from wildtype and IL-4$^{-/-}$ mice ($^{**}p < 0.01$; $^{**}p < 0.001$; ANOVA; $n = 4–8$; LPS vs respective control); the effect was significantly greater in cells prepared from IL-4$^{-/-}$ mice ($^{**}p < 0.01$; $^{+++}p < 0.001$; ANOVA; LPS in IL-4$^{-/-}$ mice vs LPS in wildtype mice).

2.6. CD200 immunofluorescent staining

Cultured cells (on cover slips) were fixed in ice-cold ethanol, blocked with 10% goat serum and incubated overnight at 4 °C with mouse monoclonal CD200 antibody (1:200; Abcam plc, UK). Cover slips were washed and incubated with Alexa 488 secondary antibody (1:4000; CD200, Molecular Probes Inc., UK), washed and mounted (Vectashield, Vector Laboratories, UK). Samples were viewed by confocal microscopy (Zeiss Ltd., UK). Negative control experiments were performed by replacing the primary antibody

with a mouse IgG antibody (Santa Cruz Biotechnology, US) and using equal gain settings during acquisition and analysis.

2.7. Statistical analysis

Data were analysed, as appropriate, using either Student's t-test for independent means, or analysis of variance (ANOVA) followed by post-hoc Student Newman–Keuls test to determine which conditions were significantly different from each other. Data are expressed as means ± SEM, where the *n* values represent the number of observations per treatment group.

3. Results

3.1. Enhanced LPS-induced inflammatory cytokine in the hippocampus and in glia from IL-4$^{-/-}$ mice

We assessed the effect of LPS on mixed glia prepared from wildtype and IL-4$^{-/-}$ mice and show that, while LPS increased IL-1β, TNFα and IL-6 in cells prepared from wildtype mice ($F(3, 18) = 47.65$, $p < 0.01$; $F(3, 19) = 50.41$, $p < 0.001$; $F(3, 46) = 84.22$, $p < 0.001$, respectively; Fig. 1), the effect of LPS was significantly greater in cells prepared from IL-4$^{-/-}$, compared with wildtype, mice ($F(3, 18) = 47.65$, $p < 0.01$; $F(3, 19) = 50.41$, $p < 0.01$; $F(3, 46) = 84.22$, $p < 0.001$, respectively). In addition to this effect, i.p. injection of LPS led to a significant increase in IL-1β concentration in hippocampal and cortical homogenates ($F(3, 79) = 8.22$, $p < 0.05$; $F(3, 23) = 10.94$, $p < 0.05$; Fig. 2a and b) and the LPS-induced change in tissue prepared from IL-4$^{-/-}$ mice was significantly greater than that in wildtype mice ($F(3, 79) = 8.22$, $p < 0.05$; $F(3, 23) = 10.94$, $p < 0.01$; Fig. 2a and b). Unstimulated cortical IL-1β concentration was significantly greater in IL-4$^{-/-}$, compared with wildtype mice ($F(3, 23) = 10.94$, $p < 0.05$).

3.2. Enhanced sickness behaviour and reduced exploratory behaviour in LPS-treated IL-4$^{-/-}$ mice

It has been suggested that the key factor triggering sickness behaviour is IL-1β and here we demonstrate that LPS (50 μg/mouse) induced sickness behaviour in wildtype and IL-4$^{-/-}$ mice ($F(11, 50) = 38.33$, $p < 0.001$; ANOVA; pre- vs post-injection of LPS in both groups of mice; $n = 8$; Fig. 2c) but that the effect was significantly greater in IL-4$^{-/-}$ mice ($F(11, 50) = 38.33$, $p < 0.001$). Analysis of the exploratory behaviour of control-treated and LPS-treated wildtype and IL-4$^{-/-}$ mice revealed that the distance covered by all animals was similar in the first trial (i.e., pre-injection of LPS) but decreased in the second and third trials compared with the first ($F(11, 56) = 20.50$, $p < 0.001$; Fig. 2d). Exploratory behaviour was not significantly affected by LPS in wildtype mice, but it was significantly decreased in IL-4$^{-/-}$ mice ($F(11, 56) = 20.50$, $p < 0.001$; for control-treated vs LPS-treated IL-4$^{-/-}$ mice). The mean time spent in the outer zone (i.e., within 12 cm of the walls of the open field) was significantly greater during trials 2 and 3 in LPS-treated IL-4$^{-/-}$ mice compared with trials 2 and 3 in control-treated IL-4$^{-/-}$ mice ($F(7, 56) = 93.61$, $p < 0.001$; Fig. 2e), and compared with trials 2 and 3 in both groups of wildtype mice.

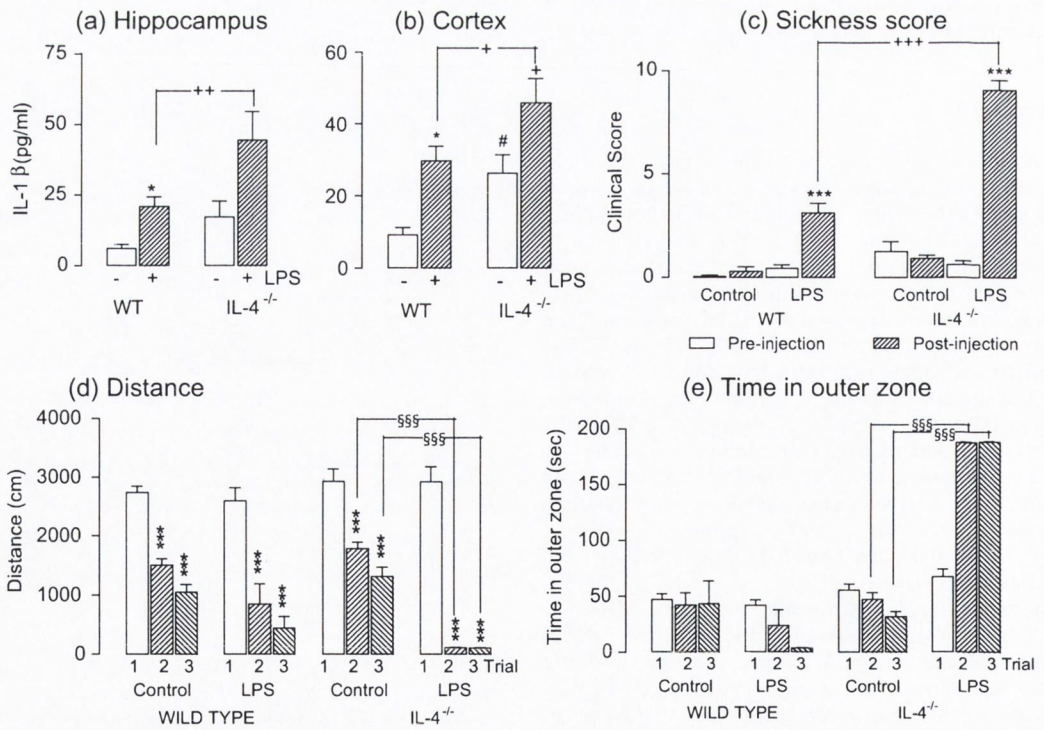

Fig. 2. IL-4$^{-/-}$ mice exhibit enhanced LPS-induced inflammatory cytokine production and sickness behaviour *in vivo*. Intraperitoneal injection of LPS significantly increased IL-1β concentration in hippocampal (a) and cortical (b) tissue prepared from wildtype and IL-4$^{-/-}$ mice ($^{*}p < 0.05$; ANOVA; $n = 12$); the effect was significantly greater in tissue prepared from IL-4$^{-/-}$ mice ($^{*}p < 0.05$; $^{**}p < 0.01$; ANOVA; LPS in IL-4$^{-/-}$ mice vs LPS in wildtype mice). Basal cortical IL-1β concentration was significantly greater in IL-4$^{-/-}$, compared with wildtype mice ($^{\#}p < 0.05$; ANOVA). (c) LPS significantly increased the clinical score for sickness behaviour in wildtype and IL-4$^{-/-}$ mice ($^{***}p < 0.001$; ANOVA; pre-injection vs post-injection) and it was significantly greater in LPS-treated IL-4$^{-/-}$ mice compared with LPS-treated wildtype mice ($^{***}p < 0.001$; ANOVA; $n = 8$). (d) Exploratory behaviour was decreased in all animals with familiarity (i.e., in trials 2 and 3 compared with trial 1; $^{***}p < 0.001$; ANOVA; $n = 8$), but whereas the effect of LPS (50 μg/mouse) was minimal in wildtype mice, it significantly reduced exploration in IL-4$^{-/-}$ mice ($^{§§§}p < 0.001$; ANOVA). (e) Time spend in the outer zone of the open field was significantly increased in LPS-treated IL-4$^{-/-}$, compared with wildtype mice ($^{§§§}p < 0.001$; ANOVA).

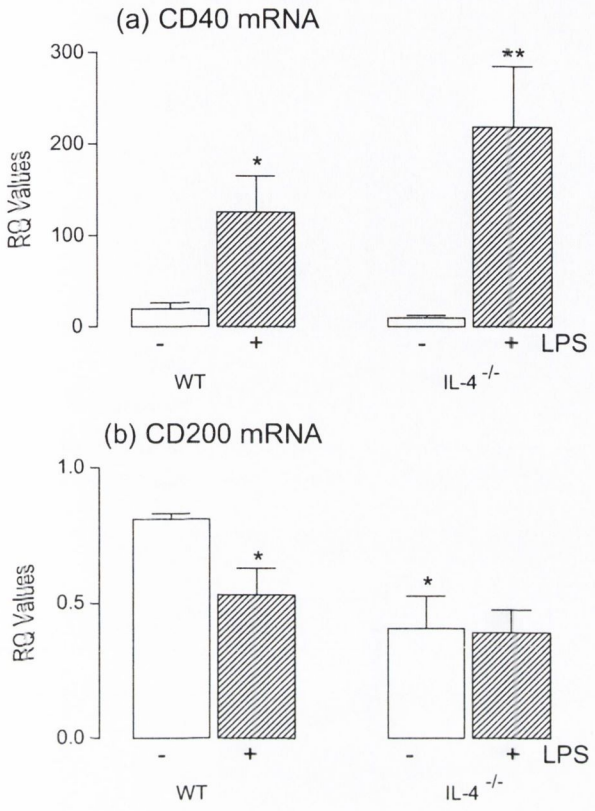

Fig. 3. Enhanced LPS-induced inflammation in IL-4$^{-/-}$ mice correlates with a reduced expression of CD200 *in vivo*. Intraperitoneal injection of LPS significantly increased CD40 mRNA (a) and significantly decreased CD200 mRNA (b) in hippocampus prepared from wildtype and IL-4$^{-/-}$ mice ($^{*}p < 0.05$; $^{**}p < 0.01$; ANOVA; $n = 6$). CD200 mRNA was also significantly reduced in tissue prepared control-treated IL-4$^{-/-}$, compared with wildtype, mice ($^{*}p < 0.05$; ANOVA; $n = 5$).

3.3. Enhanced LPS-induced CD40 and decreased CD200 expression in microglia from IL-4$^{-/-}$ mice

The LPS-induced increase in IL-1β was accompanied by a significant increase in microglial activation as revealed by upregulation of CD40 mRNA in hippocampal tissue prepared from wildtype mice ($F(3, 16) = 6.935$, $p < 0.05$; Fig. 3a) and this effect was more pronounced in tissue prepared from IL-4$^{-/-}$ mice ($F(3, 16) = 6.935$, $p < 0.01$). Previous evidence coupled an increase in microglial activation with a decrease in CD200 (Lyons et al., 2007a) and the data presented here provide support for this; Fig. 3b shows that LPS significantly decreased CD200 mRNA expression in tissue prepared from wildtype mice ($F(3, 11) = 4.736$, $p < 0.05$), and that CD200 expression was also significantly decreased in tissue prepared from IL-4$^{-/-}$, compared with wildtype mice ($F(3, 11) = 4.736$, $p < 0.05$). There was no significant difference in CD200 mRNA expression observed between control and LPS-treated IL-4$^{-/-}$ mice.

3.4. Neurons attenuate LPS-induced pro-inflammatory cytokine production by glia through CD200

To further explore the roles of CD200 and IL-4 in modulating microglial activation, cultured glia were incubated in the presence and absence of LPS and in the presence and absence of neurons, which express CD200; LPS significantly increased IL-1β mRNA ($F(3, 12) = 5.814$, $p < 0.01$; Fig. 4a) and addition of neurons significantly attenuated the LPS-induced change ($F(3, 12) = 5.814$, $p < 0.05$). In a separate experiment, we found that the attenuating effect of neurons on the LPS-induced increase in IL-1β protein was partially inhibited by including anti-CD200 antibody during incubation; thus LPS significantly increased IL-1β ($F(6, 56) = 67.35$, $p < 0.001$; Fig. 4b) and this effect was attenuated by addition of neurons ($F(6, 56) = 67.35$, $p < 0.001$; LPS + neurons vs LPS alone), and the further addition of the anti-CD200 antibody blocked the action of the neurons ($F(6, 56) = 67.35$, $p < 0.001$; LPS + neurons vs LPS + neurons + anti-CD200; Fig. 4b), however, addition of an isotype control did not block the action of neurons ($F(6, 56) = 67.35$, $p < 0.001$; LPS + neurons + isotype control vs LPS + neurons + anti-CD200), thus showing the specificity of the anti-CD200 antibody in blocking CD200–CD200R interaction. Similarly, LPS increased TNFα and IL-6 ($F(6, 39) = 36.32$, $p < 0.001$; $F(6, 54) = 34.28$, $p < 0.001$; Fig. 4c and d, respectively); addition of neurons partially attenuated these changes ($F(6, 39) = 36.32$, $p < 0.001$; $F(6, 54) = 34.28$, $p < 0.001$; LPS + neurons vs LPS alone), and the further addition of anti-CD200 antibody reversed the effect of neurons ($F(6, 39) = 36.32$, $p < 0.001$; $F(6, 54) = 34.28$, $p < 0.001$; LPS + neurons vs LPS + neurons + anti-CD200; TNFα and IL-6, respectively).

Consistent with our previously-reported studies (Lyons et al., 2007a), we found that CD200 expression was decreased on neurons prepared from IL-4$^{-/-}$ mice, as shown by a significant decrease in relative fluorescent intensity ($p = 0.0003$, unpaired Students' t-test; Fig. 5a). Because of the importance of CD200 in attenuating the effect of LPS, we argued that the effect of neurons prepared from IL-4$^{-/-}$ mice would be reduced compared with neurons prepared from wildtype mice. Consistent with this, the data in Fig. 5b–d show that the LPS-induced increases in IL-1β, TNFα and IL-6 ($F(5, 38) = 31.88$, $p < 0.001$; $F(5, 30) = 57.55$, $p < 0.001$; $F(5, 37) = 86.83$, $p < 0.001$; respectively) were significantly attenuated by addition of neurons prepared from wildtype mice ($F(5, 38) = 31.88$, $p < 0.001$; $F(5, 30) = 57.55$, $p < 0.01$; $F(5, 37) = 86.83$, $p < 0.01$; LPS + neurons vs LPS alone, for IL-1β, TNFα and IL-6, respectively) but not by neurons prepared from IL-4$^{-/-}$ mice ($F(5, 38) = 31.88$, $p < 0.001$; $F(5, 30) = 57.55$, $p < 0.05$; $F(5, 37) = 86.83$, $p < 0.01$).

4. Discussion

The results of this study demonstrate that IL-4 plays a critical role in controlling microglial activation and that this is mediated through modulation of CD200 expression. The TLR4 agonist, LPS, is a potent activator of innate immune cells, including glia and it has been reported that LPS can induce IL-1β and NO secretion by cultured glia (Costelloe et al., 2008; Loane et al., 2009; Molina-Holgado et al., 2000). Here, we found that LPS-induced production of the pro-inflammatory cytokines IL-1β, TNFα and IL-6 by mixed glia cells from C57BL/6 mice, but that this was significantly potentiated in glia from IL-4$^{-/-}$ mice. Furthermore, peripheral administration of LPS-induced IL-1β expression in the hippocampus and cortex which was significantly enhanced in IL-4$^{-/-}$, compared with wildtype, mice. It has previously been reported that IL-4 can downregulate IL-1β production by cultured mixed glial cultures and that intracerebroventricular injection of IL-4 inhibits the increase in hippocampal IL-1β concentration in LPS-treated, Aβ-treated and in aged rats (Loane et al., 2009; Lynch et al., 2007; Lyons et al., 2007b; Minogue et al., 2007). Taken together with the data of this study, these findings suggest that IL-4 is a major negative regulator of pro-inflammatory cytokine production by neuronal cells *in vitro* and *in vivo* and may have a key function in controlling neuroinflammation.

Sickness behaviour has been shown to result from an increase in pro-inflammatory cytokine concentration in the brain (Dantzer and Kelley, 2007; Laye et al., 1994; van Dam et al., 1992).

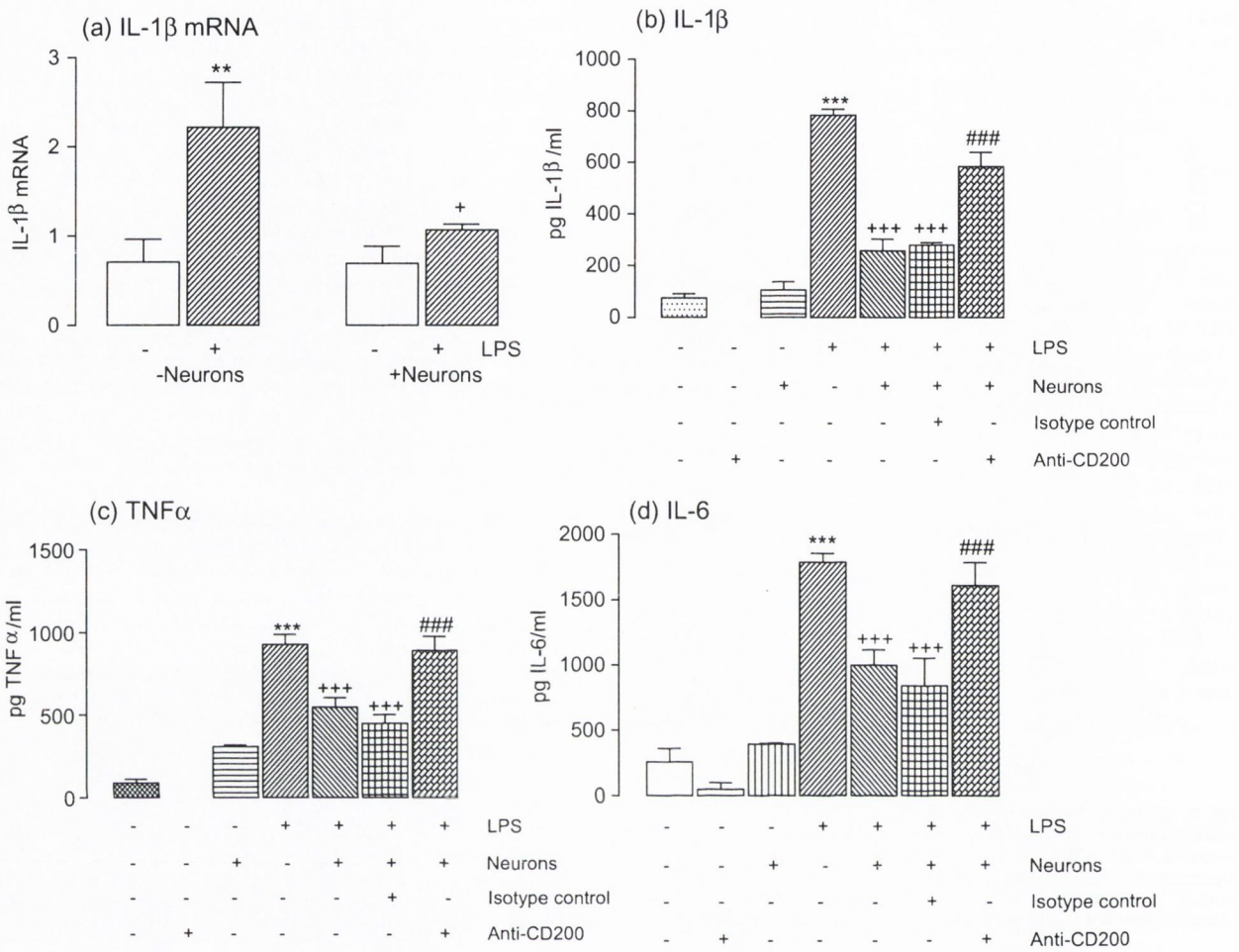

Fig. 4. Neurons attenuate LPS-induced pro-inflammatory cytokine production by glia through CD200. LPS significantly increased IL-1β mRNA (a) in glia ($^{**}p < 0.01$; ANOVA; $n = 4$). The LPS-induced effect was attenuated in the presence of neurons ($^{+}p < 0.05$; ANOVA; LPS + neurons vs LPS alone; $n = 6$). A second experiment demonstrated an LPS-induced increase in IL-1β (b), TNFα (c) and IL-6 (d; $^{***}p < 0.001$; $n = 10$) and the modulating effect of neurons which decreased the LPS-induced change ($^{+++}p < 0.001$; ANOVA; LPS + neurons vs LPS alone; $n = 10$). Incubation in the presence of anti-CD200 antibody significantly attenuated the modulating effect of neurons ($^{\#}p < 0.05$; $^{\#\#}p < 0.01$; ANOVA; LPS + neurons vs LPS + neurons + anti-CD200; $n = 10$). Substitution of anti-CD200 with an isotype control antibody demonstrated the specificity of the interaction between CD200 and CD200R ($n = 5$).

In this study, the LPS-induced increase in hippocampal and cortical concentrations of IL-1β was accompanied by decreased motor activity, which is one of the features of sickness behaviour. Importantly, LPS exerted a greater inhibitory effect on exploratory behaviour in IL-$4^{-/-}$, compared with wildtype, mice. This is consistent with the greater effect of LPS on cytokine production in IL-$4^{-/-}$ mice and with the hypothesis that anti-inflammatory cytokines can modulate the intensity of sickness behaviour. It has been demonstrated that pretreatment of rats with IL-4 intracerebroventricularly, blocked LPS-induced sickness behaviour (Bluthe et al., 2002). It has also been demonstrated that IL-10 can attenuate LPS-induced sickness behaviour (Leon et al., 1999) and that LPS-induced sickness behaviour is exacerbated in IL-$10^{-/-}$ mice (Dantzer et al., 2008). Furthermore, both IL-4 and IL-10 can attenuate the LPS-induced increases in microglial activation and pro-inflammatory cytokine production, and can reverse the LPS-induced defect in LTP (Lynch et al., 2007; Nolan et al., 2004). Thus, IL-4 alone or in combination with IL-10 may play a central role in controlling sickness behaviour induced by LPS through induction of pro-inflammatory cytokines in the brain.

Activated microglia are thought to be the primary source of inflammatory cytokines (Benveniste, 1992) although they are also released from other cells, especially astrocytes. Here, we show that the LPS-induced increase in pro-inflammatory cytokines was accompanied by an increased in expression of CD40 mRNA, which is a marker of activated microglia (Benveniste et al., 2004). We found that LPS-induced CD40 expression is exacerbated in IL-$4^{-/-}$ mice, suggesting that endogenous IL-4 can modulate microglial activation, and this is consistent with the observation that IL-4 can attenuate the increase in microglial activation observed in aged rats (Lynch et al., 2007) as well as Aβ- and IFNγ-treated rats (Clarke et al., 2007; Lyons et al., 2007b). IL-4 also modulates macrophage function and regulates production of several mediators that are integral to their function, including the pro-inflammatory cytokines IL-1, TNF-α, and IL-6 (Huang et al., 1999). While LPS enhanced CD40, it decreased CD200 expression on glia, and the extent of change was greater in tissue prepared from IL-$4^{-/-}$, compared with wildtype, mice. This inverse relationship between CD40 and CD200 provides support for recent evidence of an inverse relationship between CD200 and other markers of microglia activation, including MHCII, ICAM-1 and CD86 in aged rats and in

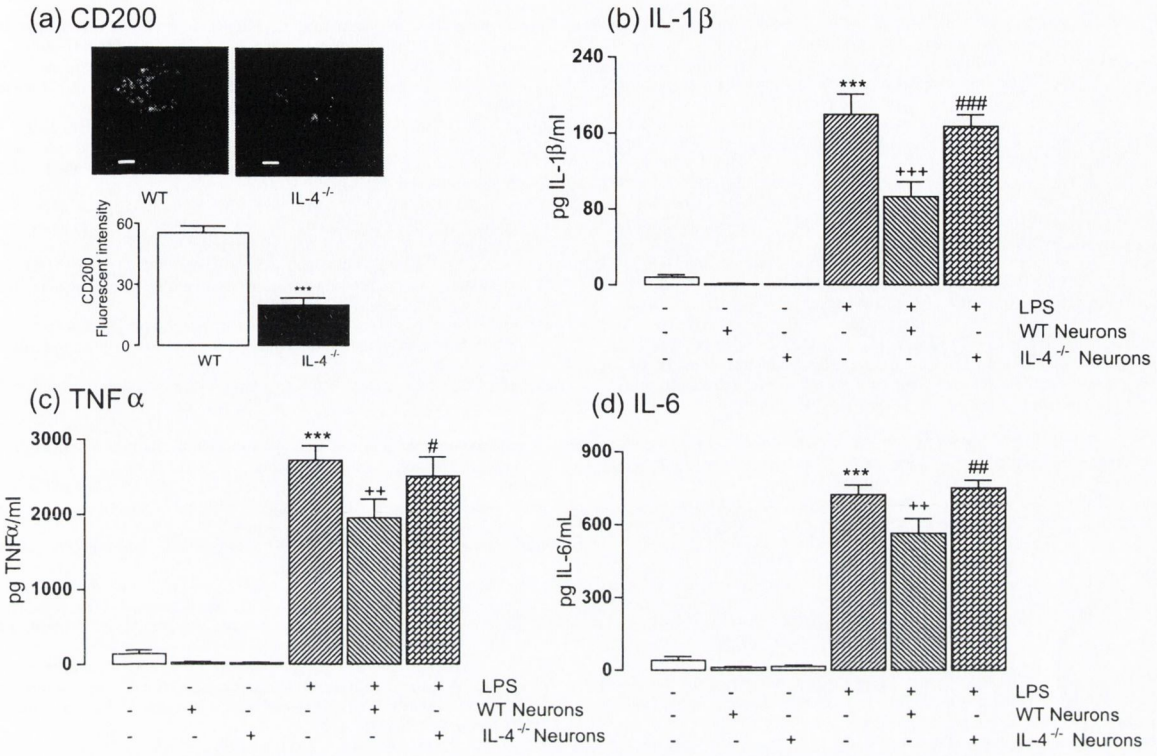

Fig. 5. IL-4 mediated neuronal expression of CD200 is required to attenuate LPS-induced pro-inflammatory cytokine production by glia. (a) CD200 was decreased in neurons prepared from IL-4$^{-/-}$ compared with wildtype, mice. The fluorescent image is representative of four independent experiments. LPS significantly increased IL-1β (b), TNFα (c) and IL-6 (d; $^{***}p < 0.001$; $n = 10$), addition of neurons prepared from wildtype mice attenuated the LPS-induced changes ($^{++}p < 0.01$; $^{+++}p < 0.001$; ANOVA; LPS + neurons vs LPS alone; $n = 6$). However, addition of neurons prepared from IL-4$^{-/-}$ mice failed to attenuate the LPS-induced changes and there was a significant difference between cytokine concentrations in glia incubated in the presence of neurons obtained from IL-4$^{-/-}$, compared with wildtype mice ($^{\#}p < 0.05$; $^{\#\#}p < 0.01$; $^{\#\#\#}p < 0.001$; ANOVA; LPS + neurons from IL-4$^{-/-}$ mice vs LPS + neurons from wildtype mice; $n = 10$).

animals treated with Aβ (Downer et al., 2009; Frank et al., 2006; Lyons et al., 2007a). Preliminary evidence suggests that, as in the case of CD200$^{-/-}$ mice (Hoek et al., 2000), microglial activation is enhanced in brain of IL-4$^{-/-}$, compared with wildtype mice, although we have not found any change in the numbers of MHCII-positive cells in IL-4$^{-/-}$ mice (Lyons et al., unpublished). Interestingly, decreased expression of CD200 ligand and protein has been reported in Alzheimer's disease and is associated with disease pathology, and with specific evidence of marked changes in the hippocampus and inferior temporal gyrus correlating with plaque deposition (Walker et al., 2009). Thus, there is growing evidence that downregulation of CD200 is associated with inflammatory changes and these findings are consistent with the original proposal of a significant immunomodulatory role for CD200 (Hoek et al., 2000; Wright et al., 2000; Frank et al., 2007).

Since CD200 is expressed on neurons, interaction with CD200R on microglia may therefore reduce their activation. Here, we show that addition of neurons to LPS-activated microglia attenuated the increases in IL-1β, IL-6 and TNF. This is consistent with the inhibitory effect of neurons on Aβ-induced glial cell activation (Lyons et al., 2007a). Interestingly however, the effect of neurons on glial release of IL-6 and TNFα was less marked than the effect on IL-1β; the reason for this is unclear at this time, but may result from proportionally greater release of these cytokines (compared with IL-1β) from astrocytes, which have not been reported to express CD200R.

It has been shown that CD200 expression on neurons is enhanced by IL-4 (Downer et al., 2009; Lyons et al., 2007a) and here we confirm this and demonstrate that CD200 was decreased in neurons prepared from IL-4$^{-/-}$ mice. Interestingly, the decreased CD200 expression which accompanies development of Alzheimer's disease is associated with a decrease in expression of IL-4 (Walker et al., 2009) and consistent with our data, this study suggested a modulatory effect of IL-4 on CD200. The importance of neuronal-derived IL-4 in controlling microglial activation was supported by the finding that, while neurons prepared from wildtype mice attenuate the LPS-triggered release of IL-1β, TNFα and IL-6, neurons from IL-4$^{-/-}$ mice failed to do so.

Maintenance of the balance between pro- and anti-inflammatory cytokines in the brain is central to regulation of neuronal function (Dantzer et al., 2008; Maher et al., 2005). The data presented here indicate that a key role for IL-4 is in the regulation of expression of CD200 on neurons which, by interaction with its receptor, determines the activation state of microglia and consequently, production of inflammatory mediators. Our findings that LPS induces a significantly greater neuroinflammatory change in cells and tissue prepared from the brain IL-4$^{-/-}$ mice compared with wildtype mice, suggest that IL-4 plays an important role in maintaining glial cells in a quiescent state.

Acknowledgments

This work was supported by grants obtained from Science Foundation Ireland, The Health Research Board (Ireland) and the EU.

References

Barclay, A.N., Wright, G.J., Brooke, G., Brown, M.H., 2002. CD200 and membrane protein interactions in the control of myeloid cells. Trends Immunol. 23, 285–290.

Benveniste, E.N., 1992. Inflammatory cytokines within the central nervous system: sources, function, and mechanism of action. Am. J. Physiol. 263, C1–C16.

Benveniste, E.N., Nguyen, V.T., Wesemann, D.R., 2004. Molecular regulation of CD40 gene expression in macrophages and microglia. Brain Behav. Immun. 18, 7–12.
Bluthe, R.M., Lestage, J., Rees, G., Bristow, A., Dantzer, R., 2002. Dual effect of central injection of recombinant rat interleukin-4 on lipopolysaccharide-induced sickness behavior in rats. Neuropsychopharmacology 26, 86–93.
Bradford, M.M., 1976. A rapid and sensitive method for the quantitation of microgram quantities of protein utilizing the principle of protein–dye binding. Anal. Biochem. 72, 248–254.
Broderick, C., Hoek, R.M., Forrester, J.V., Liversidge, J., Sedgwick, J.D., Dick, A.D., 2002. Constitutive retinal CD200 expression regulates resident microglia and activation state of inflammatory cells during experimental autoimmune uveoretinitis. Am. J. Pathol. 161, 1669–1677.
Cao, L., Fei, L., Chang, T.T., DeLeo, J.A., 2007. Induction of interleukin-1beta by interleukin-4 in lipopolysaccharide-treated mixed glial cultures: microglial-dependent effects. J. Neurochem. 102, 408–419.
Chen, Z., Duan, R.S., Lepecheur, M., Paly, E., London, J., Zhu, J., 2005. SOD-1 inhibits FAS expression in cortex of APP transgenic mice. Apoptosis 10, 499–502.
Clarke, R.M., O'Connell, F., Lyons, A., Lynch, M.A., 2007. The HMG-CoA reductase inhibitor, atorvastatin, attenuates the effects of acute administration of amyloid-beta1–42 in the rat hippocampus in vivo. Neuropharmacology 52, 136–145.
Costelloe, C., Watson, M., Murphy, A., McQuillan, K., Loscher, C., Armstrong, M.E., Garlanda, C., Mantovani, A., O'Neill, L.A., Mills, K.H., Lynch, M.A., 2008. IL-1F5 mediates anti-inflammatory activity in the brain through induction of IL-4 following interaction with SIGIRR/TIR8. J. Neurochem. 105, 1960–1969.
Dantzer, R., Kelley, K.W., 2007. Twenty years of research on cytokine-induced sickness behavior. Brain Behav. Immun. 21, 153–160.
Dantzer, R., O'Connor, J.C., Freund, G.G., Johnson, R.W., Kelley, K.W., 2008. From inflammation to sickness and depression: when the immune system subjugates the brain. Nat. Rev. Neurosci. 9, 46–56.
Downer, E.J., Cowley, T.R., Lyons, A., Mills, K.H., Berezin, V., Bock, E., Lynch, M.A., 2009. A novel anti-inflammatory role of NCAM-derived mimetic peptide, FGL. Neurobiol. Aging, in press..
Frank, M.G., Baratta, M.V., Sprunger, D.B., Watkins, L.R., Maier, S.F., 2007. Microglia serve as a neuroimmune substrate for stress-induced potentiation of CNS pro-inflammatory cytokine responses. Brain Behav. Immun. 21, 47–59.
Frank, M.G., Barrientos, R.M., Biedenkapp, J.C., Rudy, J.W., Watkins, L.R., Maier, S.F., 2006. MRNA up-regulation of MHC II and pivotal pro-inflammatory genes in normal brain aging. Neurobiol. Aging 27, 717–722.
Hoek, R.M., Ruuls, S.R., Murphy, C.A., Wright, G.J., Goddard, R., Zurawski, S.M., Blom, B., Homola, M.E., Streit, W.J., Brown, M.H., Barclay, A.N., Sedgwick, J.D., 2000. Down-regulation of the macrophage lineage through interaction with OX2 (CD200). Science 290, 1768–1771.
Huang, W.X., Huang, P., Link, H., Hillert, J., 1999. Cytokine analysis in multiple sclerosis by competitive RT-PCR: a decreased expression of IL-10 and an increased expression of TNF-alpha in chronic progression. Mult. Scler. 5, 342–348.
Iribarren, P., Chen, K., Hu, J., Zhang, X., Gong, W., Wang, J.M., 2005. IL-4 inhibits the expression of mouse formyl peptide receptor 2, a receptor for amyloid beta1–42, in TNF-alpha-activated microglia. J. Immunol. 175, 6100–6106.
Kentner, A.C., James, J.S., Miguelez, M., Bielajew, C., 2007. Investigating the hedonic effects of interferon-alpha on female rats using brain-stimulation reward. Behav. Brain Res. 177, 90–99.
Kitamura, Y., Taniguchi, T., Kimura, H., Nomura, Y., Gebicke-Haerter, P.J., 2000. Interleukin-4-inhibited mRNA expression in mixed rat glial and in isolated microglial cultures. J. Neuroimmunol. 106, 95–104.
Laye, S., Parnet, P., Goujon, E., Dantzer, R., 1994. Peripheral administration of lipopolysaccharide induces the expression of cytokine transcripts in the brain and pituitary of mice. Brain Res. Mol. Brain Res. 27, 157–162.
Leon, L.R., Kozak, W., Rudolph, K., Kluger, M.J., 1999. An antipyretic role for interleukin-10 in LPS fever in mice. Am. J. Physiol. 276, R81–R89.
Loane, D.J., Deighan, B.F., Clarke, R.M., Griffin, R.J., Lynch, A.M., Lynch, M.A., 2009. Interleukin-4 mediates the neuroprotective effects of rosiglitazone in the aged brain. Neurobiol Aging. 30, 920–931.
Lynch, A.M., Loane, D.J., Minogue, A.M., Clarke, R.M., Kilroy, D., Nally, R.E., Roche, O.J., O'Connell, F., Lynch, M.A., 2007. Eicosapentaenoic acid confers neuroprotection in the amyloid-beta challenged aged hippocampus. Neurobiol. Aging 28, 845–855.
Lyons, A., Downer, E.J., Crotty, S., Nolan, Y.M., Mills, K.H., Lynch, M.A., 2007a. CD200 ligand receptor interaction modulates microglial activation in vivo and in vitro: a role for IL-4. J. Neurosci. 27, 8309–8313.
Lyons, A., Griffin, R.J., Costelloe, C.E., Clarke, R.M., Lynch, M.A., 2007b. IL-4 attenuates the neuroinflammation induced by amyloid-beta in vivo and in vitro. J. Neurochem. 101, 771–781.
Maher, F.O., Nolan, Y., Lynch, M.A., 2005. Downregulation of IL-4-induced signalling in hippocampus contributes to deficits in LTP in the aged rat. Neurobiol. Aging 26, 717–728.
McGeer, E.G., McGeer, P.L., 1998. The importance of inflammatory mechanisms in Alzheimer disease. Exp. Gerontol. 33, 371–378.
Minogue, A.M., Lynch, A.M., Loane, D.J., Herron, C.E., Lynch, M.A., 2007. Modulation of amyloid-beta-induced and age-associated changes in rat hippocampus by eicosapentaenoic acid. J. Neurochem. 103, 914–926.
Molina-Holgado, F., Toulmond, S., Rothwell, N.J., 2000. Involvement of interleukin-1 in glial responses to lipopolysaccharide: endogenous versus exogenous interleukin-1 actions. J. Neuroimmunol. 111, 1–9.
Nemzek, J.A., Xiao, H.Y., Minard, A.E., Bolgos, G.L., Remick, D.G., 2004. Humane endpoints in shock research. Shock 21, 17–25.
Nolan, Y., Maher, F.O., Martin, D.S., Clarke, R.M., Brady, M.T., Bolton, A.E., Mills, K.H., Lynch, M.A., 2005. Role of interleukin-4 in regulation of age-related inflammatory changes in the hippocampus. J. Biol. Chem. 280, 9354–9362.
Nolan, Y., Martin, D., Campbell, V.A., Lynch, M.A., 2004. Evidence of a protective effect of phosphatidylserine-containing liposomes on lipopolysaccharide-induced impairment of long-term potentiation in the rat hippocampus. J. Neuroimmunol. 151, 12–23.
Strle, K., Zhou, J.H., Shen, W.H., Broussard, S.R., Johnson, R.W., Freund, G.G., Dantzer, R., Kelley, K.W., 2001. Interleukin-10 in the brain. Crit. Rev. Immunol. 21, 427–449.
van Dam, A.M., Brouns, M., Louisse, S., Berkenbosch, F., 1992. Appearance of interleukin-1 in macrophages and in ramified microglia in the brain of endotoxin-treated rats: a pathway for the induction of non-specific symptoms of sickness? Brain Res. 588, 291–296.
Walker, D.G., Dalsing-Hernandez, J.E., Campbell, N.A., Lue, L.F., 2009. Decreased expression of CD200 and CD200 receptor in Alzheimer's disease: a potential mechanism leading to chronic inflammation. Exp. Neurol. 215, 5–19.
Wright, G.J., Puklavec, M.J., Willis, A.C., Hoek, R.M., Sedgwick, J.D., Brown, M.H., Barclay, A.N., 2000. Lymphoid/neuronal cell surface OX2 glycoprotein recognizes a novel receptor on macrophages implicated in the control of their function. Immunity 13, 233–242.
Ye, S.M., Johnson, R.W., 1999. Increased interleukin-6 expression by microglia from brain of aged mice. J. Neuroimmunol. 93, 139–148.
Ye, S.M., Johnson, R.W., 2001. An age-related decline in interleukin-10 may contribute to the increased expression of interleukin-6 in brain of aged mice. Neuroimmunomodulation 9, 183–192.
Zhao, W., Xie, W., Xiao, Q., Beers, D.R., Appel, S.H., 2006. Protective effects of an anti-inflammatory cytokine, interleukin-4, on motoneuron toxicity induced by activated microglia. J. Neurochem. 99, 1176–1187.

THE JOURNAL OF BIOLOGICAL CHEMISTRY VOL. 283, NO. 4, pp. 1808–1817, January 25, 2008

A Pivotal Role for Interleukin-4 in Atorvastatin-associated Neuroprotection in Rat Brain*

Received for publication, September 5, 2007, and in revised form, October 31, 2007 Published, JBC Papers in Press, November 2, 2007, DOI 10.1074/jbc.M707442200

Rachael M. Clarke[‡], Anthony Lyons[‡1], Florence O'Connell[‡1], Brian F. Deighan[‡1], Claire E. Barry[‡], Ngozi G. Anyakoha[§], Anna Nicolaou[§], and Marina A. Lynch[‡2]

From the [‡]Trinity College Institute for Neuroscience, Physiology Department, Trinity College, Dublin 2, Ireland and the [§]School of Pharmacy, University of Bradford, Bradford BD7 DP, United Kingdom

Inflammatory changes, characterized by an increase in pro-inflammatory cytokine production and up-regulation of the corresponding signaling pathways, have been described in the brains of aged rats and rats treated with the potent immune modulatory molecule lipopolysaccharide (LPS). These changes have been coupled with a deficit in long-term potentiation (LTP) in hippocampus. The evidence suggests that anti-inflammatory agents, which attenuate the LPS-induced and age-associated increase in hippocampal interleukin-1β (IL-1β) concentration, lead to restoration of LTP. Here we report that atorvastatin, a member of the family of agents that act as inhibitors of 3-hydroxy-3-methylglutaryl-CoA reductase, exerts powerful anti-inflammatory effects in brain and that these effects are mediated by IL-4 and independent of its cholesterol-lowering actions. Treatment of rats with atorvastatin increased IL-4 concentration in hippocampal tissue prepared from LPS-treated and aged rats and abrogated the age-related and LPS-induced increases in pro-inflammatory cytokines, interferon-γ (IFNγ) and IL-1β, and the accompanying deficit in LTP. The effect of atorvastatin on the LPS-induced increases in IFNγ and IL-1β was absent in tissue prepared from IL-4$^{-/-}$ mice. The increase in IL-1β in LPS-treated and aged rats is associated with increased microglial activation, assessed by analysis of major histocompatibility complex II expression, and the evidence suggests that IFNγ may trigger this activation. We propose that the primary effect of atorvastatin is to increase IL-4, which antagonizes the effects of IFNγ, the associated increase in microglial activation, and the subsequent cascade of events.

The adverse effects of inflammation in the brain have been shown to include down-regulation of synaptic function. One manifestation of this is a decrease in the ability of rats to sustain long-term potentiation (LTP),[3] a form of synaptic plasticity that is considered to be a potential biological substrate for learning and/or memory. Inflammatory changes, typified by an increase in concentration of the pro-inflammatory cytokine, interleukin-1β (IL-1β), have been observed in aged rats (1, 2) and in rats treated with lipopolysaccharide (LPS (3, 4)) or β-amyloid peptides (Aβ (5)). In each of these conditions, LTP is impaired and, in some cases, the impairment is abrogated by strategies that restore IL-1β concentration to the lower values observed in control conditions (4). A role for IL-4 in modulating IL-1β production has been demonstrated (6), and we have observed that two treatments with anti-inflammatory properties, the polyunsaturated fatty acid, eicosapentaenoic acid (6) and rosiglitazone,[4] abrogate age- and LPS-induced neuroinflammation by increasing IL-4 concentration in hippocampus. These data highlight the potential of anti-inflammatory treatments to restore functional deficits associated with inflammation and draw an interesting parallel with the observation that the incidence of Alzheimer disease is reduced in individuals undergoing anti-inflammatory treatments for other conditions (7).

It seems likely that the increase in IL-1β concentration in the brain in inflammatory conditions is derived from activated microglia, and therefore parallel changes in IL-1β concentration and microglial activation have been identified in brain of aged and LPS-treated rats (8). However, the trigger leading to activation of microglia has not been identified, although results from several studies have suggested that one of the most potent activators of microglia *in vitro* is interferon-γ (IFNγ (9–11)).

Recent work has identified anti-inflammatory properties of 3-hydroxy-3-methylglutaryl coenzyme A reductase inhibitors (*i.e.* statins) that are distinct from their ability to lower cholesterol. It has been shown that statins reduce Aβ deposition and inflammatory changes in mouse models of Alzheimer disease (12–14), block paralysis in chronic and relapsing experimental autoimmune encephalomyelitis (15), reduce infarct size in ischemia, and improve neurologic outcome by directly up-regulating brain endothelial nitric-oxide synthase (16). Statins have also been shown to decrease symptoms and mortality in stroke-prone spontaneously hypertensive rats (17).

Because of their reported anti-inflammatory effects, it might be predicted that statins will counteract the inflammatory changes induced by age and by LPS treatment. To test this prediction, we investigated the effect of atorvastatin treatment on the age-related and LPS-induced changes in rat hippocampus. We report that the age- and LPS-associated microglial activation, increase in concentrations of IFNγ and IL-1β, and deficit

* The costs of publication of this article were defrayed in part by the payment of page charges. This article must therefore be hereby marked "*advertisement*" in accordance with 18 U.S.C. Section 1734 solely to indicate this fact.

[1] These authors contributed equally to the work.

[2] To whom correspondence should be addressed. Tel.: 353-1-608-1770; Fax: 353-1-679-3545; E-mail: lynchma@tcd.ie.

[3] The abbreviations used are: LTP, long-term potentiation; IL-1, interleukin-1; Aβ, β-amyloid peptide; IFNγ, interferon-γ; BSA, bovine serum albumin; MHCII, major histocompatibility complex II; JNK, c-Jun NH_2-terminal kinase; TBS, Tris-buffered saline; ANOVA, analysis of variance; LPS, lipopolysaccharide; EPSP, excitatory postsynaptic potential.

[4] Loane, D. J., Deighan, B. F., Clarke, R. M., Griffin, R. J., Lynch, A. M., and Lynch, M. A. (2007) *Neurobiol. Aging*, in press.

in LTP were abrogated in atorvastatin-treated rats. Because atorvastatin failed to attenuate the LPS-induced increases in cytokine concentrations in tissue prepared from IL-$4^{-/-}$ mice, we propose that the primary action of atorvastatin may be to trigger production of IL-4 and thereby prevent the IFNγ-induced microglial activation.

EXPERIMENTAL PROCEDURES

Animals—Twenty-four, 2- to 3-month-old male Wistar rats (BioResources Unit, Trinity College, Dublin, Ireland), were used in the first study, and 18 aged (22–24 months) and 12 young (3–4 months) animals (Bantham and Kingman, UK) were used in the second study. We also used 24 2- to 5-month-old C57BL/6 (Harlan UK Ltd.) and C57BL/6 IL-4-defective (IL-$4^{-/-}$) mice (B&K Universal, UK). Rats were housed in groups of 2–6, and mice were housed singly, under a 12-h light schedule. Ambient temperature was controlled between 22 and 23 °C, and animals were maintained under veterinary supervision throughout the study. These experiments were performed under a license issued by the Department of Health (Ireland) and with ethical approval from the local ethical review group.

Atorvastatin Treatment Regimen—Food and water intake was assessed daily for 1 week, and animals were then randomly assigned to a control treatment or atorvastatin treatment group. Atorvastatin (5 and 10 mg/kg/day in the case of rats and mice, respectively; Lipitor, Pfizer-Parke Davis, Ireland) was given orally for 3 weeks in the laboratory chow. In the first and third studies, the control- and atorvastatin-treated groups of rats and mice were subsequently subdivided into those that received saline intraperitoneally and those that received LPS (100 μg/kg *Escherichia coli* serotype 0111.B4, Sigma-Aldrich, UK) intraperitoneally on the day of the experiment. In the second study, young and aged rats were subdivided into control- and atorvastatin-treated groups, and treatment continued for 8 weeks. Rats and mice were given their daily allowance of food and monitored to ensure that they received their full daily dose of atorvastatin. Animals were weighed at intervals throughout the study to ensure that similar weight changes were occurring in the different treatment groups. At the end of the treatment period, mice were killed by cervical dislocation, the brain was rapidly removed, dissected on ice, sliced (350 × 350μ m) using a McIlwain tissue chopper, and stored in Krebs buffer containing $CaCl_2$ (1.13 mM) and 10% Me_2SO at −80 °C as previously described (1) until required for analysis. Rats were assessed for their ability to sustain LTP.

Induction of LTP in Vivo—Young rats were anesthetized by intraperitoneal injection of urethane (1.5 g/kg), and aged rats were initially given 1.2 g/kg urethane with further increments to a maximum of 2.0 g/kg when required. The absence of a pedal reflex was considered to be an indicator of deep anesthesia. In the case of the experiments in which the effect of atorvastatin was assessed on LPS-induced changes, LPS (100 μg/kg, Sigma, UK) or saline was injected intraperitoneally and 3 h later animals were assessed for their ability to sustain LTP. In some experiments rats were injected intracerebroventricularly (2.5 mm posterior, and 0.5 mm lateral, to Bregma) with IFNγ (50 ng/ml, 5 μl, Chemicon International, Inc.), IL-4 (20 ng/ml, 5 μl, R&D Systems, UK) or both, and 30 min later these rats were assessed for their ability to sustain LTP in perforant path-granule cell synapses as described previously (1). Briefly, a bipolar-stimulating electrode and a unipolar-recording electrode were stereotaxically positioned in the perforant path (4.4 mm lateral to lambda) and dorsal cell body region of the dentate gyrus (3.9 mm posterior, and 2.5 mm lateral, to Bregma), respectively. Test shocks were delivered at 30-s intervals, and recorded for 10 min before and 45 min after tetanic stimulation. The stimulation paradigm used involved delivery of 3 trains of stimuli (250 Hz for 200 ms) with an intertrain interval of 30 s, which has been shown to induce saturable LTP in perforant path-granule cell synapses in young adult rats (18); this stimulation paradigm has revealed a deficit in LTP in aged rats.

At the end of the recording period, rats were killed by decapitation, the brains were rapidly removed, and the hippocampus was dissected. One-third of the hippocampus was flash-frozen in liquid N_2 for later analysis of mRNA (see below), and slices (350 × 350 μm) were prepared from the rest of the tissue using a McIlwain tissue chopper. These slices were stored in Krebs buffer containing $CaCl_2$ (1.13 mM) and 10% Me_2SO at −80 °C as previously described (1) until required for analysis. Cortical tissue was similarly prepared and stored for later analysis of cholesterol.

Analysis of IL-1β, IFN-γ, and IL-4—The concentrations of IL-1β, IFNγ, and IL-4 were assessed by enzyme-linked immunosorbent assay (R&D Systems, UK) in the stored hippocampal slices prepared from rats (2). IFNγ and IL-1β concentrations were also assessed in tissue prepared from wild-type and IL-$4^{-/-}$ mice. Slices were thawed, rinsed, homogenized, and equalized for protein (19). For analysis of rat tissue the following antibodies were used to coat 96-well plates; 1.0 μg/ml goat anti-rat IL-1β antibody (R&D Systems, UK), or 2.0 μg/ml mouse anti-rat IFNγ antibody, or 2.0 μg/ml mouse anti-rat IL-4 antibody (diluted in phosphate-buffered saline, pH 7.3). For analysis of tissue prepared from mice, 1.25 μg/ml goat anti-mouse IFNγ antibody (BIOSOURCE, UK) or 4 μg/ml goat anti-mouse IL-1β antibody (R&D Systems, UK) were used. Plates were incubated overnight at room temperature, washed, blocked, and incubated with standards (0–1000 pg/ml) or samples for 2 h at room temperature. Wells were washed and incubated with the following antibodies: 350 ng/ml biotinylated goat anti-rat antibody for IL-1β, 150 ng/ml biotinylated goat anti-rat antibody for IFNγ, or 50 ng/ml biotinylated goat anti-rat antibody for IL-4, each diluted in phosphate-buffered saline containing 1% BSA and 2% normal goat serum, or 100 ng/ml biotinylated goat anti-mouse IL-1β antibody, and 125 ng/ml biotinylated goat anti-mouse IFNγ antibody (R&D Systems, UK). Horseradish peroxidase-conjugated streptavidin (1:200) and substrate solution (1:1 mixture of H_2O_2 and tetramethylbenzidine) were added, incubation continued in the dark for 20–30 min, and the reaction was stopped using 1 M H_2SO_4. Absorbance was read at 450 nm, and values were corrected for protein in the case of homogenates and expressed as picograms/mg of protein.

Analysis of Expression of MHCII—We assessed OX6 mRNA expression as an indicator of MHCII. Total RNA was extracted from hippocampal tissue using TRI reagent (Sigma), reverse transcription-PCR was undertaken (5), and cDNA synthesis

was performed on 1 μg of total RNA using oligo(dT) primers (Superscript reverse transcriptase; Invitrogen Ltd., UK). Equal amounts of cDNA were used for PCR amplification for a total of 30 cycles, and the following sequences of primers were used: upstream 5′-CAG TCA CAG AAG GCG TTT ATG-3′; downstream, 5′-TGC AGC ATC TGA CAG CAG GA-3′; and for rat β-actin mRNA expression: upstream, 5′-AGA AGA GCT ATG AGC TGC CTG AGG-3′; downstream, 5′-CTT CTG CAT CCT GTC AGC GAT GC-3′. The cycling conditions were 95 °C for 300 s, 65 °C for 60 s, and 72 °C for 120 s. The reaction was stopped by a final extension at 72 °C for 10 min. These primers generated OX-6 PCR products at 245 bp and β-actin PCR products at 250 bp. Equal volumes of PCR product from each sample were loaded onto 1.5% agarose gels, and bands were separated by application of 90 V, photographed, and quantified using densitometry. The target genes were normalized to β-actin mRNA expression (*i.e.* the housekeeping gene). No change in β-actin mRNA was observed with treatment.

Western Immunoblot Analysis of JNK, c-Jun, p38, and NFκB—Phosphorylation of JNK, c-Jun, p38, and NFκB was analyzed in samples prepared from hippocampal tissue as described for analysis of JNK phosphorylation (20); JNK phosphorylation was assessed in nuclear and cytosolic fractions and c-Jun phosphorylation, p38, and NFκB activation in nuclear fractions only. The cytosolic fraction was prepared by homogenizing hippocampal slices in lysis buffer (composition in mM: 20 HEPES, pH 7.4, 10 KCl, 1.5 $MgCl_2$, 1 EDTA, 1 EGTA, 1 dithiothreitol, 0.1 phenylmethylsulfonyl fluoride, containing pepstatin A (5 μg/ml), leupeptin (2 μg/ml), and aprotinin (2 μg/ml)), incubating for 20 min on ice, and centrifuging (15,000 × *g* for 10 min at 4 °C). The supernatant (*i.e.* cytosolic fraction) was suspended in sample buffer (Tris-HCl, 150 mM, pH 6.8; glycerol 10% v/v; SDS, 4% w/v; β-mercaptoethanol, 5% v/v; bromphenol blue, 0.002% w/v) to a final concentration of 300 μg/ml, boiled for 3 min, and loaded (10 μg/lane) onto 10% SDS gels. The nuclear fraction was prepared by homogenizing hippocampal slices in Krebs solution containing 2 mM $CaCl_2$, incubating for 15 min on ice in permeabilization buffer (composition: 70 mM KCl, 250 mM sucrose, 137 mM NaCl, 4.5 mM Na_2HPO_4, 1.4 mM KH_2PO_4, 100 μM phenylmethylsulfonyl fluoride, 10 μg/ml leupeptin, 2 μg/ml aprotinin, 200 μg/ml digitonin) and centrifuging (600 × *g* for 15 min at 4 °C). The pellet (*i.e.* nuclear fraction) was resuspended in sample buffer (Tris-HCl, 150 mM, pH 6.8; glycerol 10% v/v; SDS, 4% w/v; β-mercaptoethanol, 5% v/v; bromphenol blue, 0.002% w/v) to a final concentration of 10 μg/ml, boiled for 3 min, and loaded onto 10% SDS gels. All tissue samples were equalized for protein concentration, and 10-μl aliquots (1 mg/ml) were added to sample buffer (5 μl; Tris-HCl, 0.5 mM, pH6.8; glycerol, 10%; SDS, 10%; β-mercaptoethanol, 5%; bromphenol blue, 0.05% w/v), boiled for 5 min, and loaded onto 10% SDS gels. Proteins were separated by application of a 30-mA constant current for 25–30 min, transferred onto nitrocellulose strips (225 mA for 75 min), and immunoblotted with the appropriate antibody.

To assess JNK activity, proteins were immunoblotted with an antibody that specifically targets phosphorylated JNK (1:400 in Tris-buffered saline (TBS)-Tween (0.05% Tween-20) containing 0.1% BSA; Santa Cruz Biotechnology, Santa Cruz, CA) for 2 h at room temperature. Immunoreactive bands were detected using peroxidase-conjugated anti-mouse IgG (Sigma) and Super Signal chemiluminescence (Pierce). To assess phosphorylation of c-Jun, nitrocellulose membranes were blocked in TBS containing 5% BSA overnight at 4 °C and immunoblotted with a mouse monoclonal antibody (1:300 dilution in phosphate-buffered saline-Tween containing 2% nonfat dried milk, Cell Signaling) for 2 h at room temperature. In the case of p38, nitrocellulose membranes were blocked in 2% BSA in TBS overnight at 4 °C and immunoblotted with a mouse monoclonal antibody (1:200 dilution in TBS-Tween containing 0.1% BSA, Sigma) for 2 h at room temperature. Immunoreactive bands were detected using peroxidase-conjugated anti-mouse IgG (Sigma-Aldrich) and Super Signal chemiluminescence (Pierce). In the case of NFκB, nitrocellulose membranes were blocked in 5% BSA in TBS overnight at 4 °C and immunoblotted with a rabbit monoclonal antibody (1:300 dilution in TBS-Tween containing 0.1% BSA, Cell Signaling Technology) for 2 h at room temperature. Immunoreactive bands were detected using peroxidase-conjugated anti-rabbit IgG (Sigma-Aldrich) and Super Signal chemiluminescence (Pierce). Blots were stripped (Reblot Plus, Chemicon) and reprobed with an anti-actin antibody (Santa Cruz Biotechnology); in the case of JNK, c-Jun, and NFκB, antibodies raised against the unphosphorylated form were used to confirm equal loading.

Cholesterol Analysis—NMR spectra were recorded at room temperature on a JEOL ECA600 NMR spectrometer operating at 600-Hz proton frequency. The spectra were acquired in the Fourier transformation mode with 32 K data points, using a 45° pulse width. The residual monodeuterated water signal at ~4.7 ppm was suppressed by the application of a continuous and selective secondary irradiation during the relaxation delay. Chemical shifts were referenced to the residual methanol peak at 3.31 ppm. Spectral assignments were made by reference to data already in the literature (21, 22). Cholesterol was identified and quantified by its characteristic C-18 methyl singlet at 0.68 ppm.

Statistical Analysis—Data were analyzed, as appropriate, using either Student's *t* test for independent means or a two-way analysis of variance (ANOVA) followed by post hoc Student Newman-Keuls test to determine which conditions were significantly different from each other. Data are expressed as means with standard errors and deemed statistically significant when $p < 0.05$.

RESULTS

Atorvastatin Attenuates LPS-induced Inflammatory Changes—MHCII mRNA expression and IL-1β concentration were significantly increased in hippocampal tissue prepared from LPS-injected rats, compared with controls (*, $p < 0.05$, ANOVA, Fig. 1, *a* and *b*); both changes were attenuated in hippocampal tissue prepared from atorvastatin-treated rats so that mean values were similar in tissue prepared from control-treated rats and LPS-treated rats, which received atorvastatin. Interaction of IL-1β with its receptor IL-1RI has been shown to trigger sequential activation of JNK and c-Jun (4, 5), and activation of p38 and NFκB (23), therefore expression of the phosphorylated forms of these proteins was assessed in hippocampal tissue.

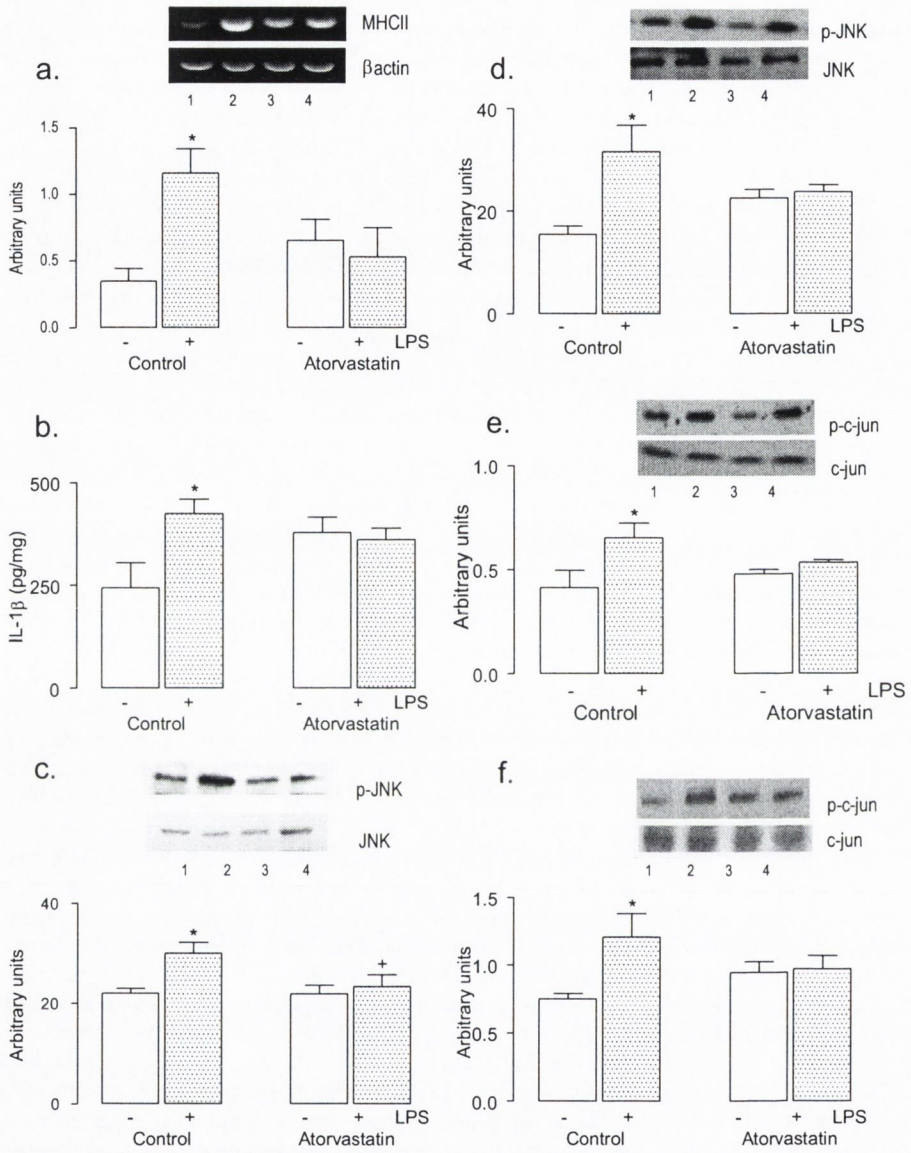

FIGURE 1. **Atorvastatin blocks the LPS-induced changes in hippocampus.** LPS injection (100 μg/kg, intraperitoneally) significantly increased expression of MHCII mRNA (*a*), IL-1β concentration (*b*), JNK activation in cytosolic (*c*), and nuclear (*d*) fractions, and phosphorylation of c-Jun on Serine-63 (*e*) and Serine-73 (*f*, *, $p < 0.05$, ANOVA). These effects were blocked in tissue prepared from animals treated orally with atorvastatin (5 mg/kg/day) for 3 weeks ($^+$, $p < 0.05$, ANOVA, *versus* LPS alone). Atorvastatin exerted no significant effect in saline-treated rats. Data in all cases are expressed as means of five or six observations (±S.E.). For *c–f*, mean arbitrary values (±S.E.) obtained from densitometric analysis are presented, and sample blots are shown (for control-treated (*lane 1*), LPS-treated (*lane 2*), atorvastatin-treated (*lane 3*), and LPS plus atorvastatin-treated (*lane 4*) rats; in all cases blots were stripped and reprobed with total JNK or total c-Jun to confirm equal loading of proteins.

actin was unchanged with treatment. In parallel with these changes, activation of c-Jun (expressed as a ratio of c-Jun phosphorylated on serine 63 or serine 73 to c-Jun) and NFκB (expressed as a ratio of phosphorylated NFκ B to total NFκB) in nuclear fractions obtained from the same tissue, were significantly increased in LPS-treated, compared with control, rats (*, $p < 0.05$; **, $p < 0.01$, ANOVA, Figs. 1*e*, 1*f*, and 2*b*). These increases were attenuated in LPS-treated rats that received atorvastatin so that the mean values in these groups were similar to those in controls, and, in the case of NFkB, significantly decreased compared with the value in tissue prepared from LPS-treated rats ($^{++}$, $p < 0.01$, ANOVA). Expression of unphosphorylated NFκB was unchanged with treatment.

Atorvastatin Attenuates the LPS-induced Inhibition of LTP—It has been consistently shown that, when hippocampal IL-1β concentration is increased, LTP is impaired and that inhibition of JNK (3) and p38 (23) antagonizes the LPS-induced inhibition of LTP. The present results support these observations and show that, in parallel with the increases in IL-1β concentration and JNK and p38 activation, LTP is impaired in LPS-treated animals. Thus, high frequency stimulation of the perforant path led to an immediate and sustained increase in population EPSP slope in control rats, whereas LTP was markedly attenuated in rats injected with LPS ($p < 0.001$, ANOVA, Fig. 3*a*). There was a significant decrease in the mean percentage change in population EPSP slope in the last 10 min of the experiment compared with the mean value in the 5 min prior to stimulation in the LPS-treated group (84.46 ± 0.62), compared with the controls (123.3 ± 1.16; **, $p < 0.01$, ANOVA, Fig. 3*b*). Mean population EPSP slope was significantly decreased in rats that received atorvastatin (109.6 ± 0.86; *, $p < 0.05$, ANOVA, Fig. 3*b*) compared with controls, and atorvastatin blocked the inhibitory effect of LPS on LTP so that the mean percentage change in EPSP sope in the last 10 min of the experiment was significantly greater in LPS-treated animals that received atorvastatin (137.0 ± 1.09) compared with controls (**, $p < 0.01$, ANOVA) or animals that received LPS ($^{++}$, $p < 0.01$, ANOVA).

Expression of phosphorylated JNK (pJNK, expressed as a ratio of pJNK to total JNK in cytosolic and nuclear fractions) and p38 (expressed in a cytosolic fraction as a ratio of phosphorylated p38 (p-p38) to actin) were significantly increased in tissue prepared from LPS-treated, compared with control-treated, rats (*, $p < 0.05$, ANOVA, Fig. 1, *c* and *d*, and Fig. 2*a*). These increases were attenuated in LPS-treated rats that received atorvastatin so that the mean values in these groups were similar to those in controls and, in the case of cytosolic pJNK, significantly reduced compared with the value in tissue prepared from LPS-treated rats ($^+$, $p < 0.05$, ANOVA). Expression of total JNK and

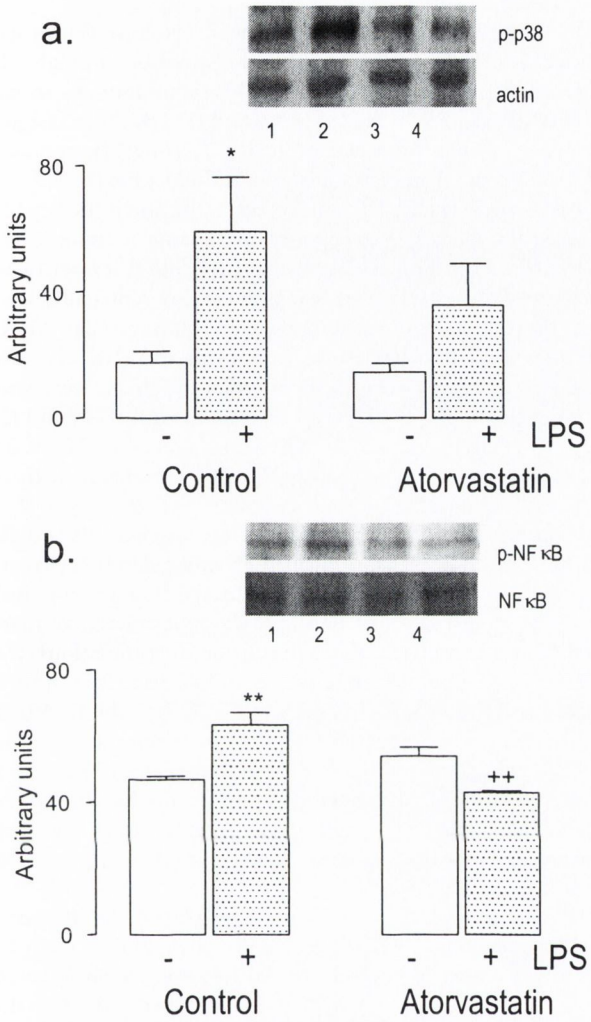

FIGURE 2. **Atorvastatin abrogates the LPS-induced activation of p38 and NFκB.** LPS injection (100 μg/kg, intraperitoneally) significantly increased activation of p38 (*a*) and NFκ B (*b*) in hippocampal tissue (* $p < 0.05$, ** $p < 0.01$, ANOVA, $n = 5$ or 6). These effects were blocked in tissue prepared from animals treated orally with atorvastatin (5 mg/kg/day) for 3 weeks ($^{++}$, $p < 0.01$, ANOVA, *versus* LPS alone). Atorvastatin exerted no significant effect in saline-treated rats. Mean arbitrary values (±S.E.) obtained from densitometric analysis are presented, and sample blots are shown; in all cases blots were stripped and reprobed with actin or total NFκB to confirm equal loading of proteins.

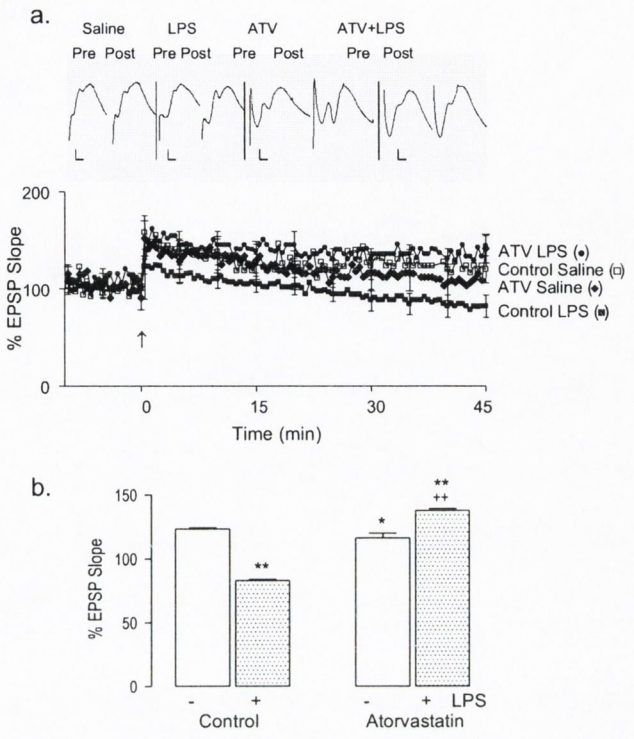

FIGURE 3. **Atorvastatin reverses the LPS-induced impairment in LTP.** *a*, intraperitoneal injection of LPS (100 μg/kg, intraperitoneally) blocked tetanus-induced LTP in perforant path-granule cell synapses, but this effect was suppressed by atorvastatin (*ATV*: 5 mg/kg/day) treatment. Data are expressed as the mean percentage change in population EPSP slope (relative to the mean population EPSP slope in the 5 min immediately prior to tetanic stimulation). Values are means and bars (denoting ± S.E.) are included at 5-min intervals. Sample recordings in the 5 min prior to tetanic stimulation (*pre*) and in the last 5 min of the experiment (*post*) are given for rats that received saline (*Saline*), LPS, ATV, or atorvastatin and LPS (*ATV+LPS*). *b*, analysis of the mean percentage changes in population EPSP slope in the last 10 min of the experiment compared with the mean value in the 5 min prior to tetanic stimulation are shown; data reveal a significant decrease in LPS-treated rats compared with control rats (**, $p < 0.01$, ANOVA); atorvastatin treatment significantly attenuated the LPS-induced effect ($^{++}$, $p < 0.01$, ANOVA, *versus* LPS alone). Mean EPSP slope was significantly reduced in saline-treated rats that received atorvastatin (*, $p < 0.05$, ANOVA, *versus* saline). The mean value in the last 10 min of the experiment was significantly reduced in atorvastatin-treated, compared with control-treated, rats (*, $p < 0.05$, ANOVA). Values are presented as means of between five and six observations (±S.E.).

Atorvastatin Also Attenuates the LPS-induced Increase in IFNγ—These data suggest that LPS-induced microglial activation may trigger the cascade of events leading to inhibition of LTP and that atorvastatin exerts its effects, because it down-regulates microglial activation or the trigger leading to activation of microglia. Because previous evidence indicated that IFNγ triggers activation of microglia *in vitro* (24) we considered that it might also trigger the response observed here *in vivo*. Mean IFNγ concentration was significantly increased in tissue prepared from LPS-treated rats (*, $p < 0.05$, ANOVA, Fig. 4*a*), and this was attenuated by atorvastatin so that IFNγ concentration was similar in tissue prepared from LPS-treated rats that received atorvastatin and in tissue prepared from control-treated rats.

IL-4 Mediates the Effects of Atorvastatin and Blocks IFNγ-induced Changes—It has been reported that atorvastatin can induce a Th2 response characterized by increased secretion of anti-inflammatory cytokines like IL-4 (15); because of this and because we have previously shown that IL-4 inhibits LPS-induced changes in hippocampus (3), we considered that the action of atorvastatin might be mediated by IL-4. We report that IL-4 concentration was significantly enhanced in hippocampal tissue prepared from atorvastatin-treated compared with control-treated rats (*, $p < 0.05$, ANOVA, Fig. 4*b*) but that IL-4 concentration was significantly decreased in tissue prepared from LPS-treated rats that did not receive atorvastatin compared with those that did ($^{+}$, $p < 0.05$, ANOVA, Fig. 4*b*). If IL-4 mediates the effects of atorvastatin, then it must be predicted that atorvastatin will not exert any effect in tissue prepared from IL-$4^{-/-}$ mice, and to check this we compared its effect on LPS-induced changes in these and wild-type mice. In

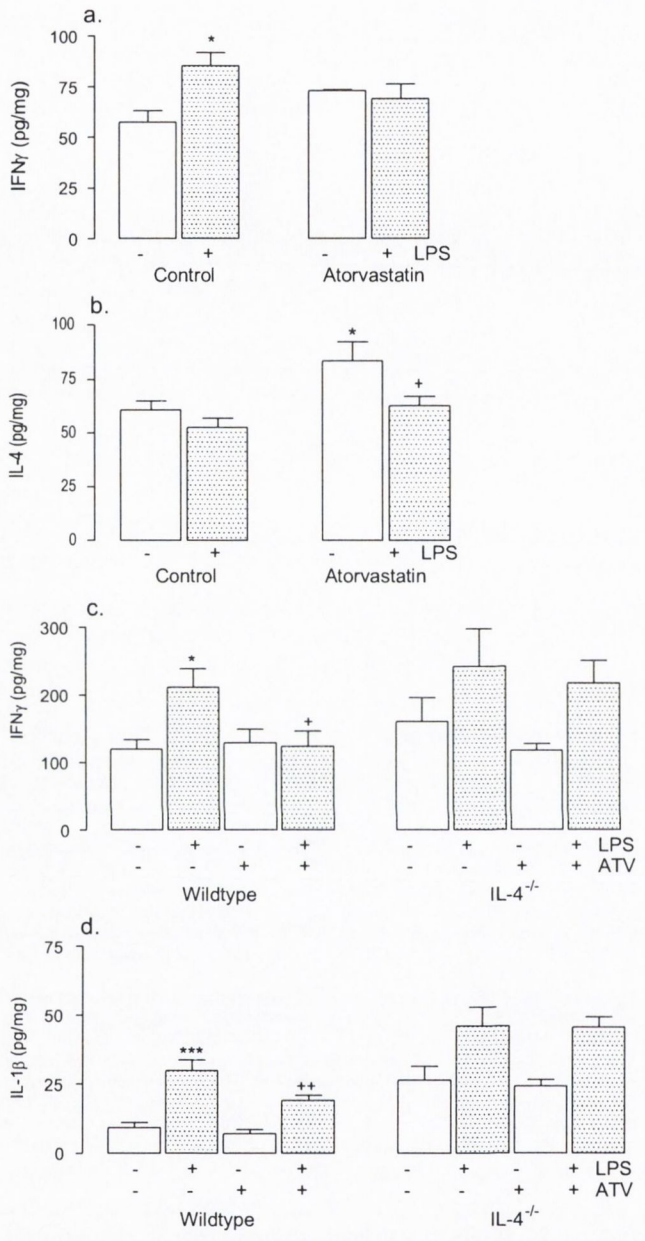

FIGURE 4. **Atorvastatin increases hippocampal IL-4 concentration and attenuates the LPS-induced changes in IFNγ hippocampal concentrations.** *a*, mean IFNγ concentration was increased in tissue prepared from LPS-treated, compared with control-treated, rats (*, $p < 0.05$, ANOVA, $n = 8/9$); this effect was attenuated in tissue prepared from atorvastatin-treated rats. *b*, mean IL-4 concentration was significantly increased with tissue prepared from atorvastatin-treated compared with control-treated, rats (*, $p < 0.05$, ANOVA); this effect was significantly reduced in tissue prepared from atorvastatin-treated animals that received LPS ($^{+}$, $p < 0.05$, ANOVA, $n = 5$). *c* and *d*, IFNγ and IL-1β concentrations were significantly increased in tissue prepared from LPS-treated wild-type mice (*, $p < 0.05$; ***, $p < 0.001$, ANOVA), and atorvastatin significantly attenuated these changes ($^{+}$, $p < 0.05$; $^{++}$, $p < 0.01$, ANOVA, *versus* LPS alone). In contrast, the effect of atorvastatin (*ATV*) was absent in tissue prepared from IL-$4^{-/-}$ mice.

parallel with the findings in rats, IFNγ and IL-1β were significantly increased in tissue prepared from LPS-treated wild-type mice (*, $p < 0.05$; ***, $p < 0.001$, ANOVA, Fig. 4, *c* and *d*), and atorvastatin significantly attenuated these changes ($^{+}$, $p < 0.05$; $^{++}$, $p < 0.01$, ANOVA), so that mean cytokine values were similar in tissue prepared from LPS-treated animals that received atorvastatin and in control-treated animals. In contrast, whereas LPS increased IFNγ and IL-1β, albeit insignificantly, in samples prepared from IL-$4^{-/-}$ mice, there was no evidence of an effect of atorvastatin in these animals.

If IL-4 mediates the effect of atorvastatin, and if the key LPS-induced action leading to degenerative change is an increase in IFNγ, then it must be predicted that IL-4, like atorvastatin, will antagonize the effects of IFNγ. Intracerebroventricular injection of IFNγ significantly increased hippocampal MHCII mRNA expression, IL-1β concentration, and JNK activation (**, $p < 0.01$, ANOVA, Fig. 5, *a–c*), and these effects were attenuated in tissue prepared from rats treated with IFNγ and IL-4 ($^{+}$, $p < 0.05$ in the case of MHCII expression and $^{++}$, $p < 0.01$ in the case of JNK activation, ANOVA). Consistent with our previous findings, the increases in microglial activation, IL-1β concentration, and JNK activation were coupled with a deficit in LTP. Thus LTP was significantly attenuated in IFNγ-treated rats (Fig. 6, *a* and *b*); the mean percentage changes in population EPSP slope in the last 10 min of the experiment (compared with the mean value in the 5 min prior to stimulation), were 129.9 ± 0.72 in control-treated rats and 86.36 ± 0.73 in IFNγ-treated animals (***, $p < 0.001$, ANOVA, Fig. 6*b*). IL-4 treatment completely abrogated the effect of IFNγ; the mean percentage change in population EPSP slope was 135.1 ± 0.81, which was not significantly different from that in control-treated rats, but was significantly greater than the value observed in rats that received IFNγ alone ($^{+++}$, $p < 0.001$, ANOVA, Fig. 6*b*).

Atorvastatin Attenuates the Age-related Inflammatory Changes and the Deficit in LTP—Previous studies from this laboratory have identified similarities in signaling events between LPS-treated rats and aged rats, in particular signaling events triggered by increased IL-1β concentration (1, 3, 4). Here we report that there were significant age-related increases in concentrations of IFNγ and IL-1β and in MHCII mRNA expression in hippocampal tissue prepared from aged, compared with young rats (*, $p < 0.05$; **, $p < 0.01$, ANOVA, Fig. 7, *a–c*) and that treatment with atorvastatin blocked these age-related changes so that the values in tissue prepared from hippocampus of aged atorvastatin-treated rats were significantly decreased compared with those in tissue prepared from aged rats that did not receive atorvastatin ($^{+}$, $p < 0.05$; $^{++}$, $p < 0.01$, ANOVA). Although atorvastatin completely reversed the IFNγ-induced increases in cytokine concentration, its effect on MHCII was partial, and, therefore, the mean value in tissue prepared from aged rats that received atorvastatin was significantly greater than in both groups of young rats (*, $p < 0.05$, ANOVA).

The data show that there was a significant age-related decrease in IL-4 concentration (*, $p < 0.05$, ANOVA, Fig. 7*d*) and that this was significantly attenuated by atorvastatin so that mean hippocampal IL-4 concentration was significantly greater in tissue prepared from aged rats that received atorvastatin compared with aged control rats ($^{+}$, $p < 0.05$, ANOVA, Fig. 7*d*). Importantly the atorvastatin-induced changes were associated with rescue of the age-related deficit in LTP; LTP was signifi-

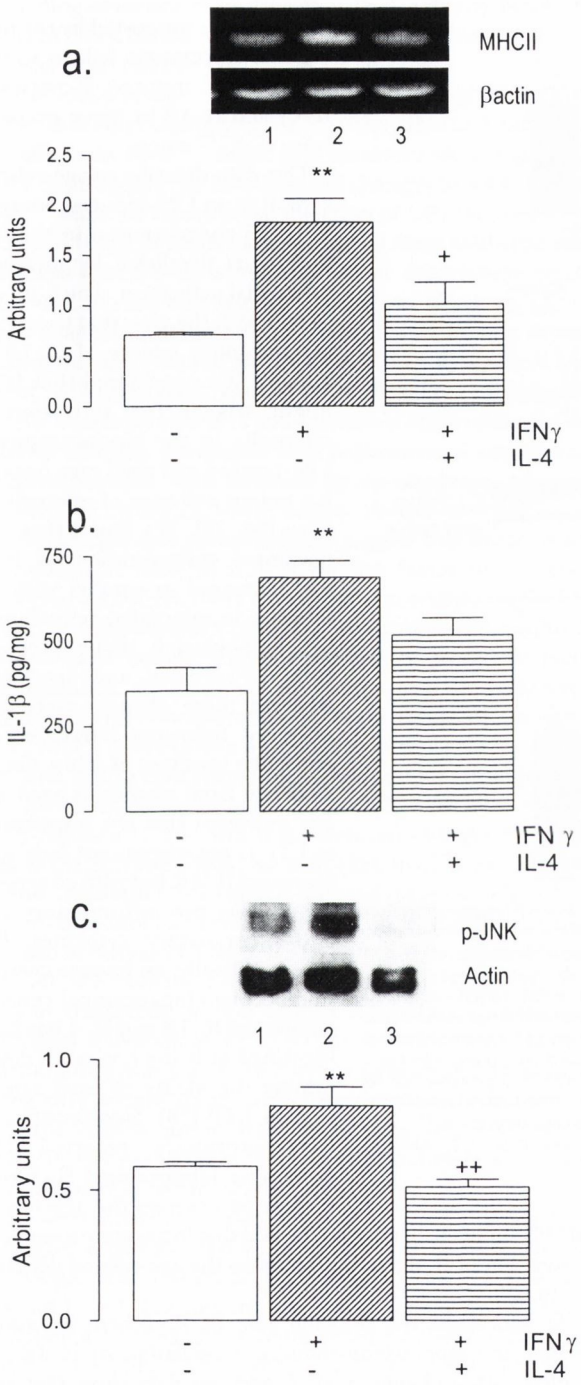

FIGURE 5. **IL-4 attenuates IFNγ-induced changes in hippocampus.** *a*, intracerebroventricular injection of IFNγ (5 μl; 50 ng/ml) significantly increased expression of MHCII mRNA (**, $p < 0.01$, ANOVA, $n = 5$), and this effect was blocked by co-injection with IL-4 (5 μl; 20 ng/ml; $^{+}$, $p < 0.05$, ANOVA). *b* and *c*, the IFNγ-induced increases in IL-1β concentration (*b*) and JNK activation (*c*) in hippocampal tissue prepared from IFNγ-treated rats were significantly greater than in saline-treated rats (**, $p < 0.01$, ANOVA), whereas the values in hippocampal tissue prepared from IFNγ and IL-4 co-injected rats were similar to those in saline-treated controls and, in the case of JNK activation, significantly decreased compared with the value observed in tissue prepared from rats treated with IFNγ alone ($^{++}$, $p < 0.01$, ANOVA). Sample blots indicating changes in phosphorylated JNK in hippocampal tissue prepared from control (*lane 1*), IFNγ- (*lane 2*), and IFNγ+IL-4- (*lane 3*)-treated rats are presented. Values are presented as means of between five and six observations (±S.E.).

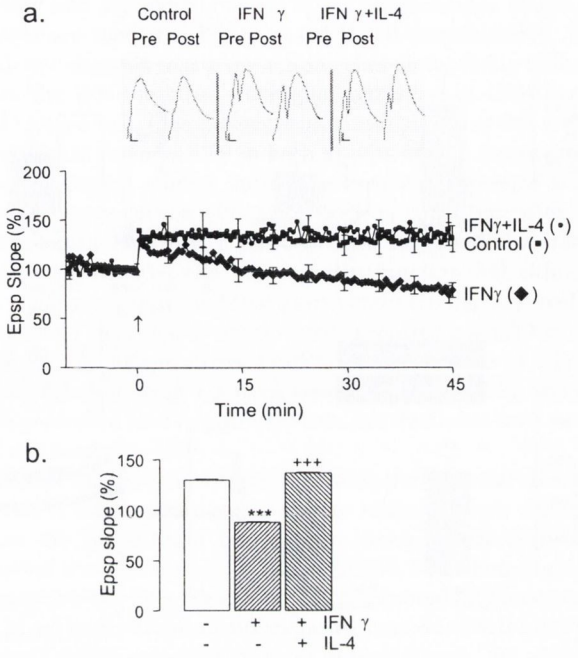

FIGURE 6. **IL-4 abrogates the IFNγ-induced inhibition of LTP.** *a*, intracerebroventricular injection of IL-4 (5 μl; 20 ng/ml) abrogated the deficit in LTP induced by IFNγ (5 μl; 50 ng/ml) so that the population EPSP slope in response to tetanic stimulation in the rats treated with IFNγ was significantly reduced compared with that in rats treated with saline, or IL-4 and IFNγ. Sample recordings in the 5 min prior to tetanic stimulation (*pre*) and in the last 5 min of the experiment (*post*) are given for control-treated, IFNγ-treated, and IFNγ+IL-4-treated rats. *b*, analysis of the mean percentage changes in population EPSP slope in the last 10 min of the experiment compared with the mean value in the 5 min prior to tetanic stimulation revealed a significant decrease in IFNγ-treated rats compared with control-treated rats (***, $p < 0.001$, ANOVA) and a significant attenuation of the IFNγ-induced change in rats treated with IFNγ and IL-4 ($^{+++}$, $p < 0.001$, ANOVA). Values are presented as means of between four and seven observations (±S.E.).

cantly decreased in aged, compared with young, rats, whereas LTP in aged rats that received atorvastatin was similar to that in young animals. The mean percentage changes in population EPSP slope in the last 10 min of the experiment (compared with the mean value in the 5 min prior to stimulation) were 118.1 ± 0.77, 94.36 ± 0.58, and 133.3 ± 0.38 in young rats, aged control-treated rats, and aged rats that received atorvastatin, respectively. These values represent a significant difference in aged control-treated rats compared with young rats (**, $p < 0.01$, ANOVA, Fig. 7*f*) and between aged control-treated and aged atorvastatin-treated rats ($^{++}$, $p < 0.01$, ANOVA, Fig. 7*f*). EPSP slope in young, atorvastatin-treated rats was also decreased (123.7 ± 0.39) compared with the value in young, control-treated rats (**, $p < 0.01$, ANOVA, Fig. 7*f*).

Atorvastatin Does Not Exert Any Effect on Cholesterol Concentration in Brain—We assessed cholesterol concentration in samples of cortical tissue prepared from control- and LPS-treated young rats that did/did not receive atorvastatin and in young and aged, control-treated, and atorvastatin-treated, rats. Cholesterol was similar in control-treated and LPS-treated rats (37.16 ± 0.3 and 36.37 ± 0.67 mol%), and atorvastatin exerted no significant effect on cholesterol (37.16 ± 0.2 and 36.57 ± 0.41 in control-treated and LPS-treated rats, respectively). In contrast cholesterol was significantly increased in tissue pre-

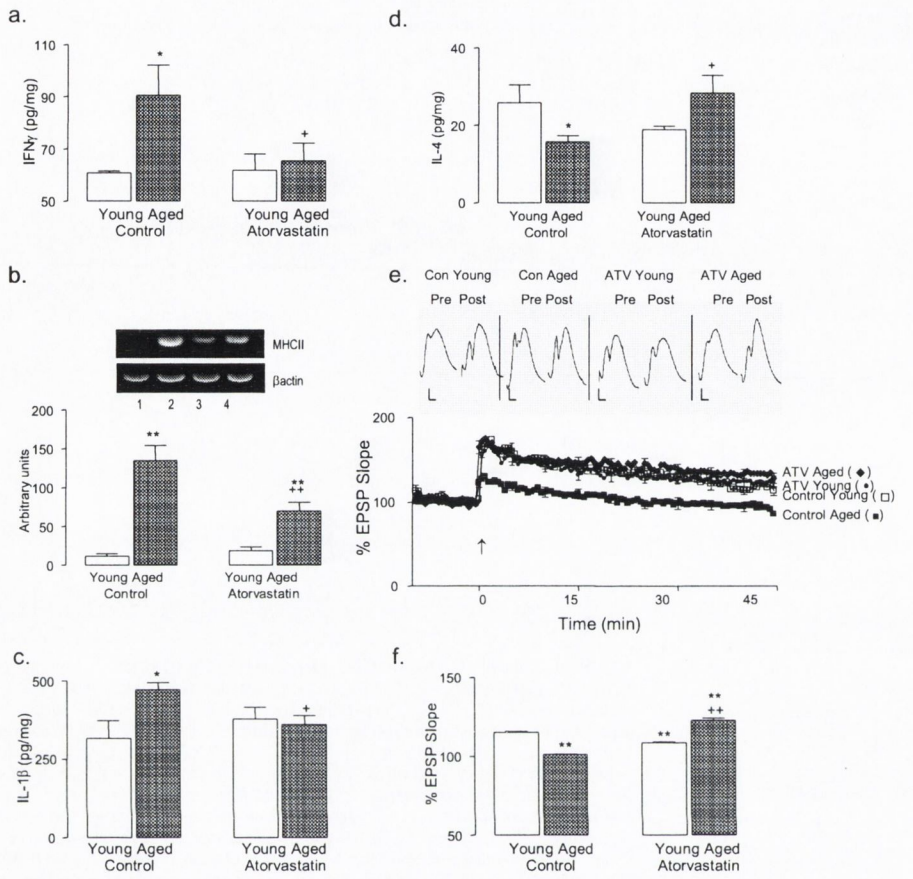

FIGURE 7. **Atorvastatin abrogates age-related changes in the rat hippocampus.** Mean IFNγ concentration (*a*), MHCII expression (*b*), and IL-1β concentration (*c*) were significantly increased and mean IL-4 concentration (*d*) was significantly decreased in hippocampal tissue prepared from aged, compared with young, rats (*, $p < 0.05$, **, $p < 0.01$, ANOVA). Atorvastatin treatment (*ATV*; 5 mg/kg/day) for 8 weeks abrogated these changes ($^{+}$, $p < 0.05$; $^{++}$, $p < 0.01$, ANOVA, *versus* LPS alone). *e*, a marked deficit in LTP was observed in aged, compared with young, rats, and treatment with ATV attenuated the age-related change. Sample recordings in the 5 min prior to tetanic stimulation (*pre*) and in the last 5 min of the experiment (*post*) are given for control-treated young and aged rats (*Con young* and *Con aged*, respectively), and atorvastatin-treated young and aged rats (*ATV young* and *ATV aged*, respectively). *f*, the mean percentage change in population EPSP slope in the last 10 min of the experiment compared with the mean value in the 5 min prior to tetanic stimulation revealed a significant age-related change (**, $p < 0.01$, ANOVA), which was significantly reversed by atorvastatin ($^{++}$, $p < 0.01$, ANOVA). Mean EPSP slope was significantly reduced in rats that received atorvastatin (*, $p < 0.05$, ANOVA, *versus* saline). Data are expressed as means of five or six observations (±S.E.).

pared from aged (39.97 ± 0.34), compared with young (37.89 ± 0.41), rats ($p < 0.01$, ANOVA), but there was no evidence of any effect of atorvastatin treatment in either age group (38.19 ± 0.20 and 40.48 ± 0.43 in young and aged atorvastatin-treated rats, respectively).

DISCUSSION

We set out to establish whether atorvastatin, which is known to possess anti-inflammatory properties, might modulate the neuro-inflammatory changes induced by LPS and age in the rat hippocampus that lead to impairment of LTP. We report that microglial activation, IFNγ, and IL-1β were increased in hippocampal tissue prepared from aged and LPS-treated rats and that these changes were accompanied by inhibition of LTP. We hypothesize that the primary action of atorvastatin is to increase IL-4 and that this prevents the IFNγ-induced microglial activation, which triggers the cascade of events. This hypothesis is supported by the finding that atorvastatin fails to attenuate the LPS-induced increases in IFNγ and IL-1β in tissue prepared from IL-$4^{-/-}$ mice.

Our data describe an age-related, as well as an LPS-induced, increase in IL-1β concentration in the hippocampus paralleled by increased microglial activation, which is consistent with the view that these cells are the likely source of IL-1β (6, 25, 26). We considered that IFNγ might trigger the activation of microglia in the hippocampus of LPS-treated and aged rats, because it a potent activator of microglia *in vitro* (24, 27). We found that hippocampal concentration of IFNγ was increased in parallel with the increase in microglial activation in the hippocampal tissue prepared from LPS-treated and aged rats, whereas these changes were also observed following intracerebroventricular injection of IFNγ. Recent evidence from studies in aged rats has indicated that the impairment in LTP is associated, not only with increased IL-1β, but with an array of changes in pro-inflammatory and anti-inflammatory cytokines, (26, 27); specifically, an inverse correlation between hippocampal concentrations of IL-1β and IL-4 has been identified as being critical in determining the ability of aged rats to sustain LTP (28). Significantly, we have previously reported that increasing hippocampal IL-4 concentration reverses the age-related and LPS-induced deficits in LTP and that intracerebroventricular injection of IL-4 partly attenuates the age-related deficit in LTP (6, 29).

We addressed the possible role of IL-4 here by asking whether the atorvastatin-induced modulation of IL-1β was coupled with a change in IL-4, and our data show that IL-4 concentration was indeed increased in atorvastatin-treated rats that received LPS and that atorvastatin treatment was associated with a reversal of the age-related decrease in IL-4. We demonstrate that IL-4 attenuates the IFNγ-triggered increases in MHCII expression and IL-1β concentration and, in parallel, antagonizes the IFNγ-induced inhibition of LTP. This antagonistic effect of IL-4 on IFNγ-induced changes indicates that the atorvastatin-induced increase in IL-4 inhibits the cascade of events triggered by the age- and LPS-induced increase in the hippocampal concentration of IFNγ and the subsequent microglial activation. Moreover it is in agreement with the previous

compelling evidence indicating that IL-4 potently blocks the effects of IFNγ, including the IFNγ-induced activation of CD40 in a microglial cell line (24).

If the action of atorvastatin is mediated through IL-4, then it follows that atorvastatin will not have the same anti-inflammatory effects in IL-$4^{-/-}$ mice, and therefore we compared its ability to attenuate the LPS-induced changes in wild-type and IL-$4^{-/-}$ mice. Intraperitoneal injection of LPS increased both IFNγ and IL-1β in brain tissue prepared from wild-type mice, and these effects were attenuated in the atorvastatin-treated mice. In contrast, atorvastatin exerted no effect on LPS-induced changes in tissue prepared from IL-$4^{-/-}$ mice, demonstrating that the effect of atorvastatin is IL-4-dependent. Consistent with these data, Youssef and colleagues (15) suggested that the beneficial effects of atorvastatin in attenuating the detrimental changes associated with experimental autoimmune encephalomyelitis were achieved by up-regulating release of Th2-derived cytokines, which include IL-4, from splenocytes.

Although the data presented here suggest that the atorvastatin-induced increase in IL-4 is the key factor in decreasing microglial activation, there is a lack of concordance in the literature regarding the effect of statins on microglial activation. On the one hand certain statins have been reported to induce inflammation, for instance lovastatin has been shown to increase IL-1β concentration in brain tissue of transgenic mice, which overexpress human amyloid precursor protein (30), and TNFα concentration in cultured hippocampal slices (13). Similarly, cerivastatin and fluvastatin have been reported to up-regulate IL-1β- and IFNγ-induced changes in smooth muscle (31, 32) and hepatoma cells (32). In contrast, simvastatin and lovastatin block the Aβ-induced increase in IL-1β production in monocytes and BV2 cells (33) and the IFNγ-induced increase in release of TNFα, IL-1β and IL-6 in cultured microglia (34). We have recently reported a beneficial effect of atorvastatin treatment *in vivo* against Aβ-induced increases in microglial activation and IL-1β concentration (35). This anti-inflammatory role is supported by a large body of evidence indicating that certain statins are protective in ischemia (36–39) and experimental autoimmune encephalomyelitis (see Ref. 40) in which the degenerative effects are attributed, at least in part, to inflammation and microglial activation.

We demonstrate that the effects of LPS and atorvastatin on microglial activation and IL-1β concentration were mirrored by changes in activation of JNK and c-Jun and in activation of p38 and NFκB. The importance of these signaling cascades in modulating LTP has been highlighted by the demonstration that the LPS-induced inhibition of LTP was blocked by inhibitors of JNK, p38, and NFκB (3, 23). To our knowledge there are no data showing that statins can attenuate LPS-induced and/or IL-1β-mediated signaling cascades in brain *in vivo* and few data documenting a modulatory effect *in vitro* (41). In contrast, several studies have revealed that statins block stimulus-induced activation of JNK and/or c-Jun in myocytes (42), Chinese hamster ovary cells (43), and macrophages (44), whereas a similar antagonistic effect on stimulus-induced activation of p38 and NFκB in monocytes (45), vascular endothelial cells (46), and macrophages (47, 48) has been reported. A significant finding of this study is that atorvastatin treatment abrogates the inflammatory and signaling changes in rat hippocampus which we believe are mediated by increased IL-1β concentration. The evidence suggests that a key action relies on its ability to modulate the IFNγ-induced microglial activation in LPS-treated and in aged rats. One downstream consequence of this is that atorvastatin restores LTP in both groups of rats. Results from epidemiological studies indicate a beneficial effect of statin therapy on cognition (49–53), which is consistent with the present data. However, it has also been suggested that statins may exert a negative effect on cognitive function (54), although a recent report indicated that atorvastatin (10 mg/day) had no such effect (55). We have previously reported a small but statistically significant atorvastatin-induced decrease in LTP in young rats following a 3-week treatment period (35), and the data presented here concur with this, but treatment for 8 weeks did not modulate LTP.

One of the key issues raised regarding the potential effects of statins in the central nervous system relates to their ability to cross the blood-brain barrier (56). Some researchers have asserted that atorvastatin is lipophilic (57, 58), whereas others suggest it is not (59). We detected small amounts of atorvastatin (~30 pg) in the brains of atorvastatin-treated animals (data not shown), which suggests that it can enter the brain, but whether this is a result of blood-brain barrier breakdown following LPS challenge, facilitated transport via atorvastatin transporters, or simple diffusion remains to be determined. Whether a statin that can cross the blood-brain barrier is advantageous or not is a question that remains, and it must be concluded that the effect of statins is dependent on the specific statin, the tissue under investigation, and the stimulus upon which the modulatory effects are analyzed.

Importantly, although we observed an age-related increase in cholesterol concentration in brain tissue (though LPS exerted no effect), atorvastatin failed to modulate brain cholesterol concentration. We conclude that the effects of atorvastatin described here are unrelated to its well described cholesterol-lowering action. The data suggest that its beneficial effects derive from its ability to maintain microglia in a quiescent state, and in particular, from its ability to increase IL-4.

REFERENCES

1. Martin, D. S., Lonergan, P. E., Boland, B., Fogarty, M. P., Brady, M., Horrobin, D. F., Campbell, V. A., and Lynch, M. A. (2002) *J. Biol. Chem.* **277,** 34239–34246
2. Nolan, Y., Maher, F. O., Martin, D. S., Clarke, R. M., Brady, M. T., Bolton, A. E., Mills, K. H., and Lynch, M. A. (2005) *J. Biol. Chem.* **280,** 9354–9362
3. Barry, C. E., Nolan, Y., Clarke, R. M., Lynch, A., and Lynch, M. A. (2005) *J. Neurochem.* **93,** 221–231
4. Lonergan, P. E., Martin, D. S., Horrobin, D. F., and Lynch, M. A. (2004) *J. Neurochem.* **91,** 20–29
5. Minogue, A. M., Schmid, A. W., Fogarty, M. P., Moore, A. C., Campbell, V. A., Herron, C. E., and Lynch, M. A. (2003) *J. Biol. Chem.* **278,** 27971–27980
6. Lynch, A. M., Loane, D. J., Minogue, A. M., Clarke, R. M., Kilroy, D., Nally, R. E., Roche, O. J., O'Connell, F., and Lynch, M. A. (2007) *Neurobiol. Aging* **28,** 845–855
7. Moore, A. H., and O'Banion, M. K. (2002) *Adv. Drug Deliv. Rev.* **54,** 1627–1656
8. Moore, M. E., Piazza, A., McCartney, Y., and Lynch, M. A. (2005) *Biochem. Soc. Trans.* **33,** 573–577
9. Milner, R., and Campbell, I. L. (2003) *J. Immunol.* **170,** 3850–3858

10. Delgado, M. (2003) *J. Biol. Chem.* **278,** 27620–27629
11. Nguyen, V. T., Walker, W. S., and Benveniste, E. N. (1998) *Eur. J. Immunol.* **28,** 2537–2548
12. Lindberg, C., Crisby, M., Winblad, B., and Schultzberg, M. (2005) *J. Neurosci. Res.* **82,** 10–19
13. Bi, X., Baudry, M., Liu, J., Yao, Y., Fu, L., Brucher, F., and Lynch, G. (2004) *J. Biol. Chem.* **279,** 48238–48245
14. Crisby, M., Carlson, L. A., and Winblad, B. (2002) *Alzheimer Dis. Assoc. Disord.* **16,** 131–136
15. Youssef, S., Stuve, O., Patarroyo, J. C., Ruiz, P. J., Radosevich, J. L., Hur, E. M., Bravo, M., Mitchell, D. J., Sobel, R. A., Steinman, L., and Zamvil, S. S. (2002) *Nature* **420,** 78–84
16. Vaughan, C. J. (2003) *Am. J. Cardiol.* **91,** 23B–29B
17. Kawashima, S., Yamashita, T., Miwa, Y., Ozaki, M., Namiki, M., Hirase, T., Inoue, N., Hirata, K., and Yokoyama, M. (2003) *Stroke* **34,** 157–163
18. Lynch, M. A., Errington, M. L., and Bliss, T. V. (1985) *Neurosci. Lett.* **62,** 123–129
19. Bradford, M. M. (1976) *Anal. Biochem.* **72,** 248–254
20. Vereker, E., O'Donnell, E., and Lynch, M. A. (2000) *J. Neurosci.* **20,** 6811–6819
21. Adosraku, R. K., Choi, G. T., Constantinou-Kokotos, V., Anderson, M. M., and Gibbons, W. A. (1994) *J. Lipid Res.* **35,** 1925–1931
22. Noula, C., Bonzom, P., Brown, A., Gibbons, W. A., Martin, J., and Nicolaou, A. (2000) *Biochim. Biophys. Acta* **1487,** 15–23
23. Kelly, A., Vereker, E., Nolan, Y., Brady, M., Barry, C., Loscher, C. E., Mills, K. H., and Lynch, M. A. (2003) *J. Biol. Chem.* **278,** 19453–19462
24. Nguyen, V. T., and Benveniste, E. N. (2000) *J. Immunol.* **165,** 6235–6243
25. Block, M. L., and Hong, J. S. (2005) *Prog. Neurobiol.* **76,** 77–98
26. Griffin, R., Nally, R., Nolan, Y., McCartney, Y., Linden, J., and Lynch, M. A. (2006) *J. Neurochem.* **99,** 1263–1272
27. Maher, F. O., Clarke, R. M., Kelly, A., Nally, R. E., and Lynch, M. A. (2006) *J. Neurochem.* **96,** 1560–1571
28. Maher, F. O., Nolan, Y., and Lynch, M. A. (2005) *Neurobiol. Aging* **26,** 717–728
29. Nolan, Y., Campbell, V. A., Bolton, A. E., and Lynch, M. A. (2005) *Neuroimmunomodulation* **12,** 113–116
30. Chauhan, N. B., Siegel, G. J., and Lichtor, T. (2004) *J. Neurosci. Res.* **78,** 732–741
31. Hattori, Y., Nakanishi, N., and Kasai, K. (2002) *Cardiovasc. Res.* **54,** 649–658
32. Menschikowski, M., Hagelgans, A., Heyne, B., Hempel, U., Neumeister, V., Goez, P., Jaross, W., and Siegert, G. (2005) *Biochim. Biophys. Acta* **1733,** 157–171
33. Cordle, A., Koenigsknecht-Talboo, J., Wilkinson, B., Limpert, A., and Landreth, G. (2005) *J. Biol. Chem.* **280,** 34202–34209
34. Townsend, K. P., Shytle, D. R., Bai, Y., San, N., Zeng, J., Freeman, M., Mori, T., Fernandez, F., Morgan, D., Sanberg, P., and Tan, J. (2004) *J. Neurosci. Res.* **78,** 167–176
35. Clarke, R. M., O'Connell, F., Lyons, A., and Lynch, M. A. (2007) *Neuropharmacology* **52,** 136–145
36. Endres, M., and Laufs, U. (2004) *Stroke* **35,** 2708–2711
37. Endres, M., Laufs, U., Huang, Z., Nakamura, T., Huang, P., Moskowitz, M. A., and Liao, J. K. (1998) *Proc. Natl. Acad. Sci. U. S. A.* **95,** 8880–8885
38. Greisenegger, S., Mullner, M., Tentschert, S., Lang, W., and Lalouschek, W. (2004) *J. Neurol. Sci.* **221,** 5–10
39. Marti-Fabregas, J., Gomis, M., Arboix, A., Aleu, A., Pagonabarraga, J., Belvis, R., Cocho, D., Roquer, J., Rodriguez, A., Garcia, M. D., Molina-Porcel, L., Diaz-Manera, J., and Marti-Vilalta, J. L. (2004) *Stroke* **35,** 1117–1121
40. Stuve, O., Youssef, S., Dunn, S., Slavin, A. J., Steinman, L., and Zamvil, S. S. (2003) *Cell Mol. Life Sci.* **60,** 2483–2491
41. Bosel, J., Gandor, F., Harms, C., Synowitz, M., Harms, U., Djoufack, P. C., Megow, D., Dirnagl, U., Hortnagl, H., Fink, K. B., and Endres, M. (2005) *J. Neurochem.* **92,** 1386–1398
42. Ito, M., Adachi, T., Pimentel, D. R., Ido, Y., and Colucci, W. S. (2004) *Circulation* **110,** 412–418
43. Bardeleben, R., Kaina, B., and Fritz, G. (2003) *Biochem. Biophys. Res. Commun.* **307,** 401–407
44. Matsumoto, M., Einhaus, D., Gold, E. S., and Aderem, A. (2004) *J. Immunol.* **172,** 7377–7384
45. Ortego, M., Gomez-Hernandez, A., Vidal, C., Sanchez-Galan, E., Blanco-Colio, L. M., Martin-Ventura, J. L., Tunon, J., Diaz, C., Hernandez, G., and Egido, J. (2005) *J. Cardiovasc. Pharmacol.* **45,** 468–475
46. Wang, H. R., Li, J. J., Huang, C. X., and Jiang, H. (2005) *Clin. Chim. Acta* **353,** 53–60
47. Huang, K. C., Chen, C. W., Chen, J. C., and Lin, W. W. (2003) *FEBS Lett.* **555,** 385–389
48. Senokuchi, T., Matsumura, T., Sakai, M., Yano, M., Taguchi, T., Matsuo, T., Sonoda, K., Kukidome, D., Imoto, K., Nishikawa, T., Kim-Mitsuyama, S., Takuwa, Y., and Araki, E. (2005) *J. Biol. Chem.* **280,** 6627–6633
49. Heart Protection Study Collaboration Group (2002) *Lancet* **360,** 7–22
50. Jick, H., Zornberg, G. L., Jick, S. S., Seshadri, S., and Drachman, D. A. (2000) *Lancet* **356,** 1627–1631
51. Law, M., and Rudnicka, A. R. (2006) *Am. J. Cardiol.* **97,** 52C–60C
52. Shepherd, J., Blauw, G. J., Murphy, M. B., Bollen, E. L., Buckley, B. M., Cobbe, S. M., Ford, I., Gaw, A., Hyland, M., Jukema, J. W., Kamper, A. M., Macfarlane, P. W., Meinders, A. E., Norrie, J., Packard, C. J., Perry, I. J., Stott, D. J., Sweeney, B. J., Twomey, C., and Westendorp, R. G. (2002) *Lancet* **360,** 1623–1630
53. Wolozin, B., Kellman, W., Ruosseau, P., Celesia, G. G., and Siegel, G. (2000) *Arch. Neurol.* **57,** 1439–1443
54. Wagstaff, L. R., Mitton, M. W., Arvik, B. M., and Doraiswamy, P. M. (2003) *Pharmacotherapy* **23,** 871–880
55. Summers, M. J., Oliver, K. R., Coombes, J. S., and Fassett, R. G. (2007) *Pharmacotherapy* **27,** 183–190
56. Sparks, D. L., Connor, D. J., Browne, P. J., Lopez, J. E., and Sabbagh, M. N. (2002) *J. Nutr. Health Aging* **6,** 324–331
57. King, D. S., Wilburn, A. J., Wofford, M. R., Harrell, T. K., Lindley, B. J., and Jones, D. W. (2003) *Pharmacotherapy* **23,** 1663–1667
58. Kobayashi, M., Otsuka, Y., Itagaki, S., Hirano, T., and Iseki, K. (2006) *Int. J. Pharm.* **317,** 19–25
59. Caballero, J., and Nahata, M. (2004) *J. Clin. Pharm. Ther.* **29,** 209–21